Investigation of the Posttranscriptional Regulator BRF1 in Embryonic Stem Cells by Inducible RNA Interference

INAUGURALDISSERTATION

zur
Erlangung der Würde eines Doktors der Philosophie
vorgelegt der
Philosophisch-Naturwissenschaftlichen Fakultät
der Universität Basel

von

Daniel Wegmüller
aus Frenkendorf, BL und Vechigen, BE

Basel, 2007

Genehmigt von der Philosophisch-Naturwissenschaftlichen Fakultät der Universität Basel auf Antrag von

Professor Yves A. Barde und Professor Christoph Moroni

Basel, den 11. Dezember 2007

<div style="text-align: right">

Prof. Dr. Hans-Peter Hauri
Dekan der Philosophisch-
Naturwissenschaftlichen Fakultät

</div>

SUMMARY

Pluripotency in murine embryonic stem (ES) cells is maintained by a hierarchy of transcription factors (Nanog, Oct4, Sox2, etc.) but nothing is known to date if ES cell self-renewal or differentiation may also involve mechanisms that act posttranscriptionally at the level of mRNA turnover. Around 8% of all transcripts contain in their 3'-untranslated region a so-called AU-rich element (ARE), a destabilizing motif, which is a key target for proteins regulating dynamic mRNA turnover control, and many of these transcripts code for growth and cell cycle regulatory genes. Our longstanding interest in the laboratory is the ARE-mRNA regulator Brf1 (Zfp36L1), and we were interested to see if this protein is also involved in ES cell pluripotency or differentiation. In early experiments we found Brf1 to be expressed in undifferentiated ES cells (CCE, CGR-8) and under positive regulation by the LIF (leukemia inhibitory factor) and Stat3 axis. As LIF removal or targeting of Stat3 by siRNA led to downregulation of Brf1, we wished to explore the consequences of only downregulating Brf1.

To do so, we developed a cassette system where a small hairpin RNA (shRNA) of choice can be introduced into a defined frt (flip-recombinase target)-site by co-transfection with the recombinase, and which can, in addition, be induced by doxycycline. CCE ES cells already expressing the Tet-repressor (TR) for doxycycline inducibility were transfected with a construct expressing both GFP and neomycin resistance markers linked to a frt-site, allowing Flp-recombinase mediated integration of the plasmid encoding the inducible shRNA. For systems control, we targeted Stat3 by shRNA and observed in response to doxycycline, as expected, the morphological and biochemical (Oct-4, Fgf4, Rex-1) signs of differentiation of ES cells even in presence of LIF, thus verifying the validity of the system.

Addition of doxycycline to clones with inducible Brf1 shRNA led to a distinct alteration of the morphology of plated embryoid bodies formed in hanging drops. Unexpectedly, downregulation of Brf1 strongly stimulated the formation of cardiac markers (Nkx2.5, Gata4) as well as the formation of beating bodies observed around day 9. To trigger these changes and to enhance cardiomyocyte formation, 4 days of doxycycline addition following LIF removal was sufficient.

A DNA microarray chip analysis was conducted to identify ARE-bearing transcripts with altered expression upon LIF removal and Brf1 downregulation by RNA interference. Based on our hypothesis, we hoped to identify ARE-bearing transcripts that would be increased by these changes. Unfortunately we could not identify any such transcripts suggesting that the effect may be subtle, or could be masked by the simultaneous changes in transcriptional regulation that accompanies these changes.

In a series of preliminary experiments to establish if posttranscriptional regulation is

operating in undifferentiated ES cells, an EGFP reporter linked to the destabilizing ARE from the IL3 gene was transduced into CCE cells. The amount of EGFP expression, as a marker for steady-state mRNA levels, was consistently lower in cells transduced with a reporter bearing the wild-type ARE when compared to cells bearing a non-functional mutant ARE suggesting reporter mRNA destabilization. In addition, when the reporter was expressed in cells bearing the Brf1 shRNA, a slight but significant increase in EGFP expression was observed upon Brf1 downregulation. These results suggest that posttranscriptional regulation of mRNAs is also active in murine ES cells.

Taken together, these findings raise the possibility that Brf1 could be a novel potential regulator of cardiomyocyte formation and suggest that posttranscriptional mechanisms may play an important role in early development. In addition, the inducible RNA interference system developed for this study can be used to investigate any gene of interest and its role in ES cell development.

1. TABLE OF CONTENTS

1. INTRODUCTION

1.1 Posttranscriptional control

Precise control of gene expression is of the utmost importance in cells and living organisms. It is vital for cells to express the right gene at the right time at the required levels. Gene expression is orchestrated at many levels. It is most commonly regarded as being responsive to cues from inside or outside of the cells by signaling pathways, which regulate the transcription of the gene or the activity of the translated protein. A mechanism that is often neglected but is becoming increasingly recognized is the posttranscriptional regulation of gene expression, which includes quality control of mRNAs, control of transcript levels by regulation of the decay rate and storage of RNAs for times when they are urgently required.

1.1.1 mRNA turnover

mRNA turnover plays a crucial role in the control of gene expression both by setting the basal level of gene expression, and as a mode of regulation (Parker and Song 2004). Eukaryotic mRNAs have a complex final structure, evolving from the maturation of primary, intron-containing transcripts. Maturation of mRNAs includes removal of the introns by splicing, adding of a 7-methyl-GTP cap to the 5' end of the mRNA and addition of a 3' poly(A) tail of about 200 nucleotides (Watson *et al*. 1988). These two modifications are crucial determinants of nuclear export, translation and transcript stability. These structures are bound by eIF4E and the poly(A)-binding protein (PABP) to protect the mRNA from degradation by exonucleases (Bernstein *et al*. 1989; Gingras *et al*. 1999). In general, transcripts in eukaryotes undergo decay after poly(A)-tail shortening.

1.1.1.1 mRNA degradation pathways

The first step in general mRNA turnover in eukaryotes is deadenylation of the poly(A) tail. There are two cytoplasmic protein complexes (CCr4-Not1 and PAN) that can catalyze deadenylation (Brown and Sachs 1998; Tucker *et al*. 2001; Denis and Chen 2003) which are common to all eukaryotes. Another enzyme known to deadenylate mRNA is PARN (poly(A) ribonuclease), a poly(A)-specific exonuclease (Astrom *et al*. 1992; Korner and Wahle 1997). PARN appears to be needed for fast deadenylation in connection with cis regulatory element-

mediated mRNA destabilization (Lai *et al*. 2003) but is also implicated in nonsense-mediated decay (NMD) (Lejeune *et al*. 2003). PARN can be found in many eukaryotes but is absent in *S.cerevisiae* and *Drosophila melanogaster*. PARN is not inhibited by the 5'-cap structure but by the poly(A) binding protein PABP1 (Dehlin *et al*. 2000; Gao *et al*. 2001; Martinez *et al*. 2001), suggesting that the preferred target of PARN would be an mRNA with both an exposed cap and a poly(A) tail lacking PABP1. Deadenylation is reversible (Huarte *et al*. 1992) as long as the transcript is not decapped or subjected to exosome-mediated decay. This reversibility of mRNA de- and readenylation is mainly described in the development of organisms as some maternal mRNAs in oocytes lack poly(A) tails which are re-added upon development (**Figure 1.1**).
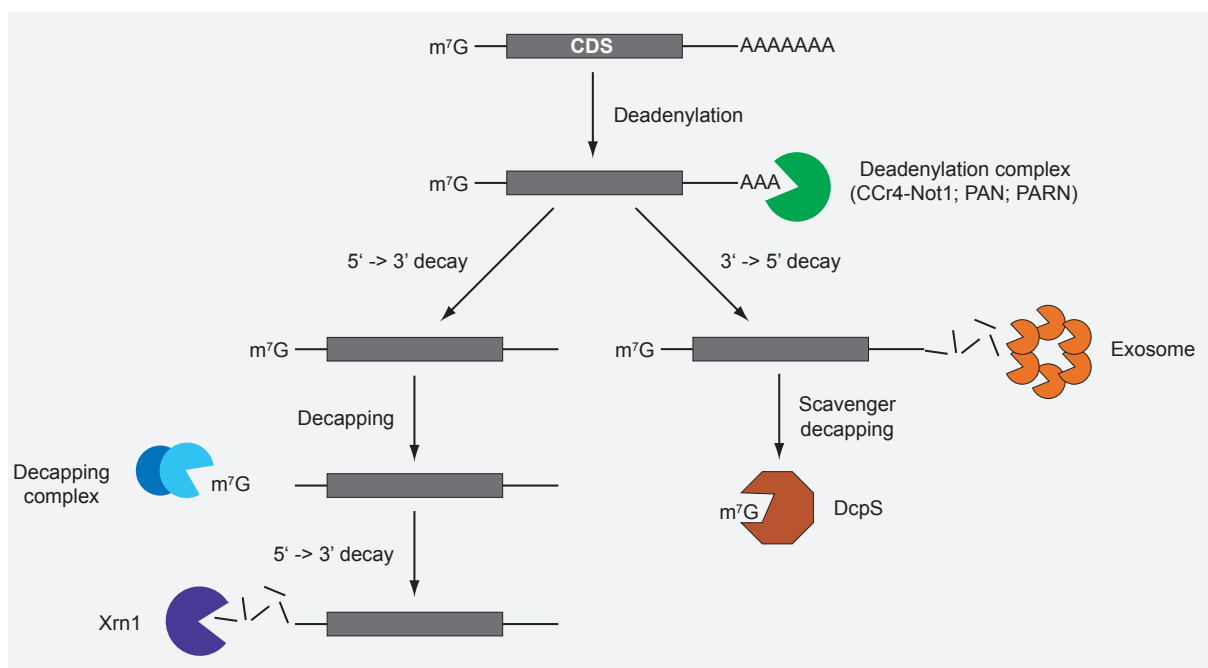
Figure 1.1: *Mechanisms of normal mRNA decay. Most mRNAs undergo decay by the deadenylation-dependent pathway.* The poly(A) tail is removed by deadenylases followed by degradation of the mRNA body by two different pathways: Either decapping followed by 5'->3' decay or 3'->5' decay by the exosome. Adapted from (Garneau *et al.* 2007).

5'-3' decay pathway

Removal of the cap structure occurs by hydrolyzation via a decapping complex releasing m^{7}GDP. Several observations suggest that this complex recognizes the substrate by interaction with the cap of the mRNA and that the decapping machinery prefers substrates larger than 25 nucleotides (Wang *et al*. 2002). Control of decapping is regulated by three inputs: the poly(A) tail inhibits decapping, the translation status of the mRNA where translation and decapping compete with each other, and the ability of the mRNA to recruit the decapping complex (Parker and Song 2004). Further decapping can be modulated either by mRNA-specific binding proteins

or by the regulation of other transacting factors. A final step in decapping is dissociation of the cap-binding complex. Decapping seems to take place in specific cytoplasmic foci, the P-bodies, where mRNA decapping factors and the 5'->3' exonucleases are concentrated (Sheth and Parker 2003). After decapping, the exposed mRNA can be degraded by the 5'->3' exonuclease Xrn1 (Muhlrad and Parker 1994) (**Figure 1.1**).

3'-5' decay pathway

The other possible decay pathway is 3'->5' degradation by the cytoplasmic exosome followed by cap hydrolyzation by DcpS (Liu *et al*. 2002). The exosome is a large protein complex that consists of 6 RNases and 3 proteins containing RNA binding domains (Shen and Kiledjian 2006). This 9-subunit core complex assembles into a ring and two of these complete rings build a barrel-like structure. In addition, there are other associated and regulatory proteins belonging to other RNase families that play a role in substrate specificity. All the ribonucleases are 3'-5' exonucleases indicating that the RNA is degraded from the 3' end (van Hoof and Parker 1999). This complex degrades mRNAs that are targeted for decay because of errors or as part of normal mRNA turnover. Several proteins that can stabilize or destabilize mRNA molecules via binding to AU-rich elements in the 3'-untranslated region (3' UTR) of mRNAs have been shown to interact with the exosome complex (Chen *et al*. 2001; Gherzi *et al*. 2004). In the nucleus it processes several small nuclear RNAs (Allmang *et al*. 1999), but most exosomal particles are present in the nucleolus where it processes 5.8S rRNA and small nucleolar RNAs. Thus substrates of the exosome can include messenger RNA, ribosomal RNA, and several species of small RNAs (**Figure 1.1**).

1.1.1.2 ARE and AUBP

Cytokine, growth factor, proto-oncogene and immediate early gene mRNAs are inherently unstable. Many of these mRNAs have regulatory elements in their 3'-untranslated region (3'-UTR). Among the most common is the AU-rich element (ARE), which is a major cis-acting element targeting mRNAs for rapid degradation (**Figure 1.2**).

The destabilizing function of AREs has been demonstrated by linking the GM-CSF 3'-UTR containing an ARE to a β-globin reporter transcript (Shaw and Kamen 1986), resulting in rapid degradation of the otherwise stable β-globin reporter. A database search indicated that up to 8% of all mRNAs might contain a functional ARE (Bakheet *et al*. 2001; Bakheet *et al*. 2003). AREs trigger rapid mRNA decay by accelerating the rate of deadenylation (Brewer and Ross 1988; Xu *et al*. 1997). In addition, it was shown that mRNA turnover could proceed through a coupled 3' to 5' exonuclease degradation–dependent decapping pathway (Wang and Kiledjian 2001).

Depending on the sequence features, AREs have been classified into three different classes (Chen and Shyu 1995) (see **Table 1.1**).
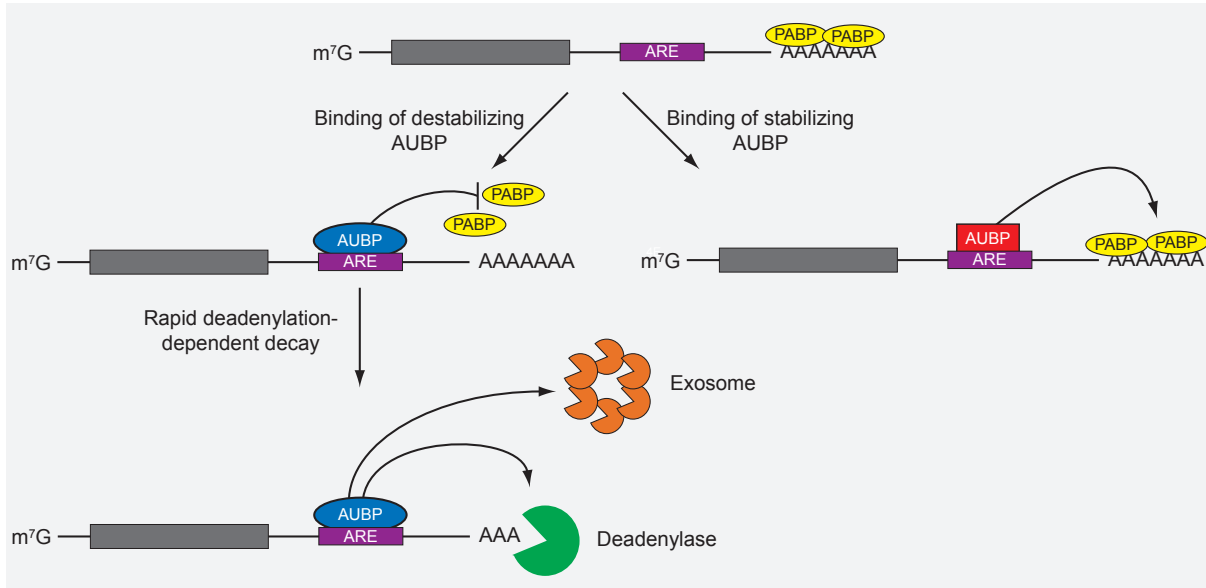
Figure 1.2: *ARE-dependent mRNA decay.* Interaction of the AU-rich element (ARE) with a destabilizing AU-binding protein (AUBP) might promote rapid deadenylation by reducing the affinity of the poly(A) binding protein (PABP) for the poly(A) tail. Conversely, stabilizing factors might enhance binding of the PABP to the poly(A) tail, thus blocking deadenylation. Adapted from (Gao *et al.* 2001).

ARE	Example	Sequence features
AUUUA-containing		
class I	c-fos	1-3 copies of scattered AUUUA motifs coupled with a nearby U-rich region or U stretch
class II	GM-CSF	At least two overlapping copies of the nonamer UUAUUUA(U/A)(U/A) in a U-rich region
Non-AUUUA	c-jun	U-rich region and other features

Table 1.1: *ARE classification* (Chen and Shyu 1995).

Recently, novel unrelated destabilizing elements have been identified in the 3'UTR of the TNFα mRNA – the constitutive decay element (CDE) (Stoecklin *et al.* 2003a), and UG-rich sequences bound by CUG-binding proteins (Moraes *et al.* 2006) - that are thought to fine-tune ARE-dependent decay.

Several AU-binding proteins (AUBPs) have been identified that specifically bind to the ARE (Mitchell and Tollervey 2000; Chen *et al.* 2001) to play an effector role in executing ARE-dependent mRNA decay.

Zfp36 family

TTP (tristetraproline, Zfp36 (Zinc finger protein 36), Tis11) was the first AU-binding protein described that contains a CCCH zinc finger motif (DuBois *et al*. 1990; Lai *et al*. 1990). In addition, BRF1 (butyrate response factor 1, Zfp36L1 (Zinc finger protein 36-like 1), Tis11b), BRF2 (butyrate response factor 2, Zfp36L2 (Zinc finger protein 36-like 2), Tis11d) and, recently, Zfp36L3 (Zinc finger protein 36-like 3) have been identified to belong to this protein family. All Zfp36 family members contain an internal repeat – YKTELC – and a repeated cysteine-histidine motif, $CX_8CX_5CX_3H$ (Varnum *et al*. 1991), which is a zinc finger motif (Hudson *et al*. 2004). The two tandem repeats separated by 13 amino acids of Zfp36 proteins have been shown to coordinate with Zn^{2+}.

Initially, the role of TTP was proposed to be a zinc finger transcription factor (Taylor and Blackshear 1995). TTP-deficient mice were then generated to investigate the physiological role of TTP (Taylor *et al*. 1996). These knockout mice appeared normal at birth but within 1-8 weeks after birth, they developed a complex syndrome of inflammatory arthritis, dermatitis, antinuclear antibodies and other symptoms. All of these aspects could be prevented by injecting the mice with monoclonal antibodies capable of neutralizing tumor necrosis factor α (TNF-α). These studies identified TTP as a modulator of TNF-α production, turnover or action *in vivo*. In further studies, TTP (Carballo *et al*. 1998; Stoecklin *et al*. 2000), BRF1 (Stoecklin *et al*. 2002) and BRF2 (Lai *et al*. 2000; Ciais *et al*. 2004) have been shown to bind ARE-containing mRNAs and target them for rapid decay by stimulation of deadenylation. Mutation of the zinc finger abolishes ARE-binding and the destabilizing activity of BRF1, BRF2 and TTP.

Knockout of Brf1 leads to embryonic lethality around embryonic day 11 (Stumpo *et al*. 2004), whereas knockout of Brf2 leads to female infertility (Ramos *et al*. 2004). Only the Brf1 knockout from the ZFP36 family showed an effect on the developing embryo whereas knockouts of either TTP or Brf2 had postnatal implications. Also observations in our and other laboratories showed that Brf1 expression changes upon differentiation of ES cells and seems to be under control of Lif/Stat3 (Sekkai *et al*. 2005; Hailesellasse Sene *et al*. 2007).

Brf1 (Zfp36L1)

Brf1 is predominantly a cytoplasmic protein and contains a nuclear export signal (NES) in its C-terminus. Nucleo-cytoplasmic shuttling of Brf1 relies on the nuclear export receptor CRM1 (Phillips *et al*. 2002). An early result showed suppression of Brf1 expression by butyrate leading to the name butyrate response factor (Maclean *et al*. 1998). In various cells or tissues ACTH (Chinn *et al*. 2002), insulin or insulin-like growth factor 1 (IGF-1) (Corps and Brown 1995) induces Brf1 expression and insulin stimulation is unique for Brf1, as it does not occur for TTP or Brf2.

Activity and stability of Brf1 is dependent on the phosphorylation at serine 92 and 203 by Akt or other kinases (Schmidlin *et al.* 2004; Benjamin *et al.* 2006), in an analogous manner to MK2 phosphorylation of TTP (Stoecklin *et al.* 2004). Phosphorylated Brf1 requires binding to 14-3-3 which stabilizes and inactivates it as isolated phospho-Brf1 is still capable of ARE binding and interaction with decay enzymes. Active Brf1 binds to ARE containing transcripts and confers rapid decay of these mRNAs by enhancing deadenylation and directly targeting them to decay enzymes (Lykke-Andersen and Wagner 2005).

Other AUBPs

Another known AUBP is the KH-type splicing regulatory protein (KSRP) that was identified as a splicing factor binding to the intronic enhancer element to induce assembly of other proteins onto the splicing enhancer (Min *et al.* 1997). KSRP activity has been found in the nucleus and the cytoplasm, it may interact with RNA molecules and participate in transcription, RNA processing, transport or catabolism (Min *et al.* 1997). KSRP has been shown to bind to ARE mRNAs and recruit the exosome for 3'-5' mRNA degradation (Gherzi *et al.* 2004).

AUF1, also known as heterogeneous nuclear ribonucleoprotein D (hnRNP D), also controls the stability of ARE-containing mRNAs (Brewer 1991; Loflin *et al.* 1999). Certain isoforms of hnRNP D can either stabilize or destabilize ARE mRNAs (Xu *et al.* 2001; Raineri *et al.* 2004), depending on the cell type investigated (Gouble *et al.* 2002). Recent data suggest that AUF1 may have additional functions besides regulating ARE-mRNA turnover, such as the ability to bind DNA (Dempsey *et al.* 1998), modulation of telomerase activity (Eversole and Maizels 2000), and linking the ubiquitin/proteasome pathway and translation to mRNA turnover (Laroia *et al.* 1999).

Nevertheless there are also AUBPS that act as stabilizers of ARE-containing mRNAs. HuR, an ubiquitously expressed member of the ELAV (embryonic lethal, abnormal vision) family, is an AUBP that binds with high affinity to the ARE (Blaxall *et al.* 2002) and prevents decay of ARE-mRNAs (Fan and Steitz 1998). HuR appears to protect the body of the mRNA from degradation, rather than slowing down the rate of deadenylation (Peng *et al.* 1998).

AU-binding proteins and cancer

There are reports indicating that levels of AU-binding proteins can be correlated with diverse cancers. Following are some examples: Brf1 is highly expressed in t(8;21) (AML-MTG8 fusion) leukemic cells and overexpression of Brf1 induces myeloid cell proliferation in response to G-CSF (Shimada *et al.* 2000). Brf1 has also been shown to be upregulated in hepatocellular

carcinomas compared to the adjacent tissues (Zindy *et al*. 2006). Additionally, two recent reports show that there is a breakpoint in Brf1 exon 1 in B-cell lymphomas (communicated by Prof. Siebert, Kiel; (Pospisilova *et al*. 2007)).

Overexpression of TTP suppresses tumor growth in an IL-3 dependent mast cell mouse model (Stoecklin *et al*. 2003b), but overexpression of AUF1 (p37) leads to tumorigenesis in transgenic mice with high cyclin D1 levels in the tumors (Gouble *et al*. 2002). Not only destabilizers but also a stabilizing AUBP such as HuR can be implicated in cancer as HuR is highly expressed in malignant brain tumors (Dixon *et al*. 2001) and cytoplasmic localization of HuR is associated with increased Cox-2 expression and high tumor stage in colon cancer (Mrena *et al*. 2005; Denkert *et al*. 2006).

1.1.2 Further posttranscriptional mechanisms, quality control

There are many mechanisms that recognize aberrant mRNA and subsequently leads to its degradation as a quality control of mRNA biogenesis. One of these mechanisms is nonsense-mediated decay (NMD), which recognizes and degrades transcripts containing a premature stop-codon. These mRNAs have to be destroyed before they can produce truncated proteins with potentially abnormal function. The NMD pathway has been found in all eukaryotes and the core-proteins are highly conserved. In mammals the exon-exon junctions are marked by a complex called the exon junction complex (EJC). This complex is placed about 20-24 nucleotides upstream of the junction upon splicing. The exon junction complex is normally displaced upon translation by the ribosome. If there is a premature stop codon, not all EJC are displaced and the mRNA is subjected to rapid, deadenylation-independent decapping (Muhlrad and Parker 1994).

mRNAs without a termination codon undergo Nonstop mRNA decay (NSD). This decay can arise due to polyadenylation occurring prematurely in the coding region, abortion of transcription or upon incomplete 3'-5' decay of ribosome-associated mRNAs. Such transcripts are normally decayed by the 3'-5' exosomal pathway.

A third mRNA quality control mechanism is No-go decay (NGD). This pathway is used when mRNA translation elongation stalls resulting in endonucleolytic cleavage near the site of ribosome stalling. These stalls can be caused by defective ribosomes or by physically altered mRNAs that cause a complete block of translation. This mechanism is thought to have evolved to purge the cell of mRNAs and their associated ribosomes that are stuck in the process of elongation.

1.2 Stem Cells

Stem cells are an ideal system to study developmental processes at the molecular level, especially embryonic stem (ES) cells as they can be genetically modified and differentiated into various cells of the different germ layers. From our perspective, it is also a very interesting system to investigate, as there is nothing described in the literature about posttranscriptional control mechanisms in ES cells, which opens a new opportunity for us to study ARE-dependent developmental mechanisms in a novel cell system.

1.2.1 General Introduction

Stem cells are primal cells found in all multicellular organisms. These cells can originate from an embryo, fetus or adult and have the capability to renew themselves for indefinite periods and to give rise to specialized mature cells. There are different definitions of stem cells: totipotent, pluripotent, multipotent and unipotent stem cells (**Figure 1.3**). For example, a fertilized egg is said to be totipotent, because it can generate all the cells and tissues necessary to make an embryo and to support its development *in utero*.

Pluripotent stem cells have the ability to produce cells from the three germ layers (endo-, ecto-, mesoderm) from which all the cells of the body arise. These cells can give rise to more than 200 different cell types. The first reported type of pluripotent stem cell was identified in the 1960s from analysis of a type of cancer called a teratocarcinoma (Stevens 1960; Kleinsmith and Pierce 1964). Researchers noted that a single cell from this cancer could be isolated and remain undifferentiated in culture. Introduced into a blastocyst, these cells participated in normal embryonic development and gave rise to normal tissue (Brinster 1974; Mintz and Illmensee 1975; Papaioannou *et al.* 1975). This type of stem cells became known as embryonic
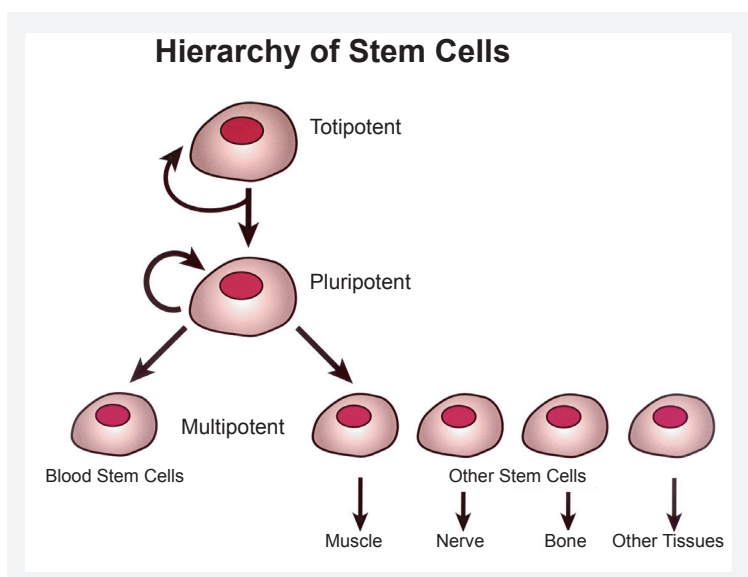

Figure 1.3: *Hierarchy of stem cells.* A totipotent stem cell can give rise to all tissues including extra-embryonic layers whereas pluripotent stem cells can only produce the tissues that arise from the three germ layers. Multipotent stem cells (e.g. hematopoietic stem cells) are stem cells in differentiated tissue and can regenerate this tissue.

carcinoma cells (EC cells) (**Figure 1.4**). Beginning in the 1980s, the first mouse embryonic stem (ES) cells were grown in the laboratory (Evans and Kaufman 1981; Martin 1981). They are derived from the inner cell mass of the blastocyst before implantation into the uterine wall (**Figure 1.4**). The third type of pluripotent stem cell is the embryonic germ cell (EG cells). Researchers also discovered that primordial germ cells of the gonadal ridges of a 5-10 week old fetus could be cultured and stimulated to produce many different cell types (Matsui *et al*. 1992; Resnick *et al*. 1992) (**Figure 1.4**). Because these cells cannot produce all of the extra-embryonic tissue required for mammalian development, they are not considered totipotent.
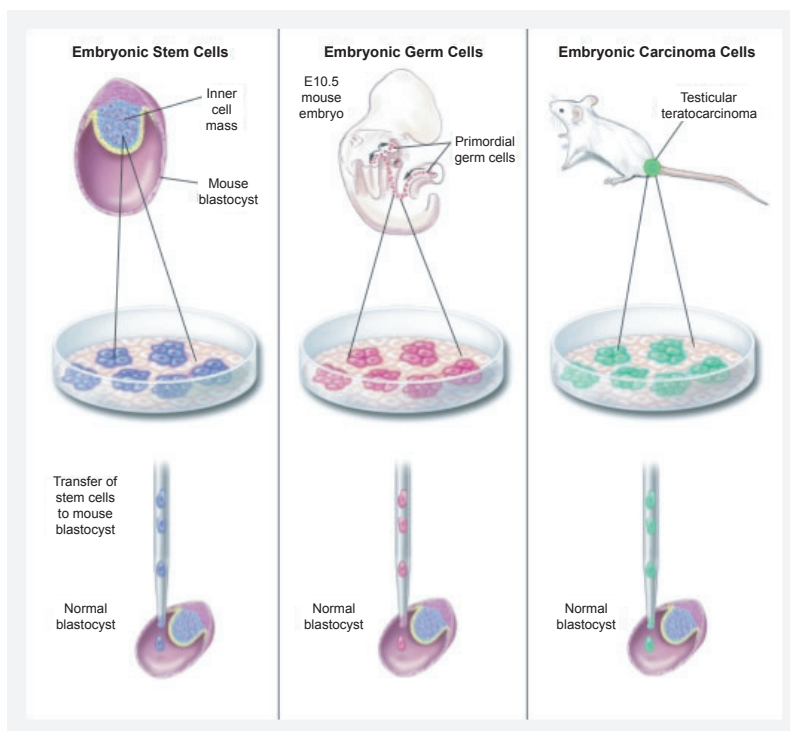
Adult stem cells are believed to be multipotent. They are undifferentiated cells present in differentiated tissue, renew themselves for the lifetime of the organism and become specialized cells of the tissue from which they originate. Usually, they generate progenitor or precursor cells (unipotent stem cells), which then differentiate into mature cells with specialized function and distinct morphology. Adult stem cells are found in blood, bone marrow, brain, skeletal muscle etc. To date there are no isolated adult stem cells that are capable of building

Figure 1.4: *Origins of mouse pluripotent stem cells.* There are three different types of pluripotent stem cells: Embryonic stem cells, embryonic germ cells and embryonic carcinoma cells (©2001 Terese Winslow).

all cells of the body, but experiments have demonstrated that they can transdifferentiate from one type of cell or tissue into another (Tosh and Slack 2002).

1.2.2 Embryonic stem cells

As mentioned, embryonic stem cells are defined by their origin from one of the earliest stages (3.5 dpc) of embryonic development, from the inner cell mass of a pre-implantation blastocyst. At this stage the embryo is made up of around 150 cells and consists of a sphere composed of an outer layer of cells (trophoectoderm), a fluid-filled cavity (blastocoel) and a cluster of cells on the interior (inner cell mass) (**Figure 1.5**).
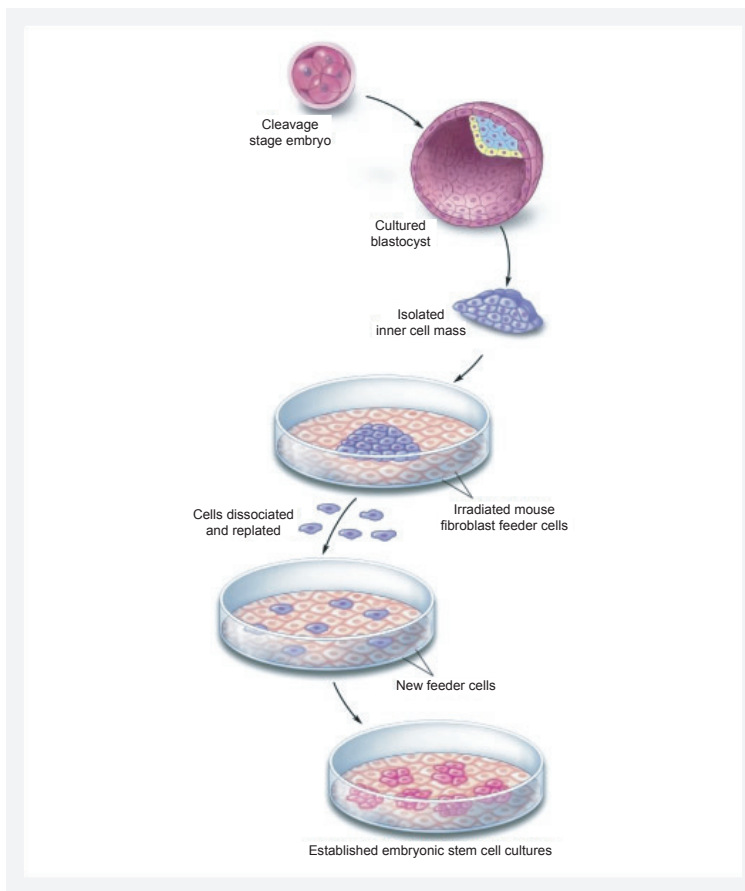
Figure 1.5: *Generating embryonic stem cell cultures.* Embryonic stem cells are derived from the inner cell mass of a blastocyst. They can be cultured on growth inhibited – either mitomycin C treated or irradiated - embryonic feeder cells. There are also ES cell lines that are independent of feeder cells (©2001 Terese Winslow).

Embryonic stem cells are capable of undergoing an unlimited number of symmetrical cell divisions without differentiating (self-renewal) and have a stable diploid normal karyotype. ES cells can differentiate into every cell type of all three germ layers of the embryo (pluripotency), but do not generate trophoblast tissue *in vivo* (**Table 1.2, Figure 1.6**). They are capable of integrating into all fetal tissues during development and of colonizing the germ line and give rise to egg or sperm cells, which allows ES cells to be used as vehicles for introducing genetic modifications into mice (Bradley *et al*. 1992). ES cells can also undergo multi-lineage differentiation *in vitro* and can be guided into well-differentiated cells (Doetschman *et al*. 1985; Keller 1995).

Undifferentiated ES cells express several transcription factors (Oct4, Nanog, Sox2, etc.) that maintain them in a continuous proliferative and non-differentiating state. ES cells lack the G1 checkpoint and spend most of their time in S phase of the cell cycle. They also do not need any external stimulus to initiate DNA replication.

The ability of ES cells to generate a complete embryo depends on the number of passages *in vitro*, but optimized culture conditions allows ES cells to retain the ability to colonize the germ line (Wolf *et al*. 1994).

Until now, long-term cultures of self-renewing ES cells have only been established for 3 mammalian species: mice, monkeys and humans.

Embryonic germ layer	Differentiated tissue
Ectoderm	Skin
	Neural tissue
	Adrenal medulla
	Pituitary gland
	Connective tissue of the head and face
	Eyes
	Ears
Endoderm	Thymus
	Thyroid, parathyroid glands
	Larynx, trachea, lung
	Urinary bladder, vagina, urethra
	Gastrointestinal organs (liver, pancreas)
	Lining of the GI tract
	Lining of the respiratory tract
Mesoderm	Bone marrow
	Adrenal cortex
	Lymphatic tissue
	Skeletal, smooth and cardiac muscle
	Connective tissues incl. bone, cartilage
	Urogenital system
	Vascular system

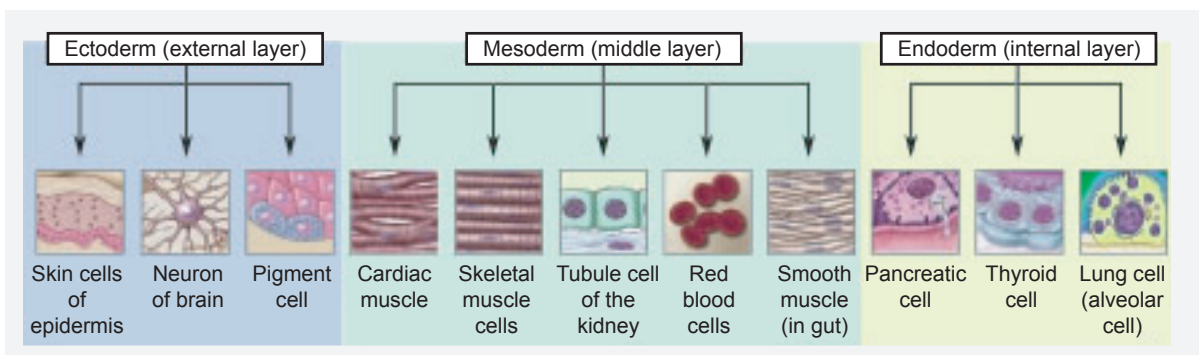**Table 1.2:** *Embryonic germ layers from which differentiated tissues develop*

Figure 1.6: *Differentiation into tissues.* Pluripotent ES cells can differentiate in cells from all three germ layers and can therefore give rise to a complete organism (©2001 Terese Winslow).

1.2.3 Regulatory mechanisms in murine ES cells

Recent experiments revealed a complex transcriptional regulatory circuit responsible for ES cell self-renewal and differentiation. Implicated in this mechanism are several signaling pathways and transcription factors like Oct4, Sox2, Nanog and others.

1.2.3.1 Signaling Pathways

LIF-Stat3

ES cells need several factors for *in vitro* cultivation in order to remain undifferentiated. These factors are normally provided by serum and feeder cells. One of the most important factors provided by feeder cells that allow murine embryonic stem cells to stay in an undifferentiated state is leukemia inhibitory factor (LIF), a cytokine from the interleukin-6 (IL-6) family (Smith *et al*. 1988). In the absence of serum, LIF alone is not sufficient to keep the cells in a pluripotent, undifferentiated condition. LIF interacts with the LIF receptor that works as a heterodimer together with the signal transducer glycoprotein 130 (gp130). This trimeric complex leads to the activation of janus kinases (Jaks) and concomitant phosphorylation of the cytoplasmic domain of gp130 (Niwa *et al*. 1998). These phospho-sites then serve as binding sites of src-homology 2 (SH2) -domain containing proteins that are then also phosphorylated by Jaks. The signal transducer and activator of transcription 3 (Stat3) protein binds to these phospho-sites, is phosphorylated by Jak2, dimerizes upon phosphorylation and translocates to the nucleus to act as a transcription factor. This cascade is sufficient to keep the ES cells pluripotent in the presence of serum. Although the essential function of this pathway is known, the targets of Stat3 still remain elusive. Recently, c-myc was identified as a key-target of LIF-Stat3 (Cartwright *et al*. 2005). Overexpression of c-myc is enough to render the self-renewal of ES cells independent of LIF (**Figure 1.7**).

However, this pathway also interacts with other pathways activated by receptor-tyrosine kinases (RTK), G-protein coupled receptors, transforming growth factor β (TGFβ) receptors and Wnt receptors.

MAPK-ERK

Another pathway that is also, but not exclusively, induced by LIF is the mitogen-activated protein kinase (MAPK) pathway (Boeuf *et al*. 1997) that phosphorylates the extracellular signal-regulated protein kinases (ERK1 and 2) (Burdon *et al*. 1999). Murine ES cells show high ERK activity upon differentiation and overexpression of a constitutively activated

member of this pathway leads to expression of mesodermal markers (LaBonne *et al*. 1995). ERK activation may not be exclusively downstream of LIF, and may also be downstream of the phosphatidylinositol-3 phosphate kinase (PI3K) (**Figure 1.7**).

PI3K-Akt

The PI3K pathway also appears to be partly under the control of LIF, but it can also be activated by BMP4 or insulin (Paling *et al*. 2004). This pathway is normally activated by multiple signals in ES cells. The activation of the PI3K pathway promotes ES cell proliferation and might also play a role in self-renewal (Takahashi *et al*. 2003; Takahashi *et al*. 2005). The PI3K-dependent proliferation of ES cells can be directly linked to its recently identified activator ERas, a member of the Ras family. ERas expression is only found in undifferentiated ES cells. ERas null cells are normal but proliferate slower (Takahashi *et al*. 2003). Inhibition of PI3K or its downstream target Akt leads to differentiation of murine ES cells even in the presence of LIF or feeders. Akt can promote a G1 to S phase transition that leads to a shorter G1 phase that contributes to the undifferentiated state of ES cells and cell cycle control may be the key role of Akt in ES cell self-renewal. This pathway can maintain pluripotency independent of Wnt/β-catenin signaling (Watanabe *et al*. 2006) (**Figure 1.7**).

Wnt-GSK3β

The canonical Wnt signaling in ES cells is endogenously activated and is downregulated upon differentiation (Sato *et al*. 2004). Activation of the pathway leads to inhibition of GSK3β, followed by nuclear accumulation of β-catenin and the expression of target genes. Activation of the pathway, for example by chemically inhibiting GSK3β, leads to maintenance of an undifferentiated phenotype and maintains expression of the pluripotent-state specific transcription factors Oct4, Rex1 and Nanog even in the absence of LIF (Sato *et al*. 2004). This pathway also upregulates Stat3 expression, suggesting a synergism with LIF-Stat3 (Hao *et al*. 2006). Another target of this pathway is p53 (Watcharasit *et al*. 2002; Qu *et al*. 2004), a transcription factor that regulates the cell cycle and suppresses Nanog expression and therefore promotes differentiation (Lin *et al*. 2005). Furthermore p53 may trigger apoptosis in ES cells to eliminate cells with DNA damage (Fluckiger *et al*. 2006). PI3K and Akt negatively regulate GSK3β (Hay and Sonenberg 2004) and may therefore contribute to self-renewal of ES cells through GSK3β, p53 and Nanog (Takahashi *et al*. 2003) (**Figure 1.7**).

TGFβ-BMP4

The TGFβ family has more than 40 members including TGFβ, Activin, Nodal and bone morphogenic proteins (BMPs). BMP4 seems to be the most important member, as it can - together with LIF in serum free medium - maintain ES cell pluripotency (Ying *et al.* 2003), possibly by blocking the MAPK signaling pathway (Qi *et al.* 2004). BMP4 is regarded as a key anti-neurogenic factor in the embryo. In the presence of LIF, BMP4 activates expression of the transcription factor similar to mothers of decapentaplegic homologue-4 (Smad4). This results in the expression of inhibitor of differentiation (Id) proteins, which inhibit neural differentiation by blocking neurogenic basic Helix-Loop-Helix (bHLH) transcription factors. Id expression can also be maintained by Nanog (Ying *et al.* 2003). In the absence of LIF,
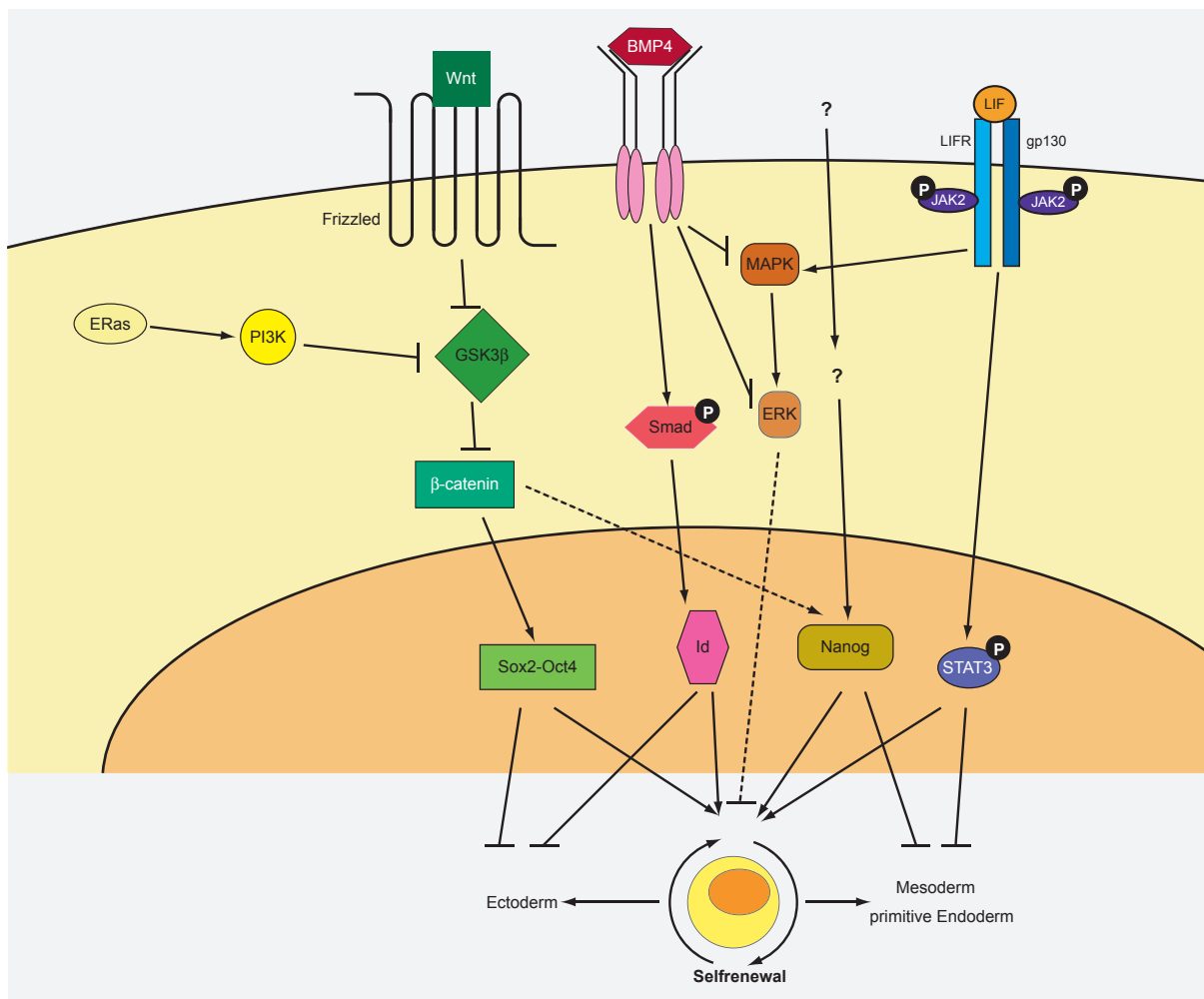
Figure 1.7: *Combinatorial signaling pathways involved in maintaining mouse ES cell pluripotency.* Cell surface receptors initiate signals that are transmitted to the nucleus and affect key pluripotency factors such as Oct4 and Nanog, and self-renewal factors such as STAT3. In the nucleus these proteins cause changes in the gene expression that result in or counteract phenotypic characteristics of embryonic stem cells. Adapted from (Boiani and Scholer 2005).

BMP4 phosphorylates different Smads (Smad1, 5 and 8) that have an inhibitory effect on Id expression. Although the TGFβ superfamily is relatively well studied, its role in ES cell self-renewal is not well understood (**Figure 1.7**).

1.2.3.2 Transcription factors

Oct4-Sox2

Oct4 (also Oct3, Oct3/4, Pou5f1) is a POU-domain containing transcription factor that binds to an octamer sequence. It is highly expressed in ES cells and decreases when these cells lose pluripotency and differentiate.

Loss of Oct4 leads to differentiation of ES cells into trophoectoderm, whereas overexpression causes differentiation into primitive endoderm and mesoderm (Yeom *et al*. 1996; Niwa 2001). Oct4 protein levels have to be maintained within a narrow window to maintain ES cells in a pluripotent state. Targets of Oct4 are Fgf4, Rex1, and Sox2. If Oct4 levels sink below the steady state, it maintains the activity of Nanog by direct binding to its promoter. If the levels rise above the steady state, Oct4 represses Nanog.

Sox2 belongs to the high mobility group (HMG)-protein family. Sox2 co-occupies many targets with Oct4 and is also required for pluripotency maintenance. When Sox2 is inactivated, formation of primitive ectoderm is defective (Avilion *et al*. 2003).

As LIF does not affect Oct4 and Oct4 does not regulate Jak-Stat signaling, Oct4 has to be regulated by, or be in itself a parallel pathway for ES cell self-renewal. However, little is known about upstream regulation of Oct4 except that Nanog or FoxD3 can also activate Oct4 expression (Pan *et al*. 2006). A combinatorial code that requires Oct4 and Sox2 specifies the first three cell lineages that emerge soon after implantation.

Nanog

Nanog is another homeobox-containing transcription factor playing an essential role in keeping the inner cell mass and ES cells pluripotent. Overexpression of Nanog renders ES cells independent of LIF, whereas the self-renewal capability of the cells is reduced (Chambers *et al*. 2003; Mitsui *et al*. 2003). The effect of Nanog overexpression is independent of Stat3 and of BMP4. Downregulation of Nanog leads to differentiation of ES cells into the endodermal lineage. It appears that Nanog also directly activates genes involved in self-renewal, such as Rex1, that are also targets of Oct4/Sox2, and it is possible that it is at the intersection of Nanog and Oct4/Sox2 (Shi *et al*. 2006). It has been proposed that Nanog mainly regulates pluripotency by repressing downstream genes that are important for differentiation (Chambers *et al*. 2003; Mitsui *et al*. 2003).

It would appear that these three transcription factors (Stat3, Oct4, Nanog) are key regulators that block differentiation and maintain ES cells in a pluripotent state (Boyer *et al.* 2005; Ivanova *et al.* 2006; Loh *et al.* 2006; Rao and Orkin 2006). Recently, further studies have shown that forcing the expression of ES-cell specific factors (Oct4, Sox2, c-myc, Klf4) in somatic cells can reprogram them to a pluripotent stem cell-like state (Takahashi and Yamanaka 2006; Wernig *et al.* 2007) where patterns of DNA methylation, gene expression and chromatin revert to that of an ES cells-like state.

1.2.3.3 Cell cycle and other features

Proliferation of differentiated mammalian cells is controlled primarily by the regulation of the progression through G1 into S phase (Burdon *et al.* 2002). ES cells have a reduced cell cycle due to a short G1 phase compared to somatic cells; this may contribute to the self-renewal. This effect could be due to the lack of cyclin-dependent kinase (CDK) 4-associated kinase activity that characterizes somatic cells as the ES cell cycle is not dependent on cyclinD: Cdk4 (Burdon *et al.* 2002). In ES cells, G1/S transition is instead dependent on cyclin E:Cdk2 and cyclin A:Cdk2 complexes, as this activity seems to be constitutive active in these cells (Savatier *et al.* 1996), suggesting that the cycle is constitutively primed for DNA replication (Stead *et al.* 2002). This pathway can be stimulated by c-myc as it is a transcription factor of cyclin E (Bartek and Lukas 2001), which links cell cycle progression to the LIF-Stat3 pathway (Hirano *et al.* 2000).

Another feature of ES cells are the high levels of telomerase activity (Thomson *et al.* 1998), which is also needed for prolonged self-renewal (Kim *et al.* 1994; Thomson *et al.* 1998). During differentiation the enzyme, and concomitantly its activity is downregulated (Qi *et al.* 2004).

Recently, it was reported that microRNAs (miRNAs) might also play a role in ES cell self-renewal as there are specific sets of miRNA expressed in ES but not in differentiated cells (Houbaviy *et al.* 2003). In addition, Dicer I null mouse ES cells fail to differentiate into all three germ layers as they are unable to produce mature miRNAs (Cheng *et al.* 2005; Kanellopoulou *et al.* 2005).

1.3 RNA Interference (RNAi)

The discovery of RNA interference has provided a useful tool to dissect gene function in cells without the need for generating gene knockouts. Recent advances have made it possible to stably introduce constructs to confer long term RNA interference for downregulation of transcripts and the concomitant loss of the protein over long time periods. Such a system is useful in ES cell research as the effect of the decrease of a gene product can be studied over the course of differentiation.

1.3.1 Discovery

RNA interference (RNAi) is defined as specific mRNA degradation by a 21 nucleotides long, double-stranded RNA molecule (small interfering RNA, siRNA) homologous to the targeted transcript. Fire and Mello were the first to describe that injection of dsRNA into the nematode *C.elegans* induced gene silencing in a gene-specific manner, a discovery rewarded with the 2006 Nobel Prize in Physiology or Medicine. Some of the resulting animals exhibited the same phenotypes as null mutants (Fire *et al*. 1998). The ability of dsRNA to induce gene silencing represents an ancient function of eukaryotic cells thought to be a defense mechanism against inverted repeats, viruses or viroids. Recently, a new category of small regulatory RNAs, called microRNAs (miRNA), was discovered (Lagos-Quintana *et al*. 2001; Lau *et al*. 2001; Lee and Ambros 2001). These RNAs are small non-protein coding genes found in many eukaryotic organisms. miRNAs are processed by the RNAi machinery, and some have been shown to regulate the expression of target-gene transcripts.

1.3.2 Mechanism of RNAi

Recently, a model for the mechanism of RNAi has been proposed. RNAi is initiated by the ATP-dependent, processive cleavage of long dsRNA or miRNAs into 21-25 nucleotide (nt) long, double-stranded fragments by the enzyme Dicer (Elbashir *et al*. 2001a; Hutvagner and Zamore 2002). These small interfering RNA (siRNA) duplexes or mature miRNAs are then incorporated into a multi-protein complex. At this point, ATP-dependent unwinding of the siRNA duplex generates an active RNA-induced silencing complex (RISC) that recognizes the target RNA complementary to the antisense strand of the siRNA or mature miRNA. Upon recognition, the mRNA is either cleaved or it comes under translational suppression (**Figure 1.8**).

Dicer is a member of the RNAse III family of dsRNA-specific endonucleases and generates RNA duplexes containing two single-stranded nucleotide overhangs at each 3' end (Elbashir *et al*. 2001b). These features are important for the entry of siRNAs or miRNAs into the RNAi pathway. RNAi can be mediated *in vitro* by synthetic siRNAs or expression of short hairpin RNAs (shRNAs) (Nykanen *et al*. 2001; Elbashir *et al*. 2001b; Brummelkamp *et al*. 2002). shRNAs are, like miRNAs, processed by Dicer to 21nt siRNAs.

The use of siRNA to downregulate a gene of interest is advantageous compared to the employment of longer dsRNA molecules (>30 nt). Transfecting mammalian cells with long dsRNAs induces an interferon response and consequently non-specific gene activation and downregulation and is often followed by cell death. By contrast, shorter siRNAs do not trigger

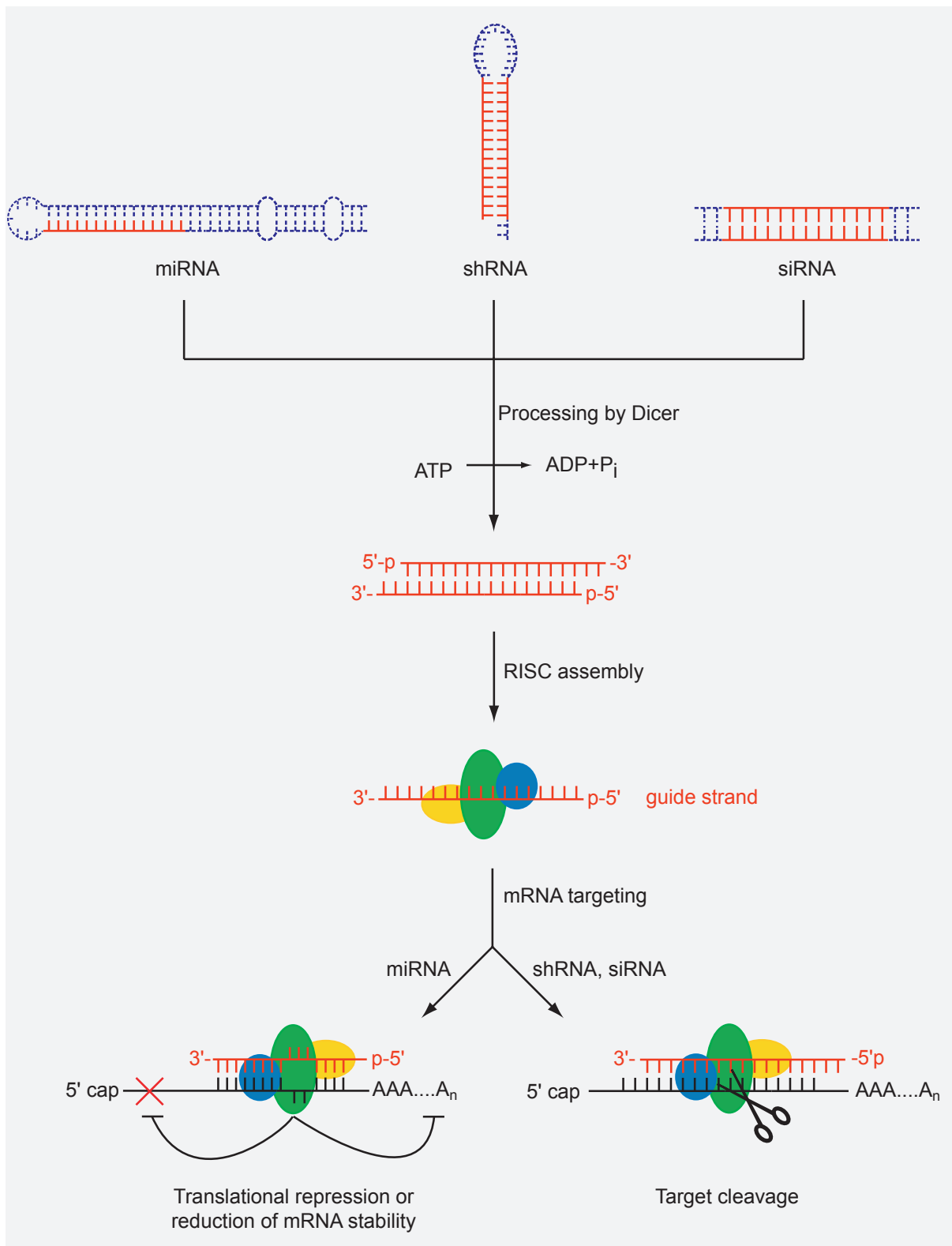**Figure 1.8:** *Mechanism of RNA interference.* dsRNA is processed by Dicer to form small active RNAs. These dsRNA intermediates are unwound and the guide strand is then incorporated into RISC, which can promote mRNA targeting resulting in either cleavage of the target transcript or translational repression or more rapid decay by accelerating deadenylation. Adapted from (Scherr and Eder 2007).

an interferon response and allow the specific downregulation of a given gene providing a method to study the "knock-out" phenotype of a protein without prior deletion of the gene by homologous recombination.

1.4 Project

In recent years, one of the main areas of interest in our laboratory has been ARE-dependent mRNA decay which is emerging as an important mechanism for posttranscriptional control of gene expression. In particular, the AU-binding protein Brf1 (Zfp36l1) was of special interest as it was shown by us to bind to ARE-mRNAs to confer rapid decay of such transcripts (Stoecklin *et al*. 2002). To investigate the role and regulation of Brf1, we have established several reporter RNA systems in human and murine cells (Stoecklin *et al*. 2002; Raineri *et al*. 2004; Schmidlin *et al*. 2004), which elucidated that Brf1 is controlled by PKB and that it counterbalances the action of the known ARE stabilizer HuR. Despite the progress made in understanding the function and regulation of Brf1, we have yet to identify a native target transcript that is regulated by it *in vivo* and a corresponding physiological role. While the number of potentially ARE-regulated transcripts is substantial (Bakheet *et al*. 2001), around 8% of all genes, only a handful of AUBPs have been identified, suggesting that each AUBP may be a master regulator responsible for many target transcripts (Keene and Lager 2005).

Dysfunctional ARE-mRNA decay has been linked to human diseases – for example altered stability of cytokine mRNA is implicated in autoimmune disorders, and transcripts for growth-factor and cell-cycle regulators are aberrantly stabilized in some cancers (Seko *et al*. 2006; Benjamin and Moroni 2007), all of which increased our interest in identifying a physiological role for Brf1. Although the knockout of Brf1 is uninformative due to embryonic lethality at E12.5 (Stumpo *et al*. 2004), it nevertheless shows the importance of Brf1 in development. As a consequence, we chose mouse embryonic stem cells as our experimental system. The advantages of ES cells is that they can be genetically manipulated to generate stable cell lines, which can be differentiated *in vitro* into different cell lineages to investigate the role of Brf1 in these mechanisms. The requirements for maintenance of pluripotency, as contrasted to the onset of differentiation, is believed to be a result of the concerted action of many genes. The coordinated changes in expression of many genes that can be observed in ES cells during initial differentiation or during the process of embryoid body formation or differentiation into various cell lineages offers a wide scope for hopefully identifying any BRF1 mediated effects. Furthermore they also offer the possibility of generating mice from these cells, which may help to identify a physiological role for Brf1. An additional reason is that to date nothing is known about the role of the mRNA turnover machinery in ES cells, despite the importance of posttranscriptional mechanisms such as ARE-dependent decay in controlling transcript levels

in mature cells. Therefore, it may very well play a role in ES cells and demonstration of this will open a new vista on stem cell research.

Early observations showed that Brf1 is indeed expressed in ES cells and that its levels decrease upon LIF removal and concomitant differentiation, encouraging us to further investigate the role of Brf1 in ES cells with the hope of identifying putative *in vivo* targets and their involvement in pluripotency and differentiation.

To establish the ES cell experimental system, we decided to use feeder-free CCE ES cells (Robertson *et al.* 1986) that are claimed to be able to form chimeras and to go germ-line for generation of transgenic animals. We wanted to establish a tetracycline-regulated system where we can inducibly downregulate Brf1 by production of endogenous shRNAs and to observe any biological consequences of Brf1 downregulation, either on ES cell pluripotency or differentiation into other cell types. To accomplish this goal, we had to first establish a cell line containing a defined locus in which the stemloop can be introduced by recombination, together with stable high expression of the Tet repressor protein for inducibility of stemloop expression. The system was validated by Tet-inducible Stat3 shRNA expression, as disruption of the LIF-Stat3 pathway is well documented to lead to the onset of differentiation. Once validated, the system can then be used as a platform for stable Brf1 shRNA induction in order to investigate the effects of Brf1 downregulation on ES cells and consequent differentiation into other lineages. A second major point that can be addressed was to identify *in vivo* Brf1 target mRNAs by DNA microarray analysis of cells undergoing BRF1 downregulation.

The main findings of this project have been published in Stem Cells (Wegmuller *et al.* 2007), and a copy of the paper is attached on page 84 and forms an integral part of this thesis. In the following section, reference will be made to figures published in the Stem Cells paper including supplementary data.

2. RESULTS

2.1 An inducible shRNA system in CCE ES cells

2.1.1 Possible Lif-Stat3 control of BRF1 expression

The initial experiments with ES cell lines were performed prior to this thesis by Dr. I. Raineri and B. Gross. Early observations were promising and showed in two different ES cell lines (**Figure 2.1A**) that Brf1 is present in pluripotent, undifferentiated ES cells but its levels decline transiently concomitant with the onset of differentiation by LIF removal (**Figure 2.1B, C**), while levels of other known AUBPs (TTP, AUF1, HuR) were unchanged (**Figure 2.1B left panel**). These results hinted that Brf1 itself might be needed to maintain the undifferentiated state by keeping certain transcripts at a low level and that Brf1 may possibly be under LIF-Stat3 control. It has been shown by Niwa *et al.* (Niwa *et al.* 1998) that blocking Stat3 by a dominant-negative form leads to same effect as LIF removal. Therefore, ES cells were treated with siRNA against Stat3, in the presence of LIF, to see if Brf1 is mainly under the control of Stat3 or if LIF signals over another pathway to Brf1. Interestingly, Brf1 downregulation was observed when Stat3 was silenced by RNAi (**Figure 2.2**), supporting the idea of Brf1 expression being under direct Stat3 control. This led us to formulate a model of how Brf1 might be involved in ES cell differentiation. This model was tested in the current work.

2.1.2 Model for Stat3 regulation of Brf1

The initial experiments showed that Stat3 is a major regulator of Brf1 expression in addition to regulating many other genes that either support self-renewal directly or by inhibition of pro-differentiation factors. We now hypothesize that Brf1 suppresses a pool of ARE-containing transcripts that partly counteract self-renewal and that are required in early differentiation to guide the cells into the correct differentiation path, and which thus have to be kept low as long as cells are in a pluripotent state. As soon as the cells begin to differentiate, Brf1 levels drop due to cessation of Stat3 signaling, leading to increased expression of these factors that now play a role in the differentiation processes (**Figure 2.3**). In contrast to Brf1, a recent publication showed that the transcription factor c-myc, which is also a Stat3 target, is a key regulator of self-renewal in murine ES cells and is able by itself to keep cells pluripotent even in the absence of LIF when over-expressed (Cartwright *et al.* 2005).
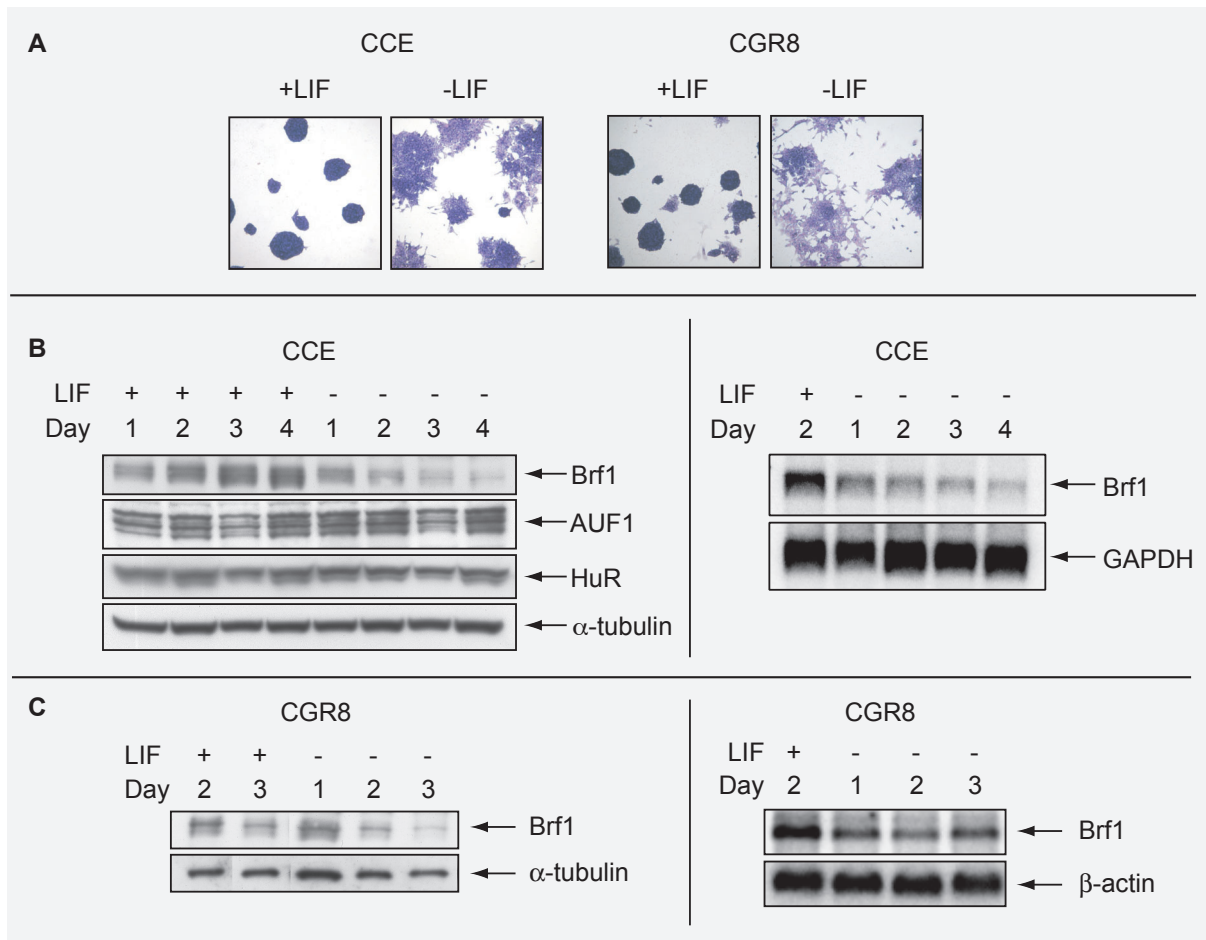
Figure 2.1: *LIF removal in CCE and CGR8 cells leads to downregulation of Brf1.*

(A) Both ES cell lines (CCE and CGR8) were grown for 3 days in medium with or without LIF.Cells grown with LIF show the dome-like colony morphology of undifferentiated cells, whereas cells kept in medium without LIF show a flat, spread-out morphology characteristic of differentiated ES cells.

(B) The left panel shows Western blots of CCE cells that were kept for 4 days either with or without LIF as indicated. Protein levels of Brf1, AUF1, HuR and α-tubulin are shown. In the right panel, Brf1 mRNA levels are monitored by Northern blot, GAPDH served as loading control.

(C) The left panel shows a Brf1 Western blot of CGR8 cells grown with or without LIF. Samples were taken at indicated days, α-tubulin served as loading control. The right panel shows a Northern blot with β-actin as loading control. Note that protein and RNA levels of Brf1 drop after LIF removal.

((A) and (C) of this figure form Supplementary Figure 1 in the Stem Cells paper on page 84)
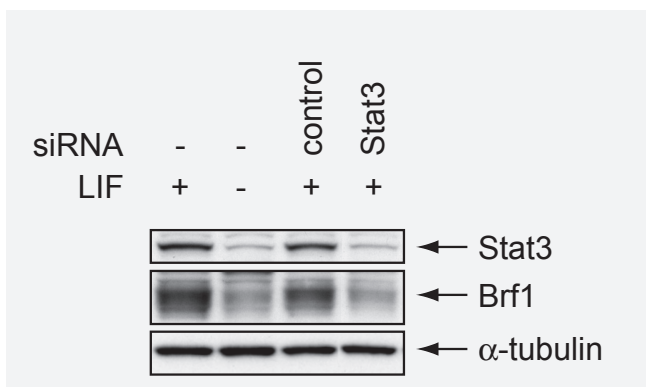

Figure 2.2: *Effect of Stat3 siRNA on Brf1 levels.* CCE cells were plated with or without LIF and, as indicated, treated for 48h with Stat3 or β-globin (control) siRNA. Expression of Stat3 and Brf1 was monitored by Western blotting.
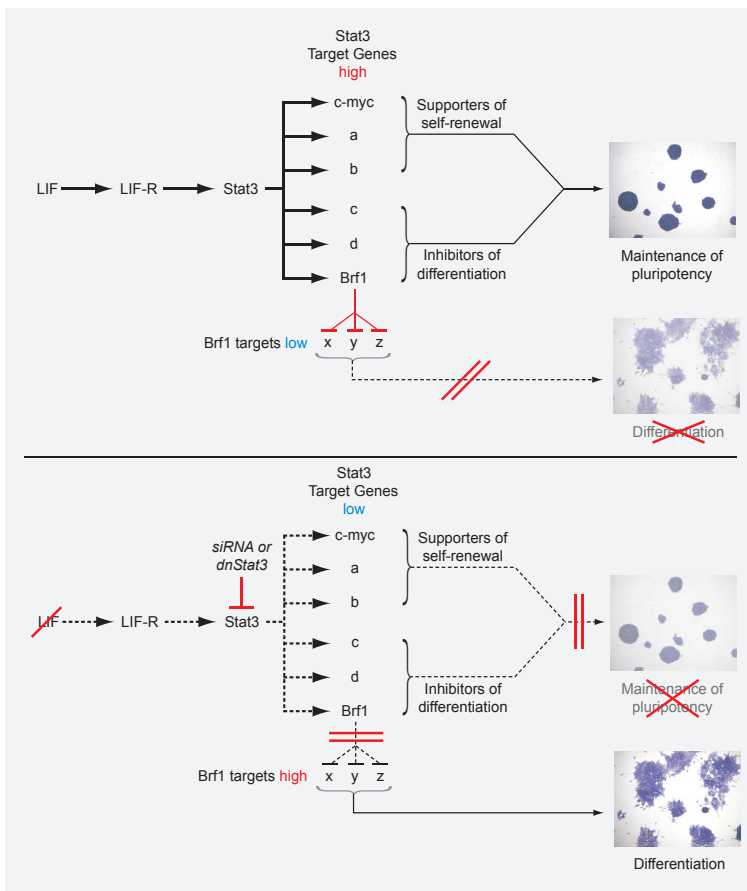
Figure 2.3: *Hypothesis of the role of Brf1 in ES cell differentiation.* LIF signals over its receptor (LIF-R) to Stat3, which has many downstream targets, including c-myc, Brf1, etc., some of them keep the cells pluripotent. These genes may be grouped into two categories: those that directly confer self-renewal and pluripotency (c-myc, a, b), and a second group that represses pro-differentiation factors (c, d, Brf1). As long as the LIF-Stat3 pathway is active (full lines; inactive path: dashed lines), both supporters of self-renewal and inhibitors of differentiation are expressed to maintain pluripotency (upper panel). In this scenario, Brf1 is high and destabilizes its targets (x, y, z), whose mRNAs contain an ARE and support differentiation.

Upon LIF removal or blocking Stat3 activity by dominant-negative (dnStat3) interference (Niwa *et al.* 1998) or siRNA (our observations), expression of both groups of genes is shut-off leading to cell differentiation (lower panel). In this case, Brf1 is low or absent and the transcripts x, y, z regulated by Brf1 are now expressed supporting differentiation.

To test the hypothesis, we needed a system to stably downregulate Brf1. Transfection of synthetic siRNA into ES cells is not ideal due to variable transfection efficiency between experiments, and siRNA transfection is transient thereby precluding the study of Brf1 downregulation in later differentiation. Therefore, we chose to test if shRNA stemloops could be generated *in vivo* that are also potent enough to downregulate Brf1 efficiently. The advantage of stable shRNA expression would be uniform downregulation of the gene of interest in all cells, minimization of unwanted off-target effects and stable long-term downregulation. Additionally, we wanted shRNA expression to be inducible, so that Brf1 downregulation can be studied at various time points of choice to uncover any stage-specific effects of Brf1 downregulation.

2.1.3 Designing and constructing the system

The system we wanted to have should consist of inducible stemloops to downregulate Brf1, or any other gene of interest, as for example in our case other AU-binding proteins like Brf2, TTP, AUF1, etc. Therefore, we decided to establish this as an inducible shRNA system as described by van de Wetering *et al.* (van de Wetering *et al.* 2003), where they described a

tetracycline-inducible promoter for shRNAs (**Figure 2.4A**) regulated by the unmodified Tet repressor (Gossen and Bujard 1992; Yao *et al*. 1998). Additionally, we wanted to have a stable, defined locus in which to introduce the inducible shRNAs, where they would be reproducibly expressed from the same site. Therefore, we chose the Flip-In system whereby constructs containing a frt (flip-recombinase target) (O'Gorman *et al*. 1991) site is inserted by the Flipase into another frt site (**Figure 2.4B**). To reach this goal, we followed a four-step protocol (**Figure 2.5**) and for validation of the functionality, we chose a stemloop against Stat3 as disruption of the LIF-Stat3 pathway leads to differentiation of murine ES cells, and thus an shRNA directed against Stat3 would be the perfect control to check for inducibility and leakiness of the system.
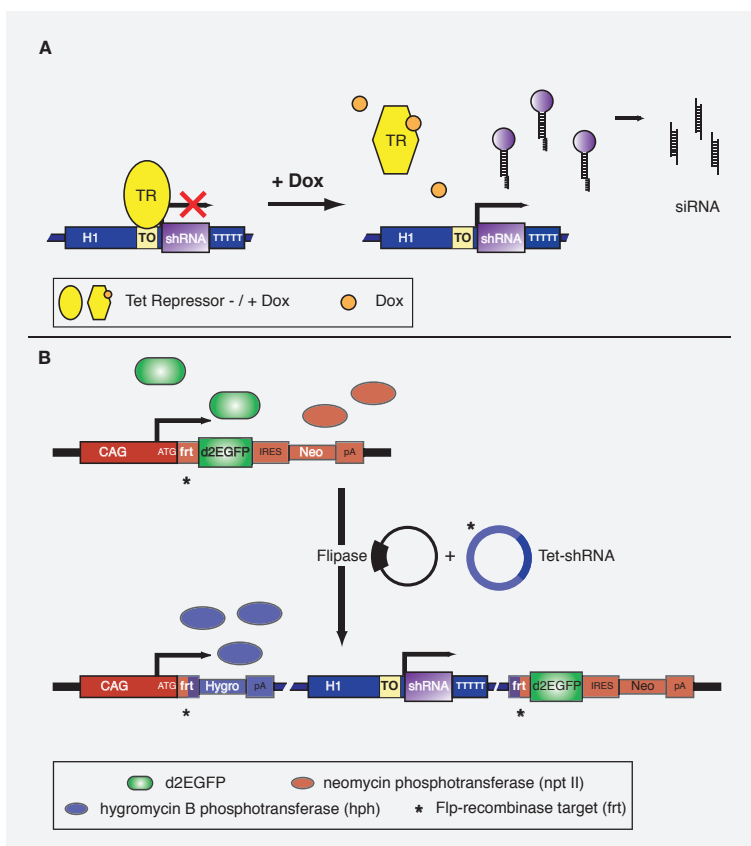

Figure 2.4: *Schematic view of doxycycline-inducible shRNA expression.*

(A) The Tet repressor (TR) binds to the Tet operator (TO) blocking RNA polymerase III. Addition of doxycycline (Dox) removes TR and shRNA is produced and processed intracellularly to 21nt siRNA as described by van de Wetering (van de Wetering *et al.* 2003).

(B) A modified Flip-In system is used to recombine a vector containing the shRNA of interest into a defined locus marked by GFP and flanked by the Flp-recombinase-target (frt) and the neomycin resistance gene. After successful recombination following cotransfection with plasmids encoding flipase and frt-containing Tet-shRNA, cells lose both GFP expression and G418 resistance after dislocation from the promoter but acquire hygromycin resistance and inducible shRNA expression. Frt is marked by an asterisk.

In the first step, the original promoter for the Tet repressor had to be replaced by a CAG promoter (CMV enhancer-chicken actin promoter fusion), as the activity of many commonly employed promoters such as the SV40 or CMV promoters are weak in undifferentiated ES cells (Chung *et al*. 2002). Behind this promoter, we cloned the Tet repressor gene linked by an IRES to a puromycin resistance marker (pCAG-TR-IRESpuro3; **Materials and Methods, Figure 4.1A**). This construct was then lipofected into CCE ES cells and the cells were selected for puromycin resistant clones. These clones were then cultured and allowed to differentiate to check for stable Tet repressor expression over time. We chose a clone (TR8) for further transfections, as it
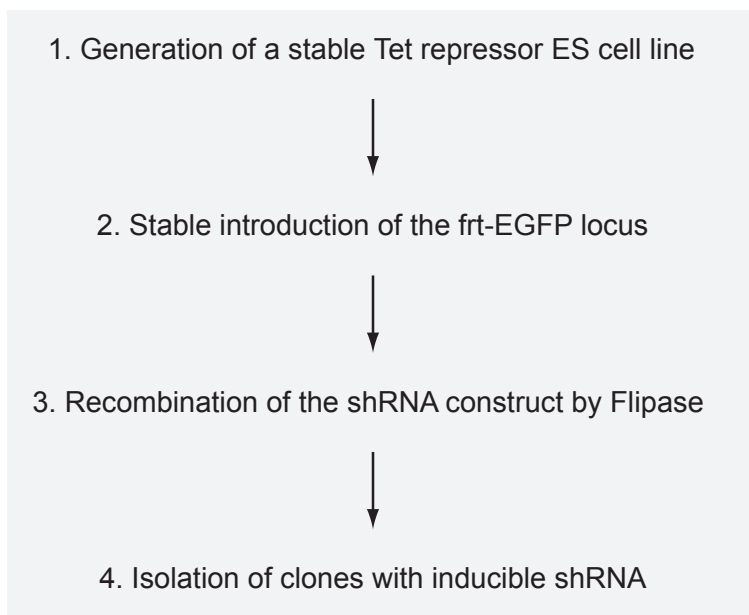
1. Generation of a stable Tet repressor ES cell line

2. Stable introduction of the frt-EGFP locus

3. Recombination of the shRNA construct by Flipase

4. Isolation of clones with inducible shRNA

Figure 2.5: *Four-step strategy.*
The indicated four steps have to be taken to generate the inducible shRNA ES cell line.

had high and stable Tet repressor expression, and showed the best inducible response upon transient transfection with inducible Brf1 shRNA.

In the second step, we wanted to have a stable frt-EGFP locus in this Tet repressor containing cell line. This required construction of a frt vector where EGFP, under the control of a CAG promoter, is flanked by a frt recombination site and an IRES sequence followed by a neomycin resistance gene (pCAG-FRTd2EGFP-IRESneo3; **Materials and Methods, Figure 4.1B**). A special feature of this construct is that the start codon is in front of the frt site and that upon recombination, the EGFP no longer has a start codon resulting in loss of EGFP expression in correctly recombined clones. The TR8 clone was then lipofected with this construct and underwent selection with geneticin for stable clones. This initial screening was easier as positive clones expressed EGFP and could be screened by FACS. Once again the same procedure was used to check for a stable 'long-term' expressing locus. From this screening, the clone (TR8-) F3 was chosen for the recombination of the inducible stemloop. However, after several passages without geneticin, the clone lost most of the GFP expression (**Figure 2.6**). This required subcloning of the F3 cell line and despite the loss of GFP expression, positive clones could be recovered by growing the cells in geneticin containing medium, which led to the eventual identification of a stable clone, F3-1, that was used for further experiments.

In the third step, a vector was constructed that would be able to target the stable frt site and containing the inducible shRNA. Therefore, a frt targeting vector, which contains a hygromycin resistance marker that can only be expressed upon correct recombination, was further modified. Into this vector we introduced an inducible H1 promoter with the cloning sites for shRNAs (pTER-shRNA-FRT; **Materials and Methods, Figure 4.1C**). As already mentioned we first cloned a shRNA against Stat3 into this vector to validate the system. This vector was cotransfected with a plasmid containing the Flip recombinase (pCAG-Flipase; **Materials and Methods, Figure 4.1D**) to introduce the stemloop and the hygromycin resistance marker into the frt locus. After selection with hygromycin, the cells were analyzed by FACS and negatively selected with geneticin, as correctly recombined F3-1-shRNA cells should have lost both EGFP and neomycin resistance (**Table 2.1**).
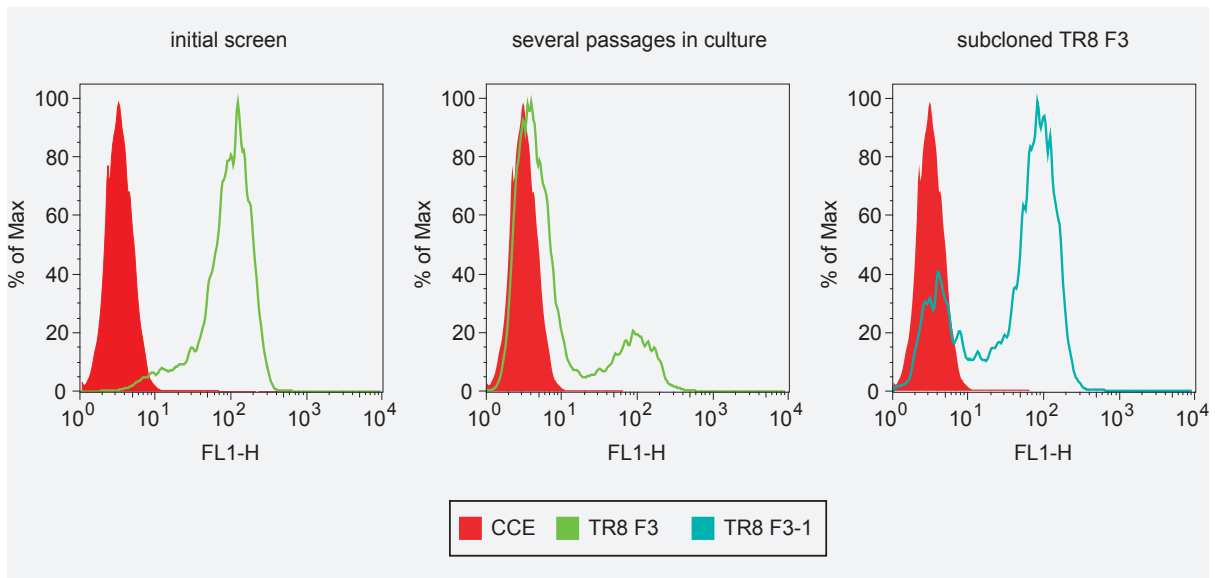
Figure 2.6: *Partial loss and recovery of EGFP.* CCE cells with stable integrated Tet repressor and the frt EGFP (TR8 F3) were FACS analysed after selection and strong EGFP expression was seen (left FACS profile), but the EGFP was almost totally lost after culturing for several passages without geneticin in the medium (middle FACS profiles). After subcloning the TR8 F3 cells, clones that again expressed EGFP were rescued (TR8 F3-1, right FACS profile).

	Puro^R	EGFP	Neo^R	Hygro^R
before recombination (TR & frt-EGFP)	+	+	+	-
after recombination (inducible shRNA)	+	-	-	+

Table 2.1. Selection markers available before and after the recombination of the shRNA into the frt locus.

The efficiency of correct recombination into the frt locus was relatively high as 15 out of 23 clones that were screened fulfilled these criteria: hygromycin resistance, geneticin sensitivity and loss of EGFP expression. Additionally, correct recombination and integration of the targeting vector was independently verified by PCR on genomic DNA from the clones (**Figure 2.7**). Primers were designed that amplify a product only upon correct recombination. We used the TR8 and the F3-1 cell lines as negative controls for the F3-1-S2 and F3-1-S3 Stat3 stemloop clones. As expected, only the clones with the Stat3 shRNA (F3-1-S2 and F3-1-S3) gave bands of the expected size of 600bp and 750bp, while nothing was amplified from the negative controls (**Figure 2.7**).
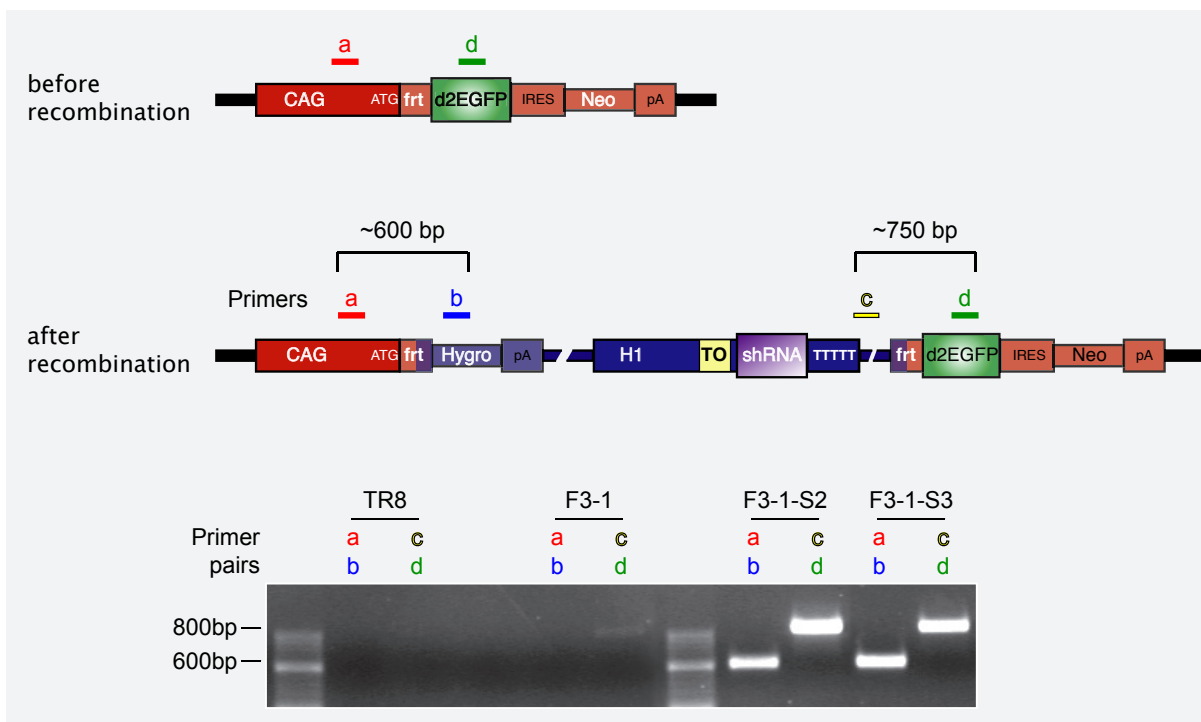
Figure 2.7: *Control of correct integration by PCR*. The Stat3 shRNA clones F3-1-S2 and F3-1-S3) were tested for correct integration by PCR, as negative controls the TR8 cells (with only the Tet repressor) or F3-1 were used. Before recombination Primer pair a/b or c/d do not give bands by PCR, as shown with TR8 and F3-1 cells. Only upon correct recombination bands at around 600bp (primers a/b) and 750bp (c/d) can be seen (F3-1-S2 and -S3).

2.1.4 Validating the system: Downregulation of Stat3 by doxycycline

To test that the system works on an actual target, Stat3 was inducibly downregulated in the Stat3 shRNA clones F3-1-S2 and F3-1-S3 by addition of doxycycline. The cells were cultured for 7 days in LIF-containing medium with or without doxycycline. As anticipated, the stemloop was strongly induced upon doxycycline addition to these clones but little or no signal was observed in the absence of doxycycline induction in the Stat3 shRNA clones or the F3-1 negative control respectively (**Figure 2.8A**). To check if the Stat3 protein is downregulated by induction of the stemloop, we performed a time-course over 7 days to measure Stat3 levels. In the control F3-1, we observed that Stat3 protein levels decline upon LIF removal but recover after day 5, while in the other conditions (+LIF or +LIF/Dox) no effect on Stat3 levels was seen (**Figure 2.8B**). In the F3-1-S2 and F3-1-S3 clones, we also saw a downregulation of Stat3 protein upon doxycycline addition in the presence of LIF, with a stronger effect on the F3-1-S3 clone. Also surprising is that the levels of Stat3 recovered even in the presence of doxycycline, but to a later time point (day 6 or later) as seen with LIF removal. The results of the other two conditions (-LIF or +LIF alone) were the same as for the control, demonstrating very tight regulation of the system with almost no leakiness for stemloop expression. Furthermore, we also used this opportunity to ascertain what happens to BRF1 levels upon Stat3 downregulation
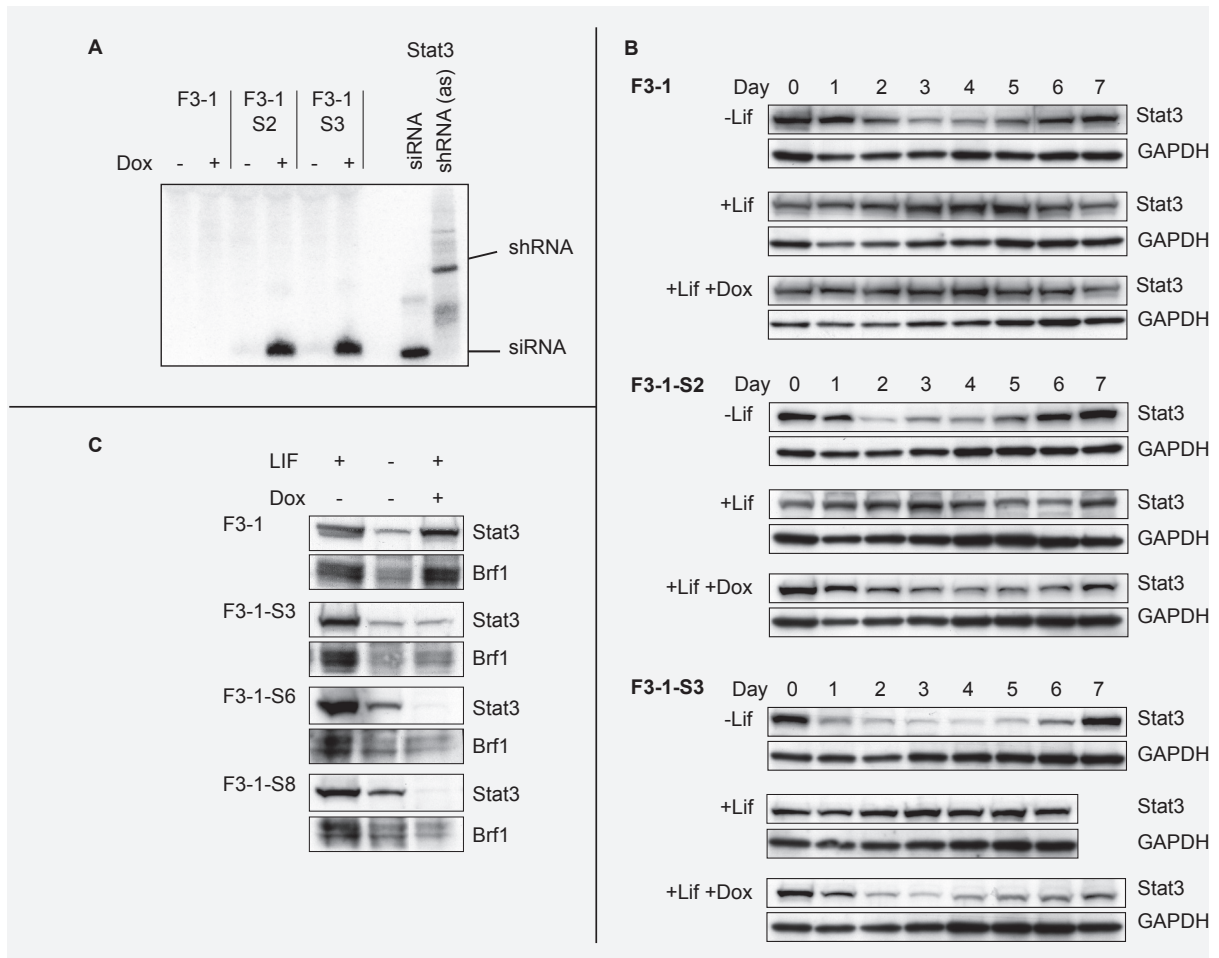
Figure 2.8: *Inducible downregulation of Stat3.*

(A) After 7 days in culture (+LIF; -/+Dox) RNA from indicated cells was isolated and processed for Northern blotting using a 5'-labeled Stat3 oligonucleotide probe. Markers shown on the right include synthetic 21nt Stat3 siRNA and 58nt Stat3 shRNA.

(B) A time-course experiment over 7 days in presence or absence of LIF and doxycycline as indicated is shown. Lysates from F3-1 control cells and the two Stat3 shRNA clones F3-1-S2 and F3-1-S3 were analyzed by Western blot against Stat3. GAPDH served as loading control. (C) Western blot analysis for Stat3 and Brf1 was performed for F3-1 control cells and three additional Stat3 shRNA clones (F3-1-S3, F3-1-S6 and F3-1-S8). Cells were culture for 7 days in presence or absence of LIF and with doxycycline as indicated. (Part (C) forms Supplementary Figure 2 in the Stem Cells paper on page 84)

with F3-1 as negative and F3-1-S3 as positive control, plus two additional Stat3 shRNA clones (F3-1-S6 and F3-1-S8). As expected, we observed in all cells a downregulation of Stat3 and Brf1 protein upon LIF removal (**Figure 2.8C**). We repeated the observation that Brf1 levels are reduced following downregulation of Stat3 by inducible shRNA. This finding substantiates the Model (**Figure 2.3**) of Brf1 being regulated by Stat3.
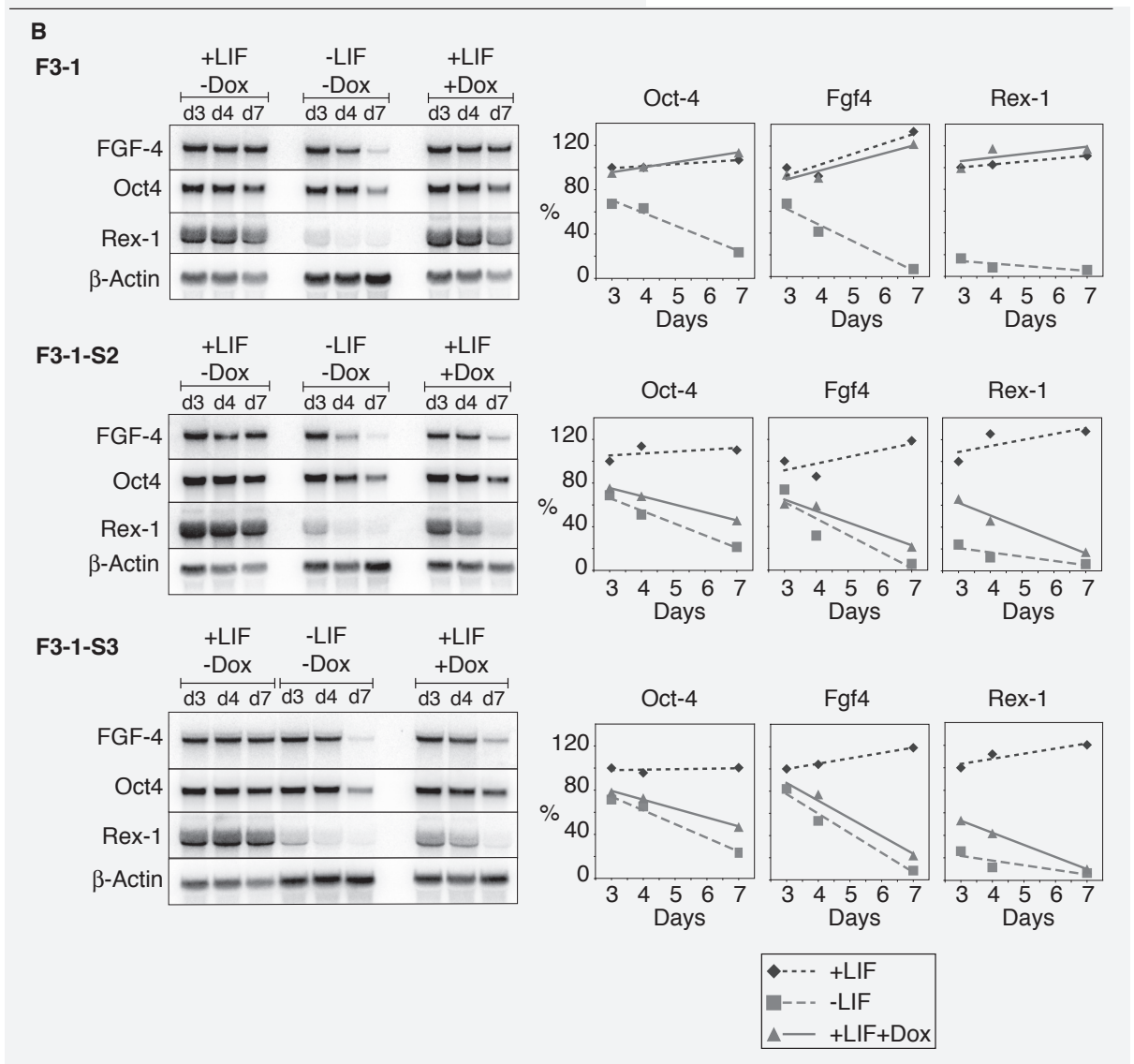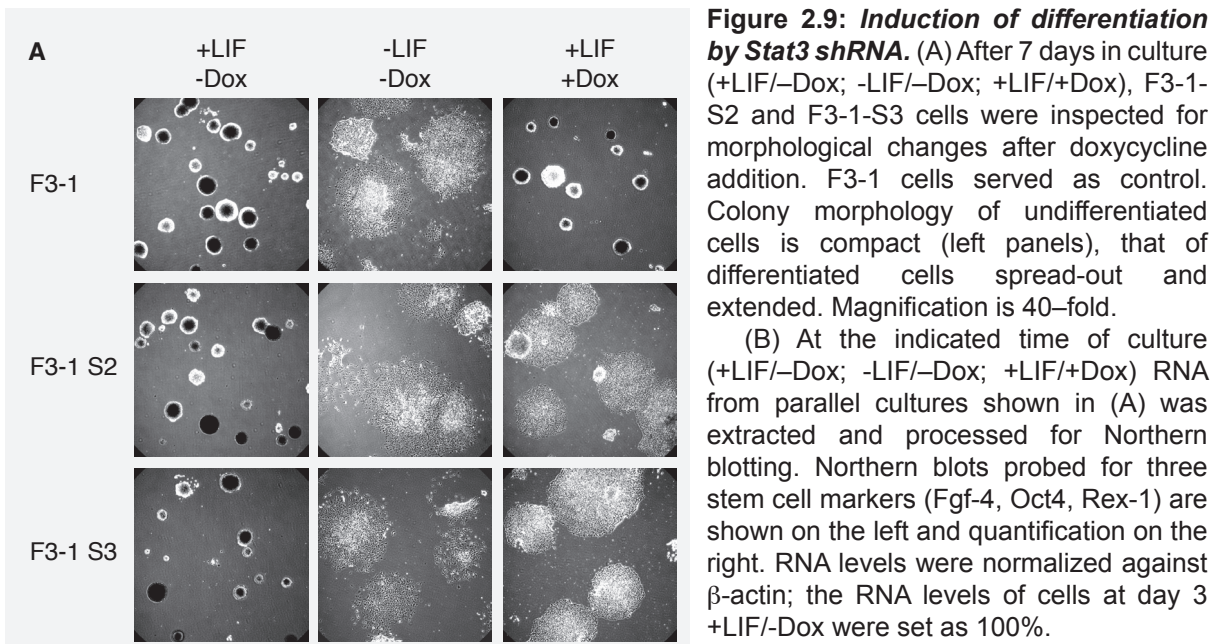
As disruption of the LIF-Stat3 pathway leads to differentiation, we investigated if induced downregulation of Stat3 is sufficient to give the same effects as LIF removal. To resolve this

question we again used F3-1 cells as negative control and the F3-1-S2 and F3-1-S3 cells. Upon Stat3 downregulation in F3-1-S2 and F3-1-S3, the cells had an altered morphology where they lost their round and compact shape to form loose and spread-out colonies resembling that of cells differentiated by LIF removal (**Figure 2.9A**). To conclusively prove that the cells were indeed differentiated, the expression of several known markers of differentiation was checked. Oct4, Sox2 and Rex-1 were chosen, as they are known to decrease upon differentiation (Yuan *et al*. 1995; Ben-Shushan *et al*. 1998; Niwa *et al*. 2000). To check for changes in expression of these markers, we performed a time-course experiment over 7 days to assess the mRNA levels. As expected, the levels of the three transcripts declined upon LIF removal in all cells, whereas with doxycycline addition, a decrease was only observed in the F3-1 cells containing the inducible Stat3 stemloop (**Figure 2.9B**). These experiments validated the inducible system for specific gene downregulation and showed robust controlled induction of the shRNA with minimal leakiness. In addition they provided corroborating evidence for Stat3 control of Brf1 expression in ES cells.

2.1.5 Recombination of the Brf1 stemloop

In order to investigate an effect of Brf1 on ES cells and differentiation, we had to first insert an inducible shRNA against Brf1 in the F3-1 cells. Therefore, the F3-1 clone was cotransfected with a pTER-shRNA-FRT vector containing a stemloop against Brf1 together with the Flipase plasmid. Cells were selected as before with hygromycin, and screened for loss of EGFP expression and neomycin resistance, to identify correctly recombined clones. Once again we obtained a high degree of correct integration, as 25 of 33 clones had the correct marker pattern (**see Table 2.1 above**). Selected clones (F3-1-B9 and F3-1-B14) were tested for inducibility of the stemloop and downregulation of Brf1. Both clones had a similar inducible response as obtained with the Stat3 shRNA clones, with strong induction of the stemloop upon doxycycline addition but almost no leakiness in its absence (**Figure 2.10A**). In addition, Brf1 protein levels decreased upon doxycycline addition (**Figure 2.10B**), although not as strongly as compared to the Stat3 protein levels after induced downregulation of Stat3.

In initial experiments with the F3-1-B9 and F3-1-B14 cells, we did not see an immediate effect upon downregulation of Brf1 in ES cells grown with LIF, indicating that Brf1 is not critical for self-renewal in the presence of LIF signaling. As ES cells can be differentiated into various lineages, we wanted to see if and what effects Brf1 downregulation would have on lineage-specific differentiation. We followed protocols by which ES cells can be guided into specific differentiation pathways. The first attempt to differentiate into the hematopoietic lineage was unsuccessful with the CCE ES cells, however later experiments using a different ES cell line (R1) were successful. The cells were also subjected to a neuron specific differentiation protocol (performed in the laboratory of Yves Barde, Biozentrum) but this also failed as the

A

	+LIF -Dox	-LIF -Dox	+LIF +Dox
F3-1			
F3-1 S2			
F3-1 S3			

Figure 2.9: *Induction of differentiation by Stat3 shRNA.* (A) After 7 days in culture (+LIF/–Dox; -LIF/–Dox; +LIF/+Dox), F3-1-S2 and F3-1-S3 cells were inspected for morphological changes after doxycycline addition. F3-1 cells served as control. Colony morphology of undifferentiated cells is compact (left panels), that of differentiated cells spread-out and extended. Magnification is 40–fold.

(B) At the indicated time of culture (+LIF/–Dox; -LIF/–Dox; +LIF/+Dox) RNA from parallel cultures shown in (A) was extracted and processed for Northern blotting. Northern blots probed for three stem cell markers (Fgf-4, Oct4, Rex-1) are shown on the left and quantification on the right. RNA levels were normalized against β-actin; the RNA levels of cells at day 3 +LIF/-Dox were set as 100%.
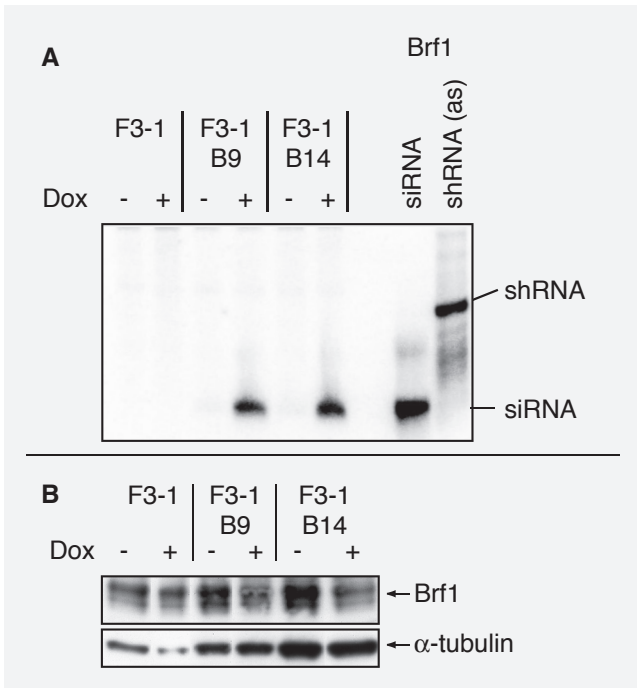
B

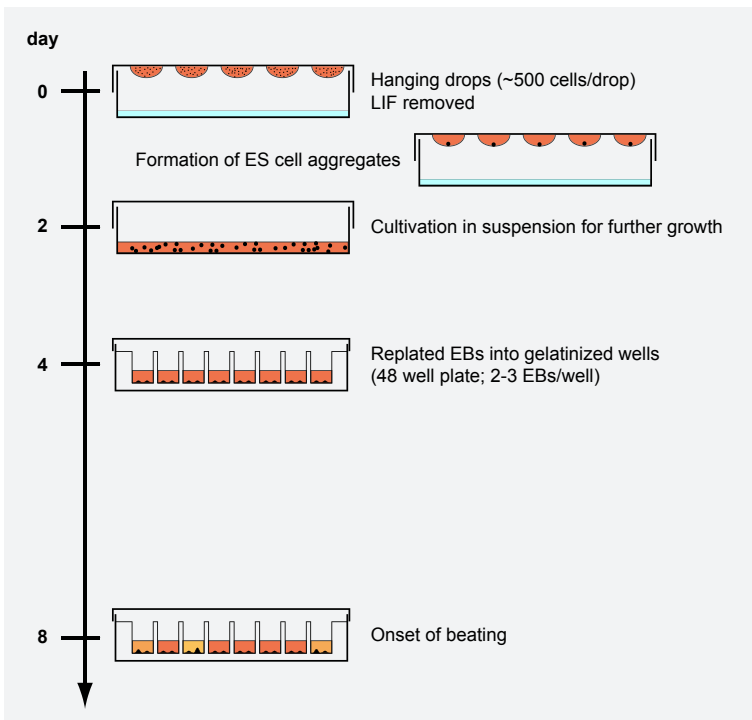**Figure 2.10:** *Doxycycline-inducible downregulation of Brf1.*

(A) After 7 days in culture (+LIF; -/+Dox) RNA from indicated cells was isolated and processed for Northern blotting using a 5'-labeled Brf1 oligonucleotide probe. Markers shown on the right include synthetic 21nt Brf1 siRNA and 58nt Brf1 shRNA.

(B) After 3 days in culture in the presence of LIF (-/+Dox) as indicated, Brf1 was examined by Western blot analysis. α-tubulin served as loading control.

cells died during differentiation and no neurons were obtained.

We proceeded to try to differentiate the cells into cardiomyocytes, as this is a simple and robust protocol, where cells are incubated as hanging drops to generate embryoid bodies that are subsequently plated into multi-well plates (**Figure 2.11**, and see Materials and Methods: Cell culture). Gratifyingly, we could see an effect on the morphology of the plated bodies generated from Brf1 downregulated cells which showed a loosening of the central mass with increased outgrowth and formation of satellite "microbodies" (**Figure 2.12**) compared to the F3-1 control. As we could observe changes on ES cell morphology, we decided to conduct further experiments to investigate the effects that Brf1 downregulation has on the cardiomyocyte differentiation pathway. Cardiomyocytes have further advantages in that they are visibly beating under the microscope and there are several well-described cell-type markers.

In the following experiments, we observed an effect on

Figure 2.11: *Generation of beating bodies.* Cells are first cultured in hanging drops for 2 days, washed down into suspension culture for additional 2 days and then 2-3 bodies are plated into gelatinized 48 well plates. After around 8 days of total culture onset of beating can be observed. Adapted from (Boheler *et al.* 2002).
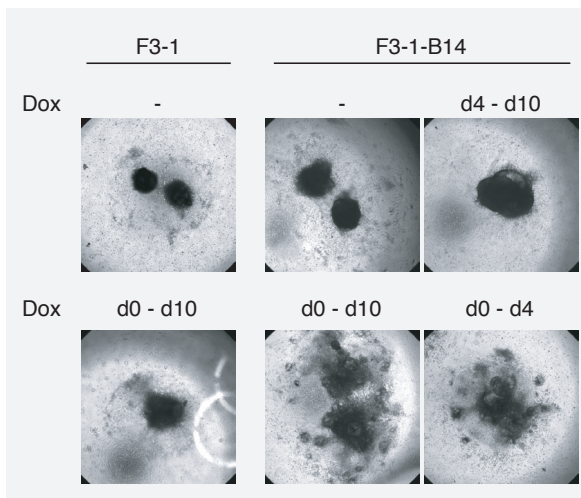
Figure 2.12: *Embryoid body morphology.* Morphology of embryoid bodies (EBs) at d10 from F3-1 and F3-1-B14 cells either kept with or without doxycycline from day 0 to day 18. Additionally, F3-1-B14 EBs were either kept with doxycycline during the first four days or from day 4 until the end of the experiment.
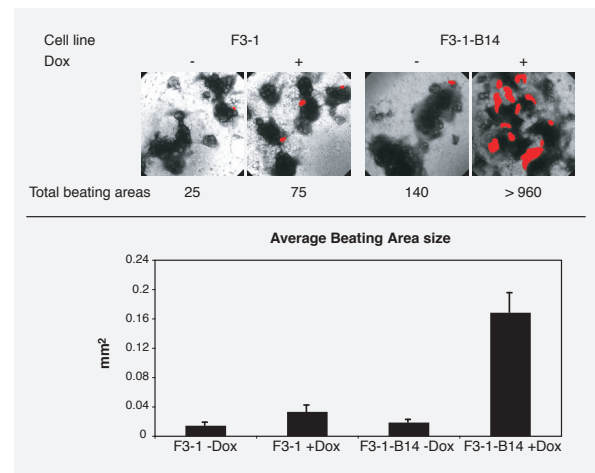

Figure 2.13: *Increase of beating areas within EBs.* Embryoid bodies from F3-1 and F3-1-B14 cells were plated with or without doxycycline into 24 well plates. For each cell and condition around 720 EBs were plated and beating areas were counted at day 18.

Upper panel: Shown in red are beating areas. Note that a single EB may contain more than one beating area, and beating areas may become confluent with time. Numbers indicate beating areas from 720 bodies plated.

Lower panel: The size of beating areas from 3 experiments was quantified, averaged and is shown with standard error of the mean.

cardiomyocyte formation, namely that cells where Brf1 is downregulated (F3-1-B14 +Dox) developed more beating bodies and beating areas per body with a greater size of the areas compared to controls F3-1 ±Dox or F3-1-B14 -Dox (**Figure 2.13**). To check if downregulation of Brf1 influences the onset of beating, we performed experiments where the plated embryoid bodies were inspected daily for the onset of beating. The experiments with the F3-1-B14 cell showed that the onset of beating was not altered by Brf1 downregulation (**Figure 2.14A**) but the number of beating bodies was significantly increased in the F3-1-B14 cells cultured in the presence of doxycycline compared to the control F3-1 ±doxycycline or F3-1-B14 -doxycycline. To confirm this, an independent clone, F3-1-B9, was put through the same protocol and we again saw no difference in the onset of beating, but a significant increase in beating bodies compared to the F3-1 control (**Figure 2.14B**) although in this case, the untreated F3-1-B9 cell did not give any visible beating. These results show that Brf1 downregulation leads to an increase in the size and number of beating areas rather than a change in the onset of beating indicating an effect on the magnitude rather than the kinetics of beating area formation.

As the dip in Brf1 levels following LIF removal is transient with recovery around day 5, we wondered if it is necessary to downregulate Brf1 throughout the whole differentiation process
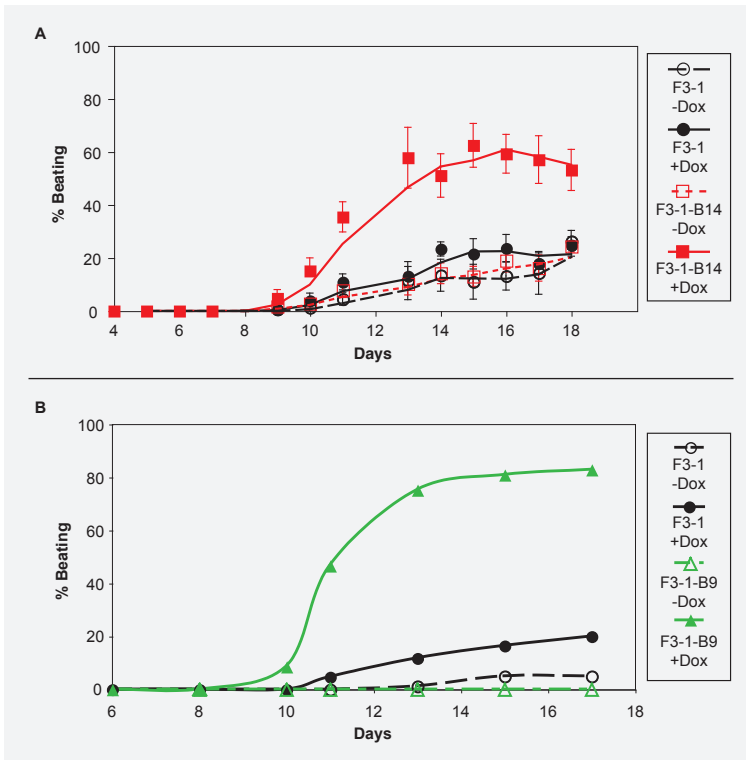
Figure 2.14: *Kinetics of cardiomyogenesis*. F3-1, F3-1-B14 and F3-1-B9 EBs were plated into 48-well plates at two bodies per well and cultured with or without doxycycline. EBs were checked daily for onset of beating and scored. The data is shown as percentage of beating bodies to total plated.

(A) F3-1 and F3-1-B14 EBs cultured with doxycycline for the total length of the experiment. For each time point at least 3 experiments are averaged and standard errors of the mean are shown.

(B) F3-1 and F3-1-B9 EBs cultured without or with doxycycline for the total length of the experiment.

or if there is a time-window in which it is necessary for Brf1 to be kept low. Therefore, we tested different time-windows in which to induce the stemloop against Brf1 to reproduce the effects described above. We found it to be sufficient to decrease Brf1 levels only for the first 4 days of differentiation (**Figure 2.11 and Figure 2.15A**), whereas downregulation post day 4 gave the same morphology and amount of beating as in the controls (**Figure 2.15B**).
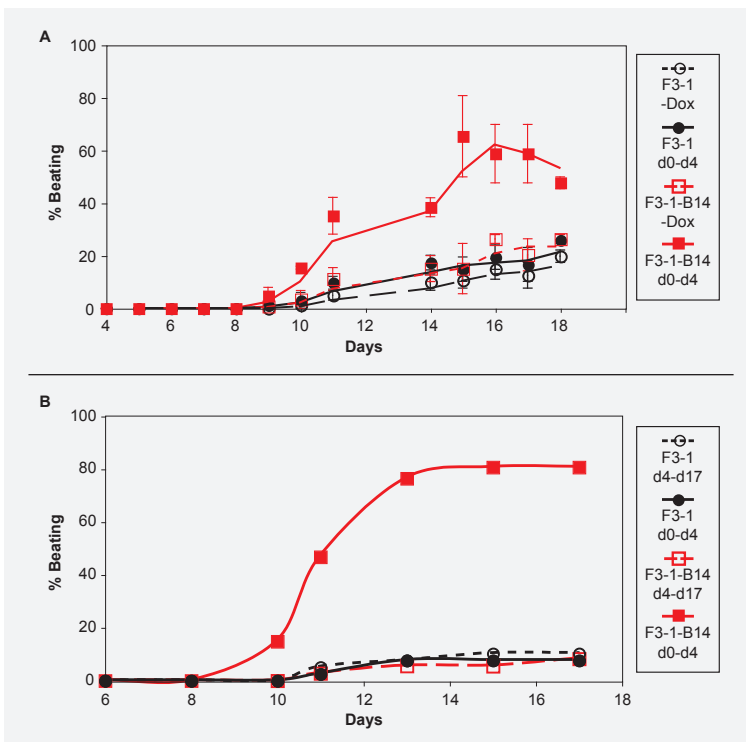

Figure 2.15: *Brf1 downregulation is sufficient during the first 4 days to trigger enhanced cardiomyogenesis*. F3-1 and F3-1-B14 EBs were plated into 48-well plates at two bodies per well and cultured with or without doxycycline. EBs were checked daily for onset of beating and scored. The data is shown as percentage of beating bodies to total plated.

(A) F3-1 and F3-1-B14 EBs were cultured with doxycycline only from day 0 to day 4 where indicated. For each time point the average and standard errors of the mean of at least 3 experiments are shown.

(B) F3-1 and F3-1-B14 EBs were plated as above, but doxycycline was present where indicated only from day 0 to day 4 or from day 4 onwards.
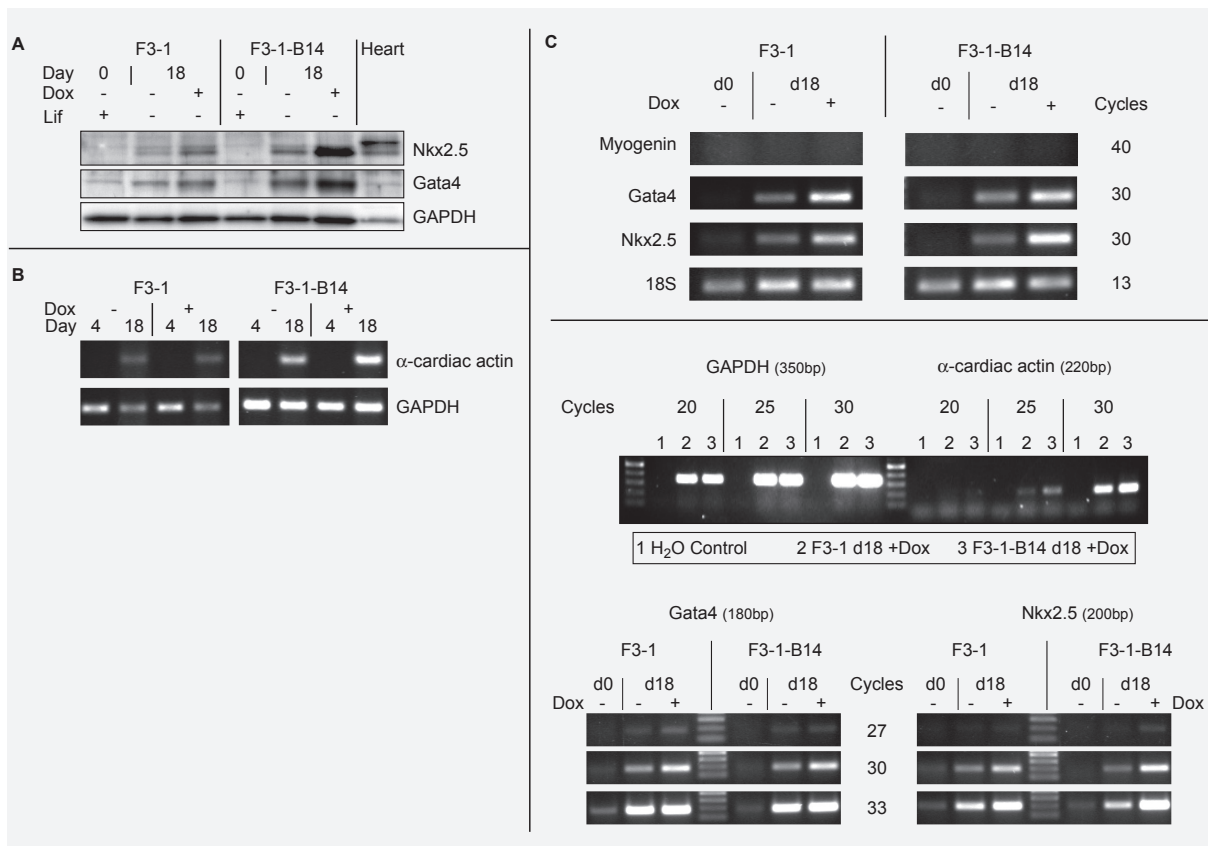
Figure 2.16: *Western blot and semi-quantitative PCR analysis of cardiac markers.*
(A) Control cells (F3-1) and Brf1 shRNA cells (F3-1-B14) were cultured in the absence of LIF with or without doxycycline for 18 days. Western blot analysis was performed for Nkx2.5, Gata4 and GAPDH. Also shown are undifferentiated F3-1 and F3-1-B14 cells grown in LIF and mouse heart as controls.
(B) Semi-quantitative RT-PCR of the cardiac marker α-cardiac actin at indicated days after LIF removal. GAPDH served as control.
(C) The upper panel shows the semi-quantitative RT-PCR analysis of myogenin, Gata4 and Nkx2.5 at indicated days after LIF removal. 18S rRNA served as loading control. Numbers of PCR cycles are shown on the right. In the lower panel the variation of cycles are shown for the semi-quantitative analysis shown in (B) and in (C) upper panel. Analysis of α-cardiac actin, Gata4, Nkx2.5 and GAPDH using different cycle numbers as indicated. (Part (C) of this Figure forms Supplementary Figure 4 in the Stem Cells paper on page 84)

To verify if the observed beating is really due to an increase in the presence of cardiomyocytes, we examined known cardiac markers by western blot (Nkx2.5, Gata4) and semi-quantitative RT-PCR (Nkx2.5, Gata4, α-cardiac actin). The western blot showed that both Nkx2.5 and Gata4 are increased compared to the controls (F3-1 ±doxycycline; F3-1-B14 -doxycycline; **Figure 2.16A**). Doxycycline by itself gave a slight enhancement of cardiomyogenesis as revealed by the cardiac markers, but this effect is negligible compared to doxycycline treated F3-1-B14 cells. The semi-quantitative RT-PCR results agreed with the western blot, namely that the cardiac markers are always strongly enhanced in F3-1-B14 cells treated with doxycycline compared to the controls (F3-1 ±doxycycline; F3-1-B14 -doxycycline) and that the skeletal muscle marker myogenin is absent in all cells (**Figure 2.16B and C**). These final results show that the

enhancement of beating is indeed due to increased differentiation of Brf1 downregulation in doxycycline-treated F3-1-B14 cells into cardiomyocytes.

All these results are described in the publication "A Cassette System to Study Embryonic Stem Cell Differentiation by Inducible RNA Interference" in *Stem Cells*, 2007; Vol. 25: p1178-1185.

2.2 Gene expression analysis in CCE cells

In further experiments, a DNA microarray chip analysis was conducted to identify native Brf1 target transcripts that may be involved in differentiation, as downregulation of Brf1 in CCE ES cells increased the formation of cardiomyocyte. Therefore, F3-1, F3-1-S2 and F3-1-B14 cells were grown ±LIF, and with LIF in presence of doxycycline for 3 days, and were then harvested for total RNA extraction for a DNA microarray analysis. The complete microarray procedure was performed by Edward J. Oakeley's laboratory at the functional genomics facility of the Friedrich Miescher Institute in Basel.

To find genes that are regulated by Brf1, we looked for transcripts that were strongly altered upon Brf1 downregulation by doxycycline but not by addition of doxycycline in the F3-1 control. We found 195 genes that were at least 1.5-fold changed only in the F3-1-B14 but not in the control (**Figure 2.17, left panel**). Of these 195 genes 161 were lower expressed upon Brf1 downregulation and 34 were increased. We expected that transcripts bearing an ARE should be found in the upregulated group as the destabilizer Brf1 is missing. Unfortunately none of the
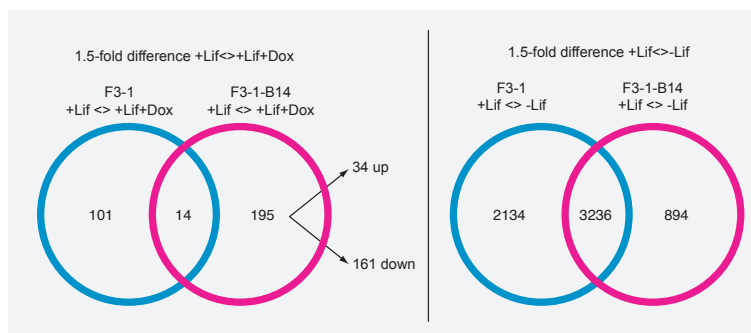

Figure 2.17: *Microarray comparison of F3-1 against F3-1-B14 cells.* Comparisons are shown as Venn diagrams of F3-1 and F3-1-B14 cells. In the left panel groups of +Lif versus +Lif+Dox are compared between the two cell lines. In the right panel the groups of +Lif versus -Lif are compared.

upregulated transcripts had any ARE-like motifs. In an earlier microarray experiment performed in our lab, CCE cells were treated for 48 hours with siRNA against Brf1 and then compared to CCE cells in LIF-containing medium. In this experiment, 10 upregulated transcripts bearing an ARE could be identified. Also upon comparing the datasets of the two experiments, no matching upregulated transcripts were found.

Comparison of F3-1 and F3-1-B14 cells treated with LIF or without LIF showed substantial differences between the two populations (**Figure 2.17, right panel**), although not many were
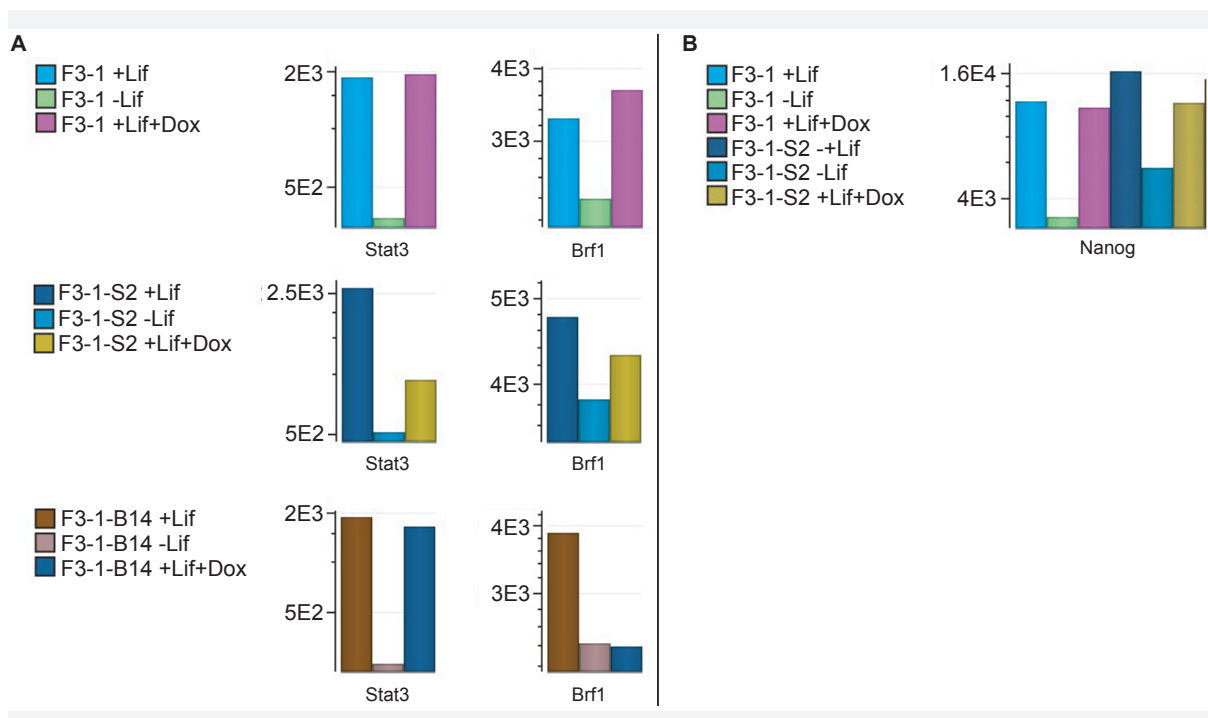
Figure 2.18: *DNA microarray analysis of Stat3, Brf1 and Nanog.* RNA from indicated cells and conditions was extracted at d3 and subjected to Affymetrix DNA microarray analysis.

(A) Shown are levels of Stat3 and Brf1 from F3-1 (control), F3-1-S2 (Stat3 shRNA) and F3-1-B14 (Brf1 shRNA) all grown with and without LIF and with LIF in presence of doxycycline as indicated.

(B) Nanog levels of F3-1 and F3-1-S2 cells under conditions as in (A).

(This Figure forms Supplementary Figure 3 in the Stem Cells paper on page 84)

anticipated, as the effects of LIF removal on the genetic program should be similar.

A pleasing outcome of the microarray experiment was that downregulation of Stat3, either upon LIF removal or doxycycline induction of the Stat3 shRNA, and the concomitant downregulation of Brf1 could also be confirmed by this method (**Figure 2.18A**). Furthermore, downregulation of the Brf1 transcript upon induction of its respective stemloop was also observed. Additionally, we could also observe that Nanog downregulation is not Stat3 dependent, and only decreases upon LIF removal and the concomitant induction of differentiation (**Figure 2.18B**).

2.3 Stability of ARE-containing mRNA in ES cells

As posttranscriptional regulation involving AU-rich elements is a major mechanism in controlling gene expression, we were interested to see if it is also active in murine ES cells. As this topic has been for several years a major research focus in our laboratory, we chose an experimentally verified system (Stoecklin *et al.* 1994) to detect whether post-transcriptional regulation is performed in ES cells. This system comprises of the 3'UTR of the IL-3 gene linked to an EGFP coding message. The IL3-3'UTR contains a strong ARE which is bound by
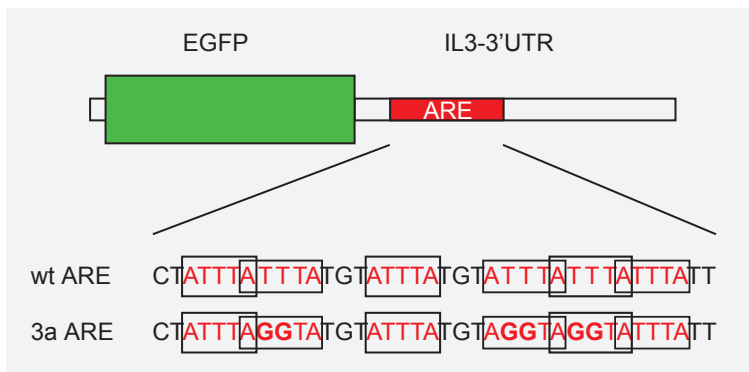
Figure 2.19: *Schematic drawing of the EGFP-IL3 3'UTR reporter.* The EGFP is followed by the whole 3'UTR of IL3. The core ARE sequence is shown which contains 6 partially overlapping AUUUA pentamers. For the 3a mutant three were mutated to AGGUA, which leads to an inactive ARE (Stoecklin *et al.* 1994).

AUBPs and subjects the message to rapid degradation, and levels of the message are reflected in EGFP expression. In addition, a mutated form of the IL-3 ARE, 3a mutant, has been demonstrated to be non-functional in ARE-mediated decay (**Figure 2.19**). To test if ES cells also show differences in the stability of ARE bearing transcripts, CCE F3-1-B14 and R1 ES cells were stably transduced with retroviruses containing the EGFP construct linked to the IL3-3'UTR with either the wildtype (wt) or the mutant (3a) ARE. After puromycin selection, clones were picked and analyzed by FACS for EGFP expression. From each cell line a clone bearing either the mutated or the wildtype ARE was then chosen for further experiments.

FACS analysis of EGFP expression showed higher EGFP levels for the mutant ARE bearing cells in both F3-1-B14 and R1 backgrounds compared to the cells containing the wildtype 3'UTR (**Figure 2.20, upper panels**). This difference may be due to the posttranscriptional regulation of mRNA levels acting at the various IL3-3'UTR constructs as previously shown
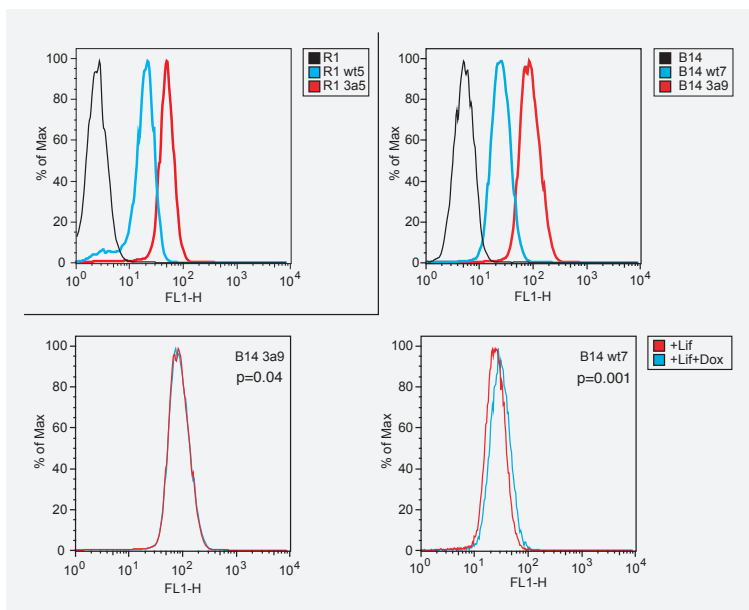

Figure 2.20: *FACS analysis of EGFP-IL3 3'UTR reporters in ES cells.* FACS profiles of R1 (upper left panel) and F3-1-B14 (upper right panel) cells either untransduced (black) or transduced with the EGFP-IL3-3'UTR wt (light blue) or 3a mutant (red). The FACS profiles from the three conditions are superimposed showing highest expression from the 3a mutant construct. The lower two panels show F3-1-B14 cells transduced with the EGFP-IL3-3'UTR wt (lower right panel) or 3a mutant (lower left panel) cultured in LIF-containing medium with (light blue) or without (red) doxycycline to induce Brf1 shRNA. FACS analysis was performed 3 days after doxycycline addition. A slight but highly significant shift can be seen when the Brf1 stemloop is induced in the cells containing the wildtype IL3-3'UTR.

in other, non-ES cell lines by our laboratory (Stoecklin *et al*. 2000; Stoecklin *et al*. 2003b). As these experiments only reflect the EGFP protein levels and not the mRNA stability of the reporter constructs, we are currently performing actinomycin D mRNA decay chase assays to investigate if the stability of the reporters are indeed different to conclusively demonstrate that ARE-dependent mRNA decay is functional in ES cells.

As described in recent publications from the laboratory, downregulation of Brf1 by siRNA leads to increased stability of a reporter bearing the wildtype IL3 ARE (Stoecklin *et al*. 2002; Raineri *et al*. 2004). Since the two reporters were introduced into the F3-1-B14 cell line, we were also able to inducibly downregulate Brf1 to investigate any changes in EGFP levels. Therefore, we cultured the cells containing the wildtype or the mutant ARE in LIF containing medium with or without doxycycline and after 3 days the cells were analyzed by FACS to monitor EGFP expression. In cells with the wildtype ARE, the levels of EGFP increased only slightly but this increase was nonetheless highly statistically significant (**Figure 2.20, lower right panel**), whereas in cells with the 3a ARE, the levels were essentially unchanged (**Figure 2.20, lower left panel**). We can therefore observe the same effect on the EGFP reporter upon Brf1 downregulation as has been previously described, but this nonetheless still requires final confirmation by mRNA stability assays.

2.4 Establishment of the system in R1 cells

Although we have developed an excellent *in vitro* culture system for downregulating any transcript of choice with a suitable stemloop, it is desirable to have it also established as a transgenic mouse model. While the original publication of the CCE cell line describes it as being able to generate transgenic animals (Robertson *et al*. 1986), the Transgenic Mouse Core Facility (TMCF) of the University was nevertheless unable to produce any chimeric mice from them. After they checked the karyotype of the untransfected CCE cell line, an abnormal chromosome distribution and even a translocation was observed by them. Furthermore, these cells have an additional disadvantage, as they do not differentiate into hematopoietic or neuronal cells.

Therefore, we decided to establish the system in a cell line that is capable of generating chimeras and giving germline transmission. The R1 cell line established by A. Nagy (Nagy *et al*. 1993) was chosen, as it was easily available by the TMCF in the Biocenter of the University of Basel.

These cells were first electroporated with the construct containing the frt-GFP-neo and selected with G418. Cells were then grown with or without LIF and feeders for 3days, or they were differentiated into beating bodies for 12 days to check for stable GFP expression over time and to see if the cells start to beat. Finally we chose two clones (3 and 21) for further electroporations with the Tet repressor construct and selected with puromycin. Stable clones were identified and are now in the process of being screened for Tet repressor expression.

3. DISCUSSION

3.1 Main Project: An inducible shRNA system in CCE ES cells

3.1.1 A model for Stat3 regulation of Brf1 expression

Our early results suggest that Brf1 is at least partially controlled by Stat3 as LIF removal leads to a decrease of Stat3 protein levels with a concomitant decrease in Brf1 levels, and this is also seen upon downregulation of Stat3 alone by siRNA. In this thesis we strengthened this model (**Figure 2.3**) by showing that induced downregulation of Stat3 in independent Stat3 shRNA clones also leads to a decrease in Brf1 levels. Furthermore, recent publications from DNA microarray experiments support the model of Brf1 being under the control of the LIF-Stat3 axis (Palmqvist *et al.* 2005; Sekkai *et al.* 2005). While these data indicate Stat3 as a major regulator of Brf1 expression in undifferentiated murine ES cells, it should be kept in mind that it may not be the sole pathway regulating Brf1, as a recent microarray analysis of DNA from chromatin immunoprecipitation in human ES cells provides support for binding of the transcription factors Oct4, Sox2 and Nanog to the promoter of Brf1 (Boyer *et al.* 2005). The finding that Brf1 is regulated by these three known transcription factors is very interesting as they regulate many developmentally important genes. As the Brf1 knock-out is embryonic lethal in mice (Stumpo *et al.* 2004), this leads to the speculation that Brf1 might also be a developmentally relevant gene. Although the binding of Oct4, Sox2 and Nanog to the Brf1 promoter has only been demonstrated for the human gene, they might also bind in murine ES cells, as we could identify *in silico* consensus binding sites for Oct4 (ATG CWA AT) and Sox2 (WWC AAW G) within 5kb of the murine Brf1 promoter region (**Figure 3.1**). These findings support the view that while regulation of Brf1 is Stat3 dependent, other known LIF-independent pluripotency factors may also be involved in its regulation.

An unexpected observation that we encountered was that upon LIF removal, Stat3 protein levels decreased transiently which has to our knowledge, never been reported. LIF removal is
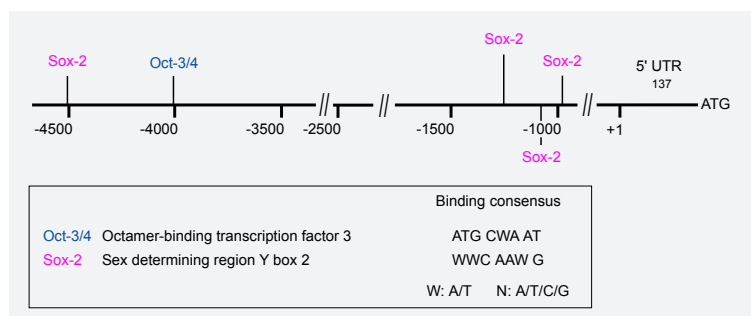

Figure 3.1: *Oct4 and Sox2 binding sites in the Brf1 promoter region.* The genomic sequence upstream of the transcription start site of the Brf1 was screened for consensus binding-sequences of Oct4 (ATG CWA AT) and Sox2 (WWC AAW G).

usually described as leading to Stat3 dephosphorylation and consequent inactivation without any change in the Stat3 protein levels (Ernst *et al.* 1999; Boeuf *et al.* 2001).

3.1.2 Designing and validating the inducible shRNA system

This work combines for the first time inducible shRNA technology with site-specific recombination in ES cells, where an EGFP-marked locus is linked to a frt recombination site and a selectable marker. As there are well-known problems associated with establishing inducible and reversible RNAi systems in murine ES cells, it was important at the outset of the project to develop a flexible and robust system that would not be affected by gene silencing.

This feature of inducible RNA interference in mouse embryonic stem cells or transgenic mice is not *per se* the novelty of our system, as there are other inducible systems where shRNA transcription can be inducibly regulated. One such group of systems are those that are irreversibly induced. Here, the shRNA expression is blocked by a floxed, e.g. neomycin, cassette in a RNA polymerase III promoter, which can be removed by Cre recombinase-mediated excision and concomitant activation of the promoter (Chang *et al.* 2004; Coumoul *et al.* 2004; Yu and McMahon 2006). An alternative system contains a loxP-Stuffer-loxP cassette inserted in front of a RNA Polymerase II promoter, which will drive shRNA production (Iovino *et al.* 2005), only upon Cre-mediated excision of the Stuffer. In yet another system, the RNAi expression is conditionally inactivated by Cre, and loxP sites are inserted flanking the RNA polymerase III promoter-shRNA cassette, so that excision leads to the loss of shRNA production and re-expression of target gene (Ventura *et al.* 2004). The advantage of all these systems is that Cre-mediated excision is conditional and can be made tissue specific using validated Cre-lines, at various times in development. The main disadvantage of these systems, as mentioned, is their irreversibility.

Another group of inducible system are the reversible ones that have been widely used to inducibly downregulate genes of which the most commonly employed has been that developed by van de Wetering and co-workers (van de Wetering *et al.* 2003). In this system, a Tet operator is introduced into a RNA polymerase III promoter and is controlled by the tetracycline regulatable Tet repressor protein. The function of this system is based on sterical hindrance of an operator bound Tet repressor to components of the transcription complex. A very recent publication showed, that inducible and reversible shRNA production with this system is also functional in transgenic animals (Seibler *et al.* 2007). A similar, but slightly different system was developed in the laboratory of Didier Trono, which is based on epigenetic repression. In their system, the Krüppel-associated box (KRAB)-domain is tethered to the Tet repressor. This KRAB-domain can silence RNA polymerase II and III promoters by inducing localized heterochromatin formation to cause transcriptional silence in the vicinity of its binding region. By introducing a Tet operator near a promoter, the fusion protein can bind and silence transcription within 3

kilobases of the binding site. Addition of doxycycline reverses Tet repressor-KRAB protein binding and relieves transcriptional repression (Wiznerowicz and Trono 2003).

The advantages of systems based on sterical hindrance or epigenetic modification are full reversibility by addition or removal of the inducer. Additionally, these reversible systems are based on well-established technology that is widely used to overexpress genes. The disadvantage of these systems is that they can be leaky and downregulation in mice cannot be performed in a tissue specific manner.

The second novel feature in our approach is the recombination locus that was introduced into the cells, in which the shRNA-containing construct is integrated. There are several possibilities for stable site-specific integration of a construct into mouse ES cells. Of these, the most commonly used is the ROSA26 locus, which confers ubiquitous transgene expression *in vivo* (Zambrowicz *et al*. 1997). Until now, this remains the only locus used for targeted integration of inducible RNAi systems into the mouse genome (Yu and McMahon 2006; Seibler *et al*. 2007). However, this locus is only present in mice and we wanted the option of establishing a similar system in future in non-murine cells. This necessitated the development of what constitutes the real novelty of our system, the introduction of a new flip-recombinase target (frt) site into mouse embryonic stem cells. Foreign DNA can be inserted by site-specific recombination promoted by the Flip-recombinase (Flipase) into the frt locus (McLeod *et al*. 1986). We chose the Flipase-frt system, which is not often used in ES cells and leaves open the possibility for adding supplemental conditional Cre-loxP regulated genes into mice generated from these cells. The frt site is located in front of an EGFP reporter linked by an IRES to a neomycin resistance gene, and unrecombined cells express EGFP and are neomycin resistant. The shRNA construct can be introduced into this locus by cotransfection with the Flip recombinase, which leads, upon correct integration, to abolished EGFP expression and neomycin sensitivity, but hygromycin resistance from the introduced construct. Theoretically, the stemloop construct can also be excised again by re-expressing the Flip recombinase. Although the ROSA26 locus is a reliable and widely used recombination target, it is only present in murine cells, whereas in principle, our system with the frt locus is species independent. Once introduced, the site offers a reliable recombination target, but clones have nevertheless to be thoroughly tested for an active locus suitable for long-term gene expression.

Establishing a working clone containing an inducible shRNA recombined into the frt locus was not as straightforward as initially expected. Stable Tet repressor expressing clones, which express the protein without being silenced over time, were relatively easy to obtain. However, cells stably transfected with the frt-EGFP construct, tended to lose EGFP expression after removal of the selection agent (neomycin). Nonetheless, reselection of the cells with neomycin and maintaining them in selective medium allowed recovery of EGFP expressing, frt containing cells. This effect could be due to heterochromatin spreading into the integration

site from adjoining regions, rather than promoter silencing from DNA methylation, as it is reversible. Nevertheless, as soon as a stemloop-bearing construct was recombined into the frt site with Tet repressor binding to the inducible H1 promoter, silencing of this region ceased to be a problem.

We first cotransfected a Stat3 shRNA construct together with the Flipase plasmid into the functional clone F3-1 as a systems control. Fortunately, the correct recombination event for the stemloop constructs was strikingly high as we had 65% positive clones as assessed by the three markers: EGFP, neomycin and hygromycin. Induction with doxycycline showed a strong expression of the Stat3 shRNA and concomitant downregulation of Stat3 protein. This was accompanied by the expected morphological and biochemical changes with negligible background in the controls. It was previously reported that tetracycline inducible expression of a dominant negative form of Stat3 in ES cells could trigger differentiation (Niwa *et al*. 1998). As our system compared favorably with the dominant negative approach, this gave us confidence in using it to target and investigate potential regulatory genes for a role in embryonic stem cell differentiation, namely our gene of interest, Brf1.

3.1.3 Inducible downregulation of Brf1

Having validated the experimental system, we then introduced the stemloop against Brf1 into the F3-1 clone and again got a high degree of correct recombination (76%) after selection. As we did not see an immediate effect upon Brf1 downregulation, we decided to differentiate the cells into more specialized cells to identify a possible *in vivo* role of Brf1. We could successfully differentiate the CCE cells into cardiomyocytes and then tested for any effect on differentiation when Brf1 is downregulated. This gave the striking observation of altered embryoid body (EB) morphology, and a dramatic increase in the number of beating areas within an EB and the total number of beating bodies compared to the controls. It is possible that the morphological changes in the cells favors the upregulation of the cardiomyogenic program, as correct *in vivo* cardiogenesis needs the presence of endoderm for differentiation of cardiac precursors and migration of the cardiac mesoderm (reviewed in Filipczyk *et al*. 2007)). Therefore, it may be possible that downregulation of Brf1 does not directly guide the cells into cardiomyocytes but rather induces an environment that is favorable for *in vitro* cardiomyogenesis (**Figure 3.2**). Interestingly, the kinetics of cardiomyogenesis was unchanged when compared between control cells, which undergo spontaneous cardiomyogenesis, and cells subjected to Brf1 downregulation. Furthermore, this effect was only observed when Brf1 was downregulated during the first 4 days of differentiation but not when Brf1 downregulation is induced after day 4. Therefore, it may well be that Brf1 activity is required to trigger the appropriate differentiation program by changing the levels of Brf1 target genes in the early onset of differentiation (**Figure 3.2**). As the cardiomyogenic program is tightly regulated and timed,
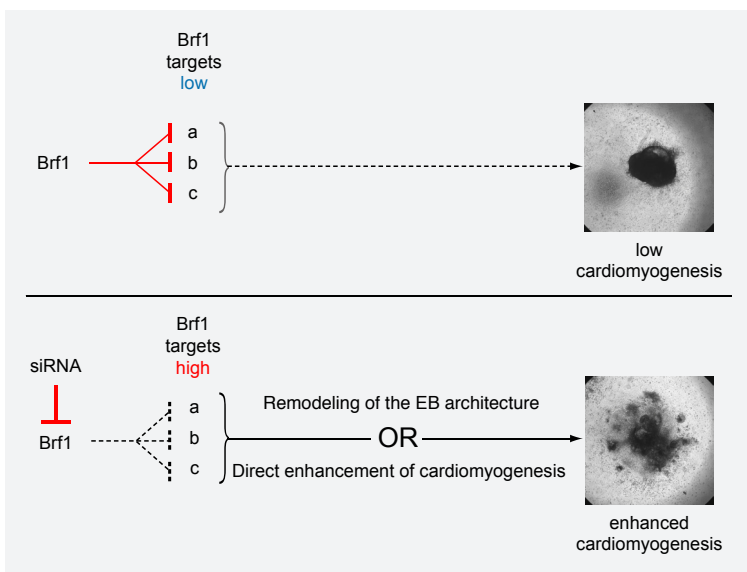
3. Discussion

Figure 3.2: *Model for the role of Brf1 in cardiomyogenesis in CCE ES cells.* In this model, Brf1 destabilizes unidentified, ARE-containing transcripts (a, b, c) that are needed for efficient cardiomyogenesis in CCE ES cells by either altering the morphology of the embryoid body or by directly enhancing the cardiomyogenic process (upper panel). Upon reduction of Brf1 protein levels by RNA interference, these mRNAs (a, b, c) are no longer subjected to degradation, leading to a rapid increase in the steady-state levels of the transcripts and their respective proteins that confer either a change in cytoskeletal architecture of the embryoid body thereby leading indirectly to enhanced cardiomyogenesis, or by directly enhancing cardiomyogenesis (lower panel).

it is important that the genes needed for differentiation are expressed at the critical time point and in precise temporal order. Whether differentiation into other cell types via downregulation of Brf1 is also affected remains to be examined.

Our results also show that doxycycline has a side-effect of enhancing cardiomyogenesis even in cells without a stemloop, which could not be circumvented by decreasing the doxycycline concentration as this also impairs shRNA induction. Nevertheless, the difference between the controls and the cells with the induced Brf1 stemloop is so large as to render the non-specific effect negligible.

The data presented in this thesis indicate that this system shows, depending on the induced shRNA, robust downregulation of the target gene with virtually no leakiness. The results for Brf1 downregulation leads to a model in which Brf1 is a suppressor of pro-differentiation transcripts and is therefore highly expressed in undifferentiated embryonic stem cells. Reductions in its levels, alters the morphology of embryoid bodies and enhances cardiomyocyte formation. As Brf1 is a known destabilizer of ARE-bearing transcripts, its targets should go up when Brf1 levels are decreased and could in our case confer enhanced cardiomyogenesis.

Until they are identified, we cannot at present distinguish whether these mRNAs are either pro-cardiomyogenic factors or favor morphological alterations of the EBs and thereby enhance indirectly cardiomyocyte formation (**Figure 3.2**). The current model for the possible mode of action of Brf1 in cardiomyogenesis is for the time being only valid for our CCE ES cells. It has yet to be tested in other ES cell lines, and a recent report in fact states that blocking the Jak2-Stat3 pathway in CCE ES cells leads to diminished cardiomyocyte development (Foshay *et al.* 2005). In this study, the CCE ES cells used had a high baseline for cardiomyogenesis (~80%, only ~20% in our case), with high Jak2 and Stat3 active protein levels in beating

versus non-beating embryoid bodies. Upon blocking of Jak2 with an inhibitor (AG490) or by blocking Stat3 by a dominant negative form (Stat3β), less beating was observed. These data may on the surface appear contradictory to our observation that decreased Brf1 levels enhance cardiomyogenesis as Stat3 seems to be the major regulator of Brf1 and blocking Stat3 leads to reduced Brf1 expression. However, in the Foshay *et al.* study, the chemical inhibitor was added after the embryoid bodies had formed at the time of plating, which is beyond the 4-day time-window in which we downregulated Brf1. The dominant-negative Stat3 form used is also of human and not mouse origin, which could conceivably generate some unintended consequences. Most importantly, Jak2 and Stat3 are upstream of Brf1 and regulate many other genes, which may have led to their observations. For this reason, both findings could be true, although one has still to keep in mind the big difference in baseline cardiomyogenesis between their CCE cells and ours, which could be due to the unbalanced karyotype of our cells. Nonetheless, it is also possible that other known transcription factors in ES cells, such as Oct4/Sox2 or Nanog, may play an important role in the regulation of Brf1 in cardiomyogenesis, as it has been found that these factors bind to the Brf1 promoter in human cells (Boyer *et al.* 2005).

A further problem for any future investigations using the CCE ES cell line is that we were unable to properly differentiate them into hematopoietic cells, and the laboratory of Prof. Yves-Alain Barde at the Biozentrum, was also unable to differentiate these cells into neurons. Attempts to generate transgenic mice with these cells at the Transgenic Core Mouse Facility (TCMF) at the Biozentrum were also unsuccessful due to a failure to form chimeras. Unfortunately, even the unmodified CCE ES cell line is karyotypically abnormal, and most cells do not have 40 chromosomes and carry a visible translocation (**Figu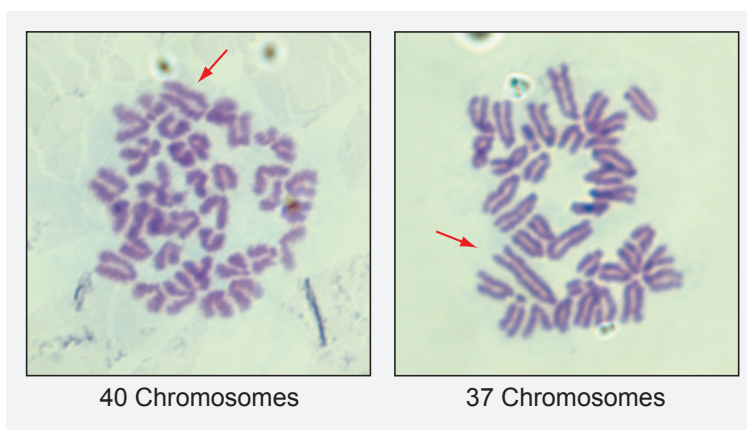re 3.3**). This leads to the need for re-establishing the system in another ES cell line that is capable of giving chimeras and going germ line. The R1 ES cell line (Nagy *et al.* 1993) was recommended by the TCMF as commonly used by them for successful transgenic mouse production. After establishing culture conditions for this cell line, we are now in the process of screening for clones stably expressing the Tet repressor and containing the frt-EGFP integration site for recombination of inducible stemloops. Upon verification of the system with Stat3 shRNA, it

40 Chromosomes   37 Chromosomes

Figure 3.3: *Karyotype of CCE cells.* Representative karyotype of the CCE cells is shown. Chromosome numbers ranged from 27 to 42. In all cells analyzed, a chromosomal translocation was seen (red arrow). (Karyotype analysis was performed by the Transgene Mouse Core Facility of the Biozentrum.)

will then be used to re-investigate the role of Brf1 in cardiomyogenesis in comparison with the CCE ES cells. It is possible that in another cell line, a decrease in Brf1 could lead to the opposite effect as observed in the CCE ES cells, similar to that reported by Foshay et al. (Foshay *et al*. 2005). As stated previously, this may be due to the unbalanced karyotype of the CCE cells, which may therefore be defective in differentiation into other cell types as observed for hematopoietic cells or neurons. Having set up the system in the R1 ES cell line, we would then be in a position to investigate the effects of Brf1 on differentiation into other lineages. In addition, it would also be worthwhile to make a transgenic mouse from the R1 cells, as it would then be possible to downregulate Brf1, or any other protein, at a given time point. Therefore, it would be possible to investigate the effects of downregulation on later embryonic developmental stages, or even in adult mice. This is particularly pertinent in the case of Brf1, where one can now circumvent the problem of embryonic lethality in Brf1 knockout mice (Stumpo *et al*. 2004).
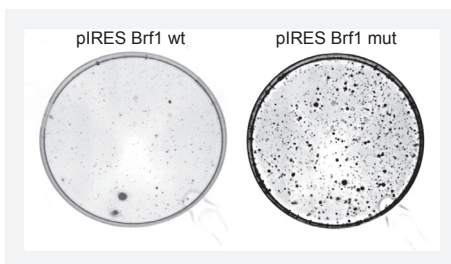

Figure 3.4: *Brf1 overexpression in ES cells.* CCE cells were transfected with Brf1 wildtype (pIRES Brf1 wt) or Brf1 zinc-finger mutant (pIRES Brf1 mut) (Stoecklin *et al.* 2002) and selected for 10 days with puromycin. Note the drastic inhibitory effect of wildtype Brf1 compared with the zinc-finger mutant, which is unable to bind mRNA. (This Figure forms Supplementary Figure 5 in the Stem Cells paper on page 84)

Theoretically, it should also be possible to use this system to inducibly overexpress any gene in R1 cells containing the Tet repressor and the frt-EGFP recombination site. It would also be extremely interesting to investigate the effects of inducible overexpression of Brf1, as inducibility could overcome the problem that continuous high overexpression of Brf1 is toxic for ES cells as was observed in early experiments (**Figure 3.4**). As Brf1 expression can be pulsed by adding doxycycline to the cells, the effects of Brf1 overexpression can also be observed at any chosen period of differentiation. This opens the possibility of checking whether overexpression of Brf1 leads to the opposite effect observed upon its downregulation.

As this system can also be used in human cells, it may prove useful for regenerative medicine. If, for example, Brf1 may also be involved in cardiomyocyte formation in human ES cells, it could be of use in replacement therapy to enhance cardiomyogenesis by altering Brf1 levels in order to replace damaged cardiac muscle. As spontaneous cardiomyocyte differentiation is very low in human ES cells (Laflamme *et al*. 2007) and requires a cocktail of different cytokines to enhance cardiomyogenesis, downregulation of Brf1 may present an alternative way to enhance this process. A problem with regard to the inducibility of this system could be that the stemloop (or gene overexpression as the case may be) is activated by addition of doxycycline. As doxycycline is an analogue of tetracycline, a broadband antibiotic, it can lead

to unwanted effects if the system in these cells is reactivated upon antibiotic therapy. Therefore, it would be necessary for the cassette to be excised from the frt locus to render the system permanently disabled, which is theoretically possible.

3.2 Gene expression analysis of CCE cells

The DNA microarray chip analysis performed to discover ARE-bearing transcripts elevated upon LIF removal or Brf1 downregulation did not identify any transcripts fulfilling these criteria (increased expression, presence of a 3'UTR ARE). As several such transcripts were found in an earlier microarray experiment, it was somewhat disappointing that we could not confirm these initial data. A major difference between the two experiments was that in the original experiment, siRNA and not shRNA, was used to transfect unmodified CCE cells. As siRNA is known to trigger off-target effects (Jackson *et al.* 2003), this may have given rise to different sets of altered genes in the chip analysis. In any case, a set of ARE-bearing transcripts was identified that were upregulated upon Brf1 downregulation in the initial experiment, although caution should be exercised in accepting this as definitive, as they were not present in the later shRNA experiment. Another reason could be the condition of the cells used for the later experiment as stocks were not freshly thawed for each independent repetition of the samples, and it is possible that the efficiency of Brf1 downregulation was variable between the samples. In addition, the single tested time point (3 days post-induction), could be either too early or late to observe the immediate effects that Brf1 may be having on its target AREs that change upon differentiation.

To definitively identify *in vivo* targets of Brf1, it would be necessary to rigorously define the best sampling points and experimental setup – normal, unguided vs. cardiomyogenic differentiation – in order to answer this question. It would also be necessary with regard to normal, unguided differentiation to perform a time course experiment over several days for mRNA isolation and concomitant chip analysis. For cardiomyogenic differentiation, it would be worth taking two time points during the critical first 4 days followed by a later one – at around day 7 or 8 – for the analysis.

It may also be helpful to first check the consequence of a change in Brf1 levels on EGFP expression in cells expressing an EGFP-IL3-3'UTR reporter (explained in the next section) in order to get an idea as to when downregulation of Brf1 has an effect on possible targets.

3.3 ARE-mRNA reporter stability in ES cells

To answer the question if ARE-dependent posttranscriptional regulation is also active in ES cells, CCE-F3-1-B14 and R1 cells were stably transfected with an EGFP vector carrying

either the wild-type IL-3 ARE or a functionally disabled mutant (3a). FACS analysis for EGFP expression gave the expected result of higher expression in the EGFP-3a transfected cells, which may reflect the greater stability of the reporter transcript. This agrees with our published data, as the same effect on EGFP reporter expression was consistently observed in other mouse or human cells (Stoecklin *et al*. 2002; Stoecklin *et al*. 2003b), namely higher fluorescence with the 3a mutant. In addition, the slightly increased EGFP level upon induced downregulation of Brf1 in CCE-F3-1-B14 cells transfected with the EGFP-wildtype construct also accords with previous experiments where an EGFP-IL3wt reporter was stabilized upon siRNA downregulation of endogenous BRF1 (Stoecklin *et al*. 2002; Raineri *et al*. 2004). These results concerning the posttranscriptional regulation of ARE-containing transcripts are still preliminary, but they hint that this regulatory mechanism is active in ES cells. Nevertheless, final confirmation awaits the results of actinomycin D time chase experiments to evaluate mRNA stability in cells with the EGFP-IL3-3a or -wt construct.

As this important mechanism has been demonstrated to function in many cell types (Stoecklin *et al*. 1994; DeMaria and Brewer 1996; Fan and Steitz 1998; Raineri *et al*. 2004), it is plausible that it could also be essential in ES cells to quickly change mRNA levels during differentiation. Therefore, it is important to determine if the AUBPs present in ES cells are in fact promoting ARE-mediated rapid mRNA decay.

This would open a new view on gene regulation in ES cells as until now, it is exclusively regarded from the viewpoint of signaling pathways that act on transcription factors to regulate gene expression. But as cell fate decisions can occasionally require a fast response, it may well be possible that there are other mechanisms needed to fine tune gene expression on the post-transcriptional level.

3.4 Final remarks and Outlook

The work presented in this thesis shows that Brf1 expression is controlled by Stat3 and proposes a model as to how Brf1 may be involved in *in vitro* cardiomyogenesis in our CCE ES cells (**Figure 3.2**), but many questions remain to be answered in the future. The present model is only valid for our CCE ES cell line, and as we would like to validate these findings, we are therefore establishing the system in another ES cell line (R1). We belief, as the R1 cell line is karyotypically normal and is able to be successfully guided into different cell types by in vitro differentiation, that we will then be able to find additional roles for Brf1 in other differentiation pathways besides the cardiomyogenic. Additionally, we hope to be able to answer the remaining questions with this cell line, namely identifying *in vivo*, ARE-containing targets of Brf1 and how they may be involved in the differentiation pathways.

This work also presents the development of a system to inducibly downregulate genes, in

the present instance Stat3 and Brf1, with almost no leakiness. To really display the robustness of this system, we would like to generate transgenic mice to confirm *in vivo* functionality of the inducible system. This will be of course require the prior construction of an inducible R1 ES cell line which is currently underway.

Preliminary results show the first hints that ARE-dependent mRNA regulation may also play a role in murine ES cells. As this has only been shown at the protein level, mRNA decay experiments have still to be performed to prove that the regulation is indeed acting posttranscriptionally at the level of mRNA turnover.

By further characterizing the role of Brf1 in embryonic stem cells, we can hopefully assign an *in vivo* function as well as targets to Brf1, and show that ARE-dependent posttranscriptional regulation is also an important mechanism in murine ES cells.

4. MATERIALS AND METHODS

Cell culture

CCE ES cells (Robertson *et al*. 1986; Keller *et al*. 1993) were cultured on gelatin-coated dishes in 250U/ml LIF (Chemicon) containing medium, consisting of high glucose DMEM (Sigma) supplemented with 15% fetal calf serum (Invitrogen), 2mM L-glutamine (Stem Cell Technologies), 0.1mM non-essential amino acids (Stem Cell Technologies), 1mM sodium pyruvate (Stem Cell Technologies) and 100μM monothioglycerol (Sigma). All cells were incubated at 37°C with 5% CO_2. Cells were frozen in medium containing 50% FCS, 40% culture medium and 10% DMSO (Sigma). Experiments with CCE-TR-FRT cells (see below) were performed in ES medium containing 100U/ml LIF in the presence or absence of 2μg/ml doxycycline (Dox).

To generate cardiomyocytes from EBs, ES cells were cultured for two days in hanging drops, followed by a two-day suspension culture. Then, 30 or 2 EBs were plated into either gelatin-coated 24- or 48-well plates, respectively, and cultured for 24 hours in maintenance medium containing IMDM (Sigma), 20% FCS (Gibco), 2mM L-glutamine (Stem Cell Technologies), 0.1mM non-essential amino acids (Stem Cell Technologies) and 100μM monothioglycerol (Sigma) to allow attachment of EBs to the culture dish. Thereafter, cells were kept for 48 hours in starvation medium consisting of maintenance medium supplemented with only 0.2% FCS, followed by culture in supplemented medium, corresponding to maintenance medium containing SRM2 (Sigma) instead of FCS.

R1 ES cells (Nagy *et al*. 1993) were cultured on mouse embryonic feeder (MEF) cells in the same medium as described for CCE ES cells except instead of 100μM monothioglycerol 50 mM 2-mercaptoethanol (Gibco) was used.

MEF cells were made according the protocol of Nagy *et al*. (Nagy *et al*. 2003). The feeder cells were treated for 1h with 10μg/ml mitomycin C and thoroughly washed before plating R1 ES cells onto them.

To generate hematopoietic cells, R1 cells were harvested and replated for 40 minutes to get rid of the feeder cells. The ES cells were then resuspended in IMDM (Sigma) containing 10% FCS, counted and diluted to 5x10^4 cells/ml. Prepare a methylcellulose medium containing: 1% Basic methylcellulose (StemCell Technologies), 15% FCS, 2mM L-Glutamine, 50mM 2-Mercatpoethanol, 40ng/ml murine Stem Cell Factor (mSCF), IMDM. Add 5000 cells/ml Methylcellulose mix and plate 1ml per 35mm dish. After 7 days primary cultures were fed either with the medium described above supplemented to a final concentration of 0,5% methylcellulose, 15% FCS, 50mM 2-mercaptoethanol, 160ng/ml mSCF, 30ng/ml murine Interleukin-3, 20ng/ml murine Interleukin-6, 3U/ml human Erythropoietin, IMDM, or embryoid bodies were plated

into gelatinized 24-well plates into IMDM containing the same supplements as above. Cells in methylcellulose were cultured for another 4 days then resuspended by incubating for 5-10 minutes in Trypsin-EDTA and plated into gelatinized 24-well plates into IMDM containing the same supplements as above.

Plasmids

Tet repressor plasmid (pCAG-TR-IRESpuro3) (Figure 4.1A): pCAG and pIRESpuro3 (Clontech) plasmids were digested (SpeI and EcoRI) and the IRESpuro3 fragment ligated into pCAG. Digestion of pcDNA6/TR (Invitrogen) vector (AflII, blunt ending, NotI) releases the TR-IVS insert. This fragment was cloned into pCAG-IRESpuro3 digested by NotI.

To generate the FRTd2EGFP plasmid (pCAG-FRTd2EGFP-IRESneo3) (Figure 4.1B), the d2EGFP was amplified without the start codon from pd2EGFP-N1 (Clontech) with BglII and NotI linkers. The CAG promoter was cut from pCAG with EcoRI and SpeI and ligated with an oligo containing an ATG, a FRT site (McLeod *et al*. 1986), EcoRI and BglII linkers to the d2EGFP fragment. This insert was finally inserted into pIRESneo3 (Clontech) digested with SpeI and NotI.

To generate shRNA plasmids (pTER-shRNA-FRT) (Figure 4.1C) the shRNAs (Stat3, Brf1) were cloned into pTER-Ni (van de Wetering *et al*. 2003) using BglII and HindIII. Plasmids were opened with NsiI and SapI and blunted, followed by insertion of an FRT-Hygro-SV40pA fragment from pcDNA5/FRT (Invitrogen) digested with PvuII.

To generate the flipase plasmid (pCAG-Flipase) (Figure 4.1D), flipase was PCR amplified from the pOG44 vector (Invitrogen) and the product digested with BsaI and blunt ended (IVS-Flipase-pA) and was then inserted into pCAG vector opened with HindIII and blunt ended.

pMS-EGFP, -IL3 wt and IL3 3avectors (Figure 4.2): The pMSCVpuro (Clontech) vector was cut with XhoI and EcoRI and a linker with two different SfiI sites was ligated into the digested vector. EGFP was PCR amplified from pEGFP-N1 (Clontech) with primers containing the SfiI restriction sites for directed cloning. The IL3 wildtype (wt) or mutated (3a) 3'UTR (Stoecklin *et al*. 1994) was amplified with primers containing NotI and EcoRI linkers and ligated behind the EGFP in the pMS-EGFP vector previously digested with NotI and EcoRI.

Transient and stable transfection of CCE cells

All transfections of CCE ES cells were done using Lipofectamine 2000 according to the standard protocol from Invitrogen; however, cells were incubated with liposome/plasmid complexes for only 3 h at 37°C/5% CO_2.

For generation of cells exhibiting Dox inducible expression of shRNAs, CCE ES cells

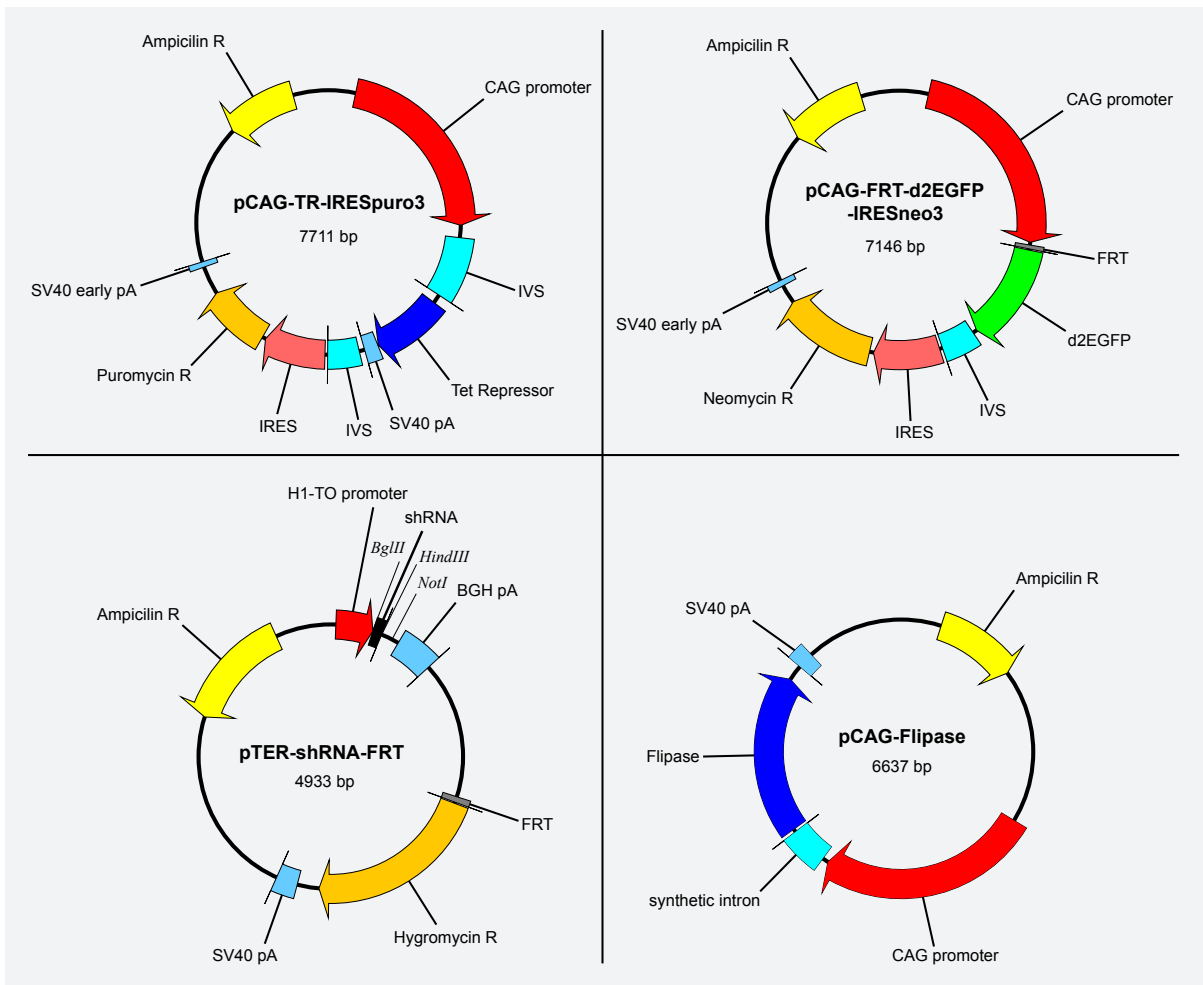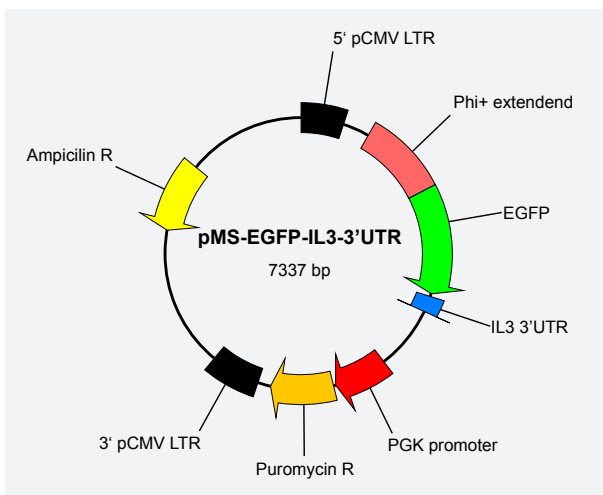**Figure 4.1:** *Plasmids of the inducible RNAi system.*

Figure 4.2: *Retroviral EGFP-IL3 3'UTR plasmid.*

were first transfected with the pCAG-TR-IRESpuro3 vector and selected with 1µg/ml puromycin (Calbiochem). Clones were identified by Western blot with mouse anti-TR monoclonal Antibody Mix (MoBiTec). A high expressing clone (TR8) was chosen for further transfection with pCAG-FRT-EGFP-IRESneo3. Selection was done with Geneticin (Gibco) at a concentration of 600 µg/ml.

Recombination of shRNA was done by co-transfection of the flipase containing vector (pCAG-Flipase) and the vector containing the shRNA (pTER-shRNA-FRT). Cells were then selected with hygromycin (Calbiochem) at a concentration of 165 U/ml. Cells were then further screened for loss of both GFP and G418 resistance.

Stable transfection of R1 cells

All R1 ES cells were electroporated using an Equibio EasyjecT Plus set to single pulse with 220 Volts and 450 μF. 3 times 10^7 cells were transfected with 30μg plasmid DNA per electroporation. First, the pCAG-FRT-EGFP-IRESneo3 was transfected and cells were selected with 150μg/ml Geneticin. By a second electroporation pCAG-TR-IRESpuro3 was transfected and cells were selected with 1 μg/ml puromycin.

Viral infection of CCE and R1 cells

Viral supernatants with pMS-EGFP vectors were produced with the Platinum-E packaging cell line (Morita *et al*. 2000). Supernatants were stabilized with Polybrene (Fluka) and added to the cells for 4 hours for infection followed by a medium change to normal DMEM maintenance medium. 24 hours after infection cells were selected with puromycin (CCE-B14: 2μg/ml; R1: 1μg/ml).

shRNA, siRNA and primers

Murine Stat3 specific oligonucleotides (5' GAT CTG AGT CAC ATG CCA CGT TGG TTC AAG AGA CCA ACG TGG CAT GTG ACT CTT TTT A 3', and 5' AGC TTA AAA AGA GTC ACA TGC CAC GTT GGT CTC TTG AAC CAA CGT GGC ATG TGA CTC A 3')

murine Stat3 siRNA: 5' GAG UCA CAU GCC ACG UUG G (XM_109608)

control siRNA (human β-globin): 5' CAA GAA AGU GCU CGG UGC C (V00497.1)

murine Brf1 specific oligonucleotides (5' GAT CTG TCC GAA TCC CCT CAC ATG TTC AAG AGA CAT GTG AGG GGA TTC GGA CTT TTT A 3', and 5' AGC TTA AAA AGT CCG AAT CCC CTC ACA TGT CTC TTG AAC ATG TGA GGG GAT TCG GAC A 3')

murine Stat3 primer 5' AGT CAC ATG CCA CGT TGG T 3'

murine α-cardiac actin PCR primers (forward 5' GCT TTG GTG TGT GAC AAT 3' GG, reverse 5' GTG ATA ATG CCA TGT TCA ATG G 3')

murine Nkx2.5 PCR primers (forward 5' CGG AAC GAC TCC CAC CTT TAG G 3', reverse 5' GGA ATC CGT CGA AAG TGC CC 3')

murine Gata4 PCR primers (forward 5' CGA GAT GGG ACG GGA CAC T 3', reverse 5' CTC ACC CTC GGC CAT TAC GA 3')

murine myogenin PCR primers (forward 5' ACA AGC CAG ACT CCC CAC TC 3', reverse 5' GCA CTC ATG TCT CTC AAA CGG T 3')

murine GAPDH PCR primers (forward 5' CAC CAC CAA CTG TTA GCC 3', reverse 5' CCT GCT TCAC CAC CTT CTT G 3')

murine 18S rRNA primers (forward 5' CGG CTA CCA CAT CCA AGG AA 3', reverse 5' GCT GGA ATT ACC GCG GCT 3')

Primers for nested PCR:

Primer a (outer: GCT GTA ATT AGC GCT TGG T, inner: CTT TGT CCC AAA TCT GTG C)

Primer b (outer: GTA TTG ACC GAT TCC TTG C, inner: GAA AGC ACG AGA TTC TTC G)

Primer c (outer: CGC ATC TAC ACATTG ATC C, inner: GTT GTA GTT GTA CTC CAG C)

Primer c (outer: GAC TCT TGT TCC AAA CTG G, inner: AGG CAG AAG TAT GCA AAG C)

Northern blot

Total RNA was harvested using Trizol (Invitrogen). To detect Brf1, Oct4, Rex-1, Fgf-4 and β-actin, Northern blots were hybridized overnight with [α^{32}P]-dCTP labeled PCR fragments generated from cDNA of the aforementioned genes (Brf1: nt 945-1328 #M58566; GAPDH, nt 589–1246, #M33197; β-actin: nt 516-1144 #NM008085; Oct4 nt 731-1101 #NM_013633; Rex-1 nt 687-1059 #NM_009556; Fgf-4 nt 250-583 #NM_010202) (Raineri *et al.* 2004). To analyze expression of shRNA in F3-1-Stat3 and F3-1-Brf1 clones, 30μg of total RNA were separated on 15% polyacrylamide gels containing 8M urea (Anamed). Gels were stained with ethidium bromide to check for equal loading before RNA was transferred by electroblotting onto Hybond-N+ (Amersham) membranes. After UV-crosslinking, filters were hybridized at 45ºC in 0.5M sodium phosphate buffer pH 7.2 containing 1% BSA (Fraction V, Sigma), 7% SDS and 5mM EDTA using a [γ^{32}P]-ATP labeled Stat3 or Brf1 specific oligonucleotide of 19 nucleotides. Blots were analyzed using the Personal Molecular Imager® FX (Biorad) and the Quantity One® software.

Western blot

The Western blot protocol employed and generation of Brf1 antibodies has recently been described (Raineri *et al.* 2004). A monoclonal anti-TR antibody mix (MoBiTec) was used to detect expression of the Tet repressor. A monoclonal antibody against α-tubulin (Clone 236-10501, Molecular Probes) was used. Stat3 (Cell Signaling), Nkx2.5 (Clone N-19, Santa Cruz Biotechnology, Inc.), Gata4 (Clone H-112, Santa Cruz Biotechnology, Inc.) and HRP-coupled GAPDH (Abcam) polyclonal antibodies were utilized. Alkaline phosphatase-coupled goat-anti-rabbit IgG (Southern Biotechnology Associates Inc.) and horseradish peroxidase-coupled

goat-anti-mouse IgG (DAKO) and rabbit anti-goat IgG (Southern Biotechnology Associates Inc.) were used as secondary antibodies. Development was performed using CDP-Star (Roche) or ECL Advance (Amersham).

Flow Cytometry

All fluorescence activated cell sorting (FACS) was performed on a Beckton-Dickinson FACSCalibur using CellQuest Software.

DNA microarray analysis

2μg of total RNA was purified using the RNeasy Mini Kit (Qiagen) and reverse transcribed and purified using the Affymetrix one-cycle cDNA synthesis kit (Affymetrix, CA, USA) as per the manufacturer's instructions. Labeled cRNA was produced using the Affymetrix IVT Labeling Kit (Affymetrix). Nucleic acid concentrations were quantified using Nanodrop and RNA quality was determined with an Agilent 2100 Bioanalyzer. 15μg of fragmented cRNA were loaded onto Affymetrix MOE430v2 GeneChips and scanned using an Affymetrix GeneChip 3000 7G scanner. The CEL files were quality controlled using Genedata's Refiner 3.1 program (Genedata AG, Basel, Switzerland). Expression values and detection P-values were estimated using Genedata's implementation of GCRMA (Wu *et al.*; Nat Biotechnol, 2004, 656-8) in Refiner 3.1. Data analysis was performed using Analyst 3.1 (Genedata AG). Experiments were performed in triplicate and for a gene to be considered it had to have a detection P-value < 0.04 in at least 2/3 of the replicates of one or more condition.

Microscopy

A Nikon Eclipse TE200 microscope equipped with a Hamamatsu digital camera (C4742-95) was used, all pictures were made at a 40X magnification. Beating areas were marked under live-microscopy using Openlab 2.2 Software (Improvision) allowing quantification.

5. REFERENCES

Allmang, C., J. Kufel, G. Chanfreau, P. Mitchell, E. Petfalski and D. Tollervey (1999). "Functions of the exosome in rRNA, snoRNA and snRNA synthesis." Embo J 18(19): 5399-410.

Astrom, J., A. Astrom and A. Virtanen (1992). "Properties of a HeLa cell 3' exonuclease specific for degrading poly(A) tails of mammalian mRNA." J Biol Chem 267(25): 18154-9.

Avilion, A. A., S. K. Nicolis, L. H. Pevny, L. Perez, N. Vivian and R. Lovell-Badge (2003). "Multipotent cell lineages in early mouse development depend on SOX2 function." Genes Dev 17(1): 126-40.

Bakheet, T., M. Frevel, B. R. Williams, W. Greer and K. S. Khabar (2001). "ARED: human AU-rich element-containing mRNA database reveals an unexpectedly diverse functional repertoire of encoded proteins." Nucleic Acids Res 29(1): 246-54.

Bakheet, T., B. R. Williams and K. S. Khabar (2003). "ARED 2.0: an update of AU-rich element mRNA database." Nucleic Acids Res 31(1): 421-3.

Bartek, J. and J. Lukas (2001). "Pathways governing G1/S transition and their response to DNA damage." FEBS Lett 490(3): 117-22.

Ben-Shushan, E., J. R. Thompson, L. J. Gudas and Y. Bergman (1998). "Rex-1, a gene encoding a transcription factor expressed in the early embryo, is regulated via Oct-3/4 and Oct-6 binding to an octamer site and a novel protein, Rox-1, binding to an adjacent site." Mol Cell Biol 18(4): 1866-78.

Benjamin, D., M. Schmidlin, L. Min, B. Gross and C. Moroni (2006). "BRF1 protein turnover and mRNA decay activity are regulated by protein kinase B at the same phosphorylation sites." Mol Cell Biol 26(24): 9497-507.

Benjamin, D. and C. Moroni (2007). "mRNA stability and cancer: an emerging link?" Expert Opin Biol Ther 7(10): 1515-29.

Bernstein, P., S. W. Peltz and J. Ross (1989). "The poly(A)-poly(A)-binding protein complex is a major determinant of mRNA stability in vitro." Mol Cell Biol 9(2): 659-70.

Blaxall, B. C., A. Pende, S. C. Wu and J. D. Port (2002). "Correlation between intrinsic mRNA stability and the affinity of AUF1 (hnRNP D) and HuR for A+U-rich mRNAs." Mol Cell Biochem 232(1-2): 1-11.

Boeuf, H., C. Hauss, F. D. Graeve, N. Baran and C. Kedinger (1997). "Leukemia inhibitory factor-dependent transcriptional activation in embryonic stem cells." J Cell Biol 138(6): 1207-17.

Boeuf, H., K. Merienne, S. Jacquot, D. Duval, M. Zeniou, C. Hauss, B. Reinhardt, Y. Huss-Garcia, A. Dierich, D. A. Frank, A. Hanauer and C. Kedinger (2001). "The ribosomal S6 kinases, cAMP-responsive element-binding, and STAT3 proteins are regulated by different leukemia inhibitory factor signaling pathways in mouse embryonic stem cells." J Biol Chem 276(49): 46204-11.

Boheler, K. R., J. Czyz, D. Tweedie, H. T. Yang, S. V. Anisimov and A. M. Wobus (2002). "Differentiation of pluripotent embryonic stem cells into cardiomyocytes." Circ Res 91(3): 189-201.

Boiani, M. and H. R. Scholer (2005). "Regulatory networks in embryo-derived pluripotent stem cells." Nat Rev Mol Cell Biol 6(11): 872-84.

Boyer, L. A., T. I. Lee, M. F. Cole, S. E. Johnstone, S. S. Levine, J. P. Zucker, M. G. Guenther, R. M. Kumar, H. L. Murray, R. G. Jenner, D. K. Gifford, D. A. Melton, R. Jaenisch and R. A. Young (2005). "Core transcriptional regulatory circuitry in human embryonic stem cells." Cell 122(6): 947-56.

Bradley, A., P. Hasty, A. Davis and R. Ramirez-Solis (1992). "Modifying the mouse: design and desire." Biotechnology (N Y) 10(5): 534-9.

Brewer, G. and J. Ross (1988). "Poly(A) shortening and degradation of the 3' A+U-rich sequences of human c-myc mRNA in a cell-free system." Mol Cell Biol 8(4): 1697-708.

Brewer, G. (1991). "An A + U-rich element RNA-binding factor regulates c-myc mRNA stability in vitro." Mol Cell Biol 11(5): 2460-6.

Brinster, R. L. (1974). "The effect of cells transferred into the mouse blastocyst on subsequent development." J Exp Med 140(4): 1049-56.

Brown, C. E. and A. B. Sachs (1998). "Poly(A) tail length control in Saccharomyces cerevisiae occurs by message-specific deadenylation." Mol Cell Biol 18(11): 6548-59.

Brummelkamp, T. R., R. Bernards and R. Agami (2002). "A system for stable expression of short interfering RNAs in mammalian cells." Science 296(5567): 550-3.

Burdon, T., C. Stracey, I. Chambers, J. Nichols and A. Smith (1999). "Suppression of SHP-2 and ERK signalling promotes self-renewal of mouse embryonic stem cells." Dev Biol 210(1): 30-43.

Burdon, T., A. Smith and P. Savatier (2002). "Signalling, cell cycle and pluripotency in embryonic stem cells." Trends Cell Biol 12(9): 432-8.

Carballo, E., W. S. Lai and P. J. Blackshear (1998). "Feedback inhibition of macrophage tumor necrosis factor-alpha production by tristetraprolin." Science 281(5379): 1001-5.

Cartwright, P., C. McLean, A. Sheppard, D. Rivett, K. Jones and S. Dalton (2005). "LIF/STAT3 controls ES cell self-renewal and pluripotency by a Myc-dependent mechanism." Development 132(5): 885-96.

Chambers, I., D. Colby, M. Robertson, J. Nichols, S. Lee, S. Tweedie and A. Smith (2003). "Functional expression cloning of Nanog, a pluripotency sustaining factor in embryonic stem cells." <u>Cell</u> 113(5): 643-55.

Chang, H. S., C. H. Lin, Y. C. Chen and W. C. Yu (2004). "Using siRNA technique to generate transgenic animals with spatiotemporal and conditional gene knockdown." <u>Am J Pathol</u> 165(5): 1535-41.

Chen, C. Y. and A. B. Shyu (1995). "AU-rich elements: characterization and importance in mRNA degradation." <u>Trends Biochem Sci</u> 20(11): 465-70.

Chen, C. Y., R. Gherzi, S. E. Ong, E. L. Chan, R. Raijmakers, G. J. Pruijn, G. Stoecklin, C. Moroni, M. Mann and M. Karin (2001). "AU binding proteins recruit the exosome to degrade ARE-containing mRNAs." <u>Cell</u> 107(4): 451-64.

Cheng, L. C., M. Tavazoie and F. Doetsch (2005). "Stem cells: from epigenetics to microRNAs." <u>Neuron</u> 46(3): 363-7.

Chinn, A. M., D. Ciais, S. Bailly, E. Chambaz, J. LaMarre and J. J. Feige (2002). "Identification of two novel ACTH-responsive genes encoding manganese-dependent superoxide dismutase (SOD2) and the zinc finger protein TIS11b [tetradecanoyl phorbol acetate (TPA)-inducible sequence 11b]." <u>Mol Endocrinol</u> 16(6): 1417-27.

Chung, S., T. Andersson, K. C. Sonntag, L. Bjorklund, O. Isacson and K. S. Kim (2002). "Analysis of different promoter systems for efficient transgene expression in mouse embryonic stem cell lines." <u>Stem Cells</u> 20(2): 139-45.

Ciais, D., N. Cherradi, S. Bailly, E. Grenier, E. Berra, J. Pouyssegur, J. Lamarre and J. J. Feige (2004). "Destabilization of vascular endothelial growth factor mRNA by the zinc-finger protein TIS11b." <u>Oncogene</u> 23(53): 8673-80.

Corps, A. N. and K. D. Brown (1995). "Insulin and insulin-like growth factor I stimulate expression of the primary response gene cMG1/TIS11b by a wortmannin-sensitive pathway in RIE-1 cells." <u>FEBS Lett</u> 368(1): 160-4.

Coumoul, X., W. Li, R. H. Wang and C. Deng (2004). "Inducible suppression of Fgfr2 and Survivin in ES cells using a combination of the RNA interference (RNAi) and the Cre-LoxP system." <u>Nucleic Acids Res</u> 32(10): e85.

Dehlin, E., M. Wormington, C. G. Korner and E. Wahle (2000). "Cap-dependent deadenylation of mRNA." <u>Embo J</u> 19(5): 1079-86.

DeMaria, C. T. and G. Brewer (1996). "AUF1 binding affinity to A+U-rich elements correlates with rapid mRNA degradation." <u>J Biol Chem</u> 271(21): 12179-84.

Dempsey, L. A., L. A. Hanakahi and N. Maizels (1998). "A specific isoform of hnRNP D interacts with DNA in the LR1 heterodimer: canonical RNA binding motifs in a sequence-specific duplex DNA binding protein." <u>J Biol Chem</u> 273(44): 29224-9.

Denis, C. L. and J. Chen (2003). "The CCR4-NOT complex plays diverse roles in mRNA metabolism." <u>Prog Nucleic Acid Res Mol Biol</u> 73: 221-50.

Denkert, C., I. Koch, N. von Keyserlingk, A. Noske, S. Niesporek, M. Dietel and W. Weichert (2006). "Expression of the ELAV-like protein HuR in human colon cancer: association with tumor stage and cyclooxygenase-2." Mod Pathol 19(9): 1261-9.

Dixon, D. A., N. D. Tolley, P. H. King, L. B. Nabors, T. M. McIntyre, G. A. Zimmerman and S. M. Prescott (2001). "Altered expression of the mRNA stability factor HuR promotes cyclooxygenase-2 expression in colon cancer cells." J Clin Invest 108(11): 1657-65.

Doetschman, T. C., H. Eistetter, M. Katz, W. Schmidt and R. Kemler (1985). "The in vitro development of blastocyst-derived embryonic stem cell lines: formation of visceral yolk sac, blood islands and myocardium." J Embryol Exp Morphol 87: 27-45.

DuBois, R. N., M. W. McLane, K. Ryder, L. F. Lau and D. Nathans (1990). "A growth factor-inducible nuclear protein with a novel cysteine/histidine repetitive sequence." J Biol Chem 265(31): 19185-91.

Elbashir, S. M., J. Harborth, W. Lendeckel, A. Yalcin, K. Weber and T. Tuschl (2001a). "Duplexes of 21-nucleotide RNAs mediate RNA interference in cultured mammalian cells." Nature 411(6836): 494-8.

Elbashir, S. M., W. Lendeckel and T. Tuschl (2001b). "RNA interference is mediated by 21- and 22-nucleotide RNAs." Genes Dev 15(2): 188-200.

Ernst, M., U. Novak, S. E. Nicholson, J. E. Layton and A. R. Dunn (1999). "The carboxyl-terminal domains of gp130-related cytokine receptors are necessary for suppressing embryonic stem cell differentiation. Involvement of STAT3." J Biol Chem 274(14): 9729-37.

Evans, M. J. and M. H. Kaufman (1981). "Establishment in culture of pluripotential cells from mouse embryos." Nature 292(5819): 154-6.

Eversole, A. and N. Maizels (2000). "In vitro properties of the conserved mammalian protein hnRNP D suggest a role in telomere maintenance." Mol Cell Biol 20(15): 5425-32.

Fan, X. C. and J. A. Steitz (1998). "Overexpression of HuR, a nuclear-cytoplasmic shuttling protein, increases the in vivo stability of ARE-containing mRNAs." Embo J 17(12): 3448-60.

Filipczyk, A. A., R. Passier, A. Rochat and C. L. Mummery (2007). "Regulation of cardiomyocyte differentiation of embryonic stem cells by extracellular signalling." Cell Mol Life Sci 64(6): 704-18.

Fire, A., S. Xu, M. K. Montgomery, S. A. Kostas, S. E. Driver and C. C. Mello (1998). "Potent and specific genetic interference by double-stranded RNA in Caenorhabditis elegans." Nature 391(6669): 806-11.

Fluckiger, A. C., G. Marcy, M. Marchand, D. Negre, F. L. Cosset, S. Mitalipov, D. Wolf, P. Savatier and C. Dehay (2006). "Cell cycle features of primate embryonic stem cells." Stem Cells 24(3): 547-56.

Foshay, K., G. Rodriguez, B. Hoel, J. Narayan and G. I. Gallicano (2005). "JAK2/STAT3 directs cardiomyogenesis within murine embryonic stem cells in vitro." <u>Stem Cells</u> 23(4): 530-43.

Gao, M., C. J. Wilusz, S. W. Peltz and J. Wilusz (2001). "A novel mRNA-decapping activity in HeLa cytoplasmic extracts is regulated by AU-rich elements." <u>Embo J</u> 20(5): 1134-43.

Garneau, N. L., J. Wilusz and C. J. Wilusz (2007). "The highways and byways of mRNA decay." <u>Nat Rev Mol Cell Biol</u> 8(2): 113-26.

Gherzi, R., K. Y. Lee, P. Briata, D. Wegmuller, C. Moroni, M. Karin and C. Y. Chen (2004). "A KH domain RNA binding protein, KSRP, promotes ARE-directed mRNA turnover by recruiting the degradation machinery." <u>Mol Cell</u> 14(5): 571-83.

Gingras, A. C., B. Raught and N. Sonenberg (1999). "eIF4 initiation factors: effectors of mRNA recruitment to ribosomes and regulators of translation." <u>Annu Rev Biochem</u> 68: 913-63.

Gossen, M. and H. Bujard (1992). "Tight control of gene expression in mammalian cells by tetracycline-responsive promoters." <u>Proc Natl Acad Sci U S A</u> 89(12): 5547-51.

Gouble, A., S. Grazide, F. Meggetto, P. Mercier, G. Delsol and D. Morello (2002). "A new player in oncogenesis: AUF1/hnRNPD overexpression leads to tumorigenesis in transgenic mice." <u>Cancer Res</u> 62(5): 1489-95.

Hailesellasse Sene, K., C. J. Porter, G. Palidwor, C. Perez-Iratxeta, E. M. Muro, P. A. Campbell, M. A. Rudnicki and M. A. Andrade-Navarro (2007). "Gene function in early mouse embryonic stem cell differentiation." <u>BMC Genomics</u> 8: 85.

Hao, J., T. G. Li, X. Qi, D. F. Zhao and G. Q. Zhao (2006). "WNT/beta-catenin pathway up-regulates Stat3 and converges on LIF to prevent differentiation of mouse embryonic stem cells." <u>Dev Biol</u> 290(1): 81-91.

Hay, N. and N. Sonenberg (2004). "Upstream and downstream of mTOR." <u>Genes Dev</u> 18(16): 1926-45.

Hirano, T., K. Ishihara and M. Hibi (2000). "Roles of STAT3 in mediating the cell growth, differentiation and survival signals relayed through the IL-6 family of cytokine receptors." <u>Oncogene</u> 19(21): 2548-56.

Houbaviy, H. B., M. F. Murray and P. A. Sharp (2003). "Embryonic stem cell-specific MicroRNAs." <u>Dev Cell</u> 5(2): 351-8.

Huarte, J., A. Stutz, M. L. O'Connell, P. Gubler, D. Belin, A. L. Darrow, S. Strickland and J. D. Vassalli (1992). "Transient translational silencing by reversible mRNA deadenylation." <u>Cell</u> 69(6): 1021-30.

Hudson, B. P., M. A. Martinez-Yamout, H. J. Dyson and P. E. Wright (2004). "Recognition of the mRNA AU-rich element by the zinc finger domain of TIS11d." <u>Nat Struct Mol Biol</u> 11(3): 257-64.

Hutvagner, G. and P. D. Zamore (2002). "RNAi: nature abhors a double-strand." <u>Curr Opin Genet Dev</u> 12(2): 225-32.

Iovino, N., M. A. Denti, I. Bozzoni and R. Cortese (2005). "A IoxP-containing pol II promoter for RNA interference is reversibly regulated by Cre recombinase." <u>RNA Biol</u> 2(3): 86-92.

Ivanova, N., R. Dobrin, R. Lu, I. Kotenko, J. Levorse, C. DeCoste, X. Schafer, Y. Lun and I. R. Lemischka (2006). "Dissecting self-renewal in stem cells with RNA interference." <u>Nature</u> 442(7102): 533-8.

Jackson, A. L., S. R. Bartz, J. Schelter, S. V. Kobayashi, J. Burchard, M. Mao, B. Li, G. Cavet and P. S. Linsley (2003). "Expression profiling reveals off-target gene regulation by RNAi." <u>Nat Biotechnol</u> 21(6): 635-7.

Kanellopoulou, C., S. A. Muljo, A. L. Kung, S. Ganesan, R. Drapkin, T. Jenuwein, D. M. Livingston and K. Rajewsky (2005). "Dicer-deficient mouse embryonic stem cells are defective in differentiation and centromeric silencing." <u>Genes Dev</u> 19(4): 489-501.

Keene, J. D. and P. J. Lager (2005). "Post-transcriptional operons and regulons co-ordinating gene expression." <u>Chromosome Res</u> 13(3): 327-37.

Keller, G., M. Kennedy, T. Papayannopoulou and M. V. Wiles (1993). "Hematopoietic commitment during embryonic stem cell differentiation in culture." <u>Mol Cell Biol</u> 13(1): 473-86.

Keller, G. M. (1995). "In vitro differentiation of embryonic stem cells." <u>Curr Opin Cell Biol</u> 7(6): 862-9.

Kim, N. W., M. A. Piatyszek, K. R. Prowse, C. B. Harley, M. D. West, P. L. Ho, G. M. Coviello, W. E. Wright, S. L. Weinrich and J. W. Shay (1994). "Specific association of human telomerase activity with immortal cells and cancer." <u>Science</u> 266(5193): 2011-5.

Kleinsmith, L. J. and G. B. Pierce, Jr. (1964). "Multipotentiality of Single Embryonal Carcinoma Cells." <u>Cancer Res</u> 24: 1544-51.

Korner, C. G. and E. Wahle (1997). "Poly(A) tail shortening by a mammalian poly(A)-specific 3'- exoribonuclease." <u>J Biol Chem</u> 272(16): 10448-56.

LaBonne, C., B. Burke and M. Whitman (1995). "Role of MAP kinase in mesoderm induction and axial patterning during Xenopus development." <u>Development</u> 121(5): 1475-86.

Laflamme, M. A., K. Y. Chen, A. V. Naumova, V. Muskheli, J. A. Fugate, S. K. Dupras, H. Reinecke, C. Xu, M. Hassanipour, S. Police, C. O'Sullivan, L. Collins, Y. Chen, E. Minami, E. A. Gill, S. Ueno, C. Yuan, J. Gold and C. E. Murry (2007). "Cardiomyocytes derived from human embryonic stem cells in pro-survival factors enhance function of infarcted rat hearts." <u>Nat Biotechnol</u> 25(9): 1015-1024.

Lagos-Quintana, M., R. Rauhut, W. Lendeckel and T. Tuschl (2001). "Identification of novel genes coding for small expressed RNAs." <u>Science</u> 294(5543): 853-8.

Lai, W. S., D. J. Stumpo and P. J. Blackshear (1990). "Rapid insulin-stimulated accumulation of an mRNA encoding a proline-rich protein." <u>J Biol Chem</u> 265(27): 16556-63.

Lai, W. S., E. Carballo, J. M. Thorn, E. A. Kennington and P. J. Blackshear (2000). "Interactions of CCCH zinc finger proteins with mRNA. Binding of tristetraprolin-related zinc finger proteins to Au-rich elements and destabilization of mRNA." <u>J Biol Chem</u> 275(23): 17827-37.

Lai, W. S., E. A. Kennington and P. J. Blackshear (2003). "Tristetraprolin and its family members can promote the cell-free deadenylation of AU-rich element-containing mRNAs by poly(A) ribonuclease." <u>Mol Cell Biol</u> 23(11): 3798-812.

Laroia, G., R. Cuesta, G. Brewer and R. J. Schneider (1999). "Control of mRNA decay by heat shock-ubiquitin-proteasome pathway." <u>Science</u> 284(5413): 499-502.

Lau, N. C., L. P. Lim, E. G. Weinstein and D. P. Bartel (2001). "An abundant class of tiny RNAs with probable regulatory roles in Caenorhabditis elegans." <u>Science</u> 294(5543): 858-62.

Lee, R. C. and V. Ambros (2001). "An extensive class of small RNAs in Caenorhabditis elegans." <u>Science</u> 294(5543): 862-4.

Lejeune, F., X. Li and L. E. Maquat (2003). "Nonsense-mediated mRNA decay in mammalian cells involves decapping, deadenylating, and exonucleolytic activities." <u>Mol Cell</u> 12(3): 675-87.

Lin, T., C. Chao, S. Saito, S. J. Mazur, M. E. Murphy, E. Appella and Y. Xu (2005). "p53 induces differentiation of mouse embryonic stem cells by suppressing Nanog expression." <u>Nat Cell Biol</u> 7(2): 165-71.

Liu, H., N. D. Rodgers, X. Jiao and M. Kiledjian (2002). "The scavenger mRNA decapping enzyme DcpS is a member of the HIT family of pyrophosphatases." <u>Embo J</u> 21(17): 4699-708.

Loflin, P., C. Y. Chen and A. B. Shyu (1999). "Unraveling a cytoplasmic role for hnRNP D in the in vivo mRNA destabilization directed by the AU-rich element." <u>Genes Dev</u> 13(14): 1884-97.

Loh, Y. H., Q. Wu, J. L. Chew, V. B. Vega, W. Zhang, X. Chen, G. Bourque, J. George, B. Leong, J. Liu, K. Y. Wong, K. W. Sung, C. W. Lee, X. D. Zhao, K. P. Chiu, L. Lipovich, V. A. Kuznetsov, P. Robson, L. W. Stanton, C. L. Wei, Y. Ruan, B. Lim and H. H. Ng (2006). "The Oct4 and Nanog transcription network regulates pluripotency in mouse embryonic stem cells." <u>Nat Genet</u> 38(4): 431-40.

Lykke-Andersen, J. and E. Wagner (2005). "Recruitment and activation of mRNA decay enzymes by two ARE-mediated decay activation domains in the proteins TTP and BRF-1." <u>Genes Dev</u> 19(3): 351-61.

Maclean, K. N., I. A. McKay and S. A. Bustin (1998). "Differential effects of sodium butyrate on the transcription of the human TIS11 family of early-response genes in colorectal cancer cells." <u>Br J Biomed Sci</u> 55(3): 184-91.

Martin, G. R. (1981). "Isolation of a pluripotent cell line from early mouse embryos cultured in medium conditioned by teratocarcinoma stem cells." Proc Natl Acad Sci U S A 78(12): 7634-8.

Martinez, J., Y. G. Ren, P. Nilsson, M. Ehrenberg and A. Virtanen (2001). "The mRNA cap structure stimulates rate of poly(A) removal and amplifies processivity of degradation." J Biol Chem 276(30): 27923-9.

Matsui, Y., K. Zsebo and B. L. Hogan (1992). "Derivation of pluripotential embryonic stem cells from murine primordial germ cells in culture." Cell 70(5): 841-7.

McLeod, M., S. Craft and J. R. Broach (1986). "Identification of the crossover site during FLP-mediated recombination in the Saccharomyces cerevisiae plasmid 2 microns circle." Mol Cell Biol 6(10): 3357-67.

Min, H., C. W. Turck, J. M. Nikolic and D. L. Black (1997). "A new regulatory protein, KSRP, mediates exon inclusion through an intronic splicing enhancer." Genes Dev 11(8): 1023-36.

Mintz, B. and K. Illmensee (1975). "Normal genetically mosaic mice produced from malignant teratocarcinoma cells." Proc Natl Acad Sci U S A 72(9): 3585-9.

Mitchell, P. and D. Tollervey (2000). "mRNA stability in eukaryotes." Curr Opin Genet Dev 10(2): 193-8.

Mitsui, K., Y. Tokuzawa, H. Itoh, K. Segawa, M. Murakami, K. Takahashi, M. Maruyama, M. Maeda and S. Yamanaka (2003). "The homeoprotein Nanog is required for maintenance of pluripotency in mouse epiblast and ES cells." Cell 113(5): 631-42.

Moraes, K. C., C. J. Wilusz and J. Wilusz (2006). "CUG-BP binds to RNA substrates and recruits PARN deadenylase." Rna 12(6): 1084-91.

Morita, S., T. Kojima and T. Kitamura (2000). "Plat-E: an efficient and stable system for transient packaging of retroviruses." Gene Ther 7(12): 1063-6.

Mrena, J., J. P. Wiksten, A. Thiel, A. Kokkola, L. Pohjola, J. Lundin, S. Nordling, A. Ristimaki and C. Haglund (2005). "Cyclooxygenase-2 is an independent prognostic factor in gastric cancer and its expression is regulated by the messenger RNA stability factor HuR." Clin Cancer Res 11(20): 7362-8.

Muhlrad, D. and R. Parker (1994). "Premature translational termination triggers mRNA decapping." Nature 370(6490): 578-81.

Nagy, A., J. Rossant, R. Nagy, W. Abramow-Newerly and J. C. Roder (1993). "Derivation of completely cell culture-derived mice from early-passage embryonic stem cells." Proc Natl Acad Sci U S A 90(18): 8424-8.

Nagy, A., M. Gertsenstein, K. Vintersten and R. Behringer (2003). "Manipulating the Mouse Embryo, 3rd Edition."

Niwa, H., T. Burdon, I. Chambers and A. Smith (1998). "Self-renewal of pluripotent embryonic stem cells is mediated via activation of STAT3." Genes Dev 12(13): 2048-60.

Niwa, H., J. Miyazaki and A. G. Smith (2000). "Quantitative expression of Oct-3/4 defines differentiation, dedifferentiation or self-renewal of ES cells." <u>Nat Genet</u> 24(4): 372-6.

Niwa, H. (2001). "Molecular mechanism to maintain stem cell renewal of ES cells." <u>Cell Struct Funct</u> 26(3): 137-48.

Nykanen, A., B. Haley and P. D. Zamore (2001). "ATP requirements and small interfering RNA structure in the RNA interference pathway." <u>Cell</u> 107(3): 309-21.

O'Gorman, S., D. T. Fox and G. M. Wahl (1991). "Recombinase-mediated gene activation and site-specific integration in mammalian cells." <u>Science</u> 251(4999): 1351-5.

Paling, N. R., H. Wheadon, H. K. Bone and M. J. Welham (2004). "Regulation of embryonic stem cell self-renewal by phosphoinositide 3-kinase-dependent signaling." <u>J Biol Chem</u> 279(46): 48063-70.

Palmqvist, L., C. H. Glover, L. Hsu, M. Lu, B. Bossen, J. M. Piret, R. K. Humphries and C. D. Helgason (2005). "Correlation of murine embryonic stem cell gene expression profiles with functional measures of pluripotency." <u>Stem Cells</u> 23(5): 663-80.

Pan, G., J. Li, Y. Zhou, H. Zheng and D. Pei (2006). "A negative feedback loop of transcription factors that controls stem cell pluripotency and self-renewal." <u>Faseb J</u> 20(10): 1730-2.

Papaioannou, V. E., M. W. McBurney, R. L. Gardner and M. J. Evans (1975). "Fate of teratocarcinoma cells injected into early mouse embryos." <u>Nature</u> 258(5530): 70-73.

Parker, R. and H. Song (2004). "The enzymes and control of eukaryotic mRNA turnover." <u>Nat Struct Mol Biol</u> 11(2): 121-7.

Peng, S. S., C. Y. Chen, N. Xu and A. B. Shyu (1998). "RNA stabilization by the AU-rich element binding protein, HuR, an ELAV protein." <u>Embo J</u> 17(12): 3461-70.

Phillips, R. S., S. B. Ramos and P. J. Blackshear (2002). "Members of the tristetraprolin family of tandem CCCH zinc finger proteins exhibit CRM1-dependent nucleocytoplasmic shuttling." <u>J Biol Chem</u> 277(13): 11606-13.

Pospisilova, H., M. Baens, L. Michaux, M. Stul, P. Van Hummelen, P. Van Loo, J. Vermeesch, M. Jarosova, Z. Zemanova, K. Michalova, I. Van den Berghe, H. D. Alexander, A. Hagemeijer, P. Vandenberghe, J. Cools, C. De Wolf-Peeters, P. Marynen and I. Wlodarska (2007). "Interstitial del(14)(q) involving IGH: a novel recurrent aberration in B-NHL." <u>Leukemia</u> 21(9): 2079-83.

Qi, X., T. G. Li, J. Hao, J. Hu, J. Wang, H. Simmons, S. Miura, Y. Mishina and G. Q. Zhao (2004). "BMP4 supports self-renewal of embryonic stem cells by inhibiting mitogen-activated protein kinase pathways." <u>Proc Natl Acad Sci U S A</u> 101(16): 6027-32.

Qu, L., S. Huang, D. Baltzis, A. M. Rivas-Estilla, O. Pluquet, M. Hatzoglou, C. Koumenis, Y. Taya, A. Yoshimura and A. E. Koromilas (2004). "Endoplasmic reticulum stress induces p53 cytoplasmic localization and prevents p53-dependent apoptosis by a pathway involving glycogen synthase kinase-3beta." <u>Genes Dev</u> 18(3): 261-77.

Raineri, I., D. Wegmueller, B. Gross, U. Certa and C. Moroni (2004). "Roles of AUF1 isoforms, HuR and BRF1 in ARE-dependent mRNA turnover studied by RNA interference." <u>Nucleic Acids Res</u> 32(4): 1279-88.

Ramos, S. B., D. J. Stumpo, E. A. Kennington, R. S. Phillips, C. B. Bock, F. Ribeiro-Neto and P. J. Blackshear (2004). "The CCCH tandem zinc-finger protein Zfp36l2 is crucial for female fertility and early embryonic development." <u>Development</u> 131(19): 4883-93.

Rao, S. and S. H. Orkin (2006). "Unraveling the transcriptional network controlling ES cell pluripotency." <u>Genome Biol</u> 7(8): 230.

Resnick, J. L., L. S. Bixler, L. Cheng and P. J. Donovan (1992). "Long-term proliferation of mouse primordial germ cells in culture." <u>Nature</u> 359(6395): 550-1.

Robertson, E., A. Bradley, M. Kuehn and M. Evans (1986). "Germ-line transmission of genes introduced into cultured pluripotential cells by retroviral vector." <u>Nature</u> 323(6087): 445-8.

Sato, N., L. Meijer, L. Skaltsounis, P. Greengard and A. H. Brivanlou (2004). "Maintenance of pluripotency in human and mouse embryonic stem cells through activation of Wnt signaling by a pharmacological GSK-3-specific inhibitor." <u>Nat Med</u> 10(1): 55-63.

Savatier, P., H. Lapillonne, L. A. van Grunsven, B. B. Rudkin and J. Samarut (1996). "Withdrawal of differentiation inhibitory activity/leukemia inhibitory factor up-regulates D-type cyclins and cyclin-dependent kinase inhibitors in mouse embryonic stem cells." <u>Oncogene</u> 12(2): 309-22.

Scherr, M. and M. Eder (2007). "Gene silencing by small regulatory RNAs in mammalian cells." <u>Cell Cycle</u> 6(4): 444-9.

Schmidlin, M., M. Lu, S. A. Leuenberger, G. Stoecklin, M. Mallaun, B. Gross, R. Gherzi, D. Hess, B. A. Hemmings and C. Moroni (2004). "The ARE-dependent mRNA-destabilizing activity of BRF1 is regulated by protein kinase B." <u>Embo J</u> 23(24): 4760-9.

Seibler, J., A. Kleinridders, B. Kuter-Luks, S. Niehaves, J. C. Bruning and F. Schwenk (2007). "Reversible gene knockdown in mice using a tight, inducible shRNA expression system." <u>Nucleic Acids Res</u> 35(7): e54.

Sekkai, D., G. Gruel, M. Herry, V. Moucadel, S. N. Constantinescu, O. Albagli, D. T. Roux, W. Vainchenker and A. Bennaceur-Griscelli (2005). "Microarray Analysis of LIF/Stat3 Transcriptional Targets in Embryonic Stem Cells." <u>Stem Cells</u> 23(10): 1634-42.

Seko, Y., S. Cole, W. Kasprzak, B. A. Shapiro and J. A. Ragheb (2006). "The role of cytokine mRNA stability in the pathogenesis of autoimmune disease." <u>Autoimmun Rev</u> 5(5): 299-305.

Shaw, G. and R. Kamen (1986). "A conserved AU sequence from the 3' untranslated region of GM-CSF mRNA mediates selective mRNA degradation." <u>Cell</u> 46(5): 659-67.

Shen, V. and M. Kiledjian (2006). "A view to a kill: structure of the RNA exosome." <u>Cell</u> 127(6): 1093-5.

Sheth, U. and R. Parker (2003). "Decapping and decay of messenger RNA occur in cytoplasmic processing bodies." <u>Science</u> 300(5620): 805-8.

Shi, W., H. Wang, G. Pan, Y. Geng, Y. Guo and D. Pei (2006). "Regulation of the pluripotency marker Rex-1 by Nanog and Sox2." <u>J Biol Chem</u> 281(33): 23319-25.

Shimada, H., H. Ichikawa, S. Nakamura, R. Katsu, M. Iwasa, I. Kitabayashi and M. Ohki (2000). "Analysis of genes under the downstream control of the t(8;21) fusion protein AML1-MTG8: overexpression of the TIS11b (ERF-1, cMG1) gene induces myeloid cell proliferation in response to G-CSF." <u>Blood</u> 96(2): 655-63.

Smith, A. G., J. K. Heath, D. D. Donaldson, G. G. Wong, J. Moreau, M. Stahl and D. Rogers (1988). "Inhibition of pluripotential embryonic stem cell differentiation by purified polypeptides." <u>Nature</u> 336(6200): 688-90.

Stead, E., J. White, R. Faast, S. Conn, S. Goldstone, J. Rathjen, U. Dhingra, P. Rathjen, D. Walker and S. Dalton (2002). "Pluripotent cell division cycles are driven by ectopic Cdk2, cyclin A/E and E2F activities." <u>Oncogene</u> 21(54): 8320-33.

Steinman, R. A. (2007). "mRNA stability control: a clandestine force in normal and malignant hematopoiesis." <u>Leukemia</u> 21(6): 1158-71.

Stevens, L. C. (1960). "Embryonic potency of embryoid bodies derived from a transplantable testicular teratoma of the mouse." <u>Dev Biol</u> 2: 285-97.

Stoecklin, G., S. Hahn and C. Moroni (1994). "Functional hierarchy of AUUUA motifs in mediating rapid interleukin-3 mRNA decay." <u>J Biol Chem</u> 269(46): 28591-7.

Stoecklin, G., X. F. Ming, R. Looser and C. Moroni (2000). "Somatic mRNA turnover mutants implicate tristetraprolin in the interleukin-3 mRNA degradation pathway." <u>Mol Cell Biol</u> 20(11): 3753-63.

Stoecklin, G., M. Colombi, I. Raineri, S. Leuenberger, M. Mallaun, M. Schmidlin, B. Gross, M. Lu, T. Kitamura and C. Moroni (2002). "Functional cloning of BRF1, a regulator of ARE-dependent mRNA turnover." <u>Embo J</u> 21(17): 4709-18.

Stoecklin, G., M. Lu, B. Rattenbacher and C. Moroni (2003a). "A constitutive decay element promotes tumor necrosis factor alpha mRNA degradation via an AU-rich element-independent pathway." <u>Mol Cell Biol</u> 23(10): 3506-15.

Stoecklin, G., B. Gross, X. F. Ming and C. Moroni (2003b). "A novel mechanism of tumor suppression by destabilizing AU-rich growth factor mRNA." <u>Oncogene</u> 22(23): 3554-61.

Stoecklin, G., T. Stubbs, N. Kedersha, S. Wax, W. F. Rigby, T. K. Blackwell and P. Anderson (2004). "MK2-induced tristetraprolin:14-3-3 complexes prevent stress granule association and ARE-mRNA decay." Embo J 23(6): 1313-24.

Stumpo, D. J., N. A. Byrd, R. S. Phillips, S. Ghosh, R. R. Maronpot, T. Castranio, E. N. Meyers, Y. Mishina and P. J. Blackshear (2004). "Chorioallantoic fusion defects and embryonic lethality resulting from disruption of Zfp36L1, a gene encoding a CCCH tandem zinc finger protein of the Tristetraprolin family." Mol Cell Biol 24(14): 6445-55.

Takahashi, K., K. Mitsui and S. Yamanaka (2003). "Role of ERas in promoting tumour-like properties in mouse embryonic stem cells." Nature 423(6939): 541-5.

Takahashi, K., M. Murakami and S. Yamanaka (2005). "Role of the phosphoinositide 3-kinase pathway in mouse embryonic stem (ES) cells." Biochem Soc Trans 33(Pt 6): 1522-5.

Takahashi, K. and S. Yamanaka (2006). "Induction of pluripotent stem cells from mouse embryonic and adult fibroblast cultures by defined factors." Cell 126(4): 663-76.

Taylor, G. A. and P. J. Blackshear (1995). "Zinc inhibits turnover of labile mRNAs in intact cells." J Cell Physiol 162(3): 378-87.

Taylor, G. A., E. Carballo, D. M. Lee, W. S. Lai, M. J. Thompson, D. D. Patel, D. I. Schenkman, G. S. Gilkeson, H. E. Broxmeyer, B. F. Haynes and P. J. Blackshear (1996). "A pathogenetic role for TNF alpha in the syndrome of cachexia, arthritis, and autoimmunity resulting from tristetraprolin (TTP) deficiency." Immunity 4(5): 445-54.

Thomson, J. A., J. Itskovitz-Eldor, S. S. Shapiro, M. A. Waknitz, J. J. Swiergiel, V. S. Marshall and J. M. Jones (1998). "Embryonic stem cell lines derived from human blastocysts." Science 282(5391): 1145-7.

Tosh, D. and J. M. Slack (2002). "How cells change their phenotype." Nat Rev Mol Cell Biol 3(3): 187-94.

Tucker, M., M. A. Valencia-Sanchez, R. R. Staples, J. Chen, C. L. Denis and R. Parker (2001). "The transcription factor associated Ccr4 and Caf1 proteins are components of the major cytoplasmic mRNA deadenylase in Saccharomyces cerevisiae." Cell 104(3): 377-86.

van de Wetering, M., I. Oving, V. Muncan, M. T. Pon Fong, H. Brantjes, D. van Leenen, F. C. Holstege, T. R. Brummelkamp, R. Agami and H. Clevers (2003). "Specific inhibition of gene expression using a stably integrated, inducible small-interfering-RNA vector." EMBO Rep 4(6): 609-15.

van Hoof, A. and R. Parker (1999). "The exosome: a proteasome for RNA?" Cell 99(4): 347-50.

Varnum, B. C., Q. F. Ma, T. H. Chi, B. Fletcher and H. R. Herschman (1991). "The TIS11 primary response gene is a member of a gene family that encodes proteins with a highly conserved sequence containing an unusual Cys-His repeat." <u>Mol Cell Biol</u> 11(3): 1754-8.

Ventura, A., A. Meissner, C. P. Dillon, M. McManus, P. A. Sharp, L. Van Parijs, R. Jaenisch and T. Jacks (2004). "Cre-lox-regulated conditional RNA interference from transgenes." <u>Proc Natl Acad Sci U S A</u> 101(28): 10380-5.

Wang, Z. and M. Kiledjian (2001). "Functional link between the mammalian exosome and mRNA decapping." <u>Cell</u> 107(6): 751-62.

Wang, Z., X. Jiao, A. Carr-Schmid and M. Kiledjian (2002). "The hDcp2 protein is a mammalian mRNA decapping enzyme." <u>Proc Natl Acad Sci U S A</u> 99(20): 12663-8.

Watanabe, S., H. Umehara, K. Murayama, M. Okabe, T. Kimura and T. Nakano (2006). "Activation of Akt signaling is sufficient to maintain pluripotency in mouse and primate embryonic stem cells." <u>Oncogene</u> 25(19): 2697-707.

Watcharasit, P., G. N. Bijur, J. W. Zmijewski, L. Song, A. Zmijewska, X. Chen, G. V. Johnson and R. S. Jope (2002). "Direct, activating interaction between glycogen synthase kinase-3beta and p53 after DNA damage." <u>Proc Natl Acad Sci U S A</u> 99(12): 7951-5.

Watson, J. D., N. H. Hopkins, J. W. Roberts, J. A. Steitz and A. M. Weiner (1988). "Molecular biology of the gene." <u>The Benjamin/Cummings Publishing Company, Inc., Menlo Park, California</u>.

Wegmuller, D., I. Raineri, B. Gross, E. J. Oakeley and C. Moroni (2007). "A cassette system to study embryonic stem cell differentiation by inducible RNA interference." <u>Stem Cells</u> 25(5): 1178-85.

Wernig, M., A. Meissner, R. Foreman, T. Brambrink, M. Ku, K. Hochedlinger, B. E. Bernstein and R. Jaenisch (2007). "In vitro reprogramming of fibroblasts into a pluripotent ES-cell-like state." <u>Nature</u> 448(7151): 318-24.

Wiznerowicz, M. and D. Trono (2003). "Conditional suppression of cellular genes: lentivirus vector-mediated drug-inducible RNA interference." <u>J Virol</u> 77(16): 8957-61.

Wolf, E., R. Kramer, I. Polejaeva, H. Thoenen and G. Brem (1994). "Efficient generation of chimaeric mice using embryonic stem cells after long-term culture in the presence of ciliary neurotrophic factor." <u>Transgenic Res</u> 3(3): 152-8.

Xu, N., C. Y. Chen and A. B. Shyu (1997). "Modulation of the fate of cytoplasmic mRNA by AU-rich elements: key sequence features controlling mRNA deadenylation and decay." <u>Mol Cell Biol</u> 17(8): 4611-21.

Xu, N., C. Y. Chen and A. B. Shyu (2001). "Versatile role for hnRNP D isoforms in the differential regulation of cytoplasmic mRNA turnover." <u>Mol Cell Biol</u> 21(20): 6960-71.

Yao, F., T. Svensjo, T. Winkler, M. Lu, C. Eriksson and E. Eriksson (1998). "Tetracycline repressor, tetR, rather than the tetR-mammalian cell transcription factor fusion derivatives, regulates inducible gene expression in mammalian cells." Hum Gene Ther 9(13): 1939-50.

Yeom, Y. I., G. Fuhrmann, C. E. Ovitt, A. Brehm, K. Ohbo, M. Gross, K. Hubner and H. R. Scholer (1996). "Germline regulatory element of Oct-4 specific for the totipotent cycle of embryonal cells." Development 122(3): 881-94.

Ying, Q. L., J. Nichols, I. Chambers and A. Smith (2003). "BMP induction of Id proteins suppresses differentiation and sustains embryonic stem cell self-renewal in collaboration with STAT3." Cell 115(3): 281-92.

Yu, J. and A. P. McMahon (2006). "Reproducible and inducible knockdown of gene expression in mice." Genesis 44(5): 252-61.

Yuan, H., N. Corbi, C. Basilico and L. Dailey (1995). "Developmental-specific activity of the FGF-4 enhancer requires the synergistic action of Sox2 and Oct-3." Genes Dev 9(21): 2635-45.

Zambrowicz, B. P., A. Imamoto, S. Fiering, L. A. Herzenberg, W. G. Kerr and P. Soriano (1997). "Disruption of overlapping transcripts in the ROSA beta geo 26 gene trap strain leads to widespread expression of beta-galactosidase in mouse embryos and hematopoietic cells." Proc Natl Acad Sci U S A 94(8): 3789-94.

Zindy, P. J., A. L'Helgoualc'h, D. Bonnier, A. Le Bechec, K. Bourd-Boitin, C. X. Zhang, O. Musso, D. Glaise, M. B. Troadec, O. Loreal, B. Turlin, J. Leger, B. Clement and N. Theret (2006). "Upregulation of the tumor suppressor gene menin in hepatocellular carcinomas and its significance in fibrogenesis." Hepatology 44(5): 1296-307.

6. ACKNOWLEDGEMENTS

7. APPENDIX

Figure and Table Index

Discussion

Materials and Methods

Publications

STEM CELLS

TECHNOLOGY DEVELOPMENT

A Cassette System to Study Embryonic Stem Cell Differentiation by Inducible RNA Interference

DANIEL WEGMÜLLER,[a] INES RAINERI,[a] BRIGITTE GROSS,[a] EDWARD J. OAKELEY,[b] CHRISTOPH MORONI[a]

[a]Institute for Medical Microbiology, Department of Biological and Clinical Sciences, University of Basel, Basel, Switzerland; [b]Friedrich Miescher Institute for Biomedical Research, Basel, Switzerland

ABSTRACT

Although differentiation of pluripotent embryonic stem cells is restricted by a hierarchy of transcription factors, little is known about whether post-transcriptional mechanisms similarly regulate early embryoid differentiation. We developed a system where small hairpin (sh)RNAs can be induced in embryonic stem (ES) cells from a defined locus following integration by Flp recombinase-mediated DNA recombination. To verify the system, the key transcription factor Stat3, which maintains pluripotency, was downregulated by shRNA, and the expected morphological and biochemical markers of differentiation were observed. Induction of shRNA specific for the post-transcriptional regulator Brf1 (*Zfp36L1*) amplified the cardiac markers with strong stimulation of cardiomyocyte formation within embryoid bodies. These findings identify Brf1 as a novel potential regulator of cardiomyocyte formation and suggest that post-transcriptional mechanisms are of importance to early development and, possibly, to regenerative medicine. The inducible RNA interference system presented here should also allow assignment of function for candidate genes with suspected roles in ES cell development. STEM CELLS 2007;25:1178–1185

Disclosure of potential conflicts of interest is found at the end of this article.

INTRODUCTION

Embryonic stem (ES) cell lines provide an attractive system to study the basically unresolved question of how stem cells decide between self-renewal and differentiation [1]. From a clinical perspective, they provide a promising tool for the emerging field of regenerative medicine. The pluripotency of cultured murine ES cells is maintained by the cytokine leukemia inhibitory factor (LIF), which restrains ES cells from differentiation and acts via LIF-receptor-dependent activation of the transcription factor Stat3 [2–5]. How the Stat3 targets maintain pluripotency and why loss of Stat3 activation leads to differentiation is not known, although recent work assigns a key role to c-myc [6]. In addition to Stat3, other transcription factors, including Oct4, nanog, Sox2, and the BMP4 regulatory protein, also play important roles in maintaining the pluripotent state of ES cells [7–13]. Recent results from human ES cells indicate that promoter regions of 353 genes, including Stat3, are co-occupied by Oct4, nanog, and Sox2 [14]. This is consistent with a model where a hierarchical system of transcription factors controls the balance between self-renewal and differentiation and where subtle changes may be sufficient for triggering differentiation [1, 15]. Although it is plausible that post-transcriptional forms of regulation may also play a role in ES differentiation, this aspect has, to the best of our knowledge, not been addressed. The control of mRNA turnover for transcripts containing an AU-rich element (ARE) in their 3′-untranslated region (UTR) is of particular interest, as this element is present in many transcription factors, cytokines, chemokines, and other regulators [16, 17]. ARE-binding proteins such as AUF1, TTP, or Brf1 have been identified, which promote ARE-dependent mRNA decay [18–21], whereas HuR acts as a stabilizer [22]. These proteins regulate access of decapping enzymes and RNases including deadenylases and exosomal enzymes to the transcripts [23–25]. The presence of common signals such as the ARE on many transcripts has suggested the concept of a "post-transcriptional operon" [26], and it may well be that a similar form of regulation also operates in ES cells and embryogenesis. We report here a system based on inducible RNA interference to assess effects of suspected regulators, post-transcriptional or otherwise. Small hairpin (sh)RNA, first introduced into a defined green fluorescent protein (GFP)-marked locus by Flp recombinase ("flipase") [27], is induced by doxycycline and triggers decay of the mRNA target. In addition to describing a generally applicable system, we report that doxycycline-induced RNA interference directed at Brf1 led to expression of cardiomyocyte-specific markers and massive amplification of beating areas within embryoid bodies (EBs).

MATERIALS AND METHODS

Cell Culture

CCE ES cells [28, 29] were cultured on gelatin-coated dishes in 250 U/ml LIF (Chemicon, Temecula, CA, http://www.chemicon.com) containing medium consisting of high glucose Dulbecco's modified Eagle's medium (Sigma-Aldrich, St. Louis, http://www.sigmaaldrich.com) supplemented with 15% fetal calf serum (FCS; Gibco, Grand Island, NY, http://www.invitrogen.com), 2 mM L-glutamine (Stem Cell Technologies, Vancouver, BC, Canada, http://www.stemcell.com), 0.1 mM nonessential amino acids (Stem Cell
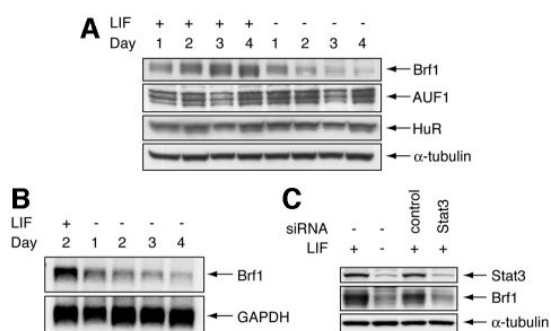
Figure 1. Brf1 expression is controlled by LIF and Stat3. **(A):** LIF removal experiment. CCE cells were kept for 4 days either with or without LIF as indicated. Protein levels of Brf1, AUF1, HuR, and α-tubulin are shown. **(B):** Brf1 mRNA levels monitored by Northern blot; GAPDH served as loading control. **(C):** Effect of Stat3 siRNA. Cells were plated with or without LIF and, as indicated, treated for 48 hours with Stat3 or β-globin (control) siRNA. Expression of Stat3 and Brf1 was monitored by Western blotting. Abbreviations: GAPDH, glyceraldehyde-3-phosphate dehydrogenase; LIF, leukemia inhibitory factor; siRNA, small interfering RNA.

Technologies), 1 mM sodium pyruvate (Stem Cell Technologies), and 100 μM monothioglycerol (Sigma-Aldrich). Cells were frozen in medium containing 50% FCS, 40% culture medium, and 10% dimethyl sulfoxide (Sigma-Aldrich). Experiments with CCE-TR-FRT cells (see below) were performed in ES medium containing 100 U/ml LIF in the presence or absence of 2 μg/ml doxycycline (Dox).

To generate cardiomyocytes from EBs, ES cells were cultured for 2 days in hanging drops followed by a 2-day suspension culture. Then, 30 or 2 EBs were plated into either gelatin-coated 24- or 48-well plates, respectively, and cultured for 24 hours in maintenance medium containing Iscove's modified Dulbecco's medium (Sigma-Aldrich), 20% FCS, 2 mM L-glutamine, 0.1 mM nonessential amino acids, and 100 μM monothioglycerol to allow attachment of EBs to the culture dish. Thereafter, cells were kept for 48 hours in starvation medium consisting of maintenance medium supplemented with only 0.2% FCS, followed by culture in supplemented medium corresponding to maintenance medium containing serum replacement (Sigma-Aldrich) instead of FCS.

Plasmids

Tet repressor plasmid (pCAG-TR-IRESpuro3): pCAG and pIRES-puro3 (Clontech, Palo Alto, CA, http://www.clontech.com) plasmids were digested (SpeI and EcoRI) and the IRESpuro3 fragment ligated into pCAG. Digestion of pcDNA6/TR (Invitrogen) vector (AflII, blunt ending, NotI) releases the Tet repressor (tetR)-intervening sequence (IVS) insert. This fragment was cloned into pCAG-IRESpuro3 digested by NotI.

To generate the FRTd2EGFP plasmid (pCAG-FRTd2EGFP-IRESneo3), the d2EGFP was amplified without the start codon from pd2EGFP-N1 (Clontech) with BglII and NotI linkers. The CAG promoter was cut from pCAG with EcoRI and SpeI and ligated with an oligo containing an ATG, a FRT site [30], EcoRI, and BglII linkers to the d2EGFP fragment. This insert was finally inserted into pIRESneo3 (Clontech) digested with SpeI and NotI.

To generate short hairpin (sh)RNA plasmids (pTER-shRNA-FRT), the shRNAs (Stat3, Brf1) were cloned into pTER-Ni [31] using BglII and NotI. Plasmids were opened with NsiI and SapI and blunted, followed by insertion of an FRT-Hygro-SV40pA fragment from pcDNA5/FRT (Invitrogen) digested with PvuII. To generate the flipase plasmid (pCAG-Flipase), flipase was polymerase chain reaction (PCR) amplified from the pOG44 vector (Invitrogen) and the product digested with BsaI and blunt ended (IVS-Flipase-pA) and was then inserted into pCAG vector opened with HindIII and blunt ended.

www.StemCells.com

Transient and Stable Transfection of CCE Cells

All transfections were done using Lipofectamine 2000 according to the standard protocol from Invitrogen; however, cells were incubated with liposome/plasmid complexes for only 3 hours at 37°C/5% CO_2. For generation of cells exhibiting Dox inducible expression of shRNAs, CCE ES cells were first transfected with the pCAG-TR-IRESpuro3 vector and selected with 1 μg/ml puromycin (Calbiochem, San Diego, http://www.emdbiosciences.com). Clones were identified by Western blot with mouse anti-tetR monoclonal antibody mix (MoBiTec, Göttingen, Germany, http://www.mobitec.de). A high expressing clone (TR8) was chosen for further transfection with pCAG-FRT-d2EGFP-IRESneo3. Selection was done with Geneticin (Gibco) at a concentration of 600 μg/ml.

Recombination of shRNA was done by cotransfection of the flipase containing vector (pCAG-Flipase) and the vector containing the shRNA (pTER-shRNA-FRT). Cells were then selected with hygromycin (Calbiochem) at a concentration of 165 U/ml. Cells were then further screened for loss of both GFP and G418 resistance.

shRNA, Small Interfering RNA, and Primers

Murine Stat3-specific oligonucleotides: 5′ GAT CTG AGT CAC ATG CCA CGT TGG TTC AAG AGA CCA ACG TGG CAT GTG ACT CTT TTT A 3′ and 5′ AGC TTA AAA AGA GTC ACA TGC CAC GTT GGT CTC TTG AAC CAA CGT GGC ATG TGA CTC A 3′.

Murine Stat3 small interfering (si)RNA: 5′ GAG UCA CAU GCC ACG UUG G 3′ (XM_109608).

Control siRNA (human β-globin): 5′ CAA GAA AGU GCU CGG UGC C 3′ (V00497.1).

Murine Brf1-specific oligonucleotides: 5′ GAT CTG TCC GAA TCC CCT CAC ATG TTC AAG AGA CAT GTG AGG GGA TTC GGA CTT TTT A 3′ and 5′ AGC TTA AAA AGT CCG AAT CCC CTC ACA TGT CTC TTG AAC ATG TGA GGG GAT TCG GAC A 3′.

Murine Stat3 primer: 5′ AGT CAC ATG CCA CGT TGG T 3′.

Murine α-cardiac actin PCR primers: forward 5′ GCT TTG GTG TGT GAC AAT 3′ GG, reverse 5′ GTG ATA ATG CCA TGT TCA ATG G 3′.

Murine Nkx2.5 PCR primers: forward 5′ CGG AAC GAC TCC CAC CTT TAG G 3′, reverse 5′ GGA ATC CGT CGA AAG TGC CC 3′.

Murine Gata4 PCR primers: forward 5′ CGA GAT GGG ACG GGA CAC T 3′, reverse 5′ CTC ACC CTC GGC CAT TAC GA 3′.

Murine myogenin PCR primers: forward 5′ ACA AGC CAG ACT CCC CAC TC 3′, reverse 5′ GCA CTC ATG TCT CTC AAA CGG T 3′.

Murine glyceraldehyde-3-phosphate dehydrogenase (GAPDH) PCR primers: forward 5′ CAC CAC CAA CTG TTA GCC 3′, reverse 5′ CCT GCT TCAC CAC CTT CTT G 3′.

Murine 18S ribosomal RNA primers: forward 5′ CGG CTA CCA CAT CCA AGG AA 3′, reverse 5′ GCT GGA ATT ACC GCG GCT 3′.

Northern Blot

Total RNA was harvested using TRIzol (Invitrogen). To detect Brf1, Oct4, Rex-1, Fgf-4, and β-actin, Northern blots were hybridized overnight with [$α^{32}$P]-dCTP-labeled PCR fragments generated from cDNA of the aforementioned genes (Brf1: nucleotide [nt] 945-1328, number M58566; GAPDH: nt 589-1246, number M33197; β-actin: nt 516-1144, number NM_008085; Oct4: nt 731-1101, number NM_013633; Rex-1: nt 687-1059, number NM_009556; Fgf-4: nt 250-583, number NM_010202) [32]. To analyze expression of shRNA in F3-1-Stat3 and F3-1-Brf1 clones, 30 μg of total RNA were separated on 15% polyacrylamide gels containing 8 M urea (Anamed Elektrophorese GmbH, Darmstadt-Arheiligen, Germany, http://www.anamed-gele.com). Gels were stained with ethidium bromide to check for equal loading before RNA was transferred by electroblotting onto Hybond-N+ (Amersham Biosciences, Piscataway, NJ, http://www.amersham.com) membranes. After UV-cross-linking, filters were hybridized at 45°C in 0.5 M sodium phosphate buffer pH 7.2 containing 1% bovine
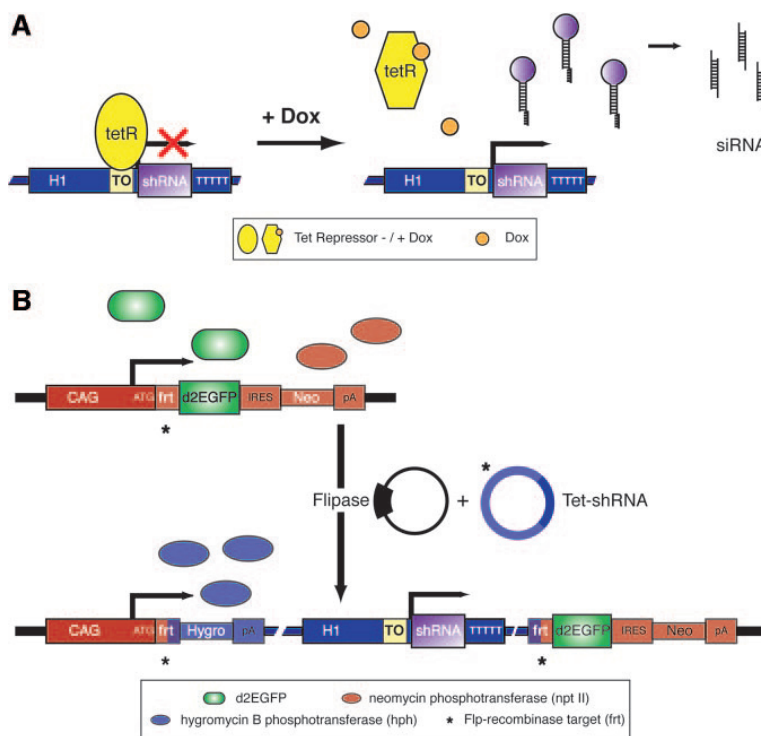
Figure 2. Schematic view of doxycycline-inducible shRNA expression. **(A):** The tetR binds to the TO, blocking RNA polymerase III. Addition of Dox removes tetR, and shRNA is produced and processed intracellularly to 21-nucleotide siRNA as described by van de Wetering [31]. **(B):** A modified Flip-In system is used to recombine a vector containing the shRNA of interest into a defined locus marked by green fluorescent protein (GFP) and flanked by the frt and the neomycin resistance gene. After successful recombination following cotransfection with plasmids encoding flipase and frt-containing Tet-shRNA, cells lose both GFP expression and G418 resistance after dislocation from the promoter but acquire hygromycin resistance and inducible shRNA expression. Frt is marked by an asterisk. Abbreviations: d2EGFP, destabilized enhanced green fluorescent protein; Dox, doxycycline; frt, Flp-recombinase-target; Hygro, hygromycin B phosphotransferase; IRES, internal ribosome entry site; Neo, neomycin phosphotransferase; pA, polyA signal; shRNA, small hairpin RNA; siRNA, small interfering RNA; tetR, Tet repressor; TO, Tet operator.

serum albumin (Fraction V, Sigma-Aldrich), 7% sodium dodecyl sulfate, and 5 mM EDTA using a [γ^{32}P]-ATP labeled Stat3 or Brf1 specific oligonucleotide of 19 nucleotides. Blots were analyzed using the Personal Molecular Imager FX (Bio-Rad, Hercules, CA, http://www.bio-rad.com) and the Quantity One software (Bio-Rad).

Western Blot

The Western blot protocol employed and generation of Brf1 antibodies has recently been described [32]. A monoclonal anti-tetR antibody mix was used to detect expression of the Tet repressor. A monoclonal antibody against α-tubulin (clone 236-10501; Molecular Probes, Carlsbad, CA, http://probes.invitrogen.com) was used. Stat3 (Cell Signaling Technology, Beverly, MA, http://www.cell-signal.com), Nkx2.5 (clone N-19; Santa Cruz Biotechnology Inc., Santa Cruz, CA, http://www.scbt.com), Gata4 (Clone H-112; Santa Cruz Biotechnology Inc.), and horseradish peroxidase-coupled GAPDH (Abcam, Cambridge, U.K., http://www.abcam.com) polyclonal antibodies were utilized. Alkaline phosphatase-coupled goat-anti-rabbit IgG (SouthernBiotech, Birmingham, AL, http://www.southernbiotech.com) and horseradish peroxidase-coupled goat-anti-mouse IgG (DAKO, Glostrup, Denmark, http://www.dako.com) and rabbit anti-goat IgG (SouthernBiotech) were used as secondary antibodies. Development was performed using CDP-Star (Roche Diagnostics, Basel, Switzerland, http://www.roche-applied-science.com) or ECL Advance (Amersham Biosciences).

Microscopy

A Nikon Eclipse TE200 (Nikon Corporation, Tokyo, http://www.nikon.com) microscope equipped with a Hamamatsu digital camera (C4742–95; Hamamatsu Photonics, Hamamatsu City, Japan, http://www.hamamatsu.com) was used, and all pictures were made at a ×40 magnification. Beating areas were marked under live-microscopy using Openlab 2.2 Software (Improvision Inc., Lexington, MA, http://www.improvision.com) allowing quantification.

RESULTS

We were interested to see whether the expression of the post-transcriptional ARE-dependent regulators Brf1, AUF1, and HuR would change under conditions at which ES cells are triggered to differentiate. When LIF was removed, CCE cells lost the compact dome-like colony morphology characteristic of undifferentiated cells and assumed the morphology of differentiated cells (supplemental online Fig. 1A; see also below). In parallel, Brf1 protein levels dropped progressively, whereas expression of HuR and AUF1 was not affected (Fig. 1A). Northern blot analysis suggested that this regulatory effect on Brf1 expression occurred at the mRNA level (Fig. 1B). The same general conclusion was obtained when a second ES line, CGR8, was similarly examined (supplemental online Fig. 1A, 1B). As LIF supports the pluripotent phenotype by activating the transcription factor Stat3, we tested whether this effect would be mimicked by siRNA downregulation of Stat3. Indeed, treatment with Stat3 specific siRNA led to a concomitant downregulation of both Stat3 and Brf1 protein levels, assessed at day 2 (Fig. 1C). As it appears that Brf1 is a target gene of the LIF-gp130-Stat3 pathway, we hypothesized that a reduction of its expression may be linked to a role in ES cell differentiation. To address this possibility, we decided to set up a system in CCE cells, in which a shRNA of choice can be inducibly expressed from a defined locus by the addition of a drug. To achieve this, we used a recently described vector system [31], illustrated in Figure 2A, where the Tet repressor protein binds to the Tet operator within the H1 promoter and acts as a "roadblock" for the RNA polymerase III. Following abrogation of repressor binding by addition of doxycycline, the downstream shRNA sequence is transcribed by RNA polymerase III and terminated by a run of five T residues [33]. CCE cells were first transfected
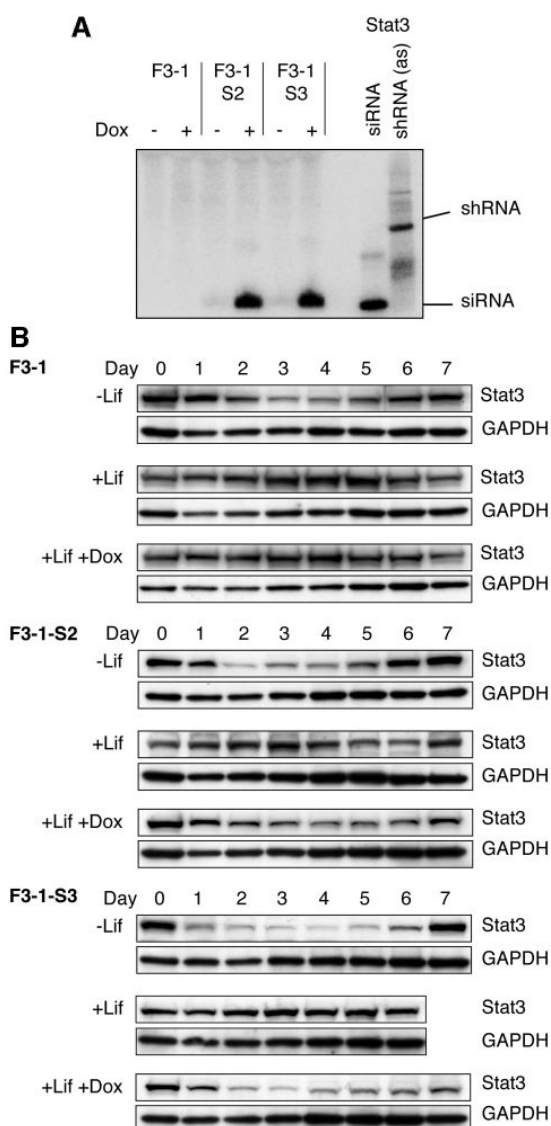
Wegmüller, Raineri, Gross et al.   1181

Figure 3. Inducible downregulation of Stat3. **(A):** After 7 days in culture (+LIF; ±Dox), RNA from indicated cells was isolated and processed for Northern blotting using a 5′-labeled Stat3 oligonucleotide probe. Markers shown on the right include synthetic 21-nucleotide (nt) Stat3 siRNA and 58-nt Stat3 shRNA. **(B):** Time-course experiment over 7 days in presence or absence of LIF and doxycycline as indicated. Lysates from F3-1 control cells and the two Stat3 shRNA clones F3-1-S2 and F3-1-S3 were analyzed by Western blot against Stat3. GAPDH served as loading control. Abbreviations: as, antisense strand; Dox, doxycycline; GAPDH, glyceraldehyde-3-phosphate dehydrogenase; LIF, leukemia inhibitory factor; shRNA, small hairpin RNA; siRNA, small interfering RNA.

with a plasmid encoding the Tet repressor [34, 35], and after puromycin selection a stable clone was selected, which maintained Tet repressor expression well over the time required for embryoid body formation (data not shown). This clone was further transfected with a construct where GFP, under control of a CAG promoter, is flanked by a Flp-recombinase-target (frt) recombination site [27] and the neomycin resistance gene. This

strategy was chosen as it allows the use of a defined locus, marked by frt-GFP-neo and allowing continuous stable gene expression, as a target for a Flp-recombinase to integrate an inducible shRNA. The GFP expressing clone F3-1, which is resistant to G418 and expresses GFP well past day 10 after induction of differentiation (data not shown), serves as the host system for a flipase-encoding plasmid together with the shRNA plasmid containing a frt site and the selectable marker hygromycin B phosphotransferase (hph). After successful recombination, the GFP gene of F3-1 is displaced by hph and inducible shRNA can now be expressed from the H1 promoter together with hygromycin resistance from the CAG promoter (Fig. 2B).

We tested this strategy first by introducing a shRNA targeting Stat3, as successful downregulation of Stat3 would be expected to trigger differentiation [5] and, hence, can be easily monitored. We selected two F3-1-derived Stat3-shRNA clones (F3-1-S2; F3-1-S3), which displayed the expected profile of GFP negative, G418 insensitive, hygromycin resistant, and correct recombination as verified by PCR (data not shown). When cells were treated for 7 days with doxycycline, both clones displayed strong siRNA induction with negligible background expression (Fig. 3A). Notably, Stat3 protein levels were downregulated in both clones tested, whereas doxycycline had no effect on F3-1 control cells (Fig. 3B). The effect was detectable after 1–2 days and was more pronounced in F3-1-S3 cells, apparently reflecting clonal variation. In contrast, LIF removal downregulated Stat3 in all three clones, including F3-1. Consistent with the result from Figure 1, arguing that Brf1 is controlled at least in part by LIF-Stat3, we observed that addition of doxycycline to clones F3-1-S2 and F3-1-S3 and in additional Stat3 shRNA expressing clones also led to downregulation of Brf1 (supplemental online Figs. 2, 3A). As with Stat3 expression, we observed some clonal variation (not shown).

Next, we checked whether addition of doxycycline would trigger the morphological changes characteristic for differentiation. As shown in Figure 4A, both shRNA clones displayed vigorous morphological differentiation upon addition of doxycycline despite the presence of LIF (right panels). To corroborate this finding, we assessed three known markers of undifferentiated ES cells (Oct4, Fgf-4, Rex-1). As expected, their levels dropped following LIF removal in all three clones tested, whereas addition of doxycycline reproduced the same effect as LIF removal in the two shRNA containing clones but not in F3-1 control cells (Fig. 4B). The stem cell marker nanog, measured at day 3, was reduced by LIF removal but not by doxycycline in both F3-1 and F3-1-S2 cells (supplemental online Fig. 3B), consistent with the fact that nanog is not controlled by Stat3 [10]. Together, these data indicated that the morphological changes induced by shRNA were accompanied by reprogramming gene expression of established regulators and show that the frt-GFP locus functions reliably as an acceptor of the shRNA cassette with the expected doxycycline inducible response. We concluded that the system can be used as a tool to investigate other genes with suspected roles in differentiation and concentrated our further studies on Brf1.

We used the same strategy as with Stat3 and isolated clones containing doxycycline-inducible Brf1 shRNA. Shown in Figure 5A are Northern blots from two representative clones (F3-1-B9 and F3-1-B14). Again, siRNA is strongly induced in both clones with negligible background expression and no signal in control cells. A parallel Western blot at day 3 showed that doxycycline led to downregulation of Brf1 protein (Fig. 5B). However, treatment with doxycycline for up to 7 days produced no morphological changes (data not shown). We wondered whether Brf1 shRNA might affect differentiation at later stages. Thus, we produced EBs and cultured these further by allowing them to attach. Unexpectedly, EBs from F3-1-B14, but not from
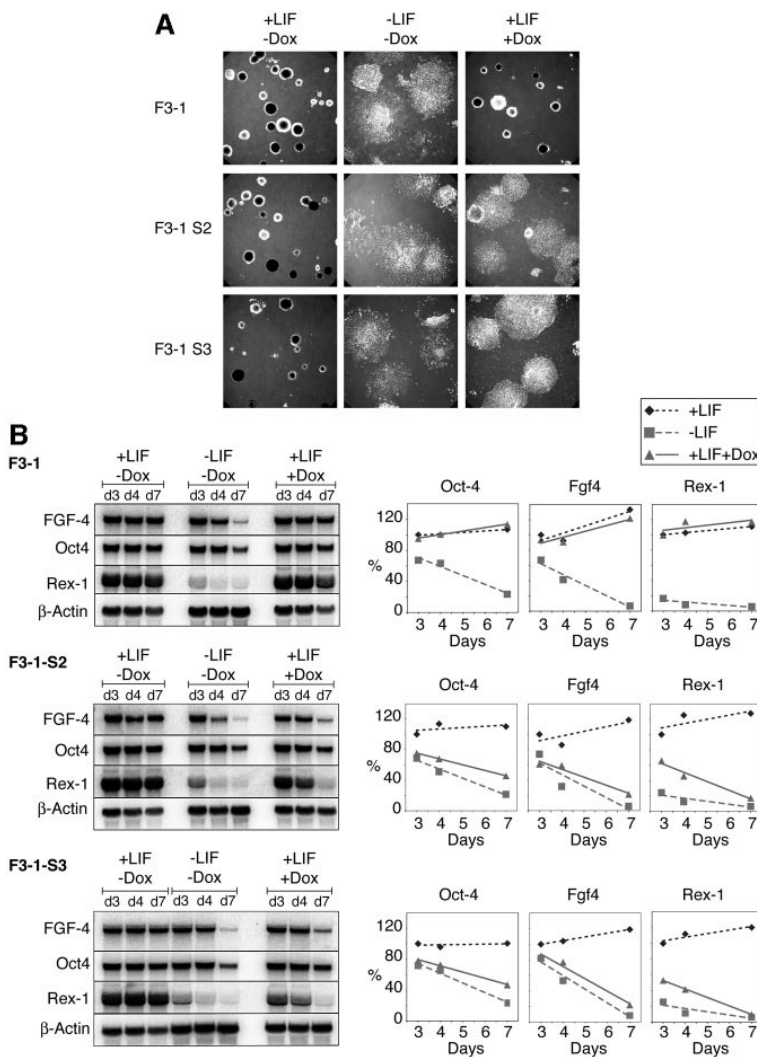
7. Appendix

Figure 4. Induction of differentiation by Stat3 small hairpin RNA. **(A):** After 7 days in culture (+LIF/−Dox; −LIF/−Dox; +LIF/+Dox), F3-1-S2 and F3-1-S3 cells were inspected for morphological changes after doxycycline addition. F3-1 cells served as control. Colony morphology of undifferentiated cells is compact (left panels), that of differentiated cells spread-out and extended. Magnification is 40-fold. **(B):** At the indicated time of culture (+LIF/−Dox; −LIF/−Dox; +LIF/+Dox), RNA from parallel cultures shown in **(A)** was extracted and processed for Northern blotting. Northern blots probed for three stem cell markers (Fgf-4, Oct4, Rex-1) are shown on the left and quantification on the right. RNA levels were normalized against β-actin; the RNA levels of cells at day 3 +LIF/−Dox were set as 100%. Abbreviations: d, day; Dox, doxycycline; LIF, leukemia inhibitory factor.

control cells, displayed a markedly altered morphology when cultured with doxycycline. Shown in Figure 6 are representative examples photographed at day 10. Although EBs from control cells appeared as compact cellular masses surrounded by a halo of outgrowing cells, doxycycline treatment of F3-1-B14 cells led to an apparent loosening of the central mass, increased outgrowth, and formation of satellite "microbodies." Interestingly, these changes were observed when doxycycline was present until day 4 but not when added after day 4. These data argue that early but not later changes in Brf1 levels affect the architecture of an embryoid body.

It is well established that cardiomyocyte formation occurs spontaneously in cultured EBs, which is easily recognizable under microscopy as "beating areas" or detectable biochemically by measuring cardiac specific markers such as the transcription factor Nkx2.5 [36, 37]. We were surprised to observe that induction of Brf1 shRNA by doxycycline led in F3-1-B14 cells to a substantial increase in number and size of beating areas (Fig. 7). We also noticed the elevated background in these cells (140 areas) compared with the F3-1 control cells, which may reflect some leakiness. Addition of doxycycline had also a

low but reproducible effect on F3-1 control cells, an effect we cannot explain but which is negligible compared with the very strong doxycycline effect in Brf1 shRNA expressing cells. To substantiate this effect of cardiomyocyte formation, we examined the expression of various markers. Eighteen days following addition of doxycycline, Nkx2.5 and Gata4 expression was weak in controls but strong in F3-1-B14 cells as shown by Western blot and PCR analysis (Fig. 8A and supplemental online Fig. 4A). The skeletal muscle marker myogenin was not expressed in ES cells (supplemental online Fig. 4A). Additionally, we monitored the cardiac marker α-cardiac actin by semi-quantitative reverse transcription-PCR at days 4 and 18 and observed weak induction in F3-1 at day 18 and higher levels in response to doxycycline in F3-1-B14 (Fig. 8B, supplemental online Fig. 4A). These findings are in agreement with the microscopic data and indicate that the appropriate change in gene expression took place.

It was of interest now whether downregulation of Brf1 would affect both the kinetics and/or the magnitude of cardiomyocyte formation and if doxycycline has to be present throughout the experiment. Thus, we plated two EBs into each
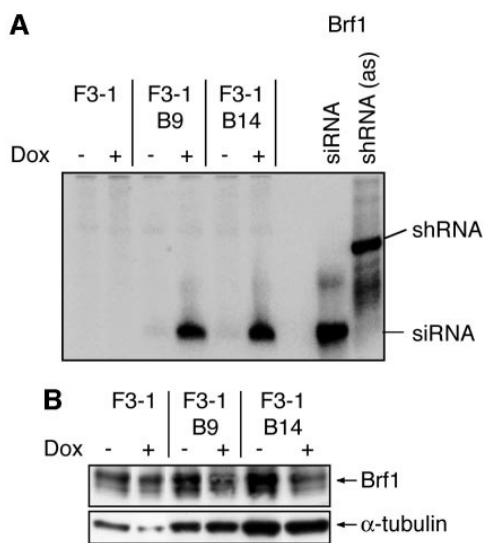
Wegmüller, Raineri, Gross et al. 1183

Figure 5. Doxycycline-inducible downregulation of Brf1. **(A):** After 7 days in culture (+leukemia inhibitory factor [LIF]; ±Dox), RNA from indicated cells was isolated and processed for Northern blotting using a 5′-labeled Brf1 oligonucleotide probe. Markers shown on the right include synthetic 21-nucleotide (nt) Brf1 siRNA and 58-nt Brf1 shRNA. **(B):** After 3 days in culture in the presence of LIF (±Dox) as indicated, Brf1 was examined by Western blot analysis. α-Tubulin served as loading control. Abbreviations: as, antisense strand; Dox, doxycycline; shRNA, small hairpin RNA; siRNA, small interfering RNA.
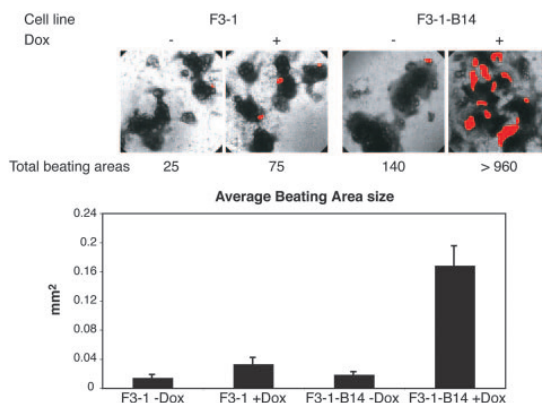

Figure 6. Embryoid body morphology. Morphology of embryoid bodies (EBs) at d10 from F3-1 and F3-1-B14 cells either kept with or without doxycycline from day 0 to day 18. Additionally, F3-1-B14 EBs were either kept with doxycycline during the first 4 days or from day 4 until the end of the experiment. Abbreviations: d, day; Dox, doxycycline.

well of a 48-well plate, which allowed daily inspection of individual beating bodies and scoring of the percentage of beating. As shown in Figure 8C (upper panel), beating body formation in doxycycline-treated F3-1-B14 cells was first observed on day 9 and reached a plateau at approximately day 14. In the absence of doxycycline, beating body formation was observed in the range of control cells. Note that, in these experiments, the number of beating bodies was scored rather than beating areas as in Figure 7. The difference between the two stimulation indices is explained by the fact that a given beating body generally contains more than one beating area that

www.StemCells.com

Figure 7. Increase of beating areas within embryoid bodies (EBs). Embryoid bodies from F3-1 and F3-1-B14 cells were plated with or without doxycycline into 24-well plates. For each cell and condition, approximately 720 EBs were plated, and beating areas were counted at day 18. Upper panel: Shown in red are beating areas. Note that a single EB may contain more than one beating area, and beating areas may become confluent with time. Numbers indicate beating areas from 720 bodies plated. Lower panel: The size of beating areas from three experiments was quantified, averaged, and is shown with standard error of the mean. Abbreviation: Dox, doxycycline.

is also of larger size. As with the morphological changes (Fig. 6), this effect on beating bodies required the presence of doxycycline early (day 0–day 4) in the experiment (Fig. 8C, lower panel), and no effect was seen when the drug was added from day 4 onwards (data not shown).
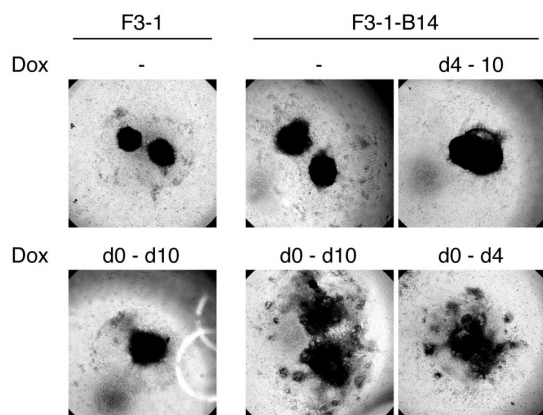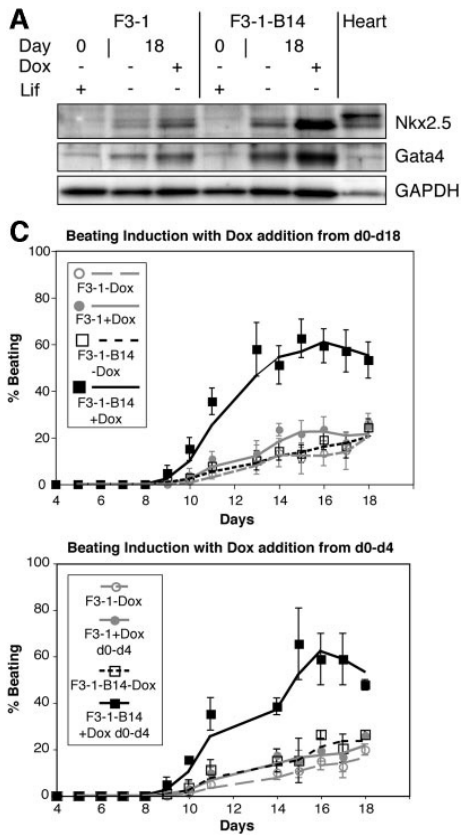
DISCUSSION

This work describes a Tet-based inducible RNA interference system, which allows the downregulation of any transcript of choice following flp recombinase mediated DNA recombination in ES cells. The power of the system is documented in experiments in which Stat3, the known regulator of ES cell differentiation, was targeted. In addition, it allowed assignment of a novel function to the post-transcriptional regulator Brf1 in ES-cell-derived cardiomyocyte formation. Clone F3-1, carrying both the Tet repressor and an frt-GFP-marked locus that integrated into genomic regions favorable for long-term gene expression (even long after onset of differentiation), is central to our system. Establishment of the doxycycline-inducible shRNA system in ES cells is of significance in view of the reported difficulties in establishing the Tet system in ES cells, thought to be due to a tendency in ES cells toward gene silencing. The efficiency of successful recombination assessed by the three selection markers GFP, neomycin, and hygromycin resistance and confirmatory PCR was remarkably high and approached approximately 50% with Stat3 and 70% with Brf1 plasmids (data not shown). With Stat3, we observed strong doxycycline-dependent induction of 21 nt siRNA formation, negligible background, and a strong morphological and biochemical response including signs of differentiation and appropriate changes of the stem-cell markers Oct4, Fgf-4, and Rex-1. Niwa et al. [5] have previously described an ES system where tetracycline induction triggered differentiation via the formation of a dominant-negative form of Stat3 protein expressed from a chromosomal site. As our system compared well with this dominant-negative system, we concluded that the RNA interference approach is suit-

Figure 8. Brf1 downregulation is correlated with stimulation of cardiomyocyte formation. **(A):** Control cells (F3-1) and Brf1 small hairpin RNA cells (F3-1-B14) were cultured in the absence of LIF with or without doxycycline for 18 days. Western blot analysis was performed for Nkx2.5, Gata4, and GAPDH. Also shown are undifferentiated F3-1 and F3-1-B14 cells grown in LIF and mouse heart as controls. **(B):** Semiquantitative RT-PCR of the cardiac marker α-cardiac actin at indicated days after LIF removal. GAPDH served as control. **(C):** F3-1 and F3-1-B14 embryoid bodies (EBs) were plated into 48-well plates at two bodies per well and cultured with or without doxycycline. EBs were checked daily for onset of beating and scored. The data are shown as percentage of beating bodies to total plated. Upper panel: F3-1 and F3-1-B14 EBs cultured with doxycycline for the total length of the experiment. For each time point, at least three experiments are averaged, and standard errors of the mean are shown. Lower panel: As above, but doxycycline was present where indicated only from day 0 to day 4. For each time point the average and standard errors of the mean of at least three experiments are shown. Abbreviations: d, day; Dox, doxycycline; GAPDH, glyceraldehyde-3-phosphate dehydrogenase; LIF, leukemia inhibitory factor; RT-PCR, reverse transcription-polymerase chain reaction.

able to probe the possible function of other suspected regulators and concentrated on Brf1, a regulator of mRNA turnover.

Brf1, originally discovered as an immediate-early gene [38], is a member of a small family of RNA-binding proteins with a conserved and characteristic CCCH zinc-finger domain recognizing AREs in the 3′UTR and promoting mRNA decay. We reported recently that the mRNA decay promoting activity of Brf1 is negatively regulated by phosphorylation via protein kinase B, which promotes complex formation to 14-3-3 [39]. Target mRNAs of Brf1 are not known but play a role in development, as mice lacking both alleles die at day 11 [40]. That Brf1 is controlled at least in part by Stat3 was suggested by the LIF removal experiment where Brf1 levels dropped (Fig. 1) and supported by transient transfection of Stat3 siRNA, which led to concomitant downregulation of Stat3 and Brf1 (Fig. 1C). In several Stat3 shRNA clones tested, doxycycline led to downregulation of Brf1 protein and transcripts (supplemental online Figs. 2, 3A). These results are consistent with DNA microarray data of others who reported Brf1 (*Zfp36L1*) downregulation after LIF removal [41, 42]. That the effect in some clones was less intense than that following LIF removal suggests that not all effects on gene expression by LIF removal are mediated by Stat3. Although a Stat3 site in the promoter region of Brf1 has been reported, support for additional control elements was provided in a recent paper on the human ES cell transcriptome where chromatin immunoprecipitation was combined with DNA microarray analysis to identify promoters of transcripts expressed in stem cells that are co-occupied by Oct4, nanog, and Sox2. Interestingly, both Stat3 and Brf1 were among the 353 transcripts that fulfilled these criteria [14]. Oct4 and Sox2 bind
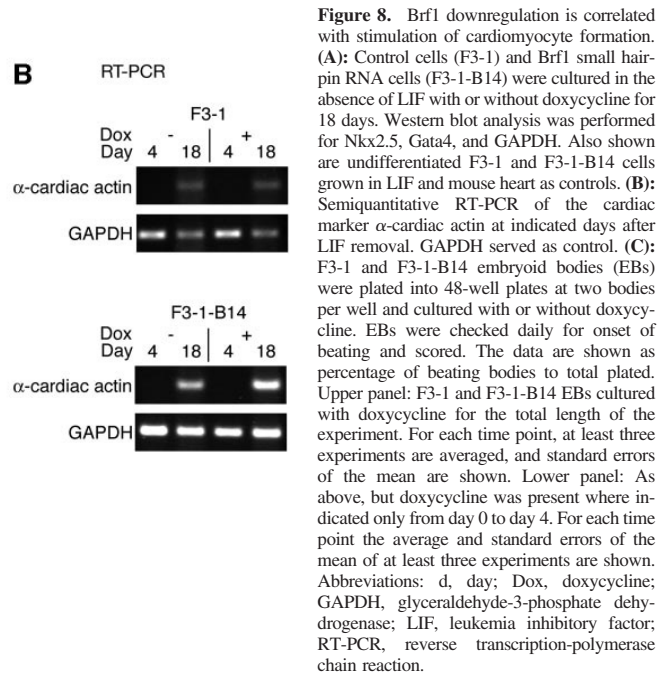
the Brf1 promoter 2497 nt upstream of the transcription initiation site and nanog at position 1733.

When we tested the effects of Brf1 shRNA induction in ES long-term cultures, we made the unexpected observation that the morphology of EBs, the number of beating areas within an embryoid body, and also the total number of beating areas was dramatically altered. We do not know whether this reflects increased survival or enhanced promotion into myogenic tissue. A time-course revealed that downregulation of Brf1 did not change the kinetics of cardiomyocyte formation, but rather amplified the spontaneous formation known to occur in cultures of murine and human EBs [37]. It is significant that both effects on general EB morphology and on cardiomyocyte formation do not occur when Brf1 is downregulated only at day 4 or later in EB cultures. This supports the hypothesis that a transient early change in Brf1 levels may set the stage for downstream processes executed by Brf1 target genes. Our data suggests the following model: Brf1, a target of Stat3, is a suppressor of differentiation expressed in undifferentiated pluripotent stem cells. Reducing its levels physiologically via reduction of LIF-Stat3 signaling or by inducible RNA interference leads to changes in embryoid body architecture and enhancement of cardiomyocyte formation. Whether generation of other cell types is similarly enhanced remains to be examined. As Brf1 regulates ARE-dependent mRNA turnover, the model predicts the existence of ARE-containing transcripts favoring cardiomyogenesis, a possibility that can now be addressed by DNA microarray analysis and suitable follow-up experiments with candidate genes. Overexpression of Brf1 would be expected to

suppress cardiomyogenesis, which, however, could not be tested, as transfected Brf1 is toxic to ES cells (supplemental online Fig. 5). If, as may well be the case, Brf1 also regulates cardiomyocyte formation in human ES cells, the protocol described here may prove useful in regenerative cardiology for replacement therapy. In addition, transgenic mice eventually generated from the lines described here might circumvent the lethality of Brf1 knockouts [40] and allow the downregulation

of Brf1 in adult tissue to reveal further functional aspects of this post-transcriptional regulator.

DISCLOSURE OF POTENTIAL CONFLICTS OF INTEREST

The authors indicate no potential conflicts of interest.

REFERENCES

1 Smith AG. Embryo-derived stem cells: Of mice and men. Annu Rev Cell Dev Biol 2001;17:435–462.

2 Williams RL, Hilton DJ, Pease S et al. Myeloid leukaemia inhibitory factor maintains the developmental potential of embryonic stem cells. Nature 1988;336:684–687.

3 Smith AG, Heath JK, Donaldson DD et al. Inhibition of pluripotential embryonic stem cell differentiation by purified polypeptides. Nature 1988;336:688–690.

4 Matsuda T, Nakamura T, Nakao K et al. STAT3 activation is sufficient to maintain an undifferentiated state of mouse embryonic stem cells. Embo J 1999;18:4261–4269.

5 Niwa H, Burdon T, Chambers I et al. Self-renewal of pluripotent embryonic stem cells is mediated via activation of STAT3. Genes Dev 1998;12:2048–2060.

6 Cartwright P, McLean C, Sheppard A et al. LIF/STAT3 controls ES cell self-renewal and pluripotency by a Myc-dependent mechanism. Development 2005;132:885–896.

7 Nichols J, Zevnik B, Anastassiadis K et al. Formation of pluripotent stem cells in the mammalian embryo depends on the POU transcription factor Oct4. Cell 1998;95:379–391.

8 Niwa H, Miyazaki J, Smith AG. Quantitative expression of Oct-3/4 defines differentiation, dedifferentiation or self-renewal of ES cells. Nat Genet 2000;24:372–376.

9 Shimozaki K, Nakashima K, Niwa H et al. Involvement of Oct3/4 in the enhancement of neuronal differentiation of ES cells in neurogenesis-inducing cultures. Development 2003;130:2505–2512.

10 Chambers I, Colby D, Robertson M et al. Functional expression cloning of Nanog, a pluripotency sustaining factor in embryonic stem cells. Cell 2003;113:643–655.

11 Mitsui K, Tokuzawa Y, Itoh H et al. The homeoprotein Nanog is required for maintenance of pluripotency in mouse epiblast and ES cells. Cell 2003;113:631–642.

12 Ying QL, Nichols J, Chambers I et al. BMP induction of Id proteins suppresses differentiation and sustains embryonic stem cell self-renewal in collaboration with STAT3. Cell 2003;115:281–292.

13 Qi X, Li TG, Hao J et al. BMP4 supports self-renewal of embryonic stem cells by inhibiting mitogen-activated protein kinase pathways. Proc Natl Acad Sci U S A 2004;101:6027–6032.

14 Boyer LA, Lee TI, Cole MF et al. Core transcriptional regulatory circuitry in human embryonic stem cells. Cell 2005;122:947–956.

15 Boiani M, Scholer HR. Regulatory networks in embryo-derived pluripotent stem cells. Nat Rev Mol Cell Biol 2005;6:872–884.

16 Chen CY, Shyu AB. AU-rich elements: Characterization and importance in mRNA degradation. Trends Biochem Sci 1995;20:465–470.

17 Bakheet T, Frevel M, Williams BR et al. ARED: Human AU-rich element-containing mRNA database reveals an unexpectedly diverse functional repertoire of encoded proteins. Nucleic Acids Res 2001;29:246–254.

18 Zhang W, Wagner BJ, Ehrenman K et al. Purification, characterization, and cDNA cloning of an AU-rich element RNA-binding protein, AUF1. Mol Cell Biol 1993;13:7652–7665.

19 Lai WS, Carballo E, Strum JR et al. Evidence that tristetraprolin binds to AU-rich elements and promotes the deadenylation and destabilization of tumor necrosis factor alpha mRNA. Mol Cell Biol 1999;19:4311–4323.

20 Lai WS, Carballo E, Thorn JM et al. Interactions of CCCH zinc finger proteins with mRNA. Binding of tristetraprolin-related zinc finger proteins to Au-rich elements and destabilization of mRNA. J Biol Chem 2000;275:17827–17837.

21 Stoecklin G, Colombi M, Raineri I et al. Functional cloning of BRF1, a regulator of ARE-dependent mRNA turnover. Embo J 2002;21:4709–4718.

22 Ma WJ, Cheng S, Campbell C et al. Cloning and characterization of HuR, a ubiquitously expressed Elav-like protein. J Biol Chem 1996;271: 8144–8151.

23 Gao M, Wilusz CJ, Peltz SW et al. A novel mRNA-decapping activity in HeLa cytoplasmic extracts is regulated by AU-rich elements. Embo J 2001;20:1134–1143.

24 Chen CY, Gherzi R, Ong SE et al. AU binding proteins recruit the exosome to degrade ARE-containing mRNAs. Cell 2001;107:451–464.

25 Lykke-Andersen J, Wagner E. Recruitment and activation of mRNA decay enzymes by two ARE-mediated decay activation domains in the proteins TTP and BRF-1. Genes Dev 2005;19:351–361.

26 Keene JD, Tenenbaum SA. Eukaryotic mRNPs may represent posttranscriptional operons. Mol Cell 2002;9:1161–1167.

27 O'Gorman S, Fox DT, Wahl GM. Recombinase-mediated gene activation and site-specific integration in mammalian cells. Science 1991;251: 1351–1355.

28 Robertson E, Bradley A, Kuehn M et al. Germ-line transmission of genes introduced into cultured pluripotential cells by retroviral vector. Nature 1986;323:445–448.

29 Keller G, Kennedy M, Papayannopoulou T et al. Hematopoietic commitment during embryonic stem cell differentiation in culture. Mol Cell Biol 1993;13:473–486.

30 McLeod M, Craft S, Broach JR. Identification of the crossover site during FLP-mediated recombination in the Saccharomyces cerevisiae plasmid 2 microns circle. Mol Cell Biol 1986;6:3357–3367.

31 van de Wetering M, Oving I, Muncan V et al. Specific inhibition of gene expression using a stably integrated, inducible small-interfering-RNA vector. EMBO Rep 2003;4:609–615.

32 Raineri I, Wegmueller D, Gross B et al. Roles of AUF1 isoforms, HuR and BRF1 in ARE-dependent mRNA turnover studied by RNA interference. Nucleic Acids Res 2004;32:1279–1288.

33 Brummelkamp TR, Bernards R, Agami R. A system for stable expression of short interfering RNAs in mammalian cells. Science 2002;296:550–553.

34 Gossen M, Bujard H. Tight control of gene expression in mammalian cells by tetracycline-responsive promoters. Proc Natl Acad Sci U S A 1992;89:5547–5551.

35 Yao F, Svensjo T, Winkler T et al. Tetracycline repressor, tetR, rather than the tetR-mammalian cell transcription factor fusion derivatives, regulates inducible gene expression in mammalian cells. Hum Gene Ther 1998;9:1939–1950.

36 Komuro I, Izumo S. Csx: A murine homeobox-containing gene specifically expressed in the developing heart. Proc Natl Acad Sci U S A 1993;90:8145–8149.

37 Sachinidis A, Fleischmann BK, Kolossov E et al. Cardiac specific differentiation of mouse embryonic stem cells. Cardiovasc Res 2003;58:278–291.

38 Gomperts M, Pascall JC, Brown KD. The nucleotide sequence of a cDNA encoding an EGF-inducible gene indicates the existence of a new family of mitogen-induced genes. Oncogene 1990;5:1081–1083.

39 Schmidlin M, Lu M, Leuenberger SA et al. The ARE-dependent mRNA-destabilizing activity of BRF1 is regulated by protein kinase B. Embo J 2004;23:4760–4769.

40 Stumpo DJ, Byrd NA, Phillips RS et al. Chorioallantoic fusion defects and embryonic lethality resulting from disruption of Zfp36L1, a gene encoding a CCCH tandem zinc finger protein of the Tristetraprolin family. Mol Cell Biol 2004;24:6445–6455.

41 Palmqvist L, Glover CH, Hsu L et al. Correlation of murine embryonic stem cell gene expression profiles with functional measures of pluripotency. STEM CELLS 2005;23:663–680.

42 Sekkai D, Gruel G, Herry M et al. Microarray analysis of LIF/Stat3 transcriptional targets in embryonic stem cells. STEM CELLS 2005;23: 1634–1642.

See www.StemCells.com for supplemental material available online.

Roles of AUF1 isoforms, HuR and BRF1 in ARE-dependent mRNA turnover studied by RNA interference

Ines Raineri, Daniel Wegmueller, Brigitte Gross, Ulrich Certa[1] and Christoph Moroni*

Institute for Medical Microbiology, University of Basel, Petersplatz 10, 4003 Basel, Switzerland and [1]Roche Center for Medical Genomics, F. Hoffmann-La Roche Ltd, Postfach, Building 93/610, CH-4070, Basel, Switzerland

ABSTRACT

HT1080 cells stably expressing green fluorescent protein (GFP) linked to a 3′ terminal AU-rich element (ARE) proved to be a convenient system to study the dynamics of mRNA stability, as changes in mRNA levels are reflected in increased or decreased fluorescence intensity. This study examined whether mRNA stability can be regulated by small interfering RNAs (siRNAs) targeted to AU-binding proteins (AUBPs), which in turn should reveal their intrinsic role as stabilizers or destabilizers of ARE-mRNAs. Indeed, siRNAs targeting HuR or BRF1 decreased or increased fluorescence, respectively. This effect was abolished if cells were treated with both siRNAs, thus indicating antagonistic control of ARE-mRNA stability. Unexpectedly, downregulation of all four AUF1 isoforms by targeting common exons did not affect fluorescence whereas selective downregulation of $p40^{AUF1}$/$p45^{AUF1}$ strongly increased fluorescence by stabilizing the GFP–ARE reporter mRNA. This observation was fully confirmed by the finding that only selective reduction of $p40^{AUF1}$/$p45^{AUF1}$ induced the production of GM-CSF, an endogenous target of AUF1. These data suggest that the relative levels of individual isoforms, rather than the absolute amount of AUF1, determine the net mRNA stability of ARE-containing transcripts, consistent with the differing ARE-binding capacities of the isoforms.

INTRODUCTION

Regulation of mRNA turnover is a key mechanism determining the intracellular abundance of transcripts, thus contributing to the controlled production of the encoded gene products (1–3). So far, the best characterized cis-elements mediating control of mRNA stability are the AU-rich elements (ARE) contained in the 3′ untranslated region (3′UTR) of cytokines, growth factors and proto-oncogenes (4,5). Presence of an ARE induces rapid shortening of the poly-A tail followed by exosomal degradation of the mRNA body (6–8). Transcripts containing an ARE usually exhibit rapid decay in resting cells, but are readily stabilized upon exposure to exogenous signals. Importantly, defective ARE function causing increased transcript stability has been reported to be a pathogenic factor in human malignancies (9–11), experimental tumors (12) and inflammatory disorders (13,14).

Several proteins binding to the ARE, AU-rich element binding proteins (AUBPs) have been identified and shown to exert a defined role in ARE-mRNA turnover. HuR, a member of the embryonic lethal abnormal vision (ELAV) RNA binding protein family has been shown to stabilize ARE-mRNAs (15,16). Two closely related proteins also containing RNA recognition motifs (RRM), TIA-1 (T-cell internal antigen-1) and TIAR (TIA-1-related protein), bind the ARE and act as translational silencers (17). Tristetraprolin (TTP, *zfp-36*) the prototype of a family of zinc-finger proteins of the unusual Cys-Cys-Cys-His (CCCH) class promotes degradation of tumor necrosis factor α (TNFα) (18,19), granulocyte-macrophage colony stimulating factor (GM-CSF) (20) and interleukin-3 (IL-3) mRNA (21). Butyrate response factor 1 (BRF1, *zfp-36l1*), a second member of the same class of zinc finger proteins, has been identified using functional genetic screening (22) and was shown to mediate rapid decay of various cytokine mRNAs, including IL-3, IL-6, GM-CSF and TNFα (23). Finally, AUF1 was first identified as a promoter of rapid ARE-mRNA decay in extracts of K562 cells (24). However, upon purification and cloning, the recombinant protein lacked decay promoting activity (25). The analysis of AUF1 has been further complicated by the existence of four isoforms that arise by differential splicing (26). This family of proteins distinguishes a 37 kDa ($p37^{AUF1}$) core protein, a 40 kDa protein ($p40^{AUF1}$) containing an N-terminal 19 amino acid insertion (exon 2), a 42 kDa protein ($p42^{AUF1}$) exhibiting a C-terminal 49 amino acids insertion (exon 7), and a 45 kDa protein ($p45^{AUF1}$) with insertions of both exon 2 and exon 7. Presence or absence of these alternatively spliced exons confers distinct biological properties to individual AUF1 isoforms. Presence of exon 7 not only affects nucleo-cytoplasmic distribution (27,28), but also blocks ubiquitination of $p42^{AUF1}$ and $p45^{AUF1}$ (29). In contrast, the lack of exon 7 targets $p37^{AUF1}$ and $p40^{AUF1}$ to the ubiquitin–proteasome pathway, which results in rapid decay of ARE-mRNAs (30,31). Importantly, absence of exon 2 in 37^{AUF1} and $p42^{AUF1}$ is associated with high affinity binding of these

*To whom correspondence should be addressed. Tel: +41 61 267 3265; Fax: +41 61 267 3283; Email: christoph.moroni@unibas.ch

isoforms (26). In addition to its role in ARE-mRNA turnover, AUF1 has been proposed to be involved in multiple cellular processes such as telomere maintenance (32) and transcriptional activation (33). The fact that AUF1 was identified to be a component of the α-globin mRNA stability complex (34) and to participate in mRNA decay directed by the c-*fos* major coding determinant (35) points to a more general function of this protein in mRNA turnover. With respect to ARE-mRNA turnover, the role of AUF1 has been extensively studied, but results were conflicting. Increased expression of AUF1 has been associated with rapid ARE-mRNA decay in peripheral blood mononuclear cells (PBMC) (36,37), smooth muscle cells (38) and monocytes (39). These data, together with the finding that forced expression of p37[AUF1] and p42[AUF1] antagonized stabilization of ARE-mRNAs accompanying hemin-induced erythroid differentiation of K562 cells (40) argue for an intrinsic destabilizing activity of AUF1. However, overexpression of all four AUF1 isoforms in NIH3T3 cells stabilized ARE-containing transcripts (41). It has not been resolved whether these disparities were due to the different cell types examined or changes in experimental conditions. Analysis of AUF1 knockout mice or studies using small interfering RNAs (siRNAs) targeted to AUF1 should help to clarify these issues.

The present study examined whether single or combined treatment of cells with siRNAs targeting HuR, BRF1 and AUF1 would affect ARE-mediated mRNA turnover. Our data indicate that BRF1 and HuR control ARE-mRNA stability in an antagonistic fashion. Furthermore, we present evidence that effects of AUF1 on ARE-containing transcripts depend on the expression level of individual AUF1 isoforms.

MATERIALS AND METHODS

Cell culture and transfection

The previously described HT1080-derived reporter cell line HTwt16 (21) was cultured in Iscove's Modified Dulbecco Medium containing 10% fetal calf serum (FCS), 50 μM 2-mercaptoethanol, 2 mM glutamine, 100 U/ml penicillin and 100 μg/ml streptomycin at 37°C/7% CO$_2$. In addition, NIH 3T3 cells stably expressing the GFP–ARE (3T3GFP–ARE) were generated and cultured as described above.

For transfections, 1.5×10^5 cells were plated per well of a 6-well plate and cultured overnight. Thereafter, siRNAs were transfected at a final concentration of 240 nM in the presence of serum free medium (OptiMEM, Invitrogen) using Oligofectamine (Invitrogen) as the carrier. Analyses were performed 48–72 h after transfection.

Oligoribonucleotides

The following 19mer oligoribonucleotide duplexes containing a 2-nt deoxythymidine overhang at each 3′ end were purchased from Xeragon. BRF1, 5′ CAA GAU GCU CAA CUA UAG U; HuR (oligo A), 5′ UAA AGU AGC AGG ACA CAG C; HuR (oligo B), 5′ CAC GCU GAA CGG CUU GAG G (42); AUF1 (exon 1), 5′ GAU UGA CGC CAG UAA GAA C; AUF1 (exon 2/oligo A), 5′ ACG AGG AGG AUG AAG GCC A (the first 16 nt are located in exon 1, the last 3 nt in exon 2); AUF1 (exon 2/oligo B), 5′ GCA GCG ACG GCA CAG CGG G; AUF1 (exon 3), 5′ GAU CCU AUC ACA GGG

CGA U; AUF1 (exon 7), 5′ CUG GAA CCA GGG AUA UAG U; β-globin, 5′ CAA GAA AGU GCU CGG UGC C.

Sequences were derived from the human sequences of HuR mRNA (accession number BC003376), BRF1 mRNA (accession number NM_007564), AUF1 mRNA (accession number NM_031370) and β-globin mRNA (accession number V00497.1). Blast search was performed on all the sequences to avoid cross-reaction with other genes.

Flow cytometry

FACS analysis of 1–2×10^4 cells was performed using a FACScan (Becton Dickinson) and the Cellquest software. GFP fluorescence was excited at 488 nm and emission was measured at 510 nm. To analyze the difference in fluorescence between medium and siRNA treated cells, Kolmogorow–Smirnow statistics calculating the greatest difference (D) in fluorescence between these two treatments were performed. The mean ± standard deviation (SD) of D for 4–9 independent experiments was calculated and Student's *t*-test comparing D of β-globin and specific siRNA-treated cells was performed.

Northern blot analysis

To analyze mRNA levels in cells treated with specific siRNAs, total RNA was harvested 72 h after transfection using Trizol® (Invitrogen). Total RNA (10–15 μg) was resolved on 1% agarose–formaldehyde gels, which were subsequently blotted onto Hybond-N+ membranes (Amersham) using 20× SSC. To detect HuR, filters were hybridized in the presence of 50% formamide (43) using a [α-32P]GTP-labeled SP6 transcribed probe spanning nt 121–488 of the murine HuR cDNA (accession number NM_010485). To detect BRF1, control β-actin and G3PDH, PCR fragments of the respective cDNAs (BRF1, nt 524–1019, accession number X99404; G3PDH, nt 589–1246, accession number M33197; murine β-actin, nt 554–815, accession number X03765) were labelled with [α-32P]dCTP using Klenow enzyme (New England Biolabs) and the gene specific 3′ primers. Filters were hybridized overnight at 65°C in 0.5 M sodium phosphate buffer pH 7.2 containing 1% BSA (Fraction V, Sigma), 7% SDS and 5 mM EDTA, and subsequently washed at 55°C each in 2× SSC/ 0.2% SDS and 0.2× SSC/0.2% SDS.

To analyze mRNA stability of the GFP–ARE reporter, cells were treated 72 h after transfection with 5 μg/ml of actinomycin D. Cytoplasmic RNA was harvested at the indicated time-points (44) and northern blot analysis performed using an SP6 transcribed [α-32P]GTP-labeled probe spanning a XbaI–EcoRI fragment containing the murine IL-3 3′UTR as described.

Signal intensities were quantified using a Personal Molecular Imager® FX (Bio-Rad) and the Quantity One™ software (Bio-Rad). To normalize for loading differences, signal intensities were normalized to the β-actin or G3PDH control.

Western blot analysis

Western blot analysis was performed as recently described (21). Briefly, 30–50 μg of total cell lysates in RIPA buffer (BRF1 and AUF1) or 15 μg of cytoplasmic cell lysate (HuR), prepared with the NE-PER® nuclear cytoplasmic extraction reagents (Pierce), were resolved on 4–20% gradient polyacrylamide gels (Anamed Electrophorese GmbH) and blotted

onto Immobilon-P (Millipore) membranes. To detect BRF1, a polyclonal antibody was generated in rabbits immunized with a C-terminal BRF1 peptide (SDSPTLDNSRRLPIFSRLSI-SDD; Neosystem) covalently linked to KLH. Antibodies were subsequently affinity purified using the BRF1 peptides employed in immunization. Monoclonal mouse-anti human HuR (Santa Cruz), polyclonal rabbit-anti human AUF1 (Upstate Biotechnology) and monoclonal mouse-anti bovine α-tubulin antibodies (Molecular Probes) served to detect the respective genes. An alkaline phosphatase-coupled goat-anti-rabbit IgG (Southern Biotechnology Associates Inc.) or a horseradish-peroxidase-coupled goat-anti-mouse IgG (DAKO) were used as secondary antibodies. Development was performed using CDP-Star (Roche) or ECL Advance (Amersham), respectively. For quantification, autoradiographs were scanned and analyzed by densitometry using the Quantity One® software (Bio-Rad).

Detection of GM-CSF by ELISA

Supernatants of triplicate cultures treated with medium or individual siRNA were harvested 72 h after transfection. GM-CSF was determined by ELISA (Pharmingen) according to the manufacturers instructions.

RESULTS

SiRNA targeting HuR and BRF1

We recently showed that siRNA targeting BRF1 increased mRNA stability of a GFP–ARE reporter and, concomitantly, fluorescence of transfected cells by FACS. Indeed, these siRNAs allowed distinction between cells with two wild-type BRF1 alleles from cells exhibiting a heterozygous inactivation of BRF1, solely based on the extent of the fluorescence shift (22). These data encouraged us to extend this approach to further AUBPs, arguing that if changes in GFP–ARE transcript stability are faithfully reflected in altered fluorescence intensity, this approach will enable the assessment of ARE-mRNA turnover rates in live cells without requiring the use of transcriptional inhibitors. As exemplified in Figure 1, downregulation of AUBPs stabilizing or destabilizing ARE-mRNAs will decrease or increase fluorescence intensity, respectively.

First, we investigated HuR, an AUBP known to stabilize ARE-mRNAs (15,16). A siRNA targeting HuR was designed that reduced HuR mRNA levels to 40% of medium or β-globin siRNA treated controls. By comparison, treatment of cells with BRF1 siRNA alone or in combination with β-globin or HuR siRNAs reduced BRF1 mRNA levels to 25% of controls (Fig. 2A). An additional HuR siRNA that had recently been described by others (42) reduced HuR protein levels to 60% of controls by western blot (Fig. 2B). Efficient inhibition of BRF1 by siRNA was also established in western blots using a polyclonal anti-BRF1 antibody generated in rabbits immunized with a C-terminal peptide of BRF1. Specific recognition of BRF1 by this antibody was confirmed by the absence of the signal in mutant slowC cells, which lack BRF1 expression compared to parental Htwt16 cells, which express wild-type BRF1 (22) (Fig. 2B).

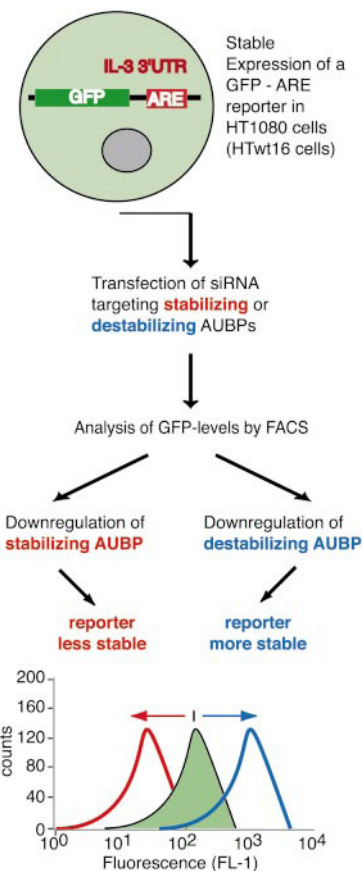Next, we determined by FACS whether siRNA treatment affected GFP expression. The results of two independent

Figure 1. Reporter system employed to reveal effects of decreased AUBP expression on ARE-mRNA stability. HT1080 cells stably expressing a GFP–ARE reporter (HTwt16) are transfected with siRNA targeting AUBP. Decreasing the level of an AUBP that stabilizes ARE-mRNAs should result in decreased fluorescence by FACS. In contrast, downregulation of an AUBP that destabilizes ARE-mRNAs should result in increased fluorescence.

experiments are shown in Figure 2C. For quantification, the greatest difference (D) in fluorescence between the curves obtained from cells treated with medium or siRNA was calculated using Kolmogorow–Smirnov statistics (Table 1). In experiment 1, no significant differences were observed between cells transfected with medium or a non-specific β-globin control siRNA (Fig. 2C, panel A). However, transfection of HuR siRNA decreased fluorescence (panel B) and BRF1siRNA increased fluorescence as previously reported (panel D) (22). To evaluate whether HuR siRNA might antagonize the stabilizing effect of BRF1 siRNA, cells were treated with combinations of siRNAs. Combined treatment with HuR or BRF1 and a non-specific β-globin siRNA led to the same shift in fluorescence as treatment with HuR or BRF1 siRNA alone (panel C and E). In contrast, combined treatment with BRF1 and HuR siRNA abolished the effects of the single
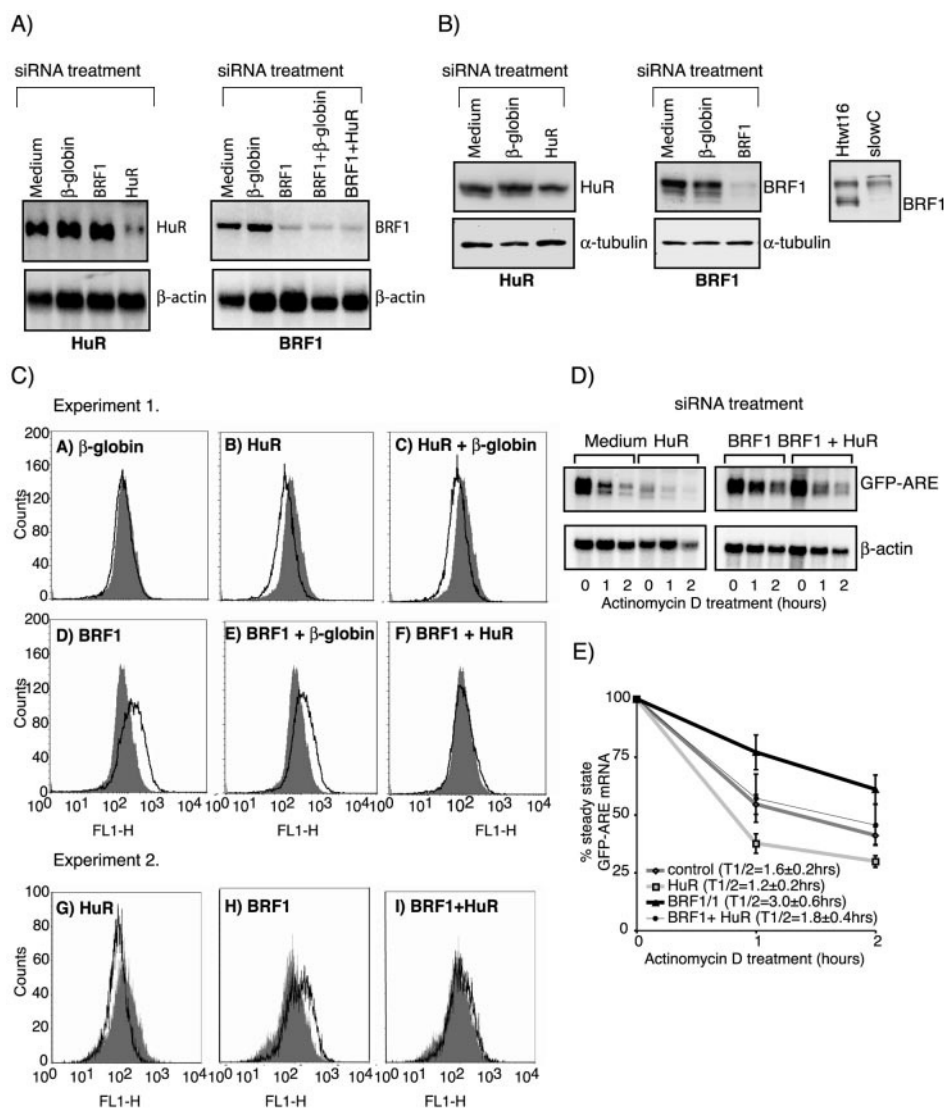
Figure 2. HuR and BRF1 siRNA have opposing effects on fluorescence and GFP–ARE mRNA stability in Htwt16 cells. (**A**) Northern blot analysis of HuR and BRF1 expression in Htwt16 cells treated for 72 h with control β-globin, HuR (oligo A), BRF1 siRNA or their combinations. (**B**) Western blots of 15 µg of cytoplasmic and 30 µg of total cell lysate to analyze cells treated with HuR (oligo B) or BRF1 siRNA. As control for the specificity of the anti-BRF1 anti-body, absence of the BRF1 signal in slowC cells lacking BRF1 expression is shown in comparison to Htwt16 cells, which express wild-type BRF1. (**C**) FACS analysis of cells treated for 72 h. In experiment 1 (A–F) the shaded areas represent medium and the overlays siRNA-treated cells; HuR (oligo A) was employed in panels B and F. In experiment 2 (G–I) the shaded curves represent cells treated with β-globin control and the overlays represent cells treated with specific BRF1 and/or HuR (oligo B) siRNA. (**D**) To evaluate the effects of siRNA on GFP–ARE mRNA stability, cells were exposed to actinomycin D for the indicated time-points 72 h after transfection of medium, β-globin control, BRF1 and/or HuR (oligo A) siRNA. Values were normalized to the β-actin control. (**E**) Quantification of the mean ± SEM of at least three independent experiments is shown and the half-life (T1/2) of the GFP–ARE reporter for each individual treatment is indicated.

siRNAs (panel F). We verified these findings with a second HuR siRNA (Fig. 2C, experiment 2). Again, HuR siRNA decreased fluorescence of transfected cells compared to β-globin siRNA-treated control cells (panel G) and annihilated the increase in fluorescence observed in cells treated solely with BRF1 siRNA (panels H and I).

Table 1. Treatment of Htwt16 cells with HuR siRNA decreases fluorescence, an effect that is reversed upon combined treatment with BRF1 siRNA

siRNA treatment	n[a]	Fluorescence[b]	$D_{Kolmogorow–Smirnow}$[c] mean $\pm$ SD	P[d]
β-globin	13	no effect	0.07 $\pm$ 0.04	
HuR	9	decreased	0.23 $\pm$ 0.08	<0.05
HuR + β-globin	4	decreased	0.24 $\pm$ 0.23	<0.05
BRF1	9	increased	0.31 $\pm$ 0.12	<0.05
BRF1 + β-globin	5	increased	0.29 $\pm$ 0.11	<0.05
HuR + BRF1	5	no effect	0.07 $\pm$ 0.03	= 0.9

[a]Number of experiments.
[b]Effect on fluorescence of medium compared to siRNA-treated cells. For statistical analysis only HuR (oligo A) was taken into consideration.
[c]Greatest distance (D) between curves obtained from medium- and siRNA-treated cells.
[d]Student's *t*-test comparing D of cells treated with control β-globin and specific siRNA.

To evaluate whether changes in fluorescence were accompanied by altered mRNA stability of the GFP–ARE reporter, actinomycin D chase experiments were performed. The results of a representative experiment are shown in Figure 2D and quantification of at least three independent experiments for each treatment is exhibited in Figure 2E. Cells treated with HuR siRNA exhibited reduced GFP–ARE mRNA levels and a slightly accelerated decay that was reflected in a decrease of the GFP–ARE half-life ($t_{1/2} = 1.2 \pm 0.2$ h) compared to controls ($t_{1/2} = 1.6 \pm 0.2$ h). The stabilization exerted by BRF1 siRNA ($t_{1/2} = 3.0 \pm 0.6$ h) was reversed by combined treatment with HuR siRNA ($t_{1/2} = 1.8 \pm 0.4$ h). In all actinomycin D chase experiments performed, we observed the decay of the GFP–ARE mRNA reporter to be fastest during the first hour of treatment. Actinomycin D has been shown to itself stabilize ARE-mRNAs (45), an effect that may be responsible for the observed impediment of decay at later time points. Together, changes in fluorescence intensity in cells treated with BRF1, HuR and combinations of these two siRNAs were qualitatively reflected in altered decay rates of the GFP–ARE reporter mRNA.

SiRNA targeting AUF1

The role of AUF1 in ARE-mediated mRNA decay is complicated by the existence of four isoforms and both destabilizing and stabilizing effects have been reported (40,41). To differentially decrease selected AUF1 isoforms we targeted siRNA to exons 1 and 3, which are common to all four isoforms, to exon 2, which is contained in p40^{AUF1} and p45^{AUF1}, and to exon 7, which is present in p42^{AUF1} and p45^{AUF1} (Fig. 3A). First, to evaluate whether the selected siRNA would specifically reduce the targeted isoforms we analyzed their distribution by western blot and quantified the respective bands by densitometry (Fig. 3B). In all experiments performed, we observed a non-specific band (marked by an asterisk) at ~55 kDa whose signal intensity correlated to the α-tubulin loading control as determined by densitometry (data not shown). The p37 and p45 isoforms were clearly distinguished in control cells (lanes 1 and 2). However, p40^{AUF1}, which is highly abundant in these cells, resolved as a very broad band obscuring simultaneous detection of the weakly expressed p42^{AUF1}. As expected, both siRNAs targeting exons

1 and 3 decreased expression of all four isoforms (lanes 3 and 6). Two independent oligoribonucleotide duplexes targeting exon 2 of AUF1 reduced only expression of p40^{AUF1}, the most abundant isoform in this cell line, and p45^{AUF1} (lanes 4 and 5). In contrast, expression of p37^{AUF1} was comparable to medium or β-globin siRNA-treated controls. Of note, the low abundant p42 isoform became visible only after selective removal of p40^{AUF1}, in cells treated with exon 2-specific siRNA. Finally, siRNA targeting exon 7 specifically reduced p45^{AUF1}. The concomitant decrease of p42^{AUF1} could not be analyzed (lane 7), due to the reasons mentioned above. In conclusion, the AUF1 siRNA employed allowed selective and efficient inhibition of the targeted isoforms, with p45^{AUF1} being reduced to 10–27% of controls by the different siRNA.

Next, we investigated how the different AUF1 siRNA affected fluorescence of transfected cells by FACS. Figure 4A shows a representative experiment and quantification is exhibited in Table 2. Decreasing the expression of all four isoforms by targeting exon 1 or 3 did not significantly alter fluorescence compared to β-globin siRNA-treated controls (panels B and E). Downregulation of both p42^{AUF1} and p45^{AUF1} led in some experiments to a slight, not consistently observed and statistically not significant, decrease of fluorescence compared to controls (panel F and Table 2). Together, these data might indicate that AUF1 does not affect expression of the GFP–ARE reporter in this cell line. However, we observed a significant increase of fluorescence in cells exhibiting reduced p40^{AUF1} and p45^{AUF1} expression after treatment with two independent exon 2-specific oligoribonucleotide duplexes (panels C and D). To substantiate these findings we performed a titration experiment, treating cells with 240–1.92 nM of the different AUF1 siRNA employed. Whereas siRNA targeting exons 1, 3 or 7 did not increase fluorescence of transfected cells at any of the concentrations tested, both siRNA targeting exon 2 increased fluorescence, with a minimal effect still being observed at 9.6 nM (data not shown).

Actinomycin D chase experiments (Fig. 4B) revealed that cells exhibiting an increased fluorescence due to selective reduction of p40^{AUF1}/p45^{AUF1} indeed showed a slower decay rate of the GFP–ARE reporter compared to β-globin siRNA- or medium-treated controls. The half-life of the GFP–ARE reporter mRNA in cells treated with AUF1 siRNA targeting exon 2 varied between individual experiments, but a consistent increase was observed compared to controls. The reduced decay rate of the GFP–ARE mRNA in cells thus treated was reflected in an accordingly increased steady-state level of the reporter, which was, however, 15–20% higher than expected. This discrepancy between the predicted and the observed increase was within the variation of the experiment. In contrast, cells exhibiting reduced levels of all four AUF1 isoforms or selectively of p42^{AUF1}/p45^{AUF1} showed decay rates of the reporter that were within the range of the controls.

In addition, NIH 3T3 cells stably expressing the GFP–ARE reporter also exhibited only an increased fluorescence if treated with AUF1 (exon 2a), but not AUF1 (exon 3) siRNA (data not shown).

Effects of HuR, BRF1 and AUF1 siRNA on endogenous GM-CSF expression

To validate these data we wished to investigate whether these siRNAs influenced expression of a physiological endogenous
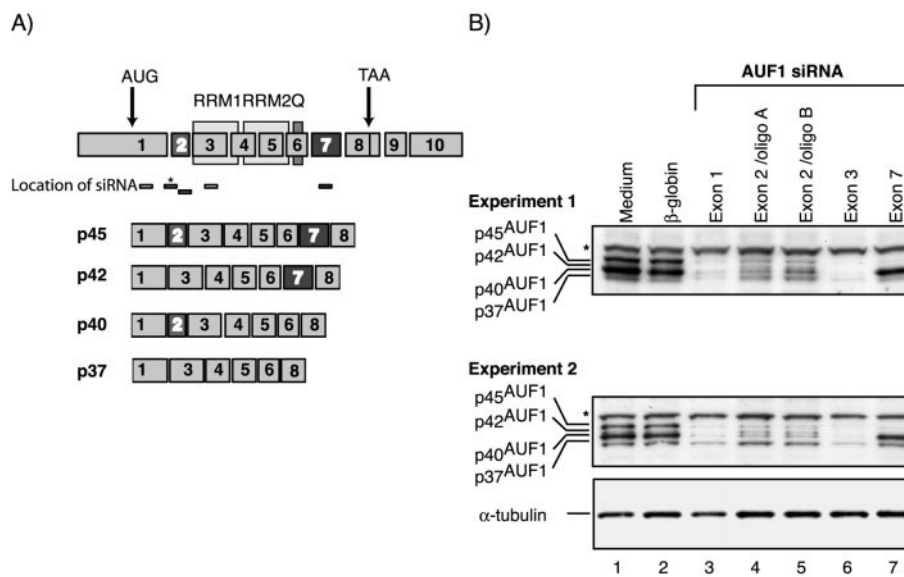
Relative Signal Intensities of Individual AUF1 Isoforms (Exp. 2)

	% Signal Intensity of Control [1]					
	Control	Exon 1	Exon 2a	Exon 2b	Exon 3	Exon 7
p45	100%	10%	27%	23%	10%	17%
p40/p42	100%	7%	27%	28%	5%	96%
p37	100%	37%	108%	87%	25%	117%

1) The integrated volumes of the AUF1 signals of experiment 2 were normalized to the α-tubulin control and expressed as percentage of the average signal obtained in the medium and β-globin treated control samples.

Figure 3. Exon-specific targeting of AUF1 allows selective reduction of specific AUF1 isoforms in Htwt16 cells. (**A**) Schematic drawing of the mRNAs coding for the different AUF1 isoforms and the localization of the siRNA employed. Location of the RRMs and the glutamine rich (Q) stretch are indicated. The siRNA AUF1 (exon 2/oligo A) marked by an asterisk targets 16 bp of exon 1 and 3 bp of exon 2. (**B**) Two independent western blots of cells treated for 72 h with AUF1 siRNA targeting exon 1 (lanes 3), exon 2 (lanes 4 and 5), exon 3 (lanes 6) and exon 7 (lanes 7). The asterisk marks a non-specific band at ~55 kDa that was observed in all experiments performed, and whose signal intensity correlated to the α-tubulin loading control in individual samples. Quantitative analysis of experiment 2 is shown in the table.

target gene. A recent cDNA microarray analysis had revealed that HT1080 cells lacking wild-type BRF1 (22) expressed at least six-fold higher GM-CSF mRNA and protein levels compared to cells with two intact BRF1 alleles, thus identifying GM-CSF as a BRF1 target gene (unpublished data). Therefore, HT1080 cells were treated for 72 h with the different siRNAs and secreted GM-CSF was subsequently determined by ELISA. Treatment with BRF1 siRNA increased GM-CSF production, an effect that was reduced upon simultaneous addition of HuR but not of β-globin siRNA (Fig. 5A). Extending this study to AUF1, a known regulator of GM-CSF expression (46), we found an even more powerful effect than with BRF1 siRNA. Of note, only selective reduction of p40^{AUF1}/p45^{AUF1} increased GM-CSF expression, whereas reduction of all four isoforms or p42^{AUF1}/p45^{AUF1} again had no effect (Fig. 5B). The increase in GM-CSF expression in cells treated with AUF1 (exon 2a) siRNA was

partially reversed if cells were simultaneously treated with HuR siRNA (Fig. 5C). Therefore, not only do the relative levels of stabilizing and destabilizing AUBPs regulate expression of GM-CSF but, surprisingly, also the relative levels of individual AUF1 isoforms.

DISCUSSION

The present study was designed to evaluate siRNA targeting AUBPs in the investigation of ARE-mRNA turnover. This seemed to be a timely objective as, with the exception of TTP (47), no AUBP knockout mice models have been reported. Results gained from loss-of-function experiments are needed to validate data previously obtained by overexpression of AUBPs. This is of particular importance because these experiments did not provide unifying conclusions (see below).
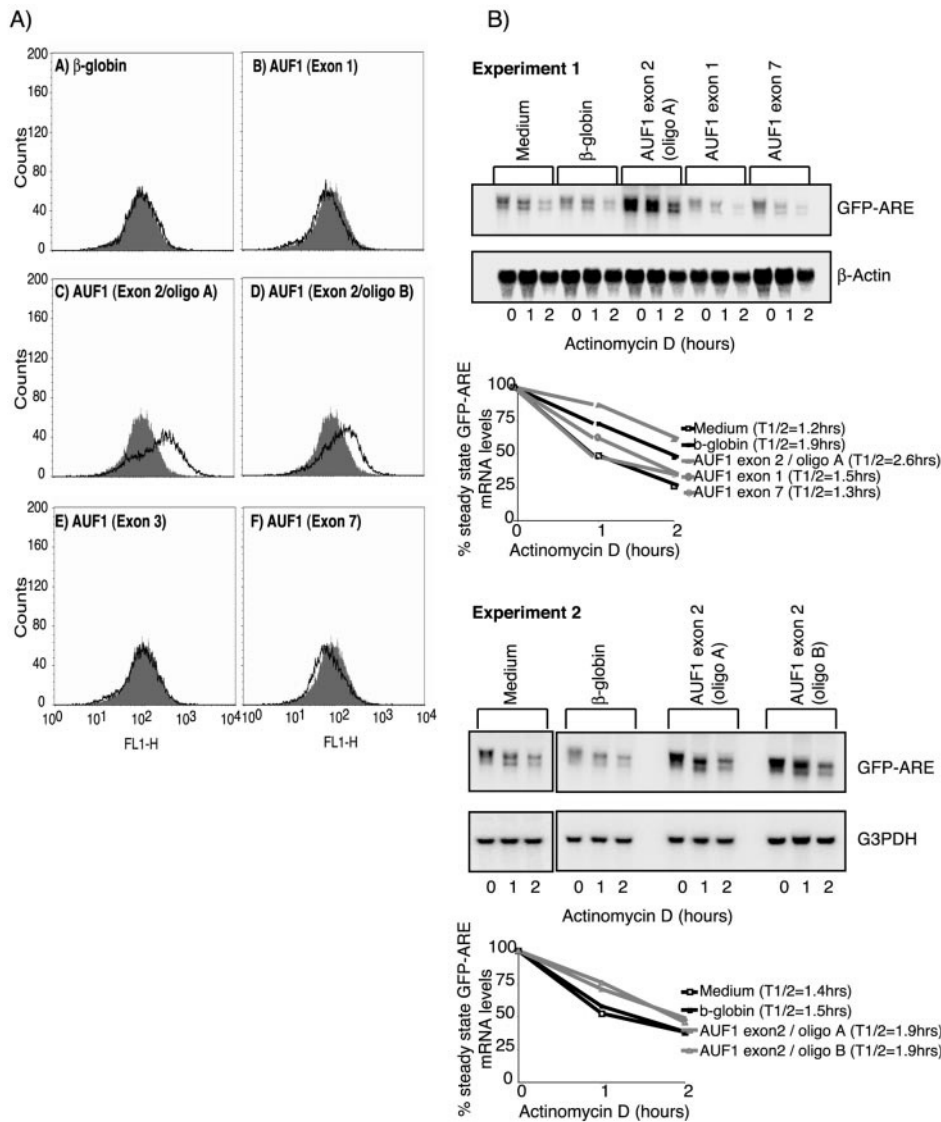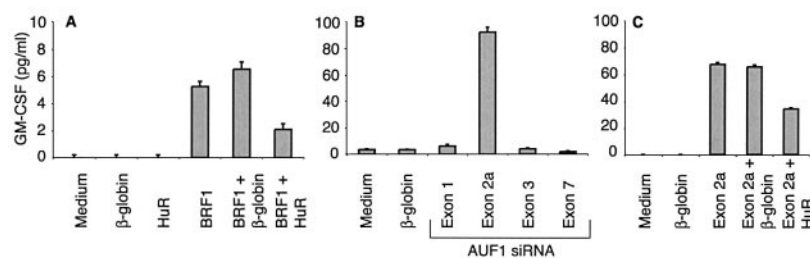
Figure 4. Selective downregulation of p40^{AUF1}/p45^{AUF1} increases fluorescence and stabilizes the GFP–ARE reporter in Htwt16 cells. (**A**) FACS analysis of cells treated for 72 h with medium or siRNA as indicated. (**B**) To evaluate the effects of siRNA on GFP–ARE mRNA stability, cells were exposed to actinomycin D for the indicated time-points 72 h after transfection of siRNA.

Indeed, treatment of Htwt16 cells with siRNA targeting HuR, a protein known to stabilize ARE-mRNAs (15,16) decreased fluorescence intensity and promoted decay of the GFP–ARE-mRNA reporter, thus confirming HuR to be a stabilizer of ARE-mRNAs. BRF1 siRNA induced the expected increase in fluorescence intensity and stabilized the GFP–ARE reporter, effects that were nullified in cells treated with a combination of HuR and BRF1 siRNAs. Inactive siRNAs have been claimed to compete with active siRNAs in a sequence-independent manner (48). However, non-specific effects were ruled out in our experiments, showing that cells treated with a combination of BRF1 and control β-globin siRNA exhibited the same shift in fluorescence as cells treated solely with BRF1 siRNA. Thus, we concluded that HuR and BRF1 control mRNA stability of the GFP–ARE reporter in an antagonistic fashion, presumably by competing for the ARE.

Table 2. Exon specific targeting of AUF1 reveals downregulation of p40[AUF1]/p45[AUF1] to increase fluorescence of transfected cells

siRNA treatment	Isoforms targeted	n^a	Fluorescence[b]	$D_{Kolmogorow-Smirnow}^c$ mean $\pm$ SD	P^d
β-globin		7	no effect	0.09 ± 0.04	
AUF1 exon 1	p37, p40, p42, p45	4	no effect	0.09 ± 0.05	= 1
AUF1 exon 2 (oligo A)	p40, p45	7	increased	0.46 ± 0.09	<0.05
AUF1 exon 2 (oligo B)	p40, p45	4	increased	0.29 ± 0.09	<0.05
AUF1 exon 3	p37, p40, p42, p45	4	no effect	0.1 ± 0.08	= 0.9
AUF1 exon 7	p42, p45	4	no effect	0.12 ± 0.03	= 0.2

[a]Number of experiments.
[b]Effect on fluorescence of medium compared to siRNA-treated cells (Fig. 4A).
[c]Greatest distance (D) between curves obtained from medium and siRNA-treated cells.
[d]Student's *t*-test comparing D of cells treated with control β-globin and specific siRNA.

Figure 5. Downregulation of p40[AUF1]/p45[AUF1] increases GM-CSF secretion of transfected Htwt16 cells. Secreted GM-CSF was measured by ELISA in the culture supernatant of cells treated for 72 h with BRF1 and HuR (oligo A) siRNA (**A**), AUF1 siRNA (**B**) and AUF1 (exon 2a) and HuR (oligo A) siRNA (**C**).

Experiments revealing that BRF1 and HuR also exerted opposing effects on expression of GM-CSF, an endogenous BRF1 target gene recently identified by cDNA microarray, further validated our findings.

In contrast to BRF1 and HuR, the role of AUF1 in ARE-mRNA turnover has not been fully clarified. Conclusions, of whether this protein acts as a stabilizer or destabilizer of ARE-mRNAs, are based on indirect evidence associating AUF1 abundance with ARE-mRNA stability (36,38,39,49) and on experiments using AUF1 overexpression, which provided ambiguous results. In NIH 3T3 cells, all four isoforms stabilized ARE-mRNAs (41). Other studies, however, showed that both p37[AUF1] and p40[AUF1] promoted decay in several cell lines investigated, including NIH 3T3 (50). Also, in K562 cells forced expression of AUF1 antagonized stabilization of ARE-mRNAs (40). The reasons for these discrepancies are not clear. Short of performing a gene knockout experiment, exon-specific targeting of AUF1 by siRNA might provide a more physiologic approach to functionally dissect this gene. At first sight, our finding that two different siRNAs efficiently inhibiting expression of all four AUF1 isoforms did not exert an effect on cellular fluorescence or mRNA stability at any of the concentrations tested would argue that, at least in HT1080 cells, AUF1 is not involved in steady-state control of ARE-mRNA turnover. However, this possibility was rejected because the decrease of p40[AUF1]/p45[AUF1] in cells treated with exon 2-specific siRNA strongly induced cellular fluorescence and stabilized the GFP–ARE reporter mRNA. This seems to be mainly due to reduction of the most abundant p40 isoform rather than to the decrease in p45[AUF1] because downregulation

of p42[AUF1] together with p45[AUF1] did not significantly affect fluorescence of transfected cells. We wish to stress that the AUF1 siRNA employed had the same effect on GM-CSF, a gene known to be controlled by AUF1 (46). Again, down-regulation of all four isoforms had no effect, whereas selective reduction of p40[AUF1] and p45[AUF1] strongly stimulated GM-CSF production. Based on these results, one might draw the conclusion that p40[AUF1], like BRF1, acts as a destabilizer of ARE-mRNAs. However, we would like to offer an alternative explanation.

The four AUF1 isoforms differ considerably in their ARE-binding affinities *in vitro*, with the rank order of p37>p42>p45>p40 (26) and the two isoforms with the highest binding affinity exert the most profound effect on ARE-mRNA stability (40,41). Thus, we propose that in HT1080 cells the highly abundant yet low-affinity p40[AUF1] competes with p37[AUF1] and p42[AUF1] for ARE-binding. After selective down-regulation of p40[AUF1], p37[AUF1] and p42[AUF1] gain access to the ARE and stabilize transcripts. This model does not exclude that post-transcriptional modifications of AUF1 might play an additional role, as the affinity of p40[AUF1] for the ARE has been shown to be affected by phosphorylation (51–53). Our proposition that alterations in ARE-mRNA stability might be induced by changes in the relative rather than the absolute levels of AUF1 isoforms would explain why the uniform reduction of all four isoforms had no effect. A key factor may well be the ratio of p37[AUF1] and possibly p42[AUF1] to p40[AUF1]. This notion is supported by two previous observations. First, the decreased stability of the β-adrenergic receptor mRNA in the failing compared to normal human heart has been

7. Appendix

associated with an increased expression of both p40[AUF1] and p45[AUF1] (38). Second, differential expression of AUF1 isoforms accompanied the decreased half-life of GM-CSF mRNA in neonatal compared to adult PBMC (36,37). Both p37[AUF1] and p40[AUF1] were decreased in the latter, whereas expression of p42[AUF1] was comparable in neonatal and adult PBMC. If our model is correct, it would follow that mRNA splicing might ultimately influence ARE-mRNA stability by determining the relative levels of individual AUF1 isoforms.

The fact that simultaneous targeting of HuR and p40[AUF1]/p45[AUF1] partially cancelled the effect of solely targeting p40[AUF1]/p45[AUF1] clearly indicates that the relative levels of the individual AUF1 isoforms can only be one determinant of ARE-mRNA stability. We propose that the quantity of all stabilizing (HuR) and destabilizing AUBPs (TTP, BRF1, BRF2), together with the relative amount of the individual AUF1 isoforms, determines the net stability of ARE-containing transcripts in a balanced fashion. Thus, silencing a single destabilizing factor will tip the balance towards increased stabilization despite the fact that other ARE-destabilizing factors may still be present. In return, decreasing the expression of any stabilizing factor will favor destabilization despite the potential presence of additional stabilizing AUBPs.

ACKNOWLEDGEMENTS

REFERENCES

1. Ross,J. (1996) Control of messenger RNA stability in higher eukaryotes. *Trends Genet.*, **12**, 171–175.
2. Guhaniyogi,J. and Brewer,G. (2001) Regulation of mRNA stability in mammalian cells. *Gene*, **265**, 11–23.
3. Wilusz,C.J., Wormington,M. and Peltz,S.W. (2001) The cap-to-tail guide to mRNA turnover. *Nat. Rev. Mol. Cell. Biol.*, **2**, 237–246.
4. Shaw,G. and Kamen,R. (1986) A conserved AU sequence from the 3′ untranslated region of GM-CSF mRNA mediates selective mRNA degradation. *Cell*, **46**, 659–667.
5. Chen,C.Y. and Shyu,A.B. (1995) AU-rich elements: characterization and importance in mRNA degradation. *Trends Biochem. Sci.*, **20**, 465–470.
6. Shyu,A.B., Belasco,J.G. and Greenberg,M.E. (1991) Two distinct destabilizing elements in the c-fos message trigger deadenylation as a first step in rapid mRNA decay. *Genes Dev.*, **5**, 221–231.
7. Chen,C.Y., Gherzi,R., Ong,S.E., Chan,E.L., Raijmakers,R., Pruijn,G.J., Stoecklin,G., Moroni,C., Mann,M. and Karin,M. (2001) AU binding proteins recruit the exosome to degrade ARE-containing mRNAs. *Cell*, **107**, 451–464.
8. Mukherjee,D., Gao,M., O'Connor,J.P., Raijmakers,R., Pruijn,G., Lutz,C.S. and Wilusz,J. (2002) The mammalian exosome mediates the efficient degradation of mRNAs that contain AU-rich elements. *EMBO J.*, **21**, 165–174.
9. Keyomarsi,K. and Pardee,A.B. (1993) Redundant cyclin overexpression and gene amplification in breast cancer cells. *Proc. Natl Acad. Sci. USA*, **90**, 1112–1116.
10. Lebwohl,D.E., Muise-Helmericks,R., Sepp-Lorenzino,L., Serve,S., Timaul,M., Bol,R., Borgen,P. and Rosen,N. (1994) A truncated cyclin D1 gene encodes a stable mRNA in a human breast cancer cell line. *Oncogene*, **9**, 1925–1929.
11. Dixon,D.A., Tolley,N.D., King,P.H., Nabors,L.B., McIntyre,T.M., Zimmerman,G.A. and Prescott,S.M. (2001) Altered expression of the mRNA stability factor HuR promotes cyclooxygenase-2 expression in colon cancer cells. *J. Clin. Invest.*, **108**, 1657–1665.
12. Nair,A.P., Hahn,S., Banholzer,R., Hirsch,H.H. and Moroni,C. (1994) Cyclosporin A inhibits growth of autocrine tumour cell lines by destabilizing interleukin-3 mRNA. *Nature*, **369**, 239–242.
13. Jacob,C.O., Lee,S.K. and Strassmann,G. (1996) Mutational analysis of TNF-alpha gene reveals a regulatory role for the 3′-untranslated region in the genetic predisposition to lupus-like autoimmune disease. *J. Immunol.*, **156**, 3043–3050.
14. Kontoyiannis,D., Pasparakis,M., Pizarro,T.T., Cominelli,F. and Kollias,G. (1999) Impaired on/off regulation of TNF biosynthesis in mice lacking TNF AU-rich elements: implications for joint and gut-associated immunopathologies. *Immunity*, **10**, 387–398.
15. Peng,S.S., Chen,C.Y., Xu,N. and Shyu,A.B. (1998) RNA stabilization by the AU-rich element binding protein, HuR, an ELAV protein. *EMBO J.*, **17**, 3461–3470.
16. Fan,X.C. and Steitz,J.A. (1998) Overexpression of HuR, a nuclear-cytoplasmic shuttling protein, increases the *in vivo* stability of ARE-containing mRNAs. *EMBO J.*, **17**, 3448–3460.
17. Piecyk,M., Wax,S., Beck,A.R., Kedersha,N., Gupta,M., Maritim,B., Chen,S., Gueydan,C., Kruys,V., Streuli,M. and Anderson,P. (2000) TIA-1 is a translational silencer that selectively regulates the expression of TNF-alpha. *EMBO J.*, **19**, 4154–4163.
18. Carballo,E., Lai,W.S. and Blackshear,P.J. (1998) Feedback inhibition of macrophage tumor necrosis factor-alpha production by tristetraprolin. *Science*, **281**, 1001–1005.
19. Lai,W.S., Carballo,E., Strum,J.R., Kennington,E.A., Phillips,R.S. and Blackshear,P.J. (1999) Evidence that tristetraprolin binds to AU-rich elements and promotes the deadenylation and destabilization of tumor necrosis factor alpha mRNA. *Mol. Cell. Biol.*, **19**, 4311–4323.
20. Carballo,E., Lai,W.S. and Blackshear,P.J. (2000) Evidence that tristetraprolin is a physiological regulator of granulocyte-macrophage colony-stimulating factor messenger RNA deadenylation and stability. *Blood*, **95**, 1891–1899.
21. Stoecklin,G., Ming,X.F., Looser,R. and Moroni,C. (2000) Somatic mRNA turnover mutants implicate tristetraprolin in the interleukin-3 mRNA degradation pathway. *Mol. Cell. Biol.*, **20**, 3753–3763.
22. Stoecklin,G., Colombi,M., Raineri,I., Leuenberger,S., Mallaun,M., Schmidlin,M., Gross,B., Lu,M., Kitamura,T. and Moroni,C. (2002) Functional cloning of BRF1, a regulator of ARE-dependent mRNA turnover. *EMBO J.*, **21**, 4709–4718.
23. Stoecklin,G., Stoeckle,P., Lu,M., Muehlemann,O. and Moroni,C. (2001) Cellular mutants define a common mRNA degradation pathway targeting cytokine AU-rich elements. *RNA*, **7**, 1578–1588.
24. Brewer,G. (1991) An A + U-rich element RNA-binding factor regulates c-myc mRNA stability in vitro. *Mol. Cell. Biol.*, **11**, 2460–2466.
25. Zhang,W., Wagner,B.J., Ehrenman,K., Schaefer,A.W., DeMaria,C.T., Crater,D., DeHaven,K., Long,L. and Brewer,G. (1993) Purification, characterization and cDNA cloning of an AU-rich element RNA-binding protein, AUF1. *Mol. Cell. Biol.*, **13**, 7652–7665.
26. Wagner,B.J., DeMaria,C.T., Sun,Y., Wilson,G.M. and Brewer,G. (1998) Structure and genomic organization of the human AUF1 gene: alternative pre-mRNA splicing generates four protein isoforms. *Genomics*, **48**, 195–202.
27. Arao,Y., Kuriyama,R., Kayama,F. and Kato,S. (2000) A nuclear matrix-associated factor, SAF-B, interacts with specific isoforms of AUF1/hnRNP D. *Arch. Biochem. Biophys.*, **380**, 228–236.
28. Sarkar,B., Lu,J.L. and Schneider,R.J. (2003) Nuclear import and export functions in the different isoforms of the AUF1/hnRNP D protein family. *J. Biol. Chem.*, **31**, 31.
29. Laroia,G. and Schneider,R.J. (2002) Alternate exon insertion controls selective ubiquitination and degradation of different AUF1 protein isoforms. *Nucleic Acids Res.*, **30**, 3052–3058.
30. Laroia,G., Cuesta,R., Brewer,G. and Schneider,R.J. (1999) Control of mRNA decay by heat shock-ubiquitin-proteasome pathway. *Science*, **284**, 499–502.
31. Laroia,G., Sarkar,B. and Schneider,R.J. (2002) Ubiquitin-dependent mechanism regulates rapid turnover of AU-rich cytokine mRNAs. *Proc. Natl Acad. Sci. USA*, **99**, 1842–1846.
32. Eversole,A. and Maizels,N. (2000) *In vitro* properties of the conserved mammalian protein hnRNP D suggest a role in telomere maintenance. *Mol. Cell. Biol.*, **20**, 5425–5432.
33. Fuentes-Panana,E.M., Peng,R., Brewer,G., Tan,J. and Ling,P.D. (2000) Regulation of the Epstein–Barr virus C promoter by AUF1 and the cyclic AMP/protein kinase A signaling pathway. *J. Virol.*, **74**, 8166–8175.

34. Kiledjian,M., DeMaria,C.T., Brewer,G. and Novick,K. (1997) Identification of AUF1 (heterogeneous nuclear ribonucleoprotein D) as a component of the alpha-globin mRNA stability complex. *Mol. Cell. Biol.*, **17**, 4870–4876.

35. Grosset,C., Chen,C.Y., Xu,N., Sonenberg,N., Jacquemin-Sablon,H. and Shyu,A.B. (2000) A mechanism for translationally coupled mRNA turnover: interaction between the poly(A) tail and a c-fos RNA coding determinant via a protein complex. *Cell*, **103**, 29–40.

36. Buzby,J.S., Lee,S.M., Van Winkle,P., DeMaria,C.T., Brewer,G. and Cairo,M.S. (1996) Increased granulocyte-macrophage colony-stimulating factor mRNA instability in cord versus adult mononuclear cells is translation-dependent and associated with increased levels of A + U-rich element binding factor. *Blood*, **88**, 2889–2897.

37. Buzby,J.S., Brewer,G. and Nugent,D.J. (1999) Developmental regulation of RNA transcript destabilization by A + U-rich elements is AUF1-dependent. *J. Biol. Chem.*, **274**, 33973–33978.

38. Pende,A., Tremmel,K.D., DeMaria,C.T., Blaxall,B.C., Minobe,W.A., Sherman,J.A., Bisognano,J.D., Bristow,M.R., Brewer,G. and Port,J. (1996) Regulation of the mRNA-binding protein AUF1 by activation of the beta-adrenergic receptor signal transduction pathway. *J. Biol. Chem.*, **271**, 8493–8501.

39. Sirenko,O.I., Lofquist,A.K., DeMaria,C.T., Morris,J.S., Brewer,G. and Haskill,J.S. (1997) Adhesion-dependent regulation of an A+U-rich element-binding activity associated with AUF1. *Mol. Cell. Biol.*, **17**, 3898–3906.

40. Loflin,P., Chen,C.Y. and Shyu,A.B. (1999) Unraveling a cytoplasmic role for hnRNP D in the *in vivo* mRNA destabilization directed by the AU-rich element. *Genes Dev.*, **13**, 1884–1897.

41. Xu,N., Chen,C.Y. and Shyu,A.B. (2001) Versatile role for hnRNP D isoforms in the differential regulation of cytoplasmic mRNA turnover. *Mol. Cell. Biol.*, **21**, 6960–6971.

42. Mazan-Mamczarz,K., Galban,S., Lopez de Silanes,I., Martindale,J.L., Atasoy,U., Keene,J.D. and Gorospe,M. (2003) RNA-binding protein HuR enhances p53 translation in response to ultraviolet light irradiation. *Proc. Natl Acad. Sci. USA*, **100**, 8354–8359.

43. Nair,A.P., Hirsch,H.H. and Moroni,C. (1992) Mast cells sensitive to v-H-ras transformation are hyperinducible for interleukin 3 expression and have lost tumor-suppressor activity. *Oncogene*, **7**, 1963–1972.

44. Gough,N.M. (1988) Rapid and quantitative preparation of cytoplasmic RNA from small numbers of cells. *Anal. Biochem.*, **173**, 93–95.

45. Chen,C.Y., Xu,N. and Shyu,A.B. (1995) mRNA decay mediated by two distinct AU-rich elements from c-fos and granulocyte-macrophage colony-stimulating factor transcripts: different deadenylation kinetics and uncoupling from translation. *Mol. Cell. Biol.*, **15**, 5777–5788.

46. Bhattacharya,S., Giordano,T., Brewer,G. and Malter,J.S. (1999) Identification of AUF-1 ligands reveals vast diversity of early response gene mRNAs. *Nucleic Acids Res.*, **27**, 1464–1472.

47. Taylor,G.A., Carballo,E., Lee,D.M., Lai,W.S., Thompson,M.J., Patel,D.D., Schenkman,D.I., Gilkeson,G.S., Broxmeyer,H.E., Haynes,B.F. and Blackshear,P.J. (1996) A pathogenetic role for TNF alpha in the syndrome of cachexia, arthritis and autoimmunity resulting from tristetraprolin (TTP) deficiency. *Immunity*, **4**, 445–454.

48. Holen,T., Amarzguioui,M., Wiiger,M.T., Babaie,E. and Prydz,H. (2002) Positional effects of short interfering RNAs targeting the human coagulation trigger Tissue Factor. *Nucleic Acids Res.*, **30**, 1757–1766.

49. Lapucci,A., Donnini,M., Papucci,L., Witort,E., Tempestini,A., Bevilacqua,A., Nicolin,A., Brewer,G., Schiavone,N. and Capaccioli,S. (2002) AUF1 Is a bcl-2 A + U-rich element-binding protein involved in bcl-2 mRNA destabilization during apoptosis. *J. Biol. Chem.*, **277**, 16139–16146.

50. Sarkar,B., Xi,Q., He,C. and Schneider,R.J. (2003) Selective degradation of AU-rich mRNAs promoted by the p37 AUF1 protein isoform. *Mol. Cell. Biol.*, **23**, 6685–6693.

51. Wilson,G.M., Sun,Y., Lu,H. and Brewer,G. (1999) Assembly of AUF1 oligomers on U-rich RNA targets by sequential dimer association. *J. Biol. Chem.*, **274**, 33374–33381.

52. Wilson,G.M., Lu,J., Sutphen,K., Suarez,Y., Sinha,S., Brewer,B., Villanueva-Feliciano,E.C., Ysla,R.M., Charles,S. and Brewer,G. (2003) Phosphorylation of p40AUF1 regulates binding to A + U-rich mRNA-destabilizing elements and protein-induced changes in ribonucleoprotein structure. *J. Biol. Chem.*, **278**, 33039–33048.

53. Wilson,G.M., Lu,J., Sutphen,K., Sun,Y., Huynh,Y. and Brewer,G. (2003) Regulation of A + U-rich element-directed mRNA turnover involving reversible phosphorylation of AUF1. *J. Biol. Chem.*, **278**, 33029–33038.

A KH Domain RNA Binding Protein, KSRP, Promotes ARE-Directed mRNA Turnover by Recruiting the Degradation Machinery

Roberto Gherzi,[1,5,*] Kyung-Yeol Lee,[2,5] Paola Briata,[1]
Daniel Wegmüller,[3] Christoph Moroni,[3]
Michael Karin,[4] and Ching-Yi Chen[2,*]
[1] Gene Transfer Laboratory
Istituto Nazionale per la Ricerca sul Cancro
Largo R. Benzi, 10
16132 Genova
Italy
[2] Department of Biochemistry and Molecular Genetics
University of Alabama at Birmingham
Birmingham, Alabama 35294
[3] Institute of Medical Microbiology
University of Basel
Petersplatz 10
4003 Basel
Switzerland
[4] Laboratory of Gene Regulation and Signal
Transduction
Department of Pharmacology
University of California, San Diego
La Jolla, California 92093

Summary

Inherently unstable mRNAs contain AU-rich elements (AREs) in their 3′ untranslated regions that act as mRNA stability determinants by interacting with ARE binding proteins (ARE-BPs). The mechanisms underlying the function of ARE and ARE-BP interactions in promoting mRNA decay are not fully understood. Here, we demonstrate that KSRP, a KH domain-containing ARE-BP, is an essential factor for ARE-directed mRNA decay. Some of the KH motifs (KHs) of KSRP directly mediate RNA binding, mRNA decay, and interactions with the exosome and poly(A) ribonuclease (PARN). The ability of KHs to promote mRNA decay correlates with their ability to bind the ARE and associate with RNA-degrading enzymes. Thus, KHs promote rapid mRNA decay by recruiting degradation machinery to ARE-containing mRNAs.

Introduction

mRNA stability varies considerably from one mRNA species to another and plays an important role in determining levels of gene expression (Guhaniyogi and Brewer, 2001; Wilusz et al., 2001). Differential mRNA decay rates are determined by specific *cis*-acting elements within the mRNA molecule. The most common *cis* element responsible for rapid mRNA decay in mammalian cells is the AU-rich element (ARE), present within the 3′ untranslated regions (UTRs) of short-lived cytokine and protooncogene mRNAs (Chen and Shyu, 1995; Bakheet et al., 2001). Recent computational analysis of the 3′ UTRs revealed that as many as 8% of human mRNAs

*Correspondence: rgherzi@yahoo.com (R.G.); cchen@uab.edu (C.-Y.C.)
[5] These authors contributed equally to this work.

contain AREs (Bakheet et al., 2001). This finding suggests that AREs may account for degradation of most unstable mRNAs.

AREs are grouped into three classes according to their sequence features and decay characteristics (Chen et al., 1995; Peng et al., 1996). Class I AREs contain one to three scattered copies of the pentanucleotide AUUUA embedded within a U-rich region, found in c-*fos* and c-*myc* mRNAs. Class II AREs contain multiple overlapping copies of the AUUUA motif, only found in cytokine mRNAs. Class III AREs, such as the one in c-*jun* mRNA, lack the hallmark AUUUA but contain a U-rich sequence. mRNA decay mediated by AREs is characterized by rapid poly(A) shortening and rapid decay of the mRNA body (Chen et al., 1995; Peng et al., 1996; Xu et al., 1997). In addition to AREs, several non-ARE-containing instability elements were also described. The stem-loop destabilizing element (SLDE) contains two predicted stem-loop structures found in the 3′ UTR of granulocyte colony-stimulating factor mRNA (Brown et al., 1996). Another *cis* element which promotes TNFα mRNA decay via an ARE-independent pathway was recently described (Stoecklin et al., 2003).

Numerous proteins were described to bind AREs (Peng et al., 1998; Bevilacqua et al., 2003). However, the functional and physiological significance of these RNA-protein interactions and their exact role in ARE-directed mRNA decay remain enigmatic. AUF1 promotes mRNA decay and is also involved in heat shock-induced stabilization of ARE-containing mRNAs (Wilson and Brewer, 1999; Sarkar et al., 2003). TTP binds to the AREs of TNFα and other cytokine mRNAs and promotes their deadenylation and decay. Mice lacking TTP exhibit decreased TNFα and GM-CSF mRNA turnover (Blackshear, 2002). BRF1, a relative of TTP, also promotes ARE-directed mRNA decay (Stoecklin et al., 2002). In contrast, HuR stabilizes ARE-containing mRNAs (Peng et al., 1998; Brennan and Steitz, 2001).

Despite intensive investigation, the mechanism by which ARE-BPs modulate mRNA decay remains nebulous. Furthermore, due to ARE sequence diversity (Bakheet et al., 2001), it is likely that additional ARE-BPs exist. Indeed, we previously purified a novel ARE-BP, KSRP (K homology Splicing Regulatory Protein), and suggested that it might promote the decay of certain ARE-containing mRNAs (Chen et al., 2001). KSRP was originally identified as a component of a protein complex that assembles on an intronic c-*src* neuronal-specific splicing enhancer (Min et al., 1997). It contains four RNA binding K homology (KH) motifs. These motifs are essential for the function of these RNA binding proteins (RBPs) since mutations within them lead to disease or differentiation defects in flies, worms, and mammals (Adinolfi et al., 1999). However, the contribution of KH motifs to specific RNA binding and hence their role within a given RBP are not well understood. It is conceivable that these motifs may be required for cooperative RNA binding. It is also possible that the KH motifs are involved in protein-protein interactions necessary for RBP functions.

Understanding the mechanisms that control mRNA

decay requires identification of the relevant enzymatic machinery. In *Saccharomyces cerevisiae*, two mRNA decay pathways exist (Tucker and Parker, 2000). Both pathways initially involve poly(A) shortening. Subsequently, the mRNA is degraded in either 5′-to-3′ or 3′-to-5′ directions. In the 5′-to-3′ decay pathway, removal of ^{7m}GDP from the ^{7m}GpppN cap by the Dcp1p/Dcp2p decapping enzyme is the next step, followed by rapid degradation of the transcript by the 5′-to-3′ exonuclease Xrn1p (Tucker and Parker, 2000). In the 3′-to-5′ decay pathway, the mRNA is rapidly degraded by the cytoplasmic exosome (Jacobs et al., 1998), a complex containing at least nine exoribonucleases (Mitchell et al., 1997).

The first step in mammalian mRNA decay also appears to be poly(A) shortening (Shyu et al., 1991). However, the mechanistic steps in mammalian mRNA decay are not as well defined as those in yeast. The use of an in vitro RNA decay system provided evidence that 3′-to-5′ degradation is mediated by the mammalian exosome, which represents the major decay pathway for ARE-containing mRNAs (Chen et al., 2001; Wang and Kiledjian, 2001; Mukherjee et al., 2002). The mammalian exosome is likely to be recruited to inherently unstable mRNAs via the AREs. Mukherjee et al. suggested that one of the core subunits of the human exosome specifically binds AREs and this binding is responsible for ARE-directed decay (Mukherjee et al., 2002). However, we found that several ARE-BPs, including KSRP, physically associate with the exosome and that the isolated exosome preferentially degrades ARE-containing RNAs (Chen et al., 2001). We have therefore suggested that the exosome is recruited to inherently unstable mRNA substrates through its interaction with destabilizing ARE-BPs, and that this recruitment provides the basic mechanism responsible for rapid and preferential decay of ARE-containing mRNAs (Chen et al., 2001; Shim and Karin, 2002).

To further understand the mechanism by which destabilizing ARE-BPs promote mRNA decay and find evidence either for or against this model, we investigated the role of KSRP in ARE-directed mRNA decay. We found that KSRP is required for rapid decay of several ARE-containing mRNAs both in vitro and in vivo. We characterized the functional domains of KSRP required for promoting mRNA decay and found that the minimal active region is composed of the third and fourth KH motifs, which together mediate high-affinity binding to the ARE, whereas the third KH motif alone is responsible for interaction with poly(A) ribonuclease, PARN, and the exosome. Additional experiments indicate that the ability of KSRP to promote rapid decay of ARE-containing mRNAs is dependent on its ability to bind the ARE and recruit the degradation machinery, thus providing strong support for the recruitment model.

We also detected a cell type-specific bias in the relative importance of individual ARE-BPs. Depletion of KSRP, but not BRF1, reduced ARE-directed mRNA decay in HeLa cells, whereas depletion of BRF1, but not KSRP, inhibited the decay of an ARE-containing mRNA in HT1080 cells. Nonetheless, simultaneous suppression of both factors resulted in additive stabilization of ARE-containing mRNAs in both cell types.

Results

KSRP Is Required for Rapid Decay of ARE-Containing RNAs In Vitro

To investigate the role of KSRP in ARE-directed mRNA decay, we generated anti-KSRP polyclonal antibodies and used them to deplete KSRP from cytoplasmic extracts (S100) of Jurkat, HeLa, and HT1080 cells (Figure 1A, top panels). No significant removal of an exosome component, hRrp4p, was detected (Figure 1A, bottom panels). Uniformly ^{32}P-labeled, capped, and nonpolyadenylated RNA substrates, including IL-2 3′ UTR, the c-*fos* ARE region (ARE^{fos}), the TNFα ARE region (ARE^{tnf}), and non-ARE-containing sequences (E4), were prepared and their decay monitored in mock- and KSRP-depleted Jurkat S100s. While all ARE-containing RNAs were rapidly degraded in the mock-depleted S100, they were stable in the KSRP-depleted S100 (Figure 1B, compare lanes 1–4 to lanes 5–8). Addition of recombinant KSRP to the KSRP-depleted S100 restored ARE-RNA decay (Figure 1B, lanes 9–12). In contrast, addition of another KH domain RBP, Nova-1, did not restore ARE-RNA decay (data not shown). None of the manipulations affected the slow decay of E4 RNA (Figure 1B). The decay of IL-2 3′ UTR RNA was also examined in depleted HeLa and HT1080 S100s. Similar stabilization of the RNA after KSRP depletion was observed and decay was restored by addition of recombinant KSRP (Figure 1C). These results suggest that KSRP is an important factor for ARE-directed RNA decay in vitro.

KSRP Is Required for Rapid Decay of ARE-Containing mRNAs In Vivo

We next used RNA interference (RNAi; Sharp, 2001; Hutvagner and Zamore, 2002) to examine whether KSRP is required for decay of ARE-containing mRNAs in living cells. A double-stranded 21 nucleotide small interfering RNA (siRNA) derived from the KSRP coding region was introduced into HeLa cells, resulting in specific reduction of KSRP levels but no effect on expression of HuR, hRRP4, or hRRP40, as judged by immunoblot analysis (Figure 2A). We examined decay of ARE-containing mRNAs in KSRP siRNA-treated cells. Vectors expressing chloramphenicol acetyltransferase (CAT) mRNAs fused to a non-ARE 3′ UTR or the 3′ UTR of IL-2 were cotransfected with KSRP or control siRNAs into HeLa cells. The half-lives of these chimeric CAT mRNAs were examined after addition of actinomycin D (act.D) by Northern blot analysis. The non-ARE CAT mRNA was stable, with no significant degradation 3 hr after act.D addition (Figure 2B). In contrast, the CAT-IL2 mRNA was rapidly degraded in luciferase siRNA-treated cells ($t_{1/2} = 45$ min) but was considerably more stable ($t_{1/2} = 180$ min) in cells treated with KSRP siRNA (Figure 2B). To examine whether KSRP is required for rapid decay of other ARE-RNAs, vectors expressing chimeric CAT mRNAs containing the AREs of c-*fos* or TNFα were cotransfected with the siRNAs. Whereas the CAT-ARE mRNAs were unstable in luciferase siRNA-treated cells, they were much more stable in KSRP siRNA-treated cells (Figure 2B).

As the first step of mammalian mRNA decay is poly(A) shortening, we determined whether the observed mRNA
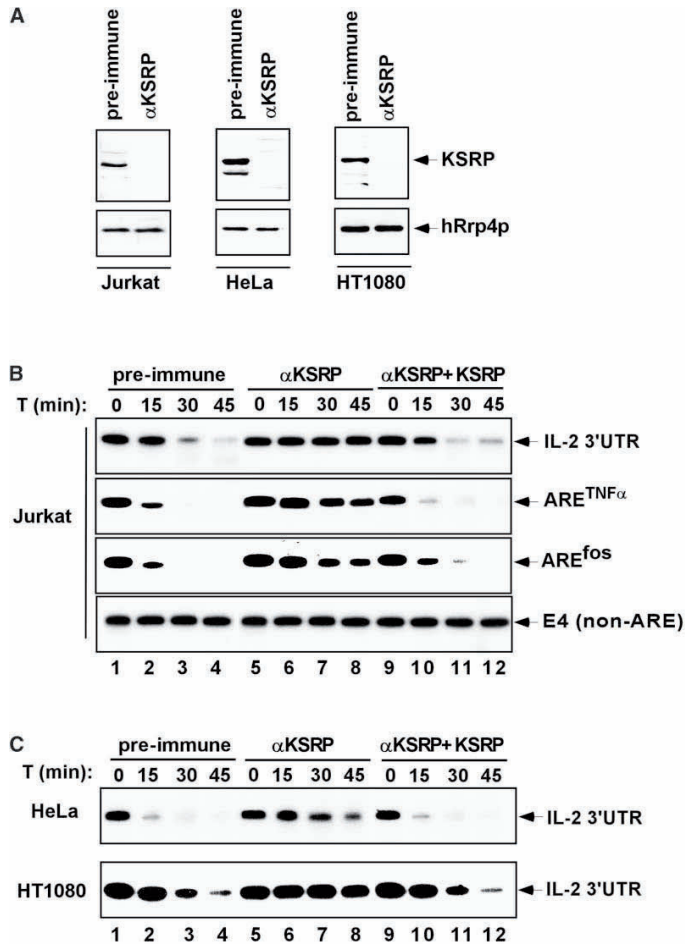
Figure 1. KSRP Is Required for ARE-Directed RNA Decay In Vitro

(A) Immunodepletion of KSRP. S100s of Jurkat, HeLa, or HT1080 cells were incubated with preimmune or anti-KSRP sera immobilized onto Protein A-Sepharose. Supernatants of mock- or KSRP-depleted reactions were analyzed by immunoblotting with anti-KSRP or anti-hRrp4p sera.

(B) In vitro RNA decay assays. Internally ^{32}P-labeled and nonpolyadenylated RNA substrates, including IL-2 3′ UTR, TNFα ARE (ARE^{tnf}), c-*fos* ARE (ARE^{fos}), or the non-ARE-containing E4, were incubated with mock- (lanes 1–4) or KSRP-depleted (lanes 5–8) Jurkat S100s. RNA degradation was analyzed by gel electrophoresis and autoradiography. The decay of the RNAs was also analyzed in KSRP-depleted S100 supplemented with recombinant KSRP$_{47-711}$ expressed in Sf9 cells (50 ng; lanes 9–12).

(C) Decay of ^{32}P-labeled IL-2 3′ UTR RNA was analyzed in mock- or KSRP-depleted HeLa or HT1080 S100s, or KSRP-depleted S100s supplemented with KSRP$_{47-711}$.

stabilization in KSRP-depleted cells is due to inhibition of deadenylation or altered degradation of the mRNA body. To evaluate this, RNA was isolated from HeLa cells transfected with the CAT-IL2 mRNA reporter and either control or KSRP siRNAs either at the time of act.D addition or 3 hr later. The RNA was subjected to oligo-nucleotide-directed RNase H cleavage by incubation with either a deoxyoligonucleotide (CAT-AS) complementary to the CAT coding region or both CAT-AS and oligo(dT)$_{12-18}$. The treated RNA was analyzed by Northern blotting using RNA probes complementary to either the CAT coding region or the 3′ UTR of IL-2. Two bands corresponding to the 5′ and 3′ fragments of the CAT transcripts were detected by the CAT probe (Figure 2C, lanes 1–8), but only one fragment, derived from the 3′ portion, was detected by the IL-2 3′ UTR probe (Figure 2C, lanes 9–16). The bands detected with either probe were dramatically decreased in cells treated with the control siRNA 3 hr after act.D addition but were considerably more abundant in cells treated with the KSRP siRNA (Figure 2C, compare lanes 2, 4, 10, and 12 with lanes 6, 8, 14, and 16).

The 3′ fragments detected at the zero time points in either siRNA-treated cells exhibited heterogeneous migration after treatment with CAT-AS (Figure 2C, lanes 1, 5, 9, and 13), but this heterogeneity was reduced after an additional treatment with oligo(dT)$_{12-18}$ (lanes 3, 7, 11, and 15). This suggests that most of the heterogeneity is due to poly(A) tail length variation. Most importantly, the stabilized 3′ fragments detected 3 hr after act.D addition in KSRP siRNA-treated cells also exhibited heterogeneous migration (lanes 6 and 14), which was eliminated by treatment with oligo(dT)$_{12-18}$ (lanes 8 and 16). These results suggest that the stabilized mRNA in KSRP-depleted cells still contains a poly(A) tail and that suppression of KSRP expression impedes the deadenylation step of ARE-directed mRNA decay.

KSRP Is Required for Rapid Decay of mRNA Containing the c-*jun* ARE But Not Required for Decay of SLDE-Containing mRNA
The results described above suggest that KSRP is essential for class I (ARE^{fos}) and II (ARE^{tnf}) ARE-directed mRNA decay. We next examined whether KSRP is required for decay of mRNAs containing either class III ARE (such as in c-*jun*) or the SLDE (the stem-loop desta-
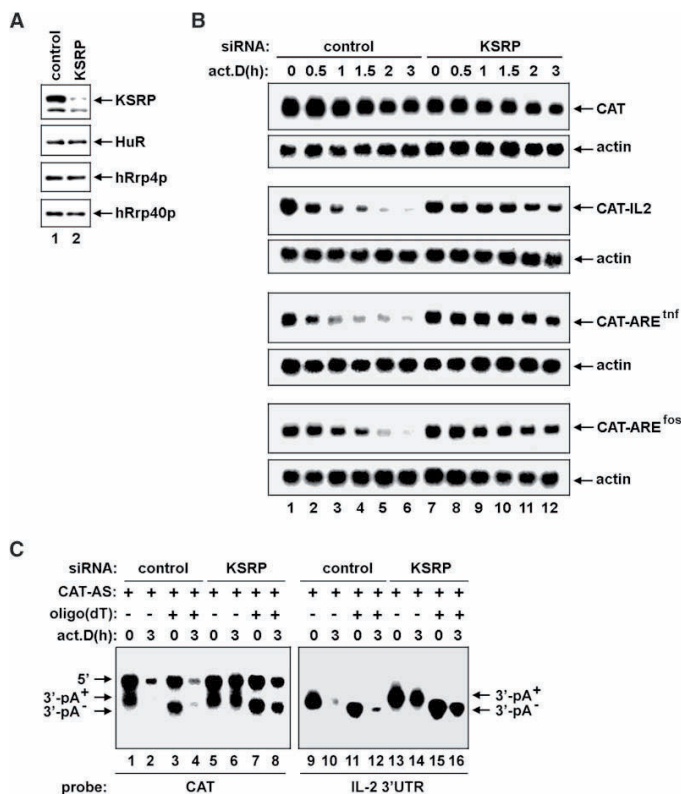
Figure 2. KSRP Is Required for ARE-Directed mRNA Decay in Living Cells

(A) Suppression of KSRP expression by RNAi. HeLa cells were transfected with a control siRNA (luciferase) or a KSRP siRNA. After 48 hr, cytoplasmic extracts were prepared and analyzed by immunoblotting with anti-KSRP, anti-HuR, anti-hRrp4p, or anti-hRrp40p sera.
(B) Stabilization of ARE-containing mRNAs in HeLa cells depleted of KSRP. HeLa cells were cotransfected with vectors expressing chimeric CAT mRNAs containing either non-ARE 3′ UTR (CAT) or various ARE-containing 3′ UTRs, including the IL-2 3′ UTR, ARE^{tnf}, or ARE^{fos} and either control or KSRP siRNAs. Total RNA was isolated at different times after act.D addition, and the levels of CAT transcripts were determined by Northern blot analysis. The membranes were rehybridized with a β-actin probe for loading control.
(C) KSRP is required for ARE-facilitated deadenylation. HeLa cells were transfected with the CAT-IL2 mRNA reporter and siRNAs. Total RNA was isolated 0 or 3 hr after act.D addition from cells treated with either control (lanes 1–4 and 9–12) or KSRP (lanes 5–8 and 13–16) siRNAs. RNAs were incubated with a CAT-AS deoxyoligonucleotide in the absence (lanes 1, 2, 5, 6, 9, 10, 13, and 14) or the presence of oligo(dT)$_{12-18}$ (lanes 3, 4, 7, 8, 11, 12, 15, and 16) and subjected to RNase H digestion. The cleaved RNAs were analyzed by Northern blotting with ^{32}P-labeled RNA probes corresponding to either the CAT coding region (lanes 1–8) or IL-2 3′ UTR (lanes 9–16). The 5′ fragment, polyadenylated 3′ fragment (3′-pA$^+$) and nonpolyadenylated 3′ fragment (3′-pA$^-$) are indicated.

bilizing element found in the 3′ UTR of G-CSF mRNA). We first determined the ability of KSRP to bind the c-*fos*, TNFα and c-*jun* AREs, and the SLDE. Recombinant KSRP bound strongly to all three ARE types but did not exhibit considerable SLDE binding activity (Figure 3A). In UV crosslinking assays using HeLa cytoplasmic extract, a 78 kDa RNA-protein complex was detected with all three AREs (Figure 3B, lanes 1, 4, and 7), but not with the SLDE (Figure 3B, lane 10). The 78 kDa RNA-protein complex was specifically immunoprecipitated by the anti-KSRP antibody, but not by a control antibody (Figure 3B, compare lanes 3, 6, and 9 to lanes 2, 5, and 8), verifying that it corresponds to the KSRP-ARE complex.

To examine whether suppression of KSRP expression inhibits mRNA decay directed by the c-*jun* ARE or the SLDE, CAT mRNA reporters containing either element were cotransfected with luciferase or KSRP siRNAs into HeLa cells. Decay of CAT-ARE^{jun} was inhibited in KSRP siRNA-treated cells, although the inhibition was not as dramatic as found for RNA decay directed by the c-*fos* or TNFα AREs (compare Figure 2B with Figure 3C). In contrast, no significant difference in the stability of CAT-SLDE mRNA was detected after siRNA treatment (Figure 3D). Altogether, these results suggest that KSRP is specifically required for rapid degradation of all three classes of ARE-containing mRNAs in living cells.

KH Motifs Mediate ARE Binding and Promote mRNA Decay
We hypothesized that at least two functions are essential for KSRP to promote mRNA decay: one being bind-

ing to AREs, possibly mediated by the KH motifs, and the other being a decay-promoting function, which may depend on recruitment of the degradation machinery (Chen et al., 2001). To identify the domains that mediate these functions, GST fusion proteins containing various regions of KSRP were produced and purified from *E. coli* (Figure 4A) and examined for their ability to restore RNA decay in KSRP-depleted S100. GST fusion proteins containing amino acids 47–569 and 130–711 of KSRP, but not amino acids 47–460, restored ARE-dependent RNA decay (Figure 4B; lanes 9–12, 17–20, and 13–16). These results suggest that sequences that flank the central KH domain are dispensable for the decay-promoting activity. This conclusion was confirmed by reconstitution of ARE-dependent RNA decay using a GST fusion protein containing only the four KH motifs (KH$_{1-4}$) (Figure 4B, lanes 21–24), whose activity was comparable to that of KSRP$_{47-711}$ expressed in Sf9 cells (lanes 5–8).

To further dissect the central KH domain, GST fusion proteins containing either individual KH motifs or combinations were produced and purified from *E. coli* (Figure 4A). We examined the ability of these proteins to bind an ARE, interact with the exosome, and restore RNA decay. In gel mobility shift assays, we did not observe significant binding of any single KH motif to ARE^{tnf} RNA using several micrograms of GST fusion proteins (data not shown). However, ARE binding was readily detected with proteins containing two adjacent KH motifs (Figure 4C), suggesting that two KH motifs are necessary for stable RNA binding. Whereas binding of either KH$_{12}$ or
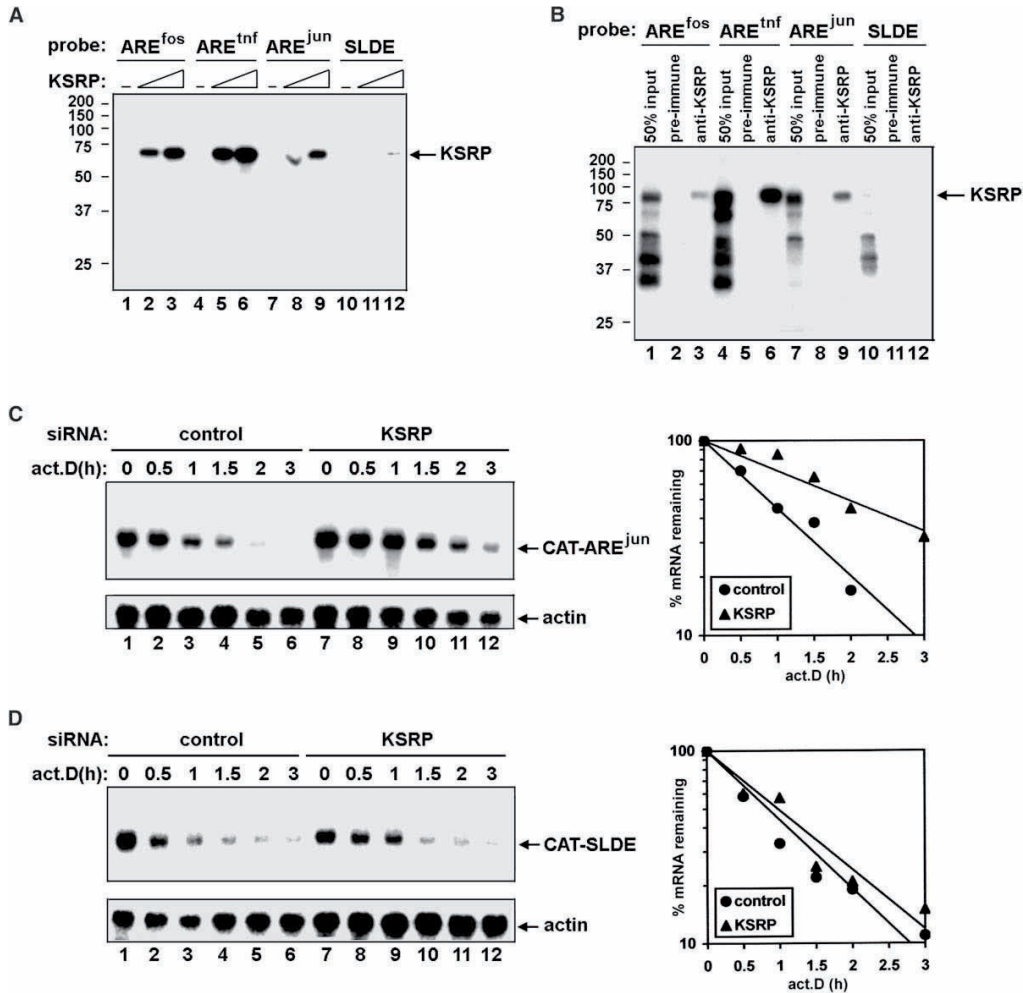
Figure 3. KSRP Is Required for Decay of CAT-ARE^{jun} mRNA, but Not for CAT-SLDE mRNA

(A) UV crosslinking assays. ^{32}P-labeled RNAs (10 fmol) including ARE^{fos}, ARE^{tnf}, ARE^{jun}, or SLDE were incubated with two different amounts (50 or 150 ng) of KSRP$_{47-711}$, and UV crosslinking assays were performed. RNA-protein complexes were analyzed by SDS-PAGE and autoradiography.
(B) ^{32}P-labeled ARE^{fos}, ARE^{tnf}, ARE^{jun}, or SLDE RNAs (10 fmol) were incubated with HeLa cytoplasmic extract, and UV crosslinking assays were performed. RNA-protein complexes were immunoprecipitated with either preimmune or anti-KSRP sera and analyzed as above. For a reference, 50% of each nonprecipitated reaction was also gel separated (lanes 1, 4, 7, and 10).
(C and D) Decay of ARE^{jun}- or SLDE-containing CAT mRNAs. HeLa cells were cotransfected with vectors expressing CAT-ARE^{jun} (C) or CAT-SLDE (D) mRNAs and either control or KSRP siRNAs. Decay of the CAT mRNAs was analyzed (left panels). Signals were quantitated with a PhosphorImager, normalized to the actin signals, and plotted on a semilogarithmic scale using a linear regression program against the time of act.D addition (right panels).

KH$_{1-3}$ to the ARE^{tnf} was barely detected at the highest input levels, binding by KH$_{34}$ or KH$_{1-4}$ was detected at lower input levels. In contrast, no binding was detected with KH$_{23}$ (Figure 4C). Thus, KH$_{34}$ mediates high-affinity interaction with the ARE.

We next examined the ability of the KH motifs to interact with the exosome. The GST-KH fusion proteins were immobilized onto GSH-Sepharose and incubated with Jurkat S100. The precipitates were analyzed for presence of the exosome by immunoblot analysis. While no hRrp4p and hRrp40p could be detected in the fractions bound to GST, GST-KH$_{12}$, and GST-KH$_4$, they were de-

tected in the fractions bound to GST-KH$_{23}$, -KH$_{34}$, -KH$_{1-4}$, -KH$_3$, and -KH$_{1-3}$ (Figure 4D). These results suggest that the KH$_3$ motif is responsible for interaction with the exosome.

To examine which KH motifs promote RNA decay, the GST-KH fusion proteins were added to KSRP-depleted S100. As described above, IL-2 3′ UTR RNA was stable in the depleted S100. Whereas addition of KH$_{12}$, which interacts weakly with the ARE but not with the exosome, or KH$_{23}$, which interacts with the exosome but not with the ARE, did not restore ARE-dependent RNA decay, addition of KH$_{34}$, which interacts with both the ARE and
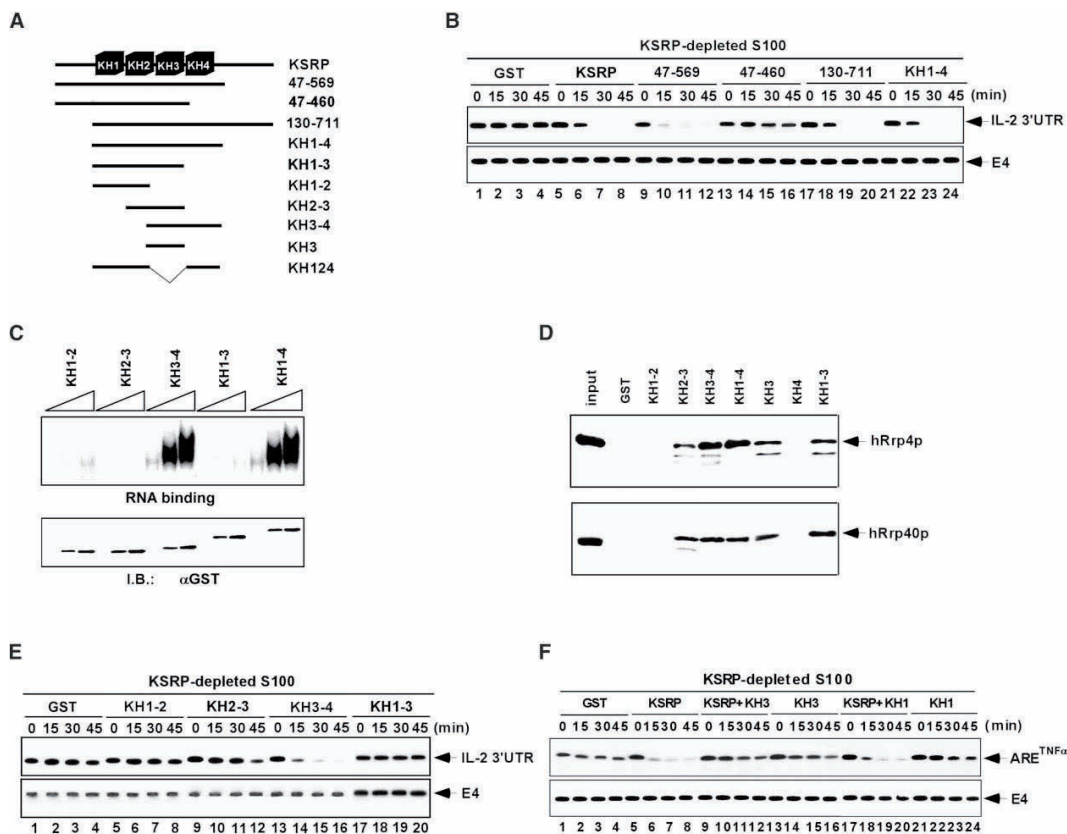
Figure 4. Some of the KH Motifs of KSRP Are Sufficient for Promoting RNA Decay In Vitro

(A) Schematic diagram of KSRP and different fragments used to prepare recombinant proteins or mammalian expression vectors. The KH motifs are indicated by black boxes.

(B) Reconstitution of RNA decay by KSRP deletion mutants. GST fusion proteins (50 ng) containing various regions of KSRP, including amino acids 47–569 (lanes 9–12), 47–460 (lanes 13–16), 130–711 (lanes 17–20), or KH_{1-4} (lanes 21–24) or his-$KSRP_{47-711}$ (lanes 5–8) expressed in Sf9 cells, were added to the KSRP-depleted S100. The decay of ^{32}P-labeled IL-2 3′ UTR or E4 RNAs was separately analyzed. All the decay assays were at least performed twice, and essentially identical results were obtained.

(C) Binding of KH motifs to ARE^{tnf}. Different amounts (50, 100, or 200 ng) of GST fusion proteins containing different KH motifs were incubated with ^{32}P-labeled ARE^{tnf} probe, and gel mobility shift assays were performed (top panel). Immunoblot analysis with anti-GST antibody was used to compare the amounts of GST fusion proteins (bottom panel).

(D) Association of KH motifs with the exosome. GST fusion proteins containing different KH motifs were immobilized onto GSH-Sepharose and incubated with Jurkat cytoplasmic extract. The associated exosome was detected by immunoblot analysis using antisera to the exosome components, hRrp4p or hRrp40p.

(E) Reconstitution of RNA decay by KH motifs. GST fusion proteins (50 ng) containing different KH motifs were added to the KSRP-depleted S100. The decay of ^{32}P-labeled IL-2 3′ UTR or E4 RNAs was separately analyzed.

(F) Excess of KH_3 inhibits the ability of KSRP to promote RNA decay. $KSRP_{47-711}$ (50 ng), $KSRP_{47-711}$ (50 ng) plus GST-KH_3 (350 ng), GST-KH_3 (350 ng), $KSRP_{47-711}$ (50 ng) plus GST-KH_1 (350 ng), or GST-KH_1 (350 ng) was added to the KSRP-depleted S100. The decay of ARE^{tnf} or E4 RNAs was separately analyzed.

the exosome, promoted RNA decay (Figure 4E). Addition of KH_{1-3}, which interacts efficiently with the exosome, but poorly with the ARE, did not restore RNA decay (Figure 4E). To further examine whether the interaction of KSRP with the exosome is necessary for RNA decay, the decay of ARE^{tnf} was examined in the KSRP-depleted S100 supplemented with KSRP and either GST-KH_3 or GST-KH_1. While addition of KSRP promoted ARE-dependent RNA decay, coincubation with KH_3, but not with KH_1, strongly inhibited the decay-promoting activity of KSRP (Figure 4F, compare lanes 9–12 with 17–20).

We suggest that KH_3, which does not bind to ARE on its own, acts in a dominant-negative fashion to inhibit RNA decay by competing with KSRP for interaction with the exosome.

Reconstitution of mRNA Decay by KH Motifs In Vivo
We investigated the role of the KH motifs in promoting mRNA decay in living cells. Vectors expressing individual or combinations of Flag-tagged KH motifs were transfected into HeLa cells. The expression levels of these proteins were similar based on anti-Flag immu-
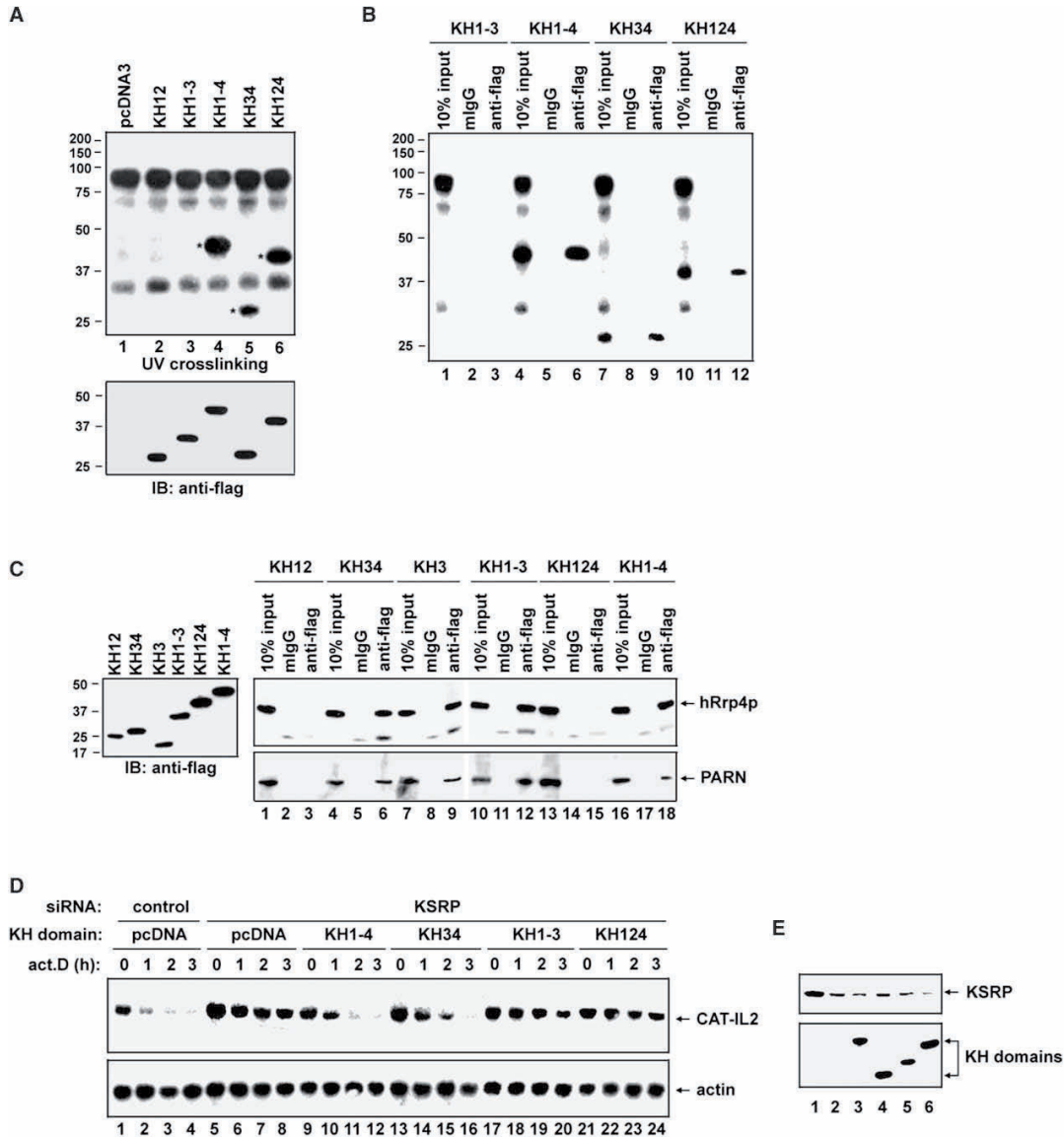
107

Figure 5. KH Motifs 3 and 4 of KSRP Are Sufficient for Promoting RNA Decay In Vivo

(A) Interaction of KH motifs with the ARE. HeLa cells were transfected with vectors expressing different Flag-tagged KH motifs. After 48 hr, cytoplasmic extracts were prepared and incubated with ^{32}P-labeled ARE^{tnf} RNA, and UV crosslinking assays were performed. RNA-protein complexes were analyzed by SDS-PAGE and autoradiography (top panel). Aliquots of cytoplasmic extracts were also analyzed by immunoblotting with anti-Flag antibody (bottom panel).

(B) UV crosslinking reactions conducted as above were immunoprecipitated with control (mouse IgG) or anti-Flag antibodies. The immunoprecipitates were analyzed by SDS-PAGE and autoradiography. A portion (10%) of each UV crosslinking reaction was loaded onto lanes 1, 4, 7, and 10.

(C) Coimmunoprecipitation of the exosome and PARN with KH motifs. Cytoplasmic extracts of transfected cells expressing various Flag-tagged KH motifs were either analyzed by immunoblotting with anti-Flag antibody (left panel) or immunoprecipitated with either mouse IgG (lanes 2, 5, 8, 11, 14, and 17) or anti-Flag antibody (lanes 3, 6, 9, 12, 15, and 18). The precipitates were analyzed by immunoblotting with anti-hRrp4p or anti-PARN sera (right panel). A portion (10%) of each immunoprecipitation reaction was loaded onto lanes 1, 4, 7, 10, 13, and 16.

(D) Reconstitution of rapid mRNA decay by KH motifs in vivo. HeLa cells were cotransfected with the CAT-IL2 mRNA reporter and either control (lanes 1–4) or KSRP (lanes 5–24) siRNAs together with pcDNA3 (lanes 1–8) or vectors expressing different KH motifs: KH$_{1-4}$ (lanes 9–12), KH$_{34}$ (lanes 13–16), KH$_{1-3}$ (lanes 17–20), or KH$_{124}$ (lanes 21–24). The decay of CAT-IL2 mRNA was examined as described in Figure 2B.

(E) Cytoplasmic extracts of the transfected cells in (D) were analyzed by immunoblotting with anti-KSRP or anti-Flag antibodies. HeLa cells were transfected with the control siRNA and pcDNA (lane 1), the KSRP siRNA and pcDNA (lane 2), KH$_{1-4}$ (lane 3), KH$_{34}$ (lane 4), KH$_{1-3}$ (lane 5), or KH$_{124}$ (lane 6).

noblotting (Figure 5A, bottom panel). The interaction of the transfected KH polypeptides with an ARE was analyzed by UV crosslinking assays. Several ARE-BPs were detected in HeLa cytoplasmic extract using ARE^{tnf} as a probe (Figure 5A, lane 1, top panel). Additional ARE-protein complexes were detected in extracts of cells expressing KH_{1-4}, KH_{34}, or KH_{124} (lanes 4–6, top panel). In contrast, no additional RNA-protein complexes could be detected in extracts of cells expressing KH_{12} or KH_{1-3} (lanes 2 and 3). To confirm that the additional ARE-protein complexes contain the corresponding KH poly-peptides, UV crosslinking reactions were immuno-precipitated with a control mouse IgG or an anti-Flag antibody. The additional RNA-protein complexes detected in extracts containing KH_{1-4}, KH_{34}, or KH_{124} were specifically precipitated by anti-Flag (Figure 5B, lanes 6, 9, and 12). No ARE-protein complexes were precipitated by anti-Flag from extracts containing KH_{1-3} (Figure 5B, lane 3). We conclude that the transfected KH_{124} and KH_{34} polypeptides, but not the KH_{12} and KH_{1-3} polypeptides, bind to the ARE.

We next examined the ability of these KH motifs to interact with the exosome. HeLa cells were transfected with vectors expressing combinations of Flag-tagged KH polypeptides, whose expression was analyzed by immunoblotting (Figure 5C, left panel). The extracts were immunoprecipitated with either control (mouse IgG) or anti-Flag antibodies, and the immunoprecipitates were examined for presence of the exosome component. hRrp4p was detected in the anti-Flag precipitates of KH polypeptides containing KH_3, such as KH_{34}, KH_3, KH_{1-3}, and KH_{1-4}, but not KH_{12} and KH_{124} (Figure 5C, right panel). We also examined the immunoprecipitates for the presence of PARN. Interestingly, PARN was present in the same precipitates that contain hRrp4p (Figure 5C, right panel).

To examine whether the KH motifs can promote mRNA decay in vivo, HeLa cells were cotransfected with the CAT-IL2 mRNA reporter, the KSRP siRNA, and vectors expressing combinations of the various KH motifs. The decay of the chimeric CAT-IL2 mRNA was examined. The knockdown of KSRP prevented rapid decay of CAT-IL2 mRNA (Figure 5D, lanes 5–8). Cotransfection of vectors expressing KH_{1-4} or KH_{34} with the KSRP siRNA restored rapid mRNA decay (lanes 9–16), while coexpression of KH_{1-3} or KH_{124} did not restore mRNA decay (lanes 17–24). The suppression of KSRP expression and expression of various KH polypeptides in the transfected cells were verified by immunoblot analysis. KSRP was similarly suppressed in all cells transfected with the siRNA (Figure 5E, lanes 2–6, top panel). The different KH polypeptides were expressed at similar levels (lanes 3–6, bottom panel). Thus, the observed effect on mRNA decay reflects the ability of third and fourth KH motifs of KSRP to promote decay. These data together with the in vitro results (Figure 4E) suggest that the ability of KH motifs to promote mRNA decay requires both binding to AREs and association with PARN and the exosome.

KSRP Simultaneously Associates with PARN and the Exosome
The results described above suggest that KSRP associates with mRNA decay enzymes and recruits them to
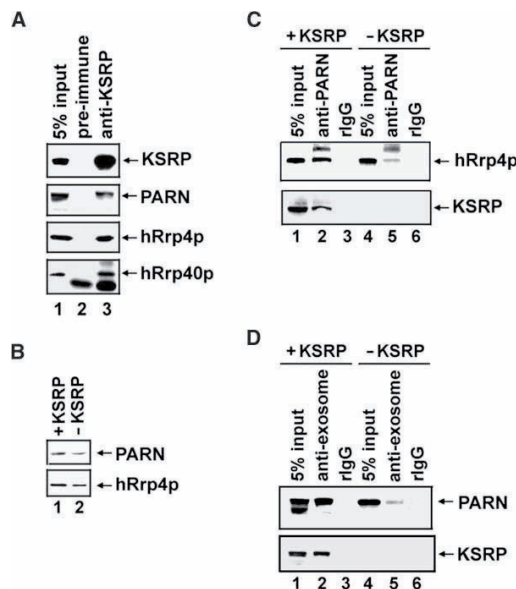

Figure 6. KSRP Simultaneously Associates with PARN and the Exosome

(A) Association of KSRP with PARN and the exosome. HeLa S100 was immunoprecipitated with preimmune (lane 2) or anti-KSRP (lane 3) sera. The precipitates were analyzed by immunoblotting with anti-KSRP, anti-PARN, anti-hRrp4p, or anti-hRrp40p sera. A portion (5%) of the immunoprecipitation reaction was loaded onto lane 1.
(B) Levels of PARN and the exosome component present in the KSRP-depleted S100. Mock- (lane 1) or KSRP-depleted (lane 2) S100s were immunoblotted with anti-PARN or anti-hRrp4p.
(C and D) Strong association of PARN with the exosome requires the presence of KSRP. Mock- (lanes 1–3) or KSRP-depleted (lanes 4–6) S100s were immunoprecipitated with anti-PARN antibody ([C], lanes 2 and 5), anti-exosome antibodies, including hRrp40p, hRrp41p, and hRrp46p ([D], lanes 2 and 5), or a rabbit serum ([C and D], lanes 3 and 6). The precipitates were analyzed by immunoblotting with anti-hRrp4p ([C], top panel), anti-PARN ([D], top panel), or anti-KSRP ([C and D], bottom panel). A portion (5%) of the immunoprecipitation reactions was loaded onto lanes 1 and 3.

degrade ARE-containing mRNAs. To provide further evidence for the recruitment mechanism, we examined whether endogenous PARN and the exosome associate with KSRP. HeLa S100 was immunoprecipitated with the anti-KSRP serum, and the immunoprecipitates were immunoblotted with anti-PARN or anti-exosome antibodies (Figure 6A). Both PARN and the exosome components, hRrp4p and hRrp40p, were detected in the anti-KSRP precipitate, but not in the control precipitate. The coimmunoprecipitation of KSRP with the decay factors was insensitive to RNase treatment (data not shown), suggesting that the associations are not mediated by an mRNA.

We next determined whether KSRP associates with both the exosome and PARN simultaneously and whether the exosome and PARN interact with each other in the absence of KSRP. S100s that were either mock depleted or depleted of KSRP with anti-KSRP antibody were immunoprecipitated with anti-PARN, anti-exosome, or a control serum. PARN and hRrp4p were both

present in the KSRP-depleted S100 (Figure 6B, compare lane 1 with lane 2), consistent with our previous observation that only a small fraction of the exosome associates with ARE-BPs (Chen et al., 2001). The immunoprecipitates were subjected to immunoblot analysis with anti-hRrp4p, anti-PARN, or anti-KSRP antibodies. hRrp4p was readily detected in the anti-PARN precipitate when KSRP was present in the S100 (Figure 6C, lane 2, top panel). Similarly, PARN was strongly detected in the anti-exosome precipitate in the presence of KSRP (Figure 6D, lane 2, top panel). KSRP was detected in the precipitates of both anti-PARN and anti-exosome (Figures 6C and 6D, lane 2, bottom panel). A small fraction composed of PARN and the exosome was still detected in the KSRP-depleted extracts (Figures 6C and 6D, lane 5, top panel). Thus, KSRP may be required to stabilize the exosome and PARN interactions. Alternatively, other decay-promoting ARE-BPs can also simultaneously associate with PARN and the exosome. Altogether these results suggest that the exosome and PARN form a stable complex in the presence of KSRP and that KSRP can simultaneously interact with both the exosome and PARN.

Both KSRP and BRF1 Are Required
for ARE-Directed mRNA Decay

To date, a number of destabilizing ARE-BPs were identified. Some of these factors are coexpressed in the same cell types and exhibit overlapping RNA binding specificities (Wilson and Brewer, 1999; Bevilacqua et al., 2003). Depletion of individual ARE-BPs results in stabilization of a subset of ARE-containing mRNAs in certain cell types (Blackshear, 2002; Stoecklin et al., 2002). However, it is not clear whether individual ARE-BPs are functionally redundant or each individual protein directs the decay of a distinct set of ARE-containing mRNAs. To explore these possibilities, the decay of ARE^{tnf} RNA was examined in S100 of an HT1080 fibrosarcoma cell line or a variant derivative (slowC), which harbors frameshift mutations in both BRF1 alleles and fails to rapidly degrade certain cytokine mRNAs (Stoecklin et al., 2000, 2001, 2002). Whereas the RNA was rapidly degraded in HT1080 S100, it was more stable in slowC S100 (Figure 7A, compare lanes 1–4 to 5–8). However, ARE^{tnf} was rapidly degraded when the amounts of slowC S100 used in the decay reaction were increased by 3-fold (Figure 7A, lanes 9–12). Under these conditions, the RNA was stabilized after depletion of KSRP (Figure 7A, lanes 13–16). These results suggest that BRF1 and KSRP act additively to direct the decay of ARE^{tnf} RNA in vitro.

To investigate whether both BRF1 and KSRP are required for mRNA decay in vivo, we knocked down both factors in HeLa or HT1080 cells using RNAi. Based on immunoblot analysis, KSRP is expressed at similar levels in these two cell types, whereas the levels of BRF1 in HT1080 cells are at least 5-fold higher than that in HeLa cells (Figure 7B). We transfected HeLa cells with the CAT-ARE^{tnf} reporter and siRNAs to BRF1 or KSRP. Expression of either BRF1 or KSRP was effectively suppressed by the corresponding siRNAs (Figure 7C, left panel). CAT-ARE^{tnf} mRNA was unstable ($t_{1/2} = 1.3$ hr) in cells treated with a control siRNA (lanes 1–5) and was only slightly stabilized ($t_{1/2} = 1.7$ hr) in cells treated with

the BRF1 siRNA (lanes 6–10). The mRNA was significantly stabilized ($t_{1/2} = 4.2$ hr) in cells treated with the KSRP siRNA (lanes 11–15) and was even more stable ($t_{1/2} = 7.0$ hr) in cells treated with both BRF1 and KSRP siRNAs (lanes 16–20).

We examined the effect of suppression of BRF1 and KSRP expression on mRNA decay in HT1080 cells. A stable HT1080 cell line expressing GFP-IL3 3′ UTR mRNA was treated with the BRF1 or KSRP siRNAs. Suppression of BRF1 and KSRP expression by the corresponding siRNAs was confirmed by immunoblotting (Figure 7D, left panel), and the decay of GFP-IL3 mRNA was examined (Figure 7D, right panel). The mRNA was unstable ($t_{1/2} = 1.2$ hr) in cells treated with a control siRNA (lanes 1–5) and was moderately stabilized ($t_{1/2} = 1.5$ hr) in cells treated with the KSRP siRNA (lanes 11–15). In contrast, the mRNA was stabilized ($t_{1/2} = 2.6$ hr) after treatment with the BRF1 siRNA (lanes 6–10) and was even more stable ($t_{1/2} = 4.5$ hr) in cells treated with both BRF1 and KSRP siRNAs (lanes 16–20). On the basis of these results, we suggest that KSRP plays a major role in decay of various ARE-containing mRNAs in HeLa cells and BRF1 may be primarily responsible for decay of IL-3′ UTR-containing mRNA in HT1080 cells.

Discussion

KSRP Is an Essential Factor
for ARE-Directed mRNA Decay

The results shown above demonstrate that KSRP is required for rapid decay of certain ARE-containing mRNAs both in vitro and in vivo. In both systems, depletion of KSRP results in stabilization of several ARE-containing mRNAs. The stabilization is observed in KSRP-depleted S100 from several cell types, including Jurkat, HeLa, and HT1080 cells (Figure 1). Furthermore, using heterologous CAT mRNAs containing various AREs in the 3′ UTR, suppression of KSRP expression compromises the rapid decay of mRNAs containing all three classes of AREs in living cells (Figures 2 and 3). Although the relative importance of KSRP in promoting ARE-directed mRNA decay may depend on either the cell type and the relative expression levels of other decay-promoting ARE-BPs or the particular mRNA species examined (as illustrated in Figure 7), the mechanistic analysis of KSRP function has provided important new insights into the mechanism of ARE-directed mRNA turnover.

Although KSRP promotes decay of reporter mRNAs containing class I, II, or III AREs in transient transfection experiments, it remains to be determined which endogenous ARE-containing mRNAs are stabilized most effectively in cells depleted of KSRP. Whereas the ARE is the major determinant of rapid mRNA turnover, additional *cis* elements can also promote mRNA decay. These additional instability elements are often present along with AREs (Shyu et al., 1991; Wisdom and Lee, 1991; Brown et al., 1996; Stoecklin et al., 2003) but are unlikely to be recognized by ARE-BPs, such as KSRP. Interestingly, only few ARE-containing mRNAs were found to be stabilized in TTP knockout mice (Blackshear, 2002). Thus, an individual ARE-BP, such as KSRP, may be most critical for only a subset of ARE-containing mRNA, and in its absence other ARE-BPs, if expressed
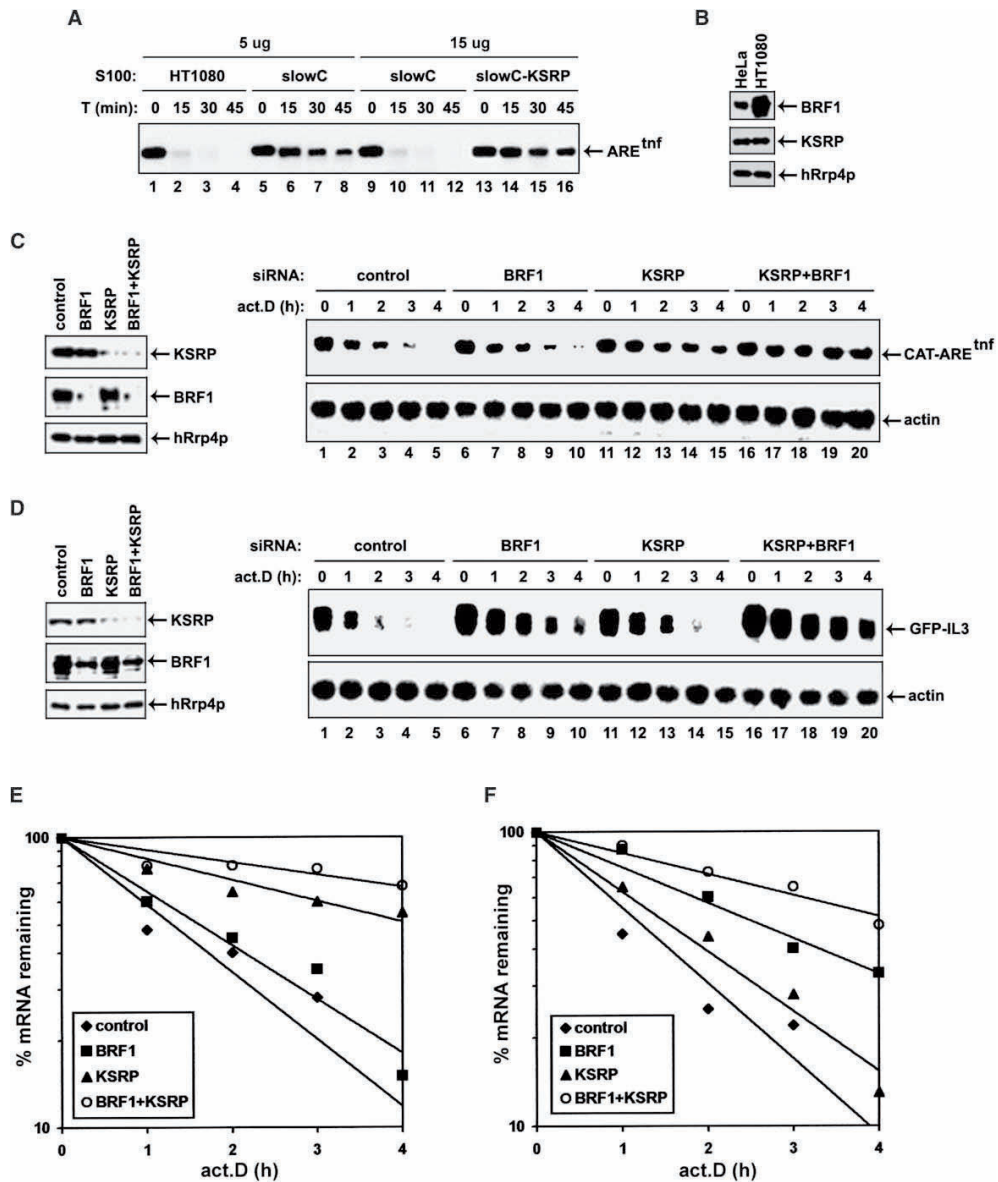
Figure 7. KSRP and BRF1 Are Both Required for ARE-Directed mRNA Decay

(A) In vitro decay of ARE^{tnf} in HT1080 or slowC S100s. ^{32}P-labeled ARE^{tnf} RNA was incubated with S100 (5 ug) of HT1080 (lanes 1–4) or slowC (lanes 5–8) cells, or S100 (15 ug) of slowC (lanes 9–12) or slowC S100 (15 ug) depleted of KSRP (lanes 13–16), and its decay was analyzed.

(B) Expression of BRF1 and KSRP in HeLa and HT1080 cells. Equivalent amounts of HeLa or HT1080 extracts were immunoblotted with anti-BRF1 or anti-KSRP antibodies. Anti-hRrp4p was also included to control gel loading.

(C) Suppression of BRF1 and KSRP expression retards rapid mRNA decay in HeLa cells. HeLa cells were cotransfected with the CAT-ARE^{tnf} mRNA reporter and either control, BRF1, KSRP, or BRF1+KSRP siRNAs. After 48 hr, cytoplasmic extracts were prepared and analyzed by immunoblotting with anti-KSRP, anti-BRF1, or anti-hRrp4p sera (left panel). Total RNA was also isolated at different times after act.D addition, and the levels of CAT-ARE^{tnf} mRNA were determined by Northern blotting (right panel).

(D) Suppression of BRF1 and KSRP expression retards rapid mRNA decay in HT1080 cells. HT1080 cells stably expressing GFP-IL3 mRNA were transfected with either control, BRF1, KSRP, or BRF1+KSRP siRNAs. After 48 hr, cytoplasmic extracts were prepared and analyzed by immunoblotting with anti-KSRP, anti-BRF1, or anti-hRrp4p sera (left panel). Total RNA was isolated at different times after act.D addition, and the levels of GFP-IL3 mRNA were determined by Northern blotting (right panel).

(E and F) The CAT-ARE^{tnf} (E) or GFP-IL3 (F) signals in (C) or (D) were quantitated with a PhosphorImager and plotted on a semilogarithmic scale using a linear regression.

7. Appendix

at sufficient levels, may take over. Indeed, we found that the loss of KSRP in HT1080 cells results in only a partial stabilization of an ARE-containing mRNA and that reduced expression of both BRF1 and KSRP results in an additive increase in mRNA stability. This redundancy suggests that different decay-promoting ARE-BPs may act via a similar mechanism despite their structural diversity. Indeed, we found that several decay-promoting ARE-BPs, including KSRP, TTP, and AUF1, copurify with the exosome (Chen et al., 2001). As discussed below, this interaction is likely to be a key feature of their function.

KH Motifs Are Necessary and Sufficient for Promoting Rapid mRNA Decay

KSRP is a member of the KH domain family of RNA binding proteins. Its central core contains four contiguous KH motifs. We found that the central KH domain of KSRP can recognize the ARE, interact with the exosome and PARN, and promote rapid decay of ARE-containing RNAs. Both N- and C-terminal sequences flanking the central KH domain are dispensable for all three activities, and their functional roles are currently unknown although they may be required for KSRP-mediated pre-mRNA splicing (Min et al., 1997) or proper subcellular localization. Using recombinant proteins containing individual KH motifs, alone or in combinations, KH_{34} was found to recognize the ARE with high affinity. As KH motif combinations lacking KH_4 did not bind ARE efficiently, we conclude that KH_4 is primarily responsible for ARE binding although an additional KH motif is needed for stabilizing the KH_4-ARE interaction. However, high-affinity ARE binding is not sufficient for promoting rapid mRNA decay. This activity also depends on interaction with the enzymatic machinery involved in mRNA degradation.

In GST pull-down and coimmunoprecipitation experiments, KH_3 is essential and sufficient for association with the exosome and PARN. Both KH_{1-4} and KH_{34} are sufficient for promoting ARE-directed mRNA decay in vitro and in vivo, whereas KH motif combinations lacking either KH_3 or KH_4 do not possess such an activity. Importantly, the overexpression of KH_3, which can interact with the exosome and PARN but not with the ARE, exerted a dominant-negative effect on the ability of KSRP to promote rapid mRNA decay. Although it is unclear whether KSRP can directly interact with the exosome or PARN or whether these interactions depend on additional factors, we believe that the ability of KH_3 to associate with the exosome and PARN is key for the decay-promoting activity of KSRP because: (1) the exosome is required for rapid mRNA decay in the in vitro decay system (Chen et al., 2001; Mukherjee et al., 2002), whereas PARN is required for deadenylation (Gao et al., 2000); (2) KH_{124}, which interacts with the ARE but fails to associate with the exosome and PARN, does not promote rapid mRNA decay; and (3) overexpression of KH_3 interferes with the ability of KSRP to promote rapid RNA decay.

A Recruitment Model for ARE-Directed mRNA Decay

Despite intensive investigation, the mechanism by which the ARE and ARE-BPs modulate mRNA decay was heretofore not well understood. For instance, it was unclear how AREs promote poly(A) shortening, 5′ decapping, and decay of the mRNA body all at once. Recent findings presented above and elsewhere shed new light on the mechanism of ARE-directed mRNA decay. TTP was recently found to promote deadenylation of ARE-containing mRNAs by PARN (Lai et al., 2003), and our results demonstrate that KSRP associates with both PARN and the exosome. These results strongly support a recruitment model that explains how certain ARE-BPs promote the rapid decay of ARE-containing mRNAs.

According to this model, certain ARE-BPs, such as KSRP, TTP, or BRF1, bind to the ARE and then recruit PARN and the exosome to the vicinity of the ARE-containing mRNAs to promote deadenylation and degradation of the mRNA body. Our results suggest that KSRP can simultaneously interact with both PARN and the exosome. Therefore, it is likely that recruitment of both factors by KSRP may occur at the same time or with little delay, but until deadenylation has occurred, the exosome may not be able to access its substrate. The ARE-BPs may also recruit decapping enzymes and the 5′-to-3′ exonuclease to promote mRNA decay via a 5′-to-3′ decay pathway. The recruitment model for ARE-directed mRNA decay is consistent with the recent finding that Upf NMD factors recruit decapping enzymes, 5′-to-3′ exonucleases, the exosome, and PARN to degrade nonsense-containing mRNAs in mammalian cells (Lejeune et al., 2003). Thus, the most important functions of decay-promoting factors are the ability to recognize specific *cis* elements on the RNA, such as the ARE, and in turn increase the local concentration of RNA-degrading enzymes.

Experimental Procedures

Plasmids

Different KH motifs of KSRP were amplified by PCR using a 5′ primer containing an EcoRI site and a 3′ primer containing an XhoI site. PCR products were subcloned between the EcoRI and XhoI sites of pGEX-JDK vector, a derivative of pGEX-2T. To construct Flag-tagged KH motifs, fragments were amplified by PCR using a 5′ primer containing a HindIII site and sequences encoding the Flag epitope and a 3′ primer containing an XbaI site. PCR products were subcloned between the HindIII and XbaI sites of pcDNA3. A fragment containing KH_{124} was obtained by two steps of overlapping PCR, in which the entire KH_3 was deleted, and subcloned between the HindIII and XbaI sites of pcDNA3.

To construct vectors expressing CAT mRNAs containing various AREs in their 3′ UTRs under control of the chicken β-actin promoter, a BglII/HindIII fragment containing the CMV promoter in pcDNA3 was replaced with a BglII/HindIII fragment from pRc/βact (Helmberg et al., 1995) to create a pβAC vector. The coding region of the CAT gene was amplified by PCR and subcloned between the HindIII and EcoRV sites of pβAC to create pβAC-CAT. CAT-IL2 3′ UTR was constructed by subcloning a PCR fragment containing the IL-2 3′ UTR between the NotI and XhoI sites of pβAC-CAT. Linkers containing the *c-fos* or TNFα ARE regions were subcloned between the NotI and XhoI or NotI and XbaI sites of pβAC-CAT, respectively, to produce CAT-ARE[fos] or CAT-ARE[tnf]. HindIII (blunt)/XhoI fragments were isolated from pSP64-ARE[jun] or pSP64-SLDE, which were constructed by subcloning HindIII/SacII fragments containing the c-*jun* ARE (Peng et al., 1998) or the SLDE of G-CSF (Brown et al., 1996) into the same sites of pSP64 (Promega), and subcloned between the NotI (blunt) and XhoI sites of pβAC-CAT. DNA templates were used to produce RNA substrates as previously described (Chen et al., 2001). E4 is a non-ARE sequence (5′-UUAUGUUGAAUGUUA AAUAUAGUAUCUAUGUAGAUUGGUUAGUAAAACU-3′).

siRNA

Doulbe-stranded 21 nucleotide RNAs (siRNAs) based on sequences within the KSRP coding region (GAUCAACCGGAGAGCAAGA) or

luciferase were purchased from Dharmacon Research, Inc. BRF1 siRNA has been described (Stoecklin et al., 2002).

Production and Purification of Recombinant Proteins and Anti-KSRP Serum

Histidine-tagged KSRP$_{47-711}$ was expressed in Sf9 cells and purified by Ni-NTA chromatography (Chen et al., 2001). GST-tagged proteins were produced in BL21(DE3) cells and purified on glutathione-Sepharose 4B. Polyclonal antiserum was raised in rabbits by immunization with purified histidine-tagged KSRP.

Immunodepletion and In Vitro RNA Decay Analysis

KSRP was removed from S100s by immunoprecipitation with anti-KSRP serum pre-bound to Protein A-Sepharose. Supernatants from preimmune serum- and antiserum-depleted reactions were used in RNA decay assays (Chen et al., 2001).

RNA Binding Analysis and Immunoprecipitation of RNA-Protein Complexes

RNA binding assays were performed as described (Chen et al., 2000). After RNase T1 treatment, RNA-protein complexes were either resolved in a 5% nondenaturing polyacrylamide gel or proceeded with UV crosslinking assays. For immunoprecipitation of RNA-protein complexes, UV crosslinking reactions were diluted with buffer (500 μl) containing 10 mM Tris-Cl (pH 8.0), 250 mM NaCl, 0.5% NP-40, and 1 mM EDTA/EGTA and incubated with antibodies (1–5 μl) and protein A/G Sepharose (20 μl) at 4°C overnight. The immunoprecipitates were washed four times and subjected to SDS-PAGE and autoradiography.

Transfection, RNA Isolation, and Northern Blot Analysis

HeLa or HT1080 cells were plated onto 6-well plates and transfected with CAT mRNA reporters (1.5 μg) and siRNAs (60 pmole) using LipofectAMINE (12 μl). Cells were incubated with the DNA-lipid mixtures for 5 hr. The following day, transfected cells were collected and replated onto 35 mm plates. After 24 hr, the cells were treated with growth medium containing actinomycin D (5 μg/ml). Total RNA was isolated using Trizol reagent at different times after act.D addition. RNA was separated by denaturing formaldehyde-agarose gel electrophoresis and transferred to Hybond-XL. The membrane was hybridized with a ^{32}P-labeled RNA probe at 68°C for 16 hr.

RNase H Analysis

RNase H digestion was performed by annealing RNA with a deoxy-oligonucleotide complementary to the CAT coding region (GCAT CAGCACCTTGTCGCCT) in RNase H buffer (0 mM Tris-Cl [pH 8.3], 75 mM KCl, 3 mM MgCl$_2$, and 10 mM DTT) for 5 min at 65°C, followed by an additional 5 min incubation at room temperature. In some reactions, oligo(dT)$_{12-18}$ was added along with the CAT oligonucleotide. RNase H (1 unit) and RNasin (20 units) were added to the mixture and incubated at 37°C for 30 min.

References

Adinolfi, S., Bagni, C., Castiglione Morelli, M.A., Fraternali, F., Musco, G., and Pastore, A. (1999). Novel RNA-binding motif: the KH module. Biopolymers 51, 153–164.

Bakheet, T., Frevel, M., Williams, B.R., Greer, W., and Khabar, K.S. (2001). ARED: human AU-rich element-containing mRNA database reveals an unexpectedly diverse functional repertoire of encoded proteins. Nucleic Acids Res. 29, 246–254.

Bevilacqua, A., Ceriani, M.C., Capaccioli, S., and Nicolin, A. (2003). Post-transcriptional regulation of gene expression by degradation of messenger RNAs. J. Cell. Physiol. 195, 356–372.

Blackshear, P.J. (2002). Tristetraprolin and other CCCH tandem zinc-finger proteins in the regulation of mRNA turnover. Biochem. Soc. Trans. 30, 945–952.

Brennan, C.M., and Steitz, J.A. (2001). HuR and mRNA stability. Cell. Mol. Life Sci. 58, 266–277.

Brown, C.Y., Lagnado, C.A., and Goodall, G.J. (1996). A cytokine mRNA-destabilizing element that is structurally and functionally distinct from A+U-rich elements. Proc. Natl. Acad. Sci. USA 93, 13721–13725.

Chen, C.Y., and Shyu, A.B. (1995). AU-rich elements: characterization and importance in mRNA degradation. Trends Biochem. Sci. 20, 465–470.

Chen, C.Y., Xu, N., and Shyu, A.B. (1995). mRNA decay mediated by two distinct AU-rich elements from c-fos and granulocyte-macrophage colony-stimulating factor transcripts: different deadenylation kinetics and uncoupling from translation. Mol. Cell. Biol. 15, 5777–5788.

Chen, C.Y., Gherzi, R., Andersen, J.S., Gaietta, G., Jürchott, K., Royer, H.D., Mann, M., and Karin, M. (2000). Nucleolin and YB-1 are required for JNK-mediated interleukin-2 mRNA stabilization during T-cell activation. Genes Dev. 14, 1236–1248.

Chen, C.Y., Gherzi, R., Ong, S.E., Chan, E.L., Raijmakers, R., Pruijn, G.J., Stoecklin, G., Moroni, C., Mann, M., and Karin, M. (2001). AU binding proteins recruit the exosome to degrade ARE-containing mRNAs. Cell 107, 451–464.

Gao, M., Fritz, D.T., Ford, L.P., and Wilusz, J. (2000). Interaction between a poly(A)-specific ribonuclease and the 5′ cap influences mRNA deadenylation rates in vitro. Mol. Cell 5, 479–488.

Guhaniyogi, J., and Brewer, G. (2001). Regulation of mRNA stability in mammalian cells. Gene 265, 11–23.

Helmberg, A., Auphan, N., Caelles, C., and Karin, M. (1995). Glucocorticoid-induced apoptosis of human leukemic cells is caused by the repressive function of the glucocorticoid receptor. EMBO J. 14, 452–460.

Hutvagner, G., and Zamore, P.D. (2002). RNAi: nature abhors a double-strand. Curr. Opin. Genet. Dev. 12, 225–232.

Jacobs, J.S., Anderson, A.R., and Parker, R.P. (1998). The 3′ to 5′ degradation of yeast mRNAs is a general mechanism for mRNA turnover that requires the SKI2 DEVH box protein and 3′ to 5′ exonucleases of the exosome complex. EMBO J. 17, 1497–1506.

Lai, W.S., Kennington, E.A., and Blackshear, P.J. (2003). Tristetraprolin and its family members can promote the cell-free deadenylation of AU-rich element-containing mRNAs by poly(A) ribonuclease. Mol. Cell. Biol. 23, 3798–3812.

Lejeune, F., Li, X., and Maquat, L.E. (2003). Nonsense-mediated mRNA decay in mammalian cells involves decapping, deadenylating, and exonucleolytic activities. Mol. Cell 12, 675–687.

Min, H., Turck, C.W., Nikolic, J.M., and Black, D.L. (1997). A new regulatory protein, KSRP, mediates exon inclusion through an intronic splicing enhancer. Genes Dev. 11, 1023–1036.

Mitchell, P., Petfalski, E., Shevchenko, A., Mann, M., and Tollervey, D. (1997). The exosome: a conserved eukaryotic RNA processing complex containing multiple 3′→5′ exoribonucleases. Cell 91, 457–466.

Mukherjee, D., Gao, M., O'Connor, J.P., Raijmakers, R., Pruijn, G., Lutz, C.S., and Wilusz, J. (2002). The mammalian exosome mediates

7. Appendix

the efficient degradation of mRNAs that contain AU-rich elements. EMBO J. *21*, 165–174.

Peng, S.S., Chen, C.Y., and Shyu, A.B. (1996). Functional characterization of a non-AUUUA AU-rich element from the c-jun proto-oncogene mRNA: evidence for a novel class of AU-rich elements. Mol. Cell. Biol. *16*, 1490–1499.

Peng, S.S., Chen, C.Y., Xu, N., and Shyu, A.B. (1998). RNA stabilization by the AU-rich element binding protein, HuR, an ELAV protein. EMBO J. *17*, 3461–3470.

Sarkar, B., Xi, Q., He, C., and Schneider, R.J. (2003). Selective degradation of AU-rich mRNAs promoted by the p37 AUF1 protein isoform. Mol. Cell. Biol. *23*, 6685–6693.

Sharp, P.A. (2001). RNA interference—2001. Genes Dev. *15*, 485–490.

Shim, J., and Karin, M. (2002). The control of mRNA stability in response to extracellular stimuli. Mol. Cells *14*, 323–331.

Shyu, A.B., Belasco, J.G., and Greenberg, M.E. (1991). Two distinct destabilizing elements in the c-fos message trigger deadenylation as a first step in rapid mRNA decay. Genes Dev. *5*, 221–231.

Stoecklin, G., Ming, X.F., Looser, R., and Moroni, C. (2000). Somatic mRNA turnover mutants implicate tristetraprolin in the interleukin-3 mRNA degradation pathway. Mol. Cell. Biol. *20*, 3753–3763.

Stoecklin, G., Stoeckle, P., Lu, M., Muehlemann, O., and Moroni, C. (2001). Cellular mutants define a common mRNA degradation pathway targeting cytokine AU-rich elements. RNA *7*, 1578–1588.

Stoecklin, G., Colombi, M., Raineri, I., Leuenberger, S., Mallaun, M., Schmidlin, M., Gross, B., Lu, M., Kitamura, T., and Moroni, C. (2002). Functional cloning of BRF1, a regulator of ARE-dependent mRNA turnover. EMBO J. *21*, 4709–4718.

Stoecklin, G., Lu, M., Rattenbacher, B., and Moroni, C. (2003). A constitutive decay element promotes tumor necrosis factor alpha mRNA degradation via an AU-rich element-independent pathway. Mol. Cell. Biol. *23*, 3506–3515.

Tucker, M., and Parker, R. (2000). Mechanisms and control of mRNA decapping in Saccharomyces cerevisiae. Annu. Rev. Biochem. *69*, 571–595.

Wang, Z., and Kiledjian, M. (2001). Functional link between the mammalian exosome and mRNA decapping. Cell *107*, 751–762.

Wilson, G.M., and Brewer, G. (1999). The search for trans-acting factors controlling messenger RNA decay. Prog. Nucleic Acid Res. Mol. Biol. *62*, 257–291.

Wilusz, C.J., Wormington, M., and Peltz, S.W. (2001). The cap-to-tail guide to mRNA turnover. Nat. Rev. Mol. Cell Biol. *2*, 237–246.

Wisdom, R., and Lee, W. (1991). The protein-coding region of c-myc mRNA contains a sequence that specifies rapid mRNA turnover and induction by protein synthesis inhibitors. Genes Dev. *5*, 232–243.

Xu, N., Chen, C.Y., and Shyu, A.B. (1997). Modulation of the fate of cytoplasmic mRNA by AU-rich elements: key sequence features controlling mRNA deadenylation and decay. Mol. Cell. Biol. *17*, 4611–4621.

Glossary

ARE: AU-rich element, adenosine/uridine rich element in the 3' untranslated region of up to 8% of all mRNAs. Sequence feature that is important for mRNA stability.

Blastocyst: Preimplantation embryo of 30-150 cells. The blastocyst consists of a sphere made of an outer layer of cells, a fluid-filled cavity, and a cluster of cells in the interior.

Cardiomyogenesis: Generation of heart muscle cells.

Cytokines: Extracellular signal protein or peptide that acts as a local mediator in cell-cell communication.

Development: Succession of changes that take place in an organism as a fertilized egg gives rise to an adult animal.

Dicer: Key enzyme for the function of RNAi. Dicer is a member of the RNAse III family of dsRNA-specific endonucleases.

Differentiation: Process whereby an unspecialized early embryonic cell acquires features of a specialized cell (heart, lungs, skin, etc.)

Ectoderm: The upper, outermost of three germ layers of the embryo; it gives rise to skin, nerves, and brain.

Embryoid bodies (EBs): Clumps of cellular structures that arise when embryonic stem cells are cultured. Embryoid bodies contain tissue from all three germ layers: endo-, meso- and ectoderm. Embryoid bodies are not part of the normal development and occur only *in vitro* conditions.

Embryonic Stem (ES) cells: Cells derived from the inner cell mass of the early mammalian embryo that can give rise to all cells in the body.

Endoderm: Lower layer of the three germ layers of the embryo; it later becomes the lungs and digestive organs.

Exosome: Multiprotein complex involved in 3'-5' RNA degradation. Consisting of different exonucleases, are found in the cytosol and nucleus.

FACS: Fluorescence activated cell sorting. Apparatus to screen cells for fluorescence.

Feeder cell layer: Cells that are utilized in co-culture to maintain pluripotent stem cells. Feeders usually consist of mouse embryonic fibroblasts.

Fibroblast: Cells of mesodermal origin that make the structural fibers and ground substance of connective tissue. They are multipotent and can give rise to other cells such as fat cells, bone cells, cartilage cells and smooth muscle cells.

Hanging drop method: A technique used to culture embryonic stem cells so that they develop into embryoid bodies.

Hematopoiesis: Generation of blood cells.

Inner cell mass: Cluster of cells inside the blastocyst. These cells give rise to the embryonic disk of the later embryo and the fetus.

in vitro (Latin for "in glass"): Term used by biochemists to describe a process taking place in an isolated cell-free extract. Also used by cell biologists to refer to cells growing in culture, as opposed to in an organism.

in vivo (Latin for "in life"): In an intact cell or organism.

Karyotype: The full set of chromosomes of a cell arranged with respect to size, shape, and number.

Mesoderm: The middle layer of the three germ layer of the embryo; it is the precursor to bone, muscle and connective tissue.

Morphology: The shape and structural makeup of a cell, tissue or organism.

miRNA: Micro-RNAs (miRNA) are single-stranded RNAs of 22-nt that are processed from ~70-nt hairpin RNA precursors. Similar to siRNAs, miRNAs can silence gene activity via destruction of homologous mRNA in plants or blocking its translation in plants and animals.

RISC: RNA induced silencing complex. Each complex consists of a single siRNA and a protein ribonuclease. Activated RISC (RISC*) can recognize and cleave a target RNA complementary to the guide strand of the siRNA.

RNAi: RNA interference. A phenomenon in which double-stranded RNA triggers the destruction of homologous mRNA.

shRNA: Short hairpin RNA. A short sequence of RNA which makes a tight hairpin turn and can be used to silence gene expression.

siRNA: Small Interfering RNA (siRNA) is 21~23-nt double-stranded RNA molecules. It guides the cleavage and degradation of its cognate RNA.

Slicer: Ribonuclease thought to be part of RISC and to perform cleavage of the target RNA.

Stem cell: A cell that has the ability to divide for indefinite periods in culture and to give rise to specialized cells.

Teratoma: A tumor composed of tissues from the three embryonic layers.

Trophoectoderm: The outer layer of the developing blastocyst that will ultimately form the embryonic side of the placenta.

Definitions are taken from:

Molecular Biology of the Cell (2002, 4th Edition). Alberts, *et al*., Garland Science

NIH Stem Cells Report (2001)

Internet

Posters

Geneva 2004

A Possible Role for the RNA-Binding Protein BRF1 in the Induction of ES Cell Differentiation

Daniel Wegmueller, Ines Raineri, Brigitte Gross, Clelia Sasseli and Christoph Moroni
Institute for Medical Microbiology, University of Basel, Basel, Switzerland.

Abstract

We are interested in the regulation of mRNA turnover, particularly in the function of BRF1. This RNA-binding protein binds to the 3' untranslated region (3'UTR) and targets the mRNA for degradation. We hypothesize that differentiation of embryonic stem (ES) cells may, in addition to transcriptional mechanisms, also involve posttranscriptional control, possibly by BRF1.

Upon induction of differentiation of murine embryonic stem (ES) cells by removal of leukemia inhibitory factor (LIF) we observed a decrease of BRF1 (Fig. 1). Small interfering RNA (siRNA) experiments targeting STAT3 (Fig. 2a) indicated that BRF1 is under STAT3 control. To test whether BRF1 may be involved in mediating the LIF -> STAT3 -> Differentiation response, we targeted BRF1 by siRNA (Fig. 2b). Unexpectedly, we observed morphological changes similar to LIF removal (Fig 2c). This suggests that BRF1 (and posttranscriptional-regulation of yet to be identified genes) contributes to induction of ES cell differentiation.

We propose a strategy in which the cDNA of BRF1 or an other RNA-binding protein or a siRNA stemloop is stably integrated and under tetracycline control (Fig. 3) in order to be able to affect posttranscriptional regulation in an inducible fashion and observe possible effects on embryoid body formation or the formation of hematopoietic colonies.

In preliminary experiments we could show (Fig. 4) that induction of a stemloop downregulated BRF1 mRNA, protein, and downregulated the marker c-kit (see arrows in Fig. 4). A model for the possible role of BRF1 in maintenance of ES cell pluripotency maintenance is shown in Figure 5.

Figure 1 Timecourse of BRF1 mRNA and protein after LIF removal.
a) Northern Blot of BRF mRNA. BRF1 mRNA decreased whereas BRF2 mRNA levels peaked at day 2 after LIF removal.
b) BRF1 and BRF2 protein levels mirror the mRNA levels. A transient increase of BRF2 was observed at day 2 after LIF removal.

1. BRF1 RNA and protein changes upon LIF removal
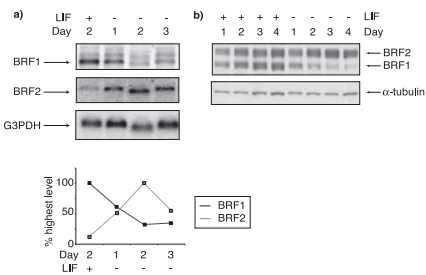
2. Cell morphology and BRF1 protein levels after treatment of cells with siRNA
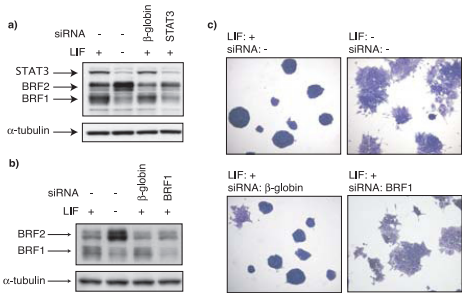
Figure 2
a) STAT3 protein levels decrease upon LIF removal and treatment of ES cells with STAT3 siRNA. The same is true for BRF1 protein levels. An increase of BRF2 is only seen in cells after LIF removal.
b) A decrease of BRF1 protein is observed when cells are treated with BRF1 siRNA or LIF is removed.
c) Morphologic changes are seen after LIF removal or treatment of ES cells with BRF1 siRNA but not in cells treated with β-globin control siRNA.

Figure 4
a) After BRF1 stemloop induction by Dox, BRF1 mRNA levels decrease to about the same level as seen at LIF removal. The same is observed with BRF1 protein (b).
c) c-kit shows the same response after Dox induction of BRF1 stemloop as after LIF removal.

4. RNA and protein levels and c-kit stain of Dox-inducible BRF1 stemloop candidate clone

3. Strategy

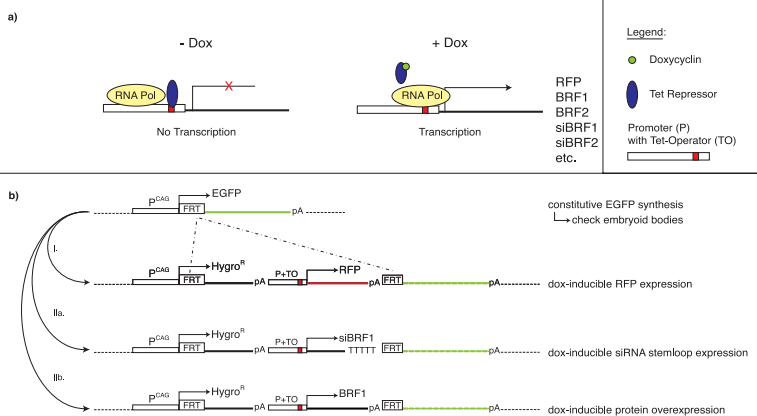### 5. Model for the Role of BRF1

Figure 3
a) A tetracycline-inducible system with the Tet-Repressor (TR) and full-length promoters containing Tet Operators (TO) to downregulate or overexpress various RNA-binding proteins.
b) After stable transfection of ES cells with the Tet-Repressor and a reporter construct containing a Flip-Site cells are screened for high reporter (EGFP) expression. These cells are transfected with Flipase and another vector containing another Flip-Site and either an inducible stemloop to downregulate (IIa) or an inducible cDNA to overexpress (IIb) the RNA-binding protein of interest. After flip recombination the construct of interest is stably integrated in the before characterized locus and can be switched on demand by addition of tetra- or doxycycline. (As a first recombination RFP (I) is used to screen for leakiness.)
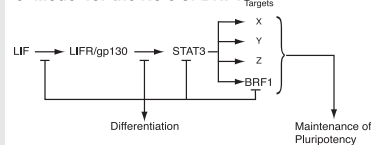
Figure 5
The LIF -> gp130 -> STAT3 pathway can be regulated at many steps. We propose that BRF1 is downstream of STAT3 and also involved in maintenance of pluripotency (directly or indirectly).

Arolla 2005

A tetracycline-inducible system to study AU-binding protein function in embryonic stem cell differentation

Daniel Wegmueller, Ines Raineri, Brigitte Gross and Christoph Moroni
Institute for Medical Microbiology, University of Basel, Basel, Switzerland.

Abstract

We are interested in the regulation of mRNA turnover, particularly in the function of BRF1. This RNA-binding protein binds to the 3' untranslated region (3'UTR) and targets the mRNA for degradation (1). We hypothesize that differentiation of embryonic stem (ES) cells may, in addition to transcriptional mechanisms, also involve posttranscriptional control, possibly by BRF1.
ES cells are kept in a undifferentiated pluripotent state by leukemia inhibitory factor (LIF) which acts via Stat3. We observed that both LIF removal and downregulation of Stat3 by siRNA leads to downregulation of BRF1.
We propose here a strategy in which a BRF1 siRNA stemloop (and later the BRF1 cDNA) is stably integrated into a defined locus marked by GFP and under tetracycline control. To evaluate the strategy we have chosen a STAT3 inducible stemloop based on its known initiation in ES cell differentiation (2).
The results with the STAT3 stemloop showed controllable downregulation of STAT3 with almost not detectable leakiness. Experiments in progress evaluate now the inducible stemloop against BRF1.
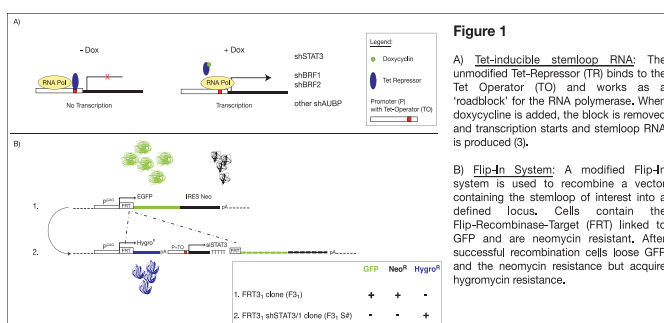
Figure 1

A) Tet-inducible stemloop RNA: The unmodified Tet-Repressor (TR) binds to the Tet Operator (TO) and works as a 'roadblock' for the RNA polymerase. When doxycycline is added, the block is removed and transcription starts and stemloop RNA is produced (3).

B) Flip-In System: A modified Flip-In system is used to recombine a vector containing the stemloop of interest into a defined locus. Cells contain the Flip-Recombinase-Target (FRT) linked to GFP and are neomycin resistant. After successful recombination cells loose GFP and the neomycin resistance but acquire hygromycin resistance.
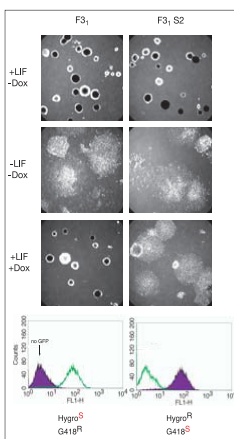
Figure 2

Stat3 stemloop RNA induces differentiation

In a first step a Stat3 stemloop was recombined into cells containing an FRT-GFP (F3₁). After 7 days in culture (+LIF –Dox, -LIF –Dox, +LIF +Dox) cells were then screened by morphological changes after doxycycline addition, for GFP presence by FACS and for antibiotic resistance. Cells that have the stemloop correctly integrated (here F3₁ S2) have lost their GFP and the neomycin resistance, but are now resistant against hygromycin. Upon addition of doxycycline cells undergo morphological changes as observed upon LIF removal.
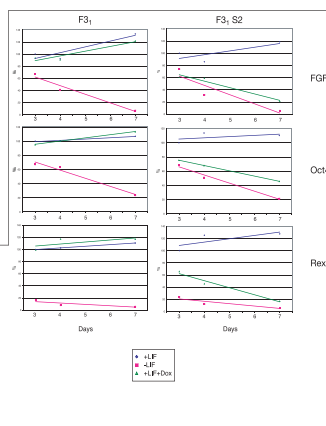

Figure 3

Doxycyclin induction of marker changes

After 7 days culture (+LIF –Dox, -LIF –Dox, +LIF +Dox) RNA was extracted and processed for northern blotting against 3 known differentiation markers (FGF-4, Oct4, Rex-1). Control cells (F3₁) displayed upon LIF removal changes in differentiation markers, whereas cells containing the Stat3 stemloop (F3₁ S2 and F3₁ S3) showed the change also following doxycycline addition.
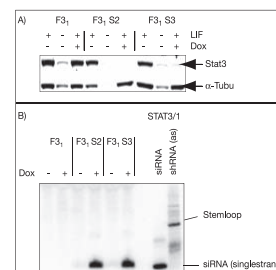

Figure 4

Doxycyclin downregulated Stat3 and induces siRNA

A) After 3 days in culture (+LIF –Dox, -LIF –Dox, +LIF +Dox) western blot analysis for Stat3 was performed for control cells and 2 Stat3 stemloop cell lines. Stat 3 levels changed in all 3 cell lines upon LIF removal. In the stemloop cell lines (F3₁ S2 and F3₁ S3) Stat3 disappeared also when doxycycline was added.

B) After 7 days in culture (+LIF -/+Dox) a stemloop northern blot was performed. Cells containing the stemloop (F3₁ S2 and F3₁ S3) showed a strong induction of the stemloop upon doxycycline addition whereas in control cell line (F3₁) and cells cultured without doxycycline no signal was observed.
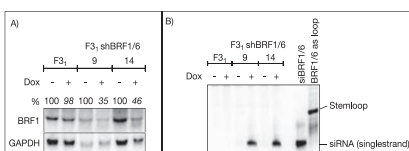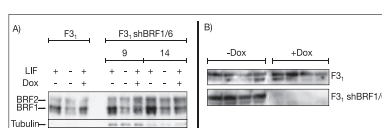

Figure 5

Downregulation of BRF1 RNA by stemloop induction

As a next step a BRF1 stemloop was then recombined in the F3₁ cell line (F3₁ shBRF1/6). After 7 days in culture (+LIF -/+Dox) northern blot experiments were performed.

A) The northern blot against BRF1 shows a reduction of BRF1 to around 40% compared to levels of cells kept without doxycycline.

B) The stemloop northern blot shows the same as observed in the Stat3 stemloop cells: Cells containing the stemloop (F3₁ shBRF1/6 9 and 14) showed a strong induction of the stemloop upon doxycycline addition whereas in control cell line (F3₁) and cells cultured without doxycycline no signal was observed.

Figure 6

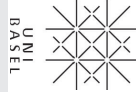Western blot analysis of BRF1 after stemloop induction

A) After 3 days in culture (+LIF –Dox, -LIF –Dox, +LIF +Dox) western blot analysis showed a low reduction of BRF1 protein upon stemloop induction.

B) After 20 days of differentiation in vitro +/- doxycycline in 24-well plates 4 wells were pooled and four replicas (4 wells each) for each condition were blotted. In cells with the BRF1 stemloop (F3₁ shBRF1/6 9) a nice reduction of BRF1 was observed whereas no change in levels was seen in control cells (F3₁) (Loading was checked by amidoblack staining of the membrane).

Discussion

The recombination of the stemloops to the FRT-GFP (F3₁) cell line is quick and straightforward. After 6 weeks a new cell line is screened and ready for experiments.
The results show that we have now a system that shows no leakiness and strong induction of stemloops upon doxycycline addition. For the Stat3 stemloop cell line experiments with longer timepoints have to be performed as well as ex vivo experiments to show its functionability in differentiation into different cell types (e.g. Hematopoietic cells, cardiac muscle cells).

References

1. G. Stoecklin et al., *Embo J* **21**, 4709 (Sep 2, 2002).
2. H. Niwa, T. Burdon, I. Chambers, A. Smith, *Genes Dev* **12**, 2048 (Jul 1, 1998).
3. M. van de Wetering et al., *EMBO Rep* **4**, 609 (Jun, 2003).

Basel 2006

Curriculum Vitae

Daniel Wegmüller

Personal Data	Marital status	Single
	Citizenship	Swiss
	Date of Birth	2. October 1978
Education	1985 – 1990	Primary school in Frenkendorf
	1990 – 1994	Progymnasium in Frenkendorf
	1994 – 1997	Gymnasium in Liestal, Matura Typus C
	1998 – 2002	Biologie II Studium at the University of Basel Diploma in Biochemistry.
	2003 – 2007	PhD in Medical-Biological Research at the Institute for Medical Microbiology in Basel
Languages	German	native language
	English	speak fluently and read/write with high proficiency
	French	speak, read, and write with basic competence
Practical Experience	2001 – 2002	Diploma-Thesis "Analysis of ARE-dependent mRNA turnover by siRNA targeted to AU-binding proteins" in the lab of Prof. Ch. Moroni at the Institute for Medical Microbiology in Basel
	2003 – 2007	PhD-Thesis "Investigation of the Posttranscriptional Regulator BRF1 in Embryonic Stem Cells by Inducible RNA Interference" in the lab of Prof. Ch. Moroni at the Institute for Medical Microbiology in Basel
Awards	2006	Roche Poster Award, 2nd Place, BioValley Science Day 2006, Basel

Publications	**Gherzi, R., K. Y. Lee, P. Briata, D. Wegmuller, C. Moroni, M. Karin and C. Y. Chen** (2004). "A KH domain RNA binding protein, KSRP, promotes ARE-directed mRNA turnover by recruiting the degradation machinery." <u>Mol Cell</u> **14**(5): 571-83.
	Raineri, I., D. Wegmueller, B. Gross, U. Certa and C. Moroni (2004). "Roles of AUF1 isoforms, HuR and BRF1 in ARE-dependent mRNA turnover studied by RNA interference." <u>Nucleic Acids Res</u> **32**(4): 1279-88.
	Wegmuller, D., I. Raineri, B. Gross, E. J. Oakeley and C. Moroni (2007). "A cassette system to study embryonic stem cell differentiation by inducible RNA interference." <u>Stem Cells</u> **25**(5): 1178-85.

Congresses	**Posters:**	
	2003	1st International Meeting on AREs and AUBPs in mRNA Stability and Translation Control, Florence, Italy
	2004	1st Swiss Stem Cell Network Meeting, Geneva, Switzerland
	2005	EMBO Workshop " Mechanisms and Regulation of mRNA Turnover", Arolla, Switzerland
	2006	Advances in Stem Cell Research, Lausanne, Switzerland
	2006	BioValley Science Day "Frontiers in Stem Cell and Cancer Research", Basel, Switzerland
	2007	USGEB Meeting, Basel, Switzerland
	Talks:	
	2005	
		2nd Swiss Stem Cell Network Meeting, Basel, Switzerland

Declaration

I declare that I wrote this thesis "*Investigation of the Posttranscriptional Regulator BRF1 in Embryonic Stem Cells by Inducible RNA Interference*" with the help indicated and only handed it in to the faculty of science of the University of Basel and to no other faculty and no other university.

Daniel Wegmüller